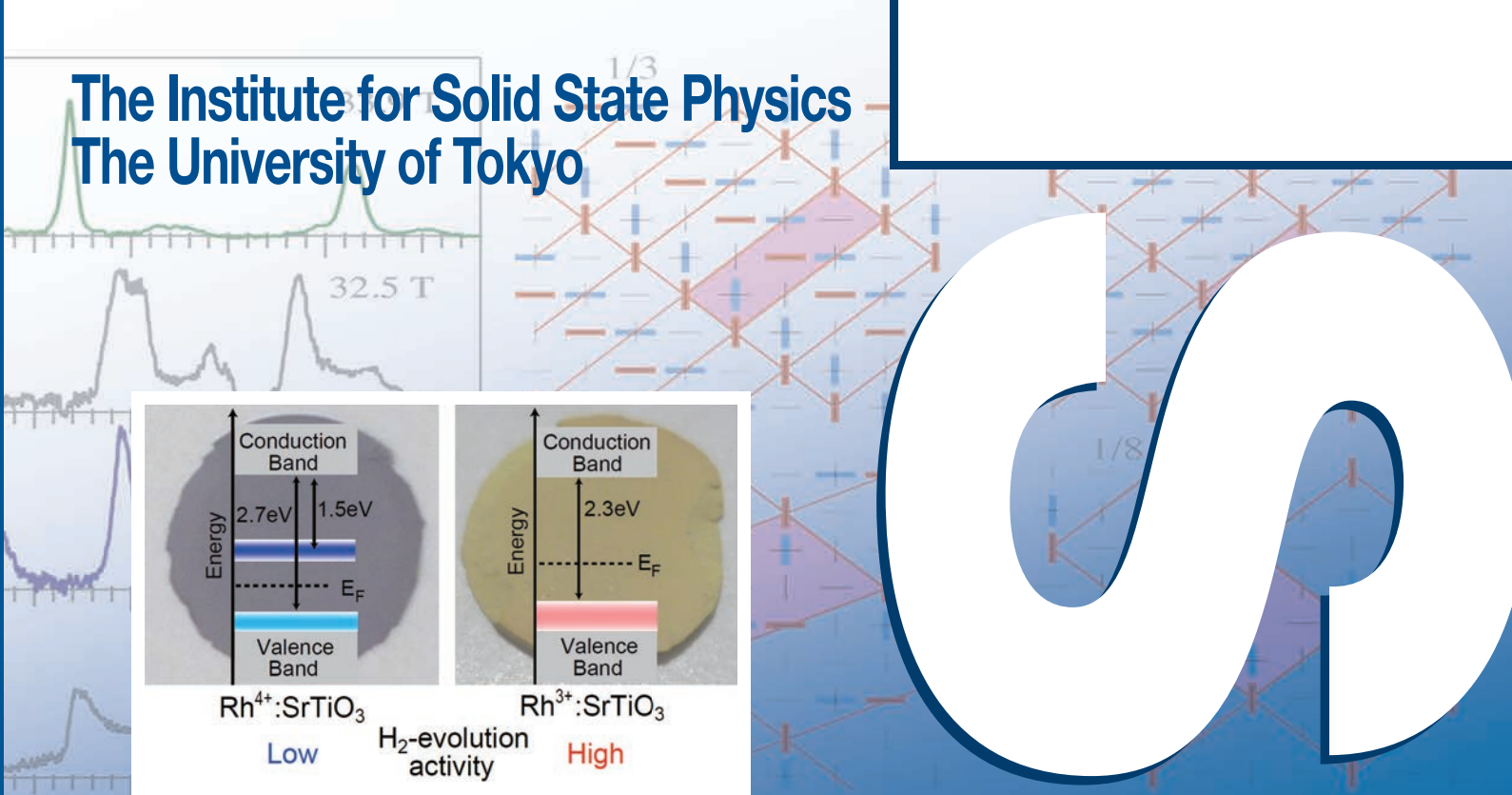
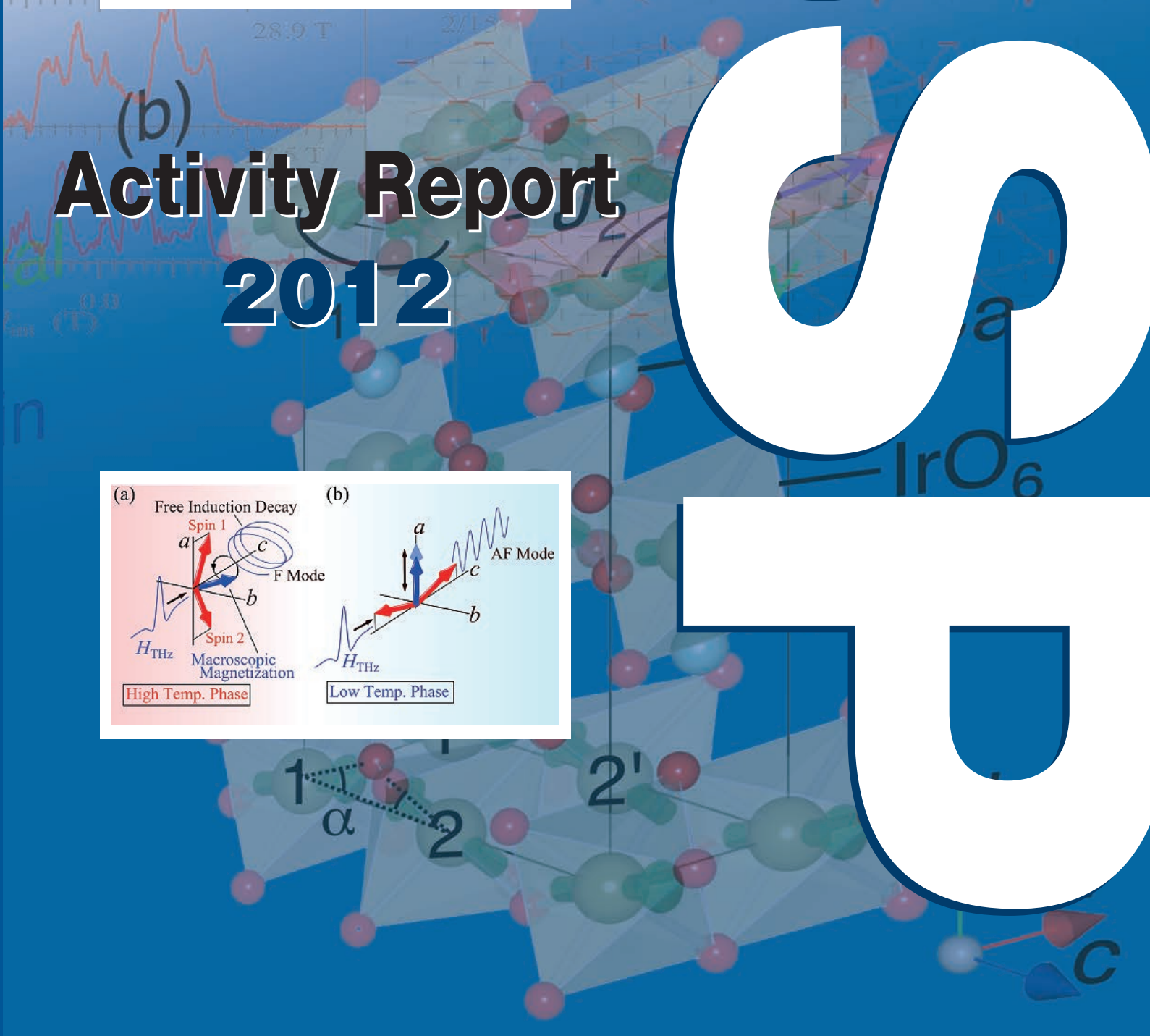
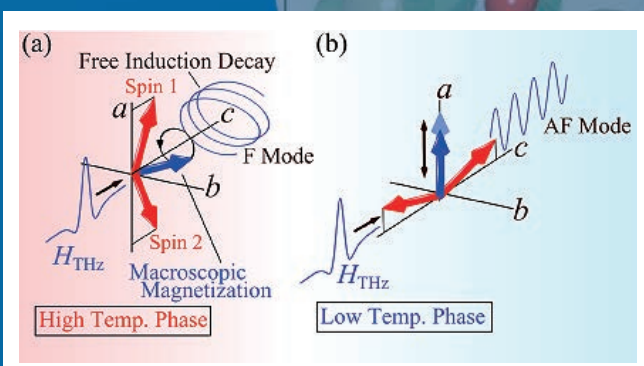


# The Institute for Solid State Physics The University of Tokyo



## (b) Activity Report 2012



# **ISSP**

## **Activity Report 2012**

<b>Contents</b>	<b>Pages</b>
Preface	1
Research Highlights	2 - 27
Highlights of Joint Research	28 - 45
International Conferences and Workshops	46 - 47
ISSP Workshops	48 - 53
Subjects of Joint Research	54 - 121
Publications	122 - 155



# Preface

We are pleased to present the annual ISSP Activity Report for the academic year 2012. ISSP (Institute for Solid State Physics) was established in 1957 as a joint-use research institution attached to the University of Tokyo. Since then both in-house research and collaboration with external users have been essential elements of the activities of ISSP.

The research at ISSP has been pursued along two major directions. Synthesis of new materials and nano-structures in search for novel phenomena and functions using advanced and original techniques is at the core of modern condensed matter science. Many groups at ISSP and their collaborators are involved in this type of “small science”. On the other hand, importance of large experimental and computational facilities in materials science has been rapidly increasing in recent years. An important mission of ISSP is to participate in the development and operation of some of those large facilities that are difficult to maintain for university faculties. Notable achievements in this direction are summarized below.

(1) ISSP has been operating supercomputers dedicated to materials science. In addition, the Center of Computational Materials Science launched in 2011 provides technical supports to facilitate use of massively parallel computational resources such as the K-computer. (2) The International MegaGauss Science Laboratory continues to develop both the destructive ultrahigh magnetic field by electromagnetic compression aimed at 1000 tesla and the non-destructive long-pulse magnetic field by a flywheel generator. (3) ISSP has been providing access to quantum beams such as neutrons and synchrotron light sources. Concerning neutron scattering, the JRR-3 reactor at Tokai is still shut down after the earthquake in 2011, however the pulse spectrometer at J-PARC is now in operation. The latest development in 2012 is the opening of the new Laser and Synchrotron Research Center, which is aimed at making a new frontier of advanced spectroscopy by combining laser, synchrotron, and X-FEL light sources in ultraviolet and soft X-ray region.



May, 2013  
Masashi Takigawa  
Director  
Institute for Solid State Physics  
The University of Tokyo

# Research Highlights

---Division of New Materials Science---

## Incomplete Devil's Staircase in the Magnetization Curve of $\text{SrCu}_2(\text{BO}_3)_2$

Takigawa and Y. Ueda Groups

Magnetization plateaus in frustrated quantum spin systems are manifestation of Wigner crystallization of magnons, resulting from competition between the kinetic energy and repulsive interaction. The layered compound  $\text{SrCu}_2(\text{BO}_3)_2$  has played a prominent role in this problem since the discovery of a sequence of plateaus at  $1/8$ ,  $1/4$ , and  $1/3$  of the saturation magnetization. Recent experiments have revealed a rich phase diagram below the  $1/4$  plateau, but with controversial results. We have performed magnetic torque and  $^{11}\text{B}$ -NMR measurements in high magnetic field up to 34 T at the Grenoble High Magnetic Field Laboratory and precisely determined the sequence and the spin structures of the plateaus [1].

The magnetization curve under static magnetic fields was accurately determined from the torque ( $\tau$ ) data (Fig. 1), which consist of two terms:  $\tau = a\mathbf{M} \times \mathbf{H} + b(\mathbf{M} \cdot \nabla)\mathbf{M}$ , the first one proportional to the transverse magnetization and the second one to the longitudinal magnetization. The first term can be eliminated by taking a linear combination of two measurements of  $\tau/H$  taken at different sample positions with the requirement that the longitudinal magnetization is zero in the dimer singlet phase below 15 T. The longitudinal magnetization thus obtained clearly shows three plateaus at the ratio  $1/8:2/15:1/6$  below the  $1/4$  plateau and two intermediate phases below and above the  $1/6$  plateau.

The plateau phases are associated with symmetry breaking commensurate spin superstructures, which were determined from the  $^{11}\text{B}$ -NMR spectrum (Fig. 2 (left)). We have established a systematic way to determine the

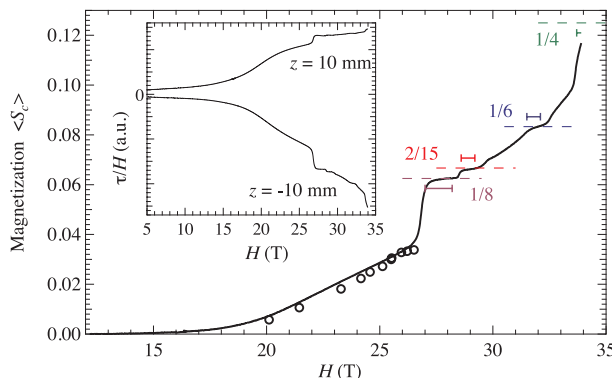


Fig. 1. Inset: The torque divided by field vs. field obtained at  $T=60\text{ mK}$  with the sample positioned at 10 mm off the nominal field center. Main panel: The thick black line represents the longitudinal magnetization with the vertical scale appropriately adjusted. The magnetization values at  $1/8$ ,  $2/15$ ,  $1/6$ , and  $1/4$  of the saturation are shown by the dashed lines. The horizontal bars indicate the field range of the plateaus determined by NMR. The open circles show the magnetization determined from the Cu NMR shift data (Kodama *et al.*, *Science* **298**, (2002) 395).

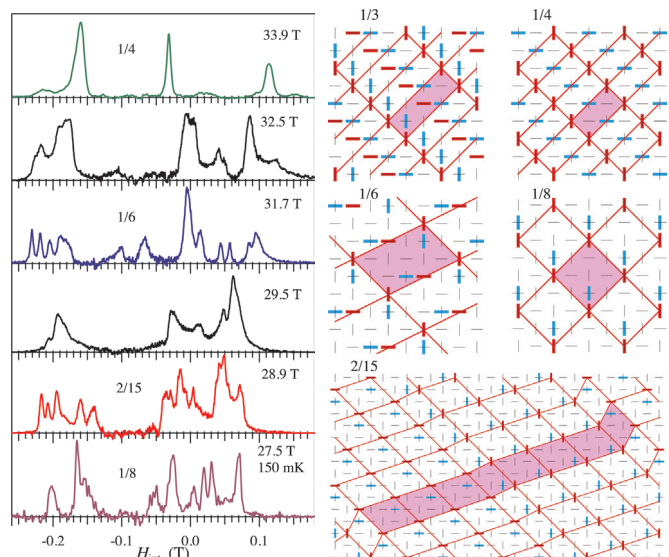


Fig. 2. (left) The distribution of internal magnetic field at the  $^{11}\text{B}$  nuclei obtained by deconvoluting the quadrupole splitting structure from the experimental NMR spectra obtained at  $T=430\text{ mK}$  unless explicitly indicated. (right) The spin superstructure of the plateau phases. The thin black lines show the lattice of orthogonal Cu dimers in one layer. The thick red lines show the triplet dimers carrying the largest magnetization in the same layer while the blue lines indicate these triplets on the neighboring layers. The unit cell of each superstructure is shown by the shaded area.

spin structure from the NMR spectra and the results are displayed in Fig. 2 (right). All plateaus show stripe order of triplets. The structure of  $1/6$  ( $1/8$ ) plateau can be obtained by removing every other triplet from the one of the  $1/3$  ( $1/4$ ) plateaus. The  $2/15$  structure exhibits a sequence of domains of  $1/8-1/8-1/8-1/6$  structure, showing how the proliferation of domain walls leads to a structure of higher order commensurability. This suggests that the plateau sequence can be interpreted as a “devil’s staircase”, which is an infinite sequence of commensurate phases [2]. However, the NMR spectra in the intermediate phase consist of only broad lines, indicating that what is observed here is an example of “incomplete devil’s staircase”, in which the infinite sequence of high order commensurate phases with small steps are replaced by incommensurate phases [3].

### References

- [1] M. Takigawa, M. Horvatić, T. Waki, S. Krämer, C. Berthier, F. Lévy-Bertrand, I. Sheikin, H. Kageyama, Y. Ueda, and F. Mila, *Phys. Rev. Lett.* **110**, 067210 (2013).
- [2] P. Bak, *Rep. Prog. Phys.* **45**, (1982) 587.
- [3] S. Arby, *Solitons and Condensed Matter Physics*, edited by A. R. Bishop and T. Schneider (Springer-Verlag, Berlin, 1979), p. 264.

### Authors

M. Takigawa, M. Horvatić, T. Waki, S. Krämer, C. Berthier, F. Lévy-Bertrand, I. Sheikin, H. Kageyama, Y. Ueda, and F. Mila

# Hidden Multipole Order in $\text{Yb}_2\text{Pt}_2\text{Pb}$ with the Orthogonal Dimer Structure

Sakakibara Group

When a  $\text{Yb}^{3+}$  ion ( $4f^{13}$ ) is situated in a crystalline electric field of low symmetry, a Kramers doublet becomes the ground state of the  $J=7/2$  multiplet. Magnetic properties of such systems can be usually described in terms of a magnetic *dipole* moment carried by the Kramers doublet. Here we show that the tetragonal compound  $\text{Yb}_2\text{Pt}_2\text{Pb}$ , which orders antiferromagnetically at  $T_N=2.1$  K [1], exhibits a very unusual ordered state in a magnetic field, whose order parameter is likely to be a high-rank magnetic *multipole* moment [2].

The Yb lattice in  $\text{Yb}_2\text{Pt}_2\text{Pb}$  can be viewed as being composed of orthogonal dimers aligned along [110] or [1-10] directions [1]; we can define two sublattices of Yb ions: sublattice A of [110] dimers and sublattice B of [1-10] dimers. In the preceding experiment, Ochiai *et al.* [3] have shown that the Yb moment has a strong Ising anisotropy along the dimer axis. When a magnetic field  $H$  is applied parallel to [110], the antiferromagnetic moments on the sublattice B are decoupled from  $H$  because their Ising axes are perpendicular to  $H$ . Accordingly, only the moments on sublattice A respond to  $H$  and the phase diagram is given in Fig. 1a, where three different ordered phases I, II' and III exist. The magnetic structures of phases I and III are shown in Figs. 2a and 2c, respectively. In phase I, both sublattices A and B are essentially in a collinear structure. In phase III, magnetic moments on sublattice B remain in a collinear structure but those on sublattice A become paramagnetic. Ochiai *et al.* [3] pointed out that the highly anisotropic magnetic properties can be understood by assuming the ground state doublet of  $\text{Yb}^{3+}$  ion to be predominantly composed of states  $|\pm 7/2\rangle$  with the local quantization axis parallel to either [110] or [1-10].

There is another phase, phase II', in the phase diagram

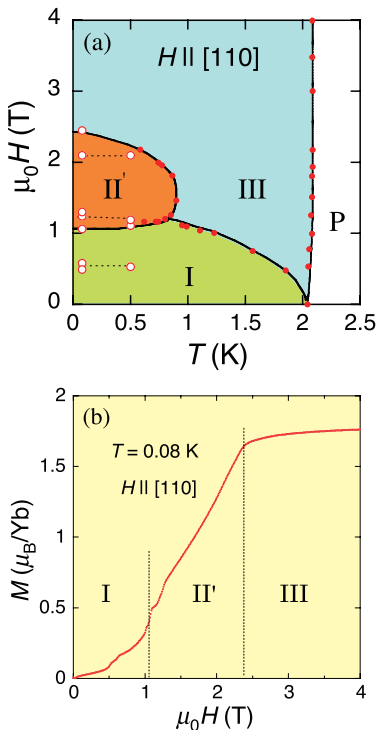


Fig. 1. (a) Magnetic phase diagram of  $\text{Yb}_2\text{Pt}_2\text{Pb}$  for  $H \parallel [110]$ . (b) Field variation of the magnetization of  $\text{Yb}_2\text{Pt}_2\text{Pb}$  for  $H \parallel [110]$  measured at 80 mK.

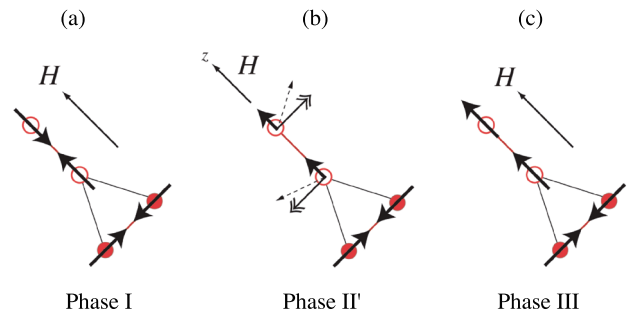


Fig. 2. Proposed magnetic structures of  $\text{Yb}_2\text{Pt}_2\text{Pb}$  for  $H \parallel [110]$ . (a) Phase I. Each Yb sublattice has a collinear structure. Thick arrows indicate the Yb magnetic moment. (b) Phase II'. Sublattice B (solid circles) remains in a collinear state, whereas sublattice A (open circles) exhibits a pseudo-spin flop. Dashed arrows denote the pseudo spins whereas double arrows indicate the multipole moments. (c) Phase III. Sublattice B remains in a collinear state, whereas sublattice A becomes paramagnetic.

[3]. The exact nature of phase II', however, has not been clear in the preceding experiments. We have examined the low temperature magnetization of  $\text{Yb}_2\text{Pt}_2\text{Pb}$  and found that the Yb magnetic moment increases almost linearly in phase II' and saturates without discontinuity; quite unexpectedly, the II'-III transition is of second order. This behavior of phase II' is apparently incompatible with the Ising anisotropy of the Yb moment. We propose that a high-rank magnetic multipole moment is the order parameter in phase II'. For simplicity, let us assume the wave functions of the Kramers doublet to be  $|\pm 7/2\rangle$ . In a pseudo-spin representation, the  $z$  component is the magnetic dipole  $J_z$ . On the other hand, the  $x$  and  $y$  components are rank-7 magnetic multipoles (*octaco-saectapoles*). It can then be shown that a pseudo-spin flop occurs in a magnetic field along the Ising axis, if an interaction between the multipole moments is sufficiently strong (Fig. 2 b) [2]. In this situation, the magnetic moment along [110] linearly increases with  $H$  and continuously saturates, as observed by experiment.

## References

- [1] M. S. Kim, M. C. Bennett, and M. C. Aronson, Phys. Rev. B **77**, 144425 (2008).
- [2] Y. Shimura, T. Sakakibara, K. Iwasawa, K. Sugiyama, and Y. Onuki, J. Phys. Soc. Jpn. **81**, 103601 (2012).
- [3] A. Ochiai, S. Matsuda, Y. Ikeda, Y. Shimizu, S. Toyoshima, H. Aoki, and K. Katoh, J. Phys. Soc. Jpn. **80**, 123705 (2011).

## Authors

Y. Shimura, T. Sakakibara, K. Iwasawa<sup>a</sup>, K. Sugiyama<sup>a</sup>, and Y. Onuki<sup>a</sup>  
<sup>a</sup>Osaka University

# Hydrogen Bond-promoted Metallic State in a Purely Organic Single-component Conductor

Mori Group

Realization of “purely organic single-component molecular metals” has been one of the long-standing open problems in chemistry, physics, and materials science. As is well known, purely organic materials are normally insulating. Recently, Mori group unveils a new type of purely organic single-component molecular conductors based on a catechol-fused ethylenedithiotetrathiafulvalene,  $\text{H}_2\text{Cat-EDT-TTF}$ , and its diselena analogue,  $\text{H}_2\text{Cat-EDT-ST}$ , which are designed and synthesized by us [1]. These conductors are the unprecedented single component systems composed of molecular units,  $\text{H}_3(\text{Cat-EDT-TTF})_2$  and  $\text{H}_3(\text{Cat-EDT-ST})_2$ ,

with the highly symmetric intra-unit hydrogen bond. Their electrical conductivity at room temperature is significantly higher than that for the previously reported purely organic single-component systems. Under the moderate physical pressure, moreover, the metallic behavior appeared in the temperature dependence of the electrical resistivity. The higher electrical conductivity observed in our systems is attributed to the hydrogen bond-promoted delocalization of charge carriers, which are generated through the partial oxidation of the H<sub>2</sub>Cat-EDT-TTF and H<sub>2</sub>Cat-EDT-ST molecules [2].

A new type of purely organic single component molecular conductors,  $\kappa$ -H<sub>3</sub>(Cat-EDT-TTF)<sub>2</sub> and  $\kappa$ -H<sub>3</sub>(Cat-EDT-ST)<sub>2</sub>, hereinafter described as  $\kappa$ -S and  $\kappa$ -Se, respectively, were obtained as black plate-like crystals by electrochemical oxidation of the corresponding donor molecules, H<sub>2</sub>Cat-EDT-TTF and H<sub>2</sub>Cat-EDT-ST, in the presence of the base, 2,2'-bipyridine. The minimal molecular unit, the H<sub>3</sub>(Cat-EDT-TTF)<sub>2</sub> composition (Fig. 1), is established by the formation of an intra-unit hydrogen bond, O..H..O, between the catechol moieties of the donor molecules, where the one hydroxyl proton is deprotonated. The oxygen–oxygen distance in the hydrogen bond, d(O..O), is 2.486(5) Å and 2.509(8) Å at room temperature, and 2.453(5) Å and 2.443(8) Å at 50 K and 30 K for  $\kappa$ -S and  $\kappa$ -Se, respectively, which are much shorter than the length of the normal O–H..O type hydrogen bond, d(O..O) 2.7 ~ 3.0 Å. Because of this strong hydrogen bonding nature, the bonded hydrogen atom is nearly located at the center between two oxygen atoms, in contrast to the asymmetric hydrogen distribution in the normal hydrogen bonds. The minimal molecular units are assembled into the purely organic single component crystal.

The electrical conductivity at room temperature is significantly high, 3.5 and 19 S cm<sup>-1</sup> for  $\kappa$ -S and  $\kappa$ -Se, respectively. These values are one or two orders of magnitude higher than the highest reported value,  $\sigma_{rt} = 10^{-1}$  S cm<sup>-1</sup>, in the purely organic single-component systems, to our best knowledge. As temperature is decreased, the electrical resistivity of these systems exponentially increases with the energy gap  $\Delta/k_B$ , of 2400 K for  $\kappa$ -S and 1200 K for  $\kappa$ -Se, respectively. The physical pressure is a good tool to change the electronic states by the modulation of the intermolecular interactions. We observed dramatic changes in the temperature variation in the electrical resistivity under pressure for  $\kappa$ -Se. Under the

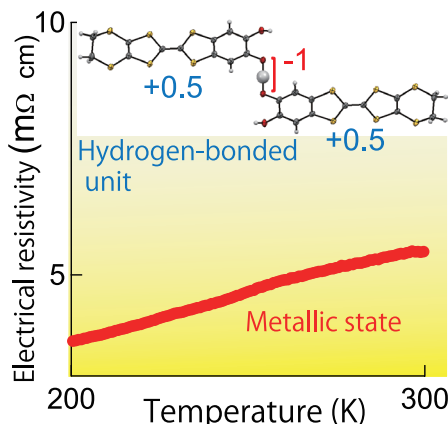


Fig. 1. Structure of the molecular unit and the metallic state in the purely organic single-component conductor. The “purely organic single-component conductor” developed by Mori’s group with the world record conductivity at room temperature (19 Scm<sup>-1</sup>) is composed of the electrically neutral and symmetric molecular units, where the charge is widely delocalized. The assembled units construct the two-dimensional conducting layers which afford the metallic state under the lowest pressure of around 1 GPa.

pressure above 1.3 GPa, the electrical resistivity monotonically decreases with reducing temperature down to around 150 K, in striking contrast with the semiconducting behavior at ambient pressure, although the resistive curve turns to increase at low temperature. Thus, the metallic states emerge with the simultaneous suppression of the semiconducting energy gap by the application of the pressure of only 1 GPa. To our knowledge, this is the lowest metallization pressure among the purely organic single-component systems.

Our system demonstrates that the symmetric hydrogen bond constructs the new type of the purely organic single-component molecular conductors which are composed of highly symmetric molecular units. Moreover, we found that the formation of the symmetric hydrogen bond promoted the intermolecular delocalization of the generated carriers, associated with the enhancement of the electrical conductivity. We believe that our new type of molecular conductors with the symmetric intra-unit hydrogen bond will realize the first purely organic single-component molecular metal at ambient pressure. A tetraselenenafulvalene (TSF)-type analogue, in which all the sulfur atoms in the TTF part of the present system are replaced with selenium atoms, is a promising candidate for the ambient-pressure metal, because the further enhanced intermolecular interactions are expected.

#### References

- [1] H. Kamo, A. Ueda, T. Isono, K. Takahashi, and H. Mori, *Tetrahedron Lett.* **53**, 4385 (2012).
- [2] T. Isono, H. Kamo, A. Ueda, K. Takahashi, A. Nakao, R. Kumai, H. Nakao, K. Kobayashi, Y. Murakami, and H. Mori, *Nature Commun.* **4**, 1344 (2013).

#### Authors

T. Isono, H. Kamo, A. Ueda, K. Takahashi<sup>a</sup>, A. Nakao<sup>b</sup>, R. Kumai<sup>c</sup>, H. Nakao<sup>c</sup>, K. Kobayashi<sup>c</sup>, Y. Murakami<sup>c</sup>, and H. Mori

<sup>a</sup>Kobe University

<sup>b</sup>Research Center for Neutron Science and Technology, CROSS

<sup>c</sup>Institute of Materials Structure Science, KEK

## Quantum Monopolar Fluctuations in the Exchange-based Spin Ice System Pr<sub>2</sub>Zr<sub>2</sub>O<sub>7</sub>

### Nakatsuji Group

Spin ice is a magnetic analogue of H<sub>2</sub>O ice that harbors dense static disorder. Dipolar interactions between classical Ising spins on pyrochlore lattice yield a frozen frustrated state with residual configurational Pauling entropy [1]. Mimicking the formation of an H<sub>3</sub>O<sup>+</sup>–OH<sup>-</sup> electric dipole in water ice, a spin flip from the spin ice manifold fractionizes into a pair of emergent magnetic monopolar quasi-particles with Coulomb attraction. In classical spin ice, monopole dynamics is diffusive –only activated thermally or by external magnetic field. The classical nature of Ising spins precludes attainment of thermal equilibrium at temperatures below the effective nearest neighbor energy scale  $J_{ff}$ . Introducing quantum fluctuations is of great interest as it enhances dynamics and might allow coherent propagation of magnetic charge (Fig. 1), much as spinons in one dimensional quantum magnets.

Here, we report the experimental observation of spin ice correlations and quantum dynamics in a new class of spin ice based on exchange interactions, Pr<sub>2</sub>Zr<sub>2</sub>O<sub>7</sub> [3]. We have succeeded in growing high quality single crystals at ISSP, which are stoichiometric to the 1-2% level. Inelastic

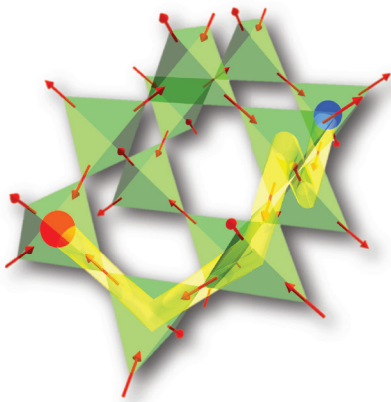


Fig. 1. Schematic illustration of magnetic monopolar quasi-particle with quantum dynamics. Red arrows denote magnetic moment. Red and Blue spheres indicate a pair of magnetic monopoles.

neutron scattering measurements revealed that the crystalline electric field (CEF) ground state of  $\text{Pr}^{3+}$  is magnetic doublet with  $\langle 111 \rangle$  Ising anisotropy, as in classical spin ice systems. AC-magnetic susceptibility and specific heat data show activated dynamics and residual entropy below 0.1 K, again similar to the behavior in classical spin ice systems. However, Curie-Weiss behavior in the temperature dependence of magnetic susceptibility for  $T < 10$  K indicated an effective moment  $\mu_{\text{eff}} = 2.5(1)\mu_B$  that is four times smaller than for dipolar spin ice  $\text{Dy}_2\text{Ti}_2\text{O}_7$  where  $\mu_{\text{eff}} = 10\mu_B$ . Correspondingly,  $\text{Pr}_2\text{Zr}_2\text{O}_7$  displays an antiferromagnetic (AFM) Weiss temperature  $\theta_{\text{CW}} = -1.4(1)$  K compared to the ferromagnetic (FM)  $\theta_{\text{CW}} \approx +0.5$  K for dipolar  $\text{Dy}_2\text{Ti}_2\text{O}_7$ .

Quasi-static spin correlations were investigated using elastic neutron scattering and the result at  $T = 0.1$  K is shown in Fig. 2(a). Sharp pinch point features near  $(111)$  and particularly  $(002)$ , bear evidence of a divergence free two-in two-out spin configuration on each tetrahedron. Indeed, the elastic  $Q$ -map resembles a classical Monte Carlo simulation for an exchange only model, which indicates dominant FM superexchange interactions in  $\text{Pr}_2\text{Zr}_2\text{O}_7$ .  $\theta_{\text{CW}}$  is however, negative and this suggests the exchange Hamiltonian includes AFM transverse terms that induce quantum dynamics. Figure 2(b) shows the  $Q$ -map of *inelastic* scattering at  $\hbar\omega = 0.25$  meV and  $T = 0.1$  K. While the overall

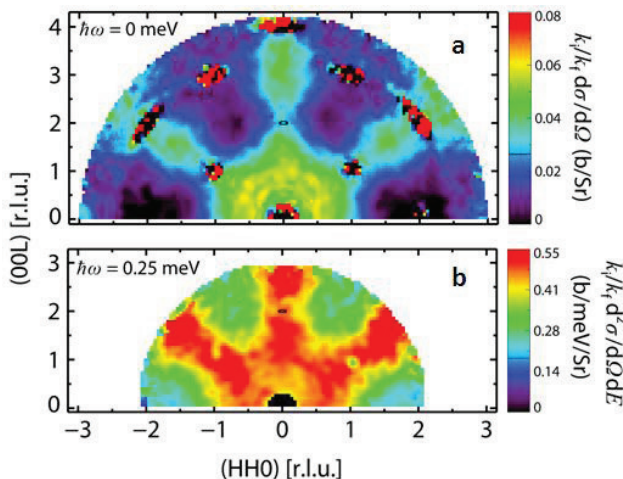


Fig. 2. Spin ice correlations and quantum dynamics in  $\text{Pr}_2\text{Zr}_2\text{O}_7$  probed through elastic and inelastic neutron scattering. (a) Elastic  $Q$ -map at 0.1 K with pinch points at  $(002)$ ,  $(111)$ , and  $(-1-11)$ . 22 K data was subtracted as a high-temperature background to cancel elastic nuclear scattering processes at Bragg peak. (b) Inelastic  $Q$ -map at  $\hbar\omega = 0.25$  meV and  $T = 0.1$  K after subtracting the corresponding data at 15 K as background [3].

pattern resembles the nominally elastic scattering (Fig. 2a), the pinch points have vanished. Excited states thus differ from the ground state by the appearance of tetrahedra that violate the ice rule or in other words by the presence of magnetic monopoles, furnishing evidence for magnetic monopolar quantum fluctuations. Such inelastic scattering accounts for  $>90\%$  of the magnetic scattering cross section at 0.1 K, showing that magnetism in  $\text{Pr}_2\text{Zr}_2\text{O}_7$  is dominated by quantum fluctuations. Our observation in  $\text{Pr}_2\text{Zr}_2\text{O}_7$  is unlike any previously documented in an insulating crystalline magnet. The interplay between monopolar quantum dynamics and itinerant electrons may play an important role in the isostructural Kondo lattice system  $\text{Pr}_2\text{Ir}_2\text{O}_7$  [4].

## References

- [1] S. T. Bramwell and M. J. P. Gingras, *Science* **294**, 1495 (2001).
- [2] C. Castelnovo, R. Moessner, and S. L. Sondhi, *Nature* **451**, 42 (2008).
- [3] K. Kimura, S. Nakatsuji, J.-J. Wen, C. Broholm, M. B. Stone, E. Nishibori, and H. Sawa, to be published in *Nature Communications* (2013).
- [4] Y. Machida, S. Nakatsuji, S. Onoda, T. Tayama, and T. Sakakibara, *Nature* **463**, 210 (2010).

## Authors

K. Kimura, S. Nakatsuji, J.-J. Wen<sup>a</sup>, C. Broholm<sup>a,b,c</sup>, M. B. Stone<sup>c</sup>, E. Nishibori<sup>d</sup>, and H. Sawa<sup>d</sup>,  
<sup>a</sup>Johns Hopkins University, USA  
<sup>b</sup>National Institute of Standards and Technology, USA  
<sup>c</sup>Oak Ridge National Laboratory, USA  
<sup>d</sup>Nagoya University

## Heavy Fermion Superconductivity in the Ferroquadrupolar State in the Quadrupolar Kondo Lattice $\text{PrTi}_2\text{Al}_{20}$

Nakatsuji Group

Orbital degree of freedom provides a various interesting phenomena such as colossal magnetoresistance, orbital ordering, and quantum spin-orbital liquid states. Although orbital degree of freedom strongly couples to spin and charge degrees of freedom in  $d$ -electron systems,  $f$ -electron systems with  $4f^2$  configuration, such as cubic Pr and U based compounds, sometimes exhibit nonmagnetic ground state with a pure orbital degree of freedom known as quadrupole moments. In analogy with magnetic Kondo lattice systems, two competing interactions, RKKY type intersite coupling and quadrupolar Kondo effect, can be induced in *quadrupolar Kondo lattice systems* due to hybridization between  $4f$  quadrupole and conduction( $c$ -) electrons, which may lead to novel quantum criticality of quadrupole order.

Recently, we revealed that  $\text{PrTr}_2\text{Al}_{20}$  ( $\text{Tr}$  = transition metal) is the first ideal quadrupolar Kondo lattice system that allows us to tune the hybridization strength and the quadrupolar ordering temperature [1]. Among them,  $\text{PrTi}_2\text{Al}_{20}$  is the best studied and established to have nonmagnetic  $\Gamma_3$  crystal electric field ground doublet with ferroquadrupolar ordering at  $T_Q = 2.0$  K [1-4] as well as strong  $c$ - $f$  hybridization [1, 5].

Here, we report the heavy fermion superconductivity at  $T_c = 0.2$  K in the ferroquadrupolar ordered state of  $\text{PrTi}_2\text{Al}_{20}$ . The temperature dependence of critical field  $B_{c2}$  and weak differential paramagnetic effect indicate type-II superconductivity. Estimated effective mass  $m^*$  from  $B_{c2}$  and Sommerfeld coefficient  $\gamma$  is  $\sim 16 m_0$ , indicating moderately enhanced  $m^*$  by hybridization. The positive  $\partial^2 B_{c2} / \partial T^2$  at  $\sim T_c$  and sensitivity of  $T_c$  to sample quality suggest the multi-gap

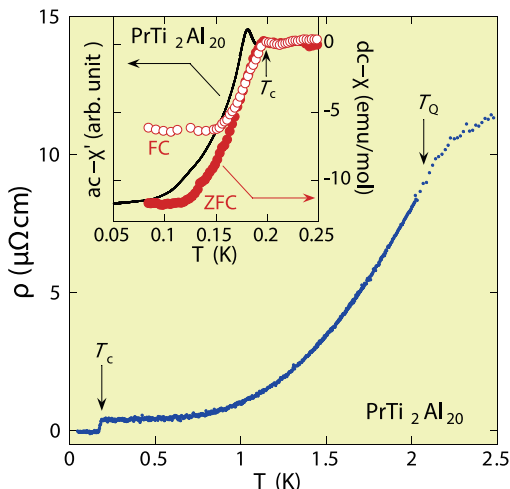


Fig. 1. Temperature dependence of the resistivity below 2.5 K in  $\text{PrTi}_2\text{Al}_{20}$  (solid circle). Arrows indicate the ferro-quadrupole transition temperature  $T_Q = 2.0$  K and superconducting transition temperature  $T_c = 0.2$  K. Inset:  $T$  dependence of the real part of the ac-susceptibility (solid line) and dc-susceptibility for zero field cooled (ZFC, solid circle) and field cooled (FC, open circle).

nature of the superconductivity. These features provide an interesting counterpart to the superconductivity at  $T_c = 50$  mK in the antiferro-quadrupole ordered state of  $\text{PrIr}_2\text{Zn}_{20}$  [7, 8], where in contrast  $4f$  electrons are well localized. More enhanced  $T_c$  and  $B_{c2}$  in  $\text{PrTi}_2\text{Al}_{20}$  should come from the mass enhancement due to the strong hybridization between  $4f$  and  $c$ -electrons.

#### References

- [1] A. Sakai and S. Nakatsuji, J. Phys. Soc. Jpn. **80**, 063701 (2011).
- [2] T. J. Sato, S. Ibuka, Y. Nambu, T. Yamazaki, A. Sakai, and S. Nakatsuji, arXiv:0301828.
- [3] T. U. Ito, W. Higemoto, K. Ninomiya, H. Luetkens, C. Baines, A. Sakai, and S. Nakatsuji, J. Phys. Soc. Jpn. **80**, 113703 (2011).
- [4] M. Koseki, Y. Nakanishi, K. Deto, G. Koseki, R. Kashiwazaki, F. Shichinomiya, M. Nakamura, M. Yoshizawa, A. Sakai, and S. Nakatsuji, J. Phys. Soc. Jpn. **80**, SA049 (2011).
- [5] M. Matsunami, M. Taguchi, A. Chainani, R. Eguchi, M. Oura, A. Sakai, S. Nakatsuji, and S. Shin, Phys. Rev. B **84**, 193101 (2011).
- [6] A. Sakai, K. Kuga, and S. Nakatsuji, J. Phys. Soc. Jpn. **81**, 083702 (2012).
- [7] T. Onimaru, K. T. Matsumoto, Y. F. Inoue, K. Umeo, Y. Saiga, Y. Matsushita, R. Tamura, K. Nishimoto, I. Ishii, T. Suzuki, and T. Takabatake, J. Phys. Soc. Jpn. **79**, 033704 (2010).
- [8] T. Onimaru, K. T. Matsumoto, Y. F. Inoue, K. Umeo, T. Sakakibara, Y. Karaki, M. Kubota, and T. Takabatake: Phys. Rev. Lett. **106**, 197201 (2011).

#### Authors

A. Sakai, K. Kuga, and S. Nakatsuji

## Evolution of $c$ - $f$ Hybridization and Two Component Hall Effect in $\beta$ -YbAlB<sub>4</sub>

### Nakatsuji Group

Several recent studies of the mixed-valence compound  $\beta$ -YbAlB<sub>4</sub> have revealed the remarkable properties which are seemingly contradictory to one another within a conventional understanding of  $f$ -electron intermetallics.  $\beta$ -YbAlB<sub>4</sub> is the first Yb-based material in which highly renormalized electronic quasiparticles (with effective masses  $> 100$  times larger than the bare electronic mass) superconduct [1, 2]. In addition,  $\beta$ -YbAlB<sub>4</sub> was found to have a quantum critical point at exactly zero magnetic field and zero pressure [3], suggesting the vanishing of an energy scale associated with

an ordered electronic state, such as magnetism. On the other hand, in apparent contradiction to these low temperature properties, the Yb  $f$ -moment in  $\beta$ -YbAlB<sub>4</sub> shows strong valence fluctuations [4] (the Yb valence is +2.75) and has a high Kondo temperature ( $T_K \sim 200 - 300$  K) [1, 3]; behaviors that usually lead to a Fermi liquid ground state with weakly renormalized quasiparticles. A study of the Hall effect sheds new light on the evolution of the electronic structure of  $\beta$ -YbAlB<sub>4</sub> and suggests how these behaviors can coexist [5].

The Hall effect measurements using high quality crystals of  $\beta$ -YbAlB<sub>4</sub> found that the Hall coefficient has strong temperature dependence and a minimum at  $T = 40$  K (see Fig. 1), that bears a close similarity to Kondo rather than mixed-valence systems. The usual interpretation of this result would put the Kondo temperature at 40 K rather than 200 - 300 K, as was measured by the longitudinal resistivity. To answer the question of how  $\beta$ -YbAlB<sub>4</sub> can appear to have two Kondo temperatures separated by almost an order of magnitude, we suggested a two component Hall effect, which was supported by the magnetic field dependence of the Hall resistivity.

As the temperature is lowered below 100 K the Hall resistivity becomes non-linear; a careful analysis showed that the field dependence can be explained by the material having two field independent Hall coefficients, the combination of which leads to a non-linear Hall resistivity. Furthermore, this analysis allowed us to show that the mobility of the material strongly increases approaching the minimum at 40 K; thus demonstrating that the minimum in the Hall coefficient is indeed due to the onset of coherent transport in a second component of the electronic transport that has just 10% of the total carrier density.

The reason that these two components have such different Kondo temperatures is suggested by the Fermi surface of  $\beta$ -YbAlB<sub>4</sub> together with a recent theoretical analysis showing that the hybridization between conduction electrons and  $f$ -moments may vanish at certain points in momentum space [6]. These nodal points lead to a large difference in hybridization strength and thereby a different Kondo temperature between the two Fermi surfaces, one of which passes close to the nodal region and the other of which is well separated.

These results therefore suggest that the emergent second component arises from the Fermi surface that lies close to the region of vanishing hybridization that may be responsible for the quantum critical and superconducting behavior observed at low temperature. This scenario is consistent with a recent

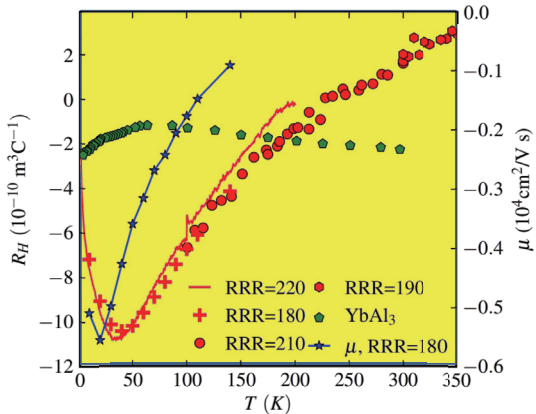


Fig. 1. The Hall coefficient ( $R_H$ ) of  $\beta$ -YbAlB<sub>4</sub> vs temperature ( $T$ ) for several different quality samples compared to a mixed valent compound YbAl<sub>3</sub> (left-hand axis).  $\beta$ -YbAlB<sub>4</sub> shows a strong temperature dependence characteristic for materials with incoherent skew-scattering from localized moments as expected when the Kondo interaction dominates. The Hall mobility  $\mu$  obtained from the two band analysis is also shown (right-hand axis).

theoretical work which provides a phenomenological model for quantum criticality in  $\beta$ -YbAlB<sub>4</sub> [6].

#### References

- [1] S. Nakatsuji, K. Kuga, Y. Machida, T. Tayama, T. Sakakibara, Y. Karaki, H. Ishimoto, S. Yonezawa, Y. Maeno, E. Pearson, G. G. Lonzarich, L. Balicas, H. Lee, and Z. Fisk, *Nature Physics* **4**, 603 (2008).
- [2] K. Kuga, Y. Karaki, Y. Matsumoto, Y. Machida, and S. Nakatsuji, *Phys. Rev. Lett.* **101**, 137004 (2008).
- [3] Y. Matsumoto, S. Nakatsuji, K. Kuga, Y. Karaki, N. Horie, Y. Shimura, T. Sakakibara, A. H. Nevidomskyy, and P. Coleman, *Science* **331**, 316 (2011).
- [4] M. Okawa, M. Matsunami, K. Ishizaka, R. Eguchi, M. Taguchi, A. Chainani, Y. Takata, M. Yabashi, K. Tamasaku, Y. Nishino, T. Ishikawa, K. Kuga, N. Horie, S. Nakatsuji, and S. Shin, *Phys. Rev. Lett.* **104**, 247201 (2010).
- [5] E. C. T. O'Farrell, Y. Matsumoto, and S. Nakatsuji, *Phys. Rev. Lett.* **109**, 176405 (2012).
- [6] A. Ramires, P. Coleman, A. H. Nevidomskyy, and A. M. Tsvelik, *Phys. Rev. Lett.* **109**, 176404 (2012).

#### Authors

E. C. T. O'Farrell, Y. Matsumoto, and S. Nakatsuji

## Quantum Compass Model Realized in Post-Perovskite Iridate CaIrO<sub>3</sub>

Ohgushi Group

There is a new trend toward exploring Mott physics in 5d transition metal oxides with a strong spin-orbit interaction. Theoretical calculations on the Hubbard model revealed that the spin-orbit interaction drives a transition from a correlated metal to an insulator [1]. This novel Mott insulating state is actually realized in a layered perovskite Sr<sub>2</sub>IrO<sub>4</sub>, including Ir<sup>4+</sup> ions with a  $(t_{2g})^5$  electronic configuration [2]. In this compound, one hole among  $t_{2g}$  manifolds takes a complex wavefunction with the spin and orbital magnetic moments of 1/3 and 2/3  $\mu_B$ , respectively, and this state is now called the  $J_{eff}=1/2$  state. The superexchange interaction across two Ir<sup>4+</sup> ions in the  $J_{eff}=1/2$  state is theoretically shown to be unique [3]. Whereas an antiferromagnetic Heisenberg interaction  $J_1 S_i \cdot S_j$  is dominant in a corner-shared IrO<sub>6</sub> bond, the magnetic interaction of the edge-shared IrO<sub>6</sub> bond becomes a highly anisotropic and ferromagnetic one,  $-J_2 S_i^z S_j^z$ , where the z direction is perpendicular to the plane expanded by the two Ir atoms and two O atoms responsible for the edge-shared bond. This interaction, which is called the quantum compass model, captures great interests since a quantum spin liquid is realized when this interaction works

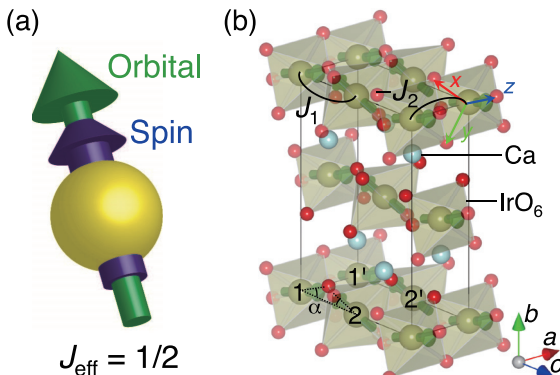


Fig. 1. (a) The schematic view of  $J_{eff}=1/2$  state. (b) Magnetic structure of the post-perovskite CaIrO<sub>3</sub>. The solid lines indicate the conventional unit cell, which is twice as large as the primitive unit cell. The magnetic interaction are also shown.

on the honeycomb lattice (Kitaev model). To test the validity of this theory, it is necessary to elucidate the magnetic structure of an Ir oxide with an edge-sharing octahedral network.

We performed resonant x-ray diffraction experiments at the  $L$  absorption edges for the post-perovskite-type compound CaIrO<sub>3</sub>, which shows a Mott insulating behavior characterized by the charge gap ~0.17 eV and undergoes a transition to a canted antiferromagnetic state at 115 K [4]. By observing the magnetic signals, we could clearly see that the magnetic structure was a striped order with an antiferromagnetic moment along the  $c$ -axis and that the wavefunction of a  $t_{2g}$  hole is strongly spin-orbit entangled, the  $J_{eff}=1/2$  state (Fig. 1). The observed spin arrangement including the weak ferromagnetic moments along the  $b$ -axis is totally consistent with the theoretical work predicting isotropic-antiferromagnetic and anisotropic-ferromagnetic superexchange interactions across the corner- and edge-sharing bonds, respectively. Our results stimulate further exploration of a novel quantum spin state in iridates.

#### References

- [1] D. Pesin and L. Balents, *Nat. Phys.* **6**, 376 (2010).
- [2] B. J. Kim, H. Ohsumi, T. Komesu, S. Sakai, T. Morita, H. Takagi, and T. Arima, *Science* **323**, 1329 (2009).
- [3] G. Jackeli and G. Khaliullin, *Phys. Rev. Lett.* **102**, 017205 (2009).
- [4] K. Ohgushi, J. Yamaura, H. Ohsumi, K. Sugimoto, S. Takeshita, A. Tokuda, H. Takagi, M. Takata, and T. Arima, *Phys. Rev. Lett.* **110**, 217212 (2013).

#### Authors

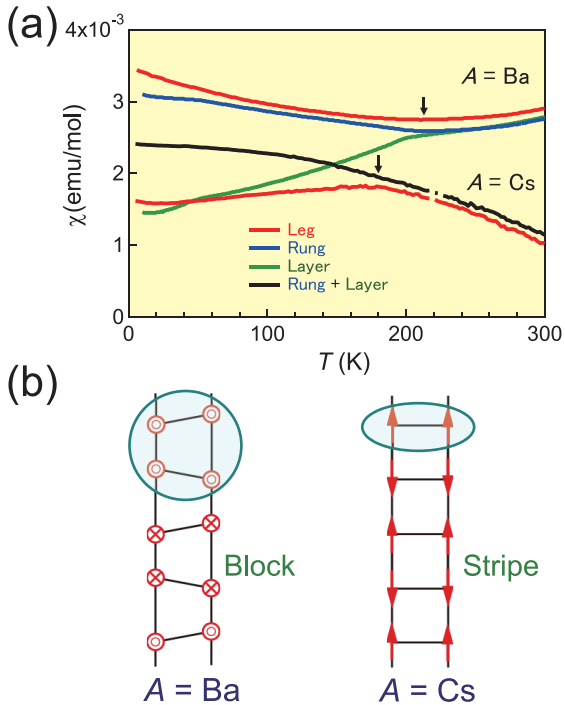
K. Ohgushi, J. Yamaura, H. Ohsumi<sup>a</sup>, K. Sugimoto<sup>b</sup>, S. Takeshita<sup>a</sup>, A. Tokuda<sup>c</sup>, H. Takagi<sup>d</sup>, M. Takata<sup>a,b</sup>, and T. Arima<sup>a,c</sup>  
<sup>a</sup>RIKEN SPring-8 Center  
<sup>b</sup>Japan Synchrotron Radiation Research Institute, SPring-8  
<sup>c</sup>Kwansei Gakuin University  
<sup>d</sup>Department of Physics, University of Tokyo  
<sup>e</sup>Department of Advanced Materials Science, University of Tokyo

## Magnetism of Fe-Based Ladder Compounds

Ohgushi, Sato, Y. Ueda, and Uwatoko Groups

Since the discovery of superconductivity at high transition temperature in LaFeAsO<sub>1-x</sub>F<sub>x</sub>, the study of Fe-based superconductors has become a main stream in condensed matter physics. The basic structural feature of Fe-based superconductors is a square lattice of Fe atoms coordinated tetrahedrally by pnictogens or chalcogens. The most common magnetic structure realized in parent materials is a stripe order, which is stabilized by Fermi surface nesting and the orbital ordering. More recently, a block order was found in A<sub>2</sub>Fe<sub>4</sub>Se<sub>5</sub> ( $A = K, Rb$ , and Cs); an important feature of this ordered phase is a large magnetic moment 3.3  $\mu_B$  as a consequence of the strong electron correlation effect [1]. To gain further insights into the mechanism and variation of these magnetic orders, investigation of Fe-based compounds with various dimensions is important, because the dimensionality strongly influences the itinerancy of electrons.

We investigated electronic properties of Fe-based chalcogenides AFe<sub>2</sub>Se<sub>3</sub> ( $A = Ba$  and Cs), in which Fe atoms form a quasi-one-dimensional ladder structure [2, 3]. Both compounds are Mott insulators due to prominence of the electron correlation effect in low-dimensional systems. The magnetic susceptibility shows anomaly corresponding to the magnetic order at 255 and 175 K for  $A = Ba$  and Cs, respectively. Interestingly, magnetic structures determined by neutron diffraction experiments are distinct in between:



## Mechanism of Enhanced Second-Harmonic Generation in Noncentrosymmetric Metal

Ohgushi, Suemoto, and Tajima Groups

Solids without spatial inversion symmetry attract great interests in the current condensed matter physics. The most common and well-studied systems without inversion symmetry are the ferroelectrics, where macroscopic polarization appears in an insulating state. Recently, conductive materials without inversion symmetry, which are known as noncentrosymmetric metals, have also attracted interest. In contrast to ferroelectrics, noncentrosymmetric metals do not exhibit macroscopic polarization due to screening by conducting electrons; instead the state is characterized by a higher-rank tensor (e.g. piezo-electric tensor). The breakdown of inversion symmetry is considered to influence the transport properties. For example, it is theoretically predicted that the inverse Faraday effect can be induced by Rashba interaction [1]. However, there have been few experimental studies [2], because noncentrosymmetric metals are rare.

We investigated electronic properties of a noncentrosymmetric metal  $\text{Pb}_2\text{Ir}_2\text{O}_6\text{O}'$ , which has the pyrochlore-type structure consisting of the  $\text{Pb}_2\text{O}'$  and  $\text{Ir}_2\text{O}_6$  building units [3]. Structural analysis revealed that the structural distortion relevant to the breakdown of the inversion symmetry is dominated by the  $\text{Pb}_2\text{O}'$  unit but is very small in the Ir-O network. Nevertheless, gigantic second-harmonic generation (SHG) signal originating from the Ir 5d electrons, which is as large as SHG signals of GaAs, was observed. First-principles electronic structure calculations reveal that the

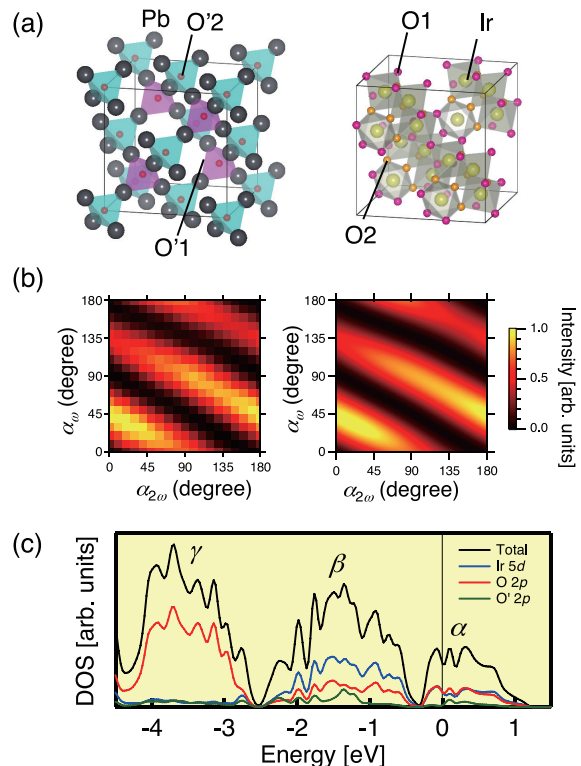


Fig. 1. (a) Crystal structure of  $\text{Pb}_2\text{Ir}_2\text{O}_6\text{O}'$ , which can be viewed as a sum of two interpenetrating units,  $\text{Pb}_2\text{O}'$  and  $\text{Ir}_2\text{O}_6$ . (b) Polarization dependence of the observed (left) and simulated (right) second-harmonic generation signals for  $\text{Pb}_2\text{Ir}_2\text{O}_6\text{O}'$ .  $\alpha_{\omega}$  and  $\alpha_{2\omega}$  stand for polarization of incident and generated beams, respectively. (c) Total and partial density of states obtained from the first-principles calculation. SHG signals originate from dipolar transitions among the bands labeled as  $\alpha$ ,  $\beta$ , and  $\gamma$ . The large hybridization of  $\text{O}' 2p$  orbitals with  $\alpha$  and  $\beta$  bands results in the observed large SHG signals.

Fig. 1. (a) Temperature ( $T$ ) dependence of the magnetic susceptibility ( $\chi$ ) at 5 T for Fe-based ladder compounds  $A\text{Fe}_2\text{Se}_3$  ( $A = \text{Ba}$  and  $\text{Cs}$ ). (b) Magnetic structures determined by neutron diffraction experiments. Brock and stripe orders are realized in  $A = \text{Ba}$  and  $\text{Cs}$ , respectively.

whereas magnetic moments of  $2.8 \mu_B$  perpendicular to the ladder plane are arranged to form a  $\text{Fe}_4$  ferromagnetic unit and each  $\text{Fe}_4$  stacks antiferromagnetically in  $A = \text{Ba}$  (block order), magnetic moments of  $1.8 \mu_B$  along the leg direction couple ferromagnetically and antiferromagnetically along the rung and leg directions, respectively, in  $A = \text{Cs}$  (stripe order). These magnetic properties are partly explained by recent Hartree-Fock calculations for the five-orbital Hubbard model [4]. Our results demonstrate that magnetism of Fe-based superconducting materials is rather complex owing to the multi-band effect and/or the electron correlation effect.

### References

- [1] P. Dai, J. Hu, and E. Dagotto, Nat. Phys. **8**, 709 (2012).
- [2] Y. Nambu, K. Ohgushi, S. Suzuki, F. Du, M. Avdeev, Y. Uwatoko, K. Munakata, H. Fukazawa, S. Chi, Y. Ueda, and T. J. Sato, Phys. Rev. B **85**, 064413 (2012).
- [3] F. Du, K. Ohgushi, Y. Nambu, T. Kawakami, M. Avdeev, Y. Hirata, Y. Watanabe, T. J. Sato, and Y. Ueda, Phys. Rev. B **85**, 214436 (2012).
- [4] Q. Luo, A. Nicholson, J. Rincón, S. Liang, J. Riera, G. Alvarez, L. Wang, W. Ku, G.D. Samolyuk, A. Moreo, and E. Dagotto, Phys. Rev. B **87**, 024404 (2013).

### Authors

K. Ohgushi, Y. Hirata, T. J. Sato, Y. Nambu, Y. Ueda, F. Du, S. Suzuki, Y. Uwatoko, K. Munakata, M. Avdeev<sup>a</sup>, T. Kawakami<sup>b</sup>, Y. Watanabe<sup>b</sup>, H. Fukazawa<sup>c</sup>, and S. Chi<sup>d</sup>

<sup>a</sup>Bragg Institute, Australian Nuclear Science and Technology Organization

<sup>b</sup>Nihon University

<sup>c</sup>Japan Atomic Energy Agency

<sup>d</sup>Oak Ridge National Laboratory

underlying mechanism for this phenomenon is the induction of the noncentrosymmetry in the Ir 5d bands by the strong hybridization with O' 2p orbitals, which are unique characteristics of Pb-containing pyrochlore-type oxides. Our results stimulate theoretical study of inversion broken iridates, where exotic quantum states such as a topological insulator and Dirac semimetal are anticipated.

#### References

- [1] V. M. Edelstein, Phys. Rev. Lett. **80**, 5766 (1998).
- [2] K. Ohgushi, J. Yamaura, M. Ichihara, Y. Kiuchi, T. Tayama, T. Sakakibara, H. Gotou, T. Yagi, and Y. Ueda, Phys. Rev. B **83**, 125103 (2011).
- [3] Y. Hirata, M. Nakajima, Y. Nomura, H. Tajima, Y. Matsushita, K. Asoh, Y. Kiuchi, A.G. Eguiluz, R. Arita, T. Suemoto, and K. Ohgushi, Phys. Rev. Lett. **110**, 187402 (2013).

#### Authors

Y. Hirata, M. Nakajima<sup>a</sup>, Y. Nomura<sup>b</sup>, H. Tajima, Y. Matsushita<sup>c</sup>, K. Asoh, Y. Kiuchi, A. G. Eguiluz<sup>d</sup>, R. Arita<sup>b</sup>, T. Suemoto, and K. Ohgushi  
<sup>a</sup>Chiba University  
<sup>b</sup>Department of Applied Physics, The University of Tokyo  
<sup>c</sup>National Institute for Materials Science  
<sup>d</sup>The University of Tennessee

---Division of Condensed Matter Theory---

## Superconductivity in a Correlated $E \otimes e$ Jahn-Teller System

Takada Group

The competition of electron-phonon (e-ph) and electron-electron (e-e) interactions in the mechanism of superconductivity is an old issue in strongly correlated systems and it has been investigated mostly in a single-orbital system, like the Hubbard-Holstein model in which the e-ph interaction enhances charge fluctuations, inducing an s-wave superconductivity in the vicinity of a charge density-wave (CDW) phase, whereas the e-e interaction suppresses such charge fluctuations but enhances spin ones, leading to a d-wave superconductivity near a spin density-wave (SDW) phase. If the effect of the e-ph interaction is about the same as that of the e-e interaction, there appears a rather complex nature of the pairing, namely, the off-site pairing (leading to either the extended s-wave or the d-wave nature, depending on the lattice structure) composed of not the bare electrons but the (phonon fully-dressed) polarons [1].

Here we add a further complication to this correlated and strongly phonon-coupled system by including the orbital degree of freedom. More specifically, we consider a two-dimensional (2D) square lattice with each site made of an  $E \otimes e$  Jahn-Teller (JT) center, namely, a site composed of doubly degenerate orbitals like the  $e_g$  orbitals in the d bands which are coupled to the doubly-degenerate JT phonons. At each center, we also consider the e-e interaction in an appropriate way to make this JT crystal as a prototype of the charge-spin-orbital complexes. Then the Hamiltonian  $H$  of this system is given by  $H=H_0+H_{e-e}+H_{e-ph}$ , where  $H_0$  is the noninteracting part composed of the electron hopping term characterized by the nearest-neighbor and next-nearest-neighbor hopping integrals,  $t$  and  $t'$ , respectively, with keeping the orbital symmetry and the degenerate-phonon term with the phonon energy  $\Omega_0$ . The orbital degree of freedom will be described by pseudospin for analogy to spin degree of freedom and the pseudospin symmetry is conserved throughout the crystal in this choice of  $H_0$ . Other terms,  $H_{e-e}$  and  $H_{e-ph}$ , consist of local-site terms written with

the intra-orbital Coulomb interaction  $U$ , the Hund's-rule coupling  $J$ , and the JT coupling  $g$ .

Due to the SU(2) symmetry in spin space and the conserved symmetry in pseudospin space, the Cooper pairing state can be specified by three quantum numbers;  $S$  the total spin of the pair,  $L$  the total pseudospin, and  $L_y$  its  $y$  component, making it possible to write the anomalous self-energy as  $\Delta_{LLy}(k)$ , where  $k$  is a combined notation of crystal momentum  $k$  and fermion Matsubara frequency  $i\omega_n=i\pi T(2n+1)$  at temperature  $T$  with an integer  $n$ . Because of the rotational symmetry around the orbital- $y$  axis,  $L_y=\pm 1$  states are degenerate and thus we treat only either  $L_y=0$  or 1 here. The group theory determines the transformation property of  $\Delta_{LLy}(k)$  in  $k$  space; it transforms in accordance with  $\Gamma$ , one of the irreducible representation of the point group  $C_{4v}$  ( $A_1$ ,  $A_2$ ,  $B_1$ ,  $B_2$ , or  $E$ ). The Pauli exclusion principle dictates that  $\Delta_{LLy}(k)$  must be antisymmetric under two-electron interchange, indicating that  $\Gamma$  must be  $E$  for  $(S,L)$  equal to either  $(0,0)$  or  $(1,1)$ ; otherwise  $\Gamma$  must be either  $A_1$ ,  $A_2$ ,  $B_1$ , or  $B_2$ . With including this transformation property in  $\Gamma$ , we can easily write down the Eliashberg equation for  $\Delta_{LLy}(k)$  at  $T=T_c$  with the pairing interaction  $V_{LLy}(q)$  containing the charge, spin, and orbital susceptibilities  $\chi_c(q)$ ,  $\chi_s(q)$  and  $\chi_o(q)$ , all of which are evaluated in the RPA with use of the irreducible susceptibility  $\chi^0(q)$ .

In Fig. 1, the phase diagram at  $T=0.02t$  is plotted in the  $U-g$  plane for the typical case of  $t'=0.125t$ ,  $U=8t$ ,  $J=t$ , and  $\Omega_0=0.10t$  at half filling. Two boundaries, denoted by  $L_I$  and  $L_{II}$ , indicates the lines where  $\chi_o(q)$ , and  $\chi_s(q)$  diverge, respectively. In the close vicinity of these boundaries, those fluctuations are enhanced strongly enough to make the system enter into various superconducting phases, each labeled by  $(\Gamma; S, L, L_y)$ . Among them, we find  $(E; 0, 0, 0)$  which is a novel chiral p-wave pairing state,  $p_x(k)\pm ip_y(k)$ , characterized by spin-singlet, orbital-singlet, and odd-parity in momentum space. This is a state very specific to the degenerate multi-orbital system and is induced by the cooperative effects of orbital and spin fluctuations that are, respectively, enhanced by e-ph and e-e interactions [2].

The conservation of the pseudospin symmetry is assumed in this study, but it is not always the case. By some tentative works, we come to know that the perturbation breaking this conservation will enhance  $T_c$  for the iron pnictides, while it reduces  $T_c$  very much for the vanadium oxides. This is an issue to be studied further in the future.

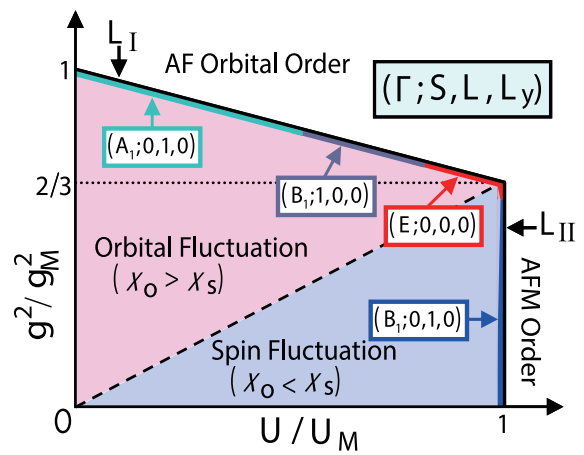


Fig. 1. Phase diagram in the  $U-g$  plane at half filling for  $U/8=J=t$ ,  $t'=0.125t$ , and  $\Omega_0=0.10t$  at  $T=0.02t$ . Units of strengths are so defined as  $U_M=32/9\chi^0(Q,0)$  and  $g_M^2/\Omega_0=1/\chi^0(Q,0)$ , where  $Q=[(\pi,\pi)]$  is the momentum maximizing both  $\chi_o(q,0)$  and  $\chi_s(q,0)$ .

## References

- [1] Y. Takada, J. Phys. Soc. Jpn. **65**, 1544 (1996).
- [2] C. Hori, H. Maebashi, and Y. Takada, J. Supercond. Nov. Magn. **25**, 1369 (2012).

## Authors

C. Hori, H. Maebashi, and Y. Takada

## Dimensional Crossover in Layered *f*-Electron Superlattices

Oshikawa Group

Dimensionality plays a crucial role in condensed matter physics, especially in systems with strong interactions. Layered structures provide an opportunity to control the dimensionality and to observe effects of reduced dimensionality and crossover behavior between two and three dimensions. In particular, recent successful fabrications of the layered superlattices of CeIn<sub>3</sub>/LaIn<sub>3</sub> [1] and CeCoIn<sub>5</sub>/YbCoIn<sub>5</sub> [2] have opened new possibilities for investigating such phenomena in *f*-electron systems. In these systems, the *f*-electrons are present only in the Ce layers, which are 2-dimensional. These systems exhibit antiferromagnetic or superconducting long-range order in regions of the phase diagram, which implies a dimensional crossover to 3 dimensions. These observations also give rise to an even more fundamental question on the dimensionality of the heavy electron states, before formation of any order. Existing theories on these systems have been based on the assumption that the *f*-electrons, separated by the spacer layers, are almost decoupled, which results in essentially 2-dimensional heavy electron states.

We reexamined [3] the heavy electron states in the layered *f*-electron superlattices, based on the inhomogeneous dynamical mean field theory combined with numerical renormalization group as an impurity solver. We show that the spectral function exhibits formation of heavy electrons in the entire system below a temperature scale  $T_0$ . On the other hand, in terms of transport, two different coherence temperatures  $T_x$  and  $T_z$  are identified in the in-plane- and the out-of-plane-resistivity, respectively. Remarkably, we find  $T_z < T_x \sim T_0$  due to scatterings between different reduced Brillouin zones. The existence of these two distinct energy scales implies a crossover in the dimensionality of the heavy

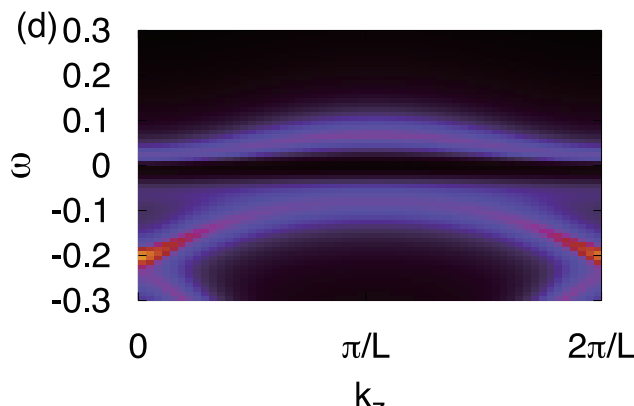


Fig. 1. Electron spectral function in a layered *f*-electron superlattice as a function of the momentum component  $k_z$  perpendicular to the layers, at a low temperature with fixed in-plane components  $k_x, k_y$ . The dispersion along the  $z$ -axis implies formation of heavy electron states extending over the entire system, coupled through the spacer layers which do not have *f*-electrons.

electrons between two and three dimensions as temperature or layer geometry is tuned. This dimensional crossover would be responsible for the characteristic behaviors in the magnetic and superconducting properties observed in the experiments.

## References

- [1] H. Shishido, T. Shibauchi, K. Yasu, T. Kato, H. Kontani, T. Terashima, and Y. Matsuda, Science **327**, 980 (2010).
- [2] Y. Mizukami, *et al.*, Nat. Phys. **7**, 849 (2012); S. K. Goh, *et al.*, Phys. Rev. Lett. **109**, 157006 (2012).
- [3] Y. Tada, R. Peters, and M. Oshikawa, preprint (2013).

## Authors

Y. Tada, R. Peters<sup>a</sup>, and M. Oshikawa

<sup>a</sup>Kyoto University

## Superconductivity near a Transverse Saturation Field in URhGe

Tsunetsugu Group

Ferromagnetic superconductivity in uranium-based heavy-fermion compounds has attracted much attention in condensed matter physics in the last decade. UGe<sub>2</sub>, URhGe, UIr, and UCoGe show unconventional superconductivity within their ferromagnetic phases. Nonunitary superconductivity is believed to appear in these compounds and their pairing mechanism and symmetry as well as novel self-induced vortex states are central issues to be clarified in the modern theory of unconventional superconductors. Among these ferromagnetic superconductors, two isomorphic compounds, UTGe ( $T = \text{Rh, Co}$ ), exhibit superconductivity at ambient pressure within their ferromagnetic state and have a similar Ising-type anisotropy of magnetization. Spontaneous moment appears parallel to the  $c$  axis, and its magnetization curve exhibits meta-magnetic behavior with a notable mass enhancement when magnetic field  $\mathbf{H}$  is applied to the  $b$  direction. This meta-magnetism is particularly prominent in URhGe and the moment gradually tilts with field and finally aligns parallel to  $\mathbf{H}$  at  $h_s = 12$  T. Superconductivity appears below the transition temperature  $T_{sc} = 0.24$  K for  $\mathbf{H} = \mathbf{0}$ , and  $T_{sc}$  decreases with  $\mathbf{H}$  and disappears at 2 T for  $\mathbf{H} \parallel b$ . Interestingly, superconductivity reappears above 8 T and shows the highest  $T_{sc} = 0.42$  K at 12 T. The mechanism of this novel re-entrant superconductivity has not been fully clarified until now.

In this project, we propose a mechanism of the re-entrant superconductivity and analyze magnetic-field dependence of the spin-components of the superconducting order parameter. We point out that there are soft magnetic excitations near the transverse-saturation field  $h_s$  in these anisotropic systems as similar to the case in the transverse Ising system, and clarify how these soft excitations couple with itinerant electrons. We develop a weak-coupling theory of p-wave superconductivity in the presence of both ferromagnetism and magnetic field.

Figure 1 shows our result of temperature-magnetic field ( $h_x$ ) phase diagram. Here,  $h_x$  represents the magnetic field strength in  $b$  direction. The superconducting transition temperatures for the polar state ( $T_{sc}^x$ ) and that for the ABM state ( $T_{sc}^z$ ) are depicted. The amplitude of the gap  $\Delta$  in the magnetic excitations and the tilting angle  $\theta$  are also plotted in Fig. 1. In the low-field region,  $T_{sc}$  is suppressed as  $h_x$  increases and disappears due to orbital pair-breaking effects. In the high-field region near the saturation field  $h_s$ ,

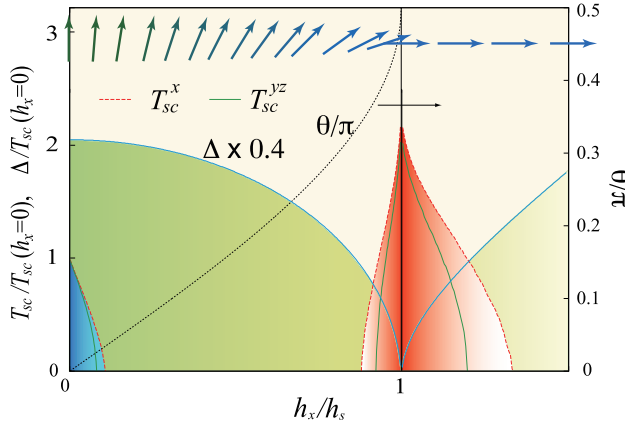


Fig. 1. Temperature - magnetic field ( $h_x$ ) phase diagram. P-wave superconducting transition temperature for the polar state ( $T_{sc}^x$ ) and that for the ABM state ( $T_{sc}^{yz}$ ) are shown. The amplitude of the gap  $\Delta$  in the magnetic excitations and the tilting angle  $\theta$  of the ferromagnetic moments measured from the zero-field direction are also plotted. The transition temperatures are scaled by the value at  $h_x = 0$ , where  $T_{sc}^x = T_{sc}^{yz}$ . Arrows depict the change in direction of the ferromagnetic moment with magnetic field.

another superconducting phase appears and the transition temperature reaches a maximum at the saturation field and then is suppressed. As we commented above, the magnetic-excitation gap  $\Delta$  gradually decreases with approaching  $h_s$  and vanishes at  $h_s$ . At the saturation field, the energy dispersion of the magnetic excitations is linear in the momentum, which represents the system is at a critical point. Above  $h_s$ , the excitations acquire a finite gap again and the gap increases linearly in  $h_x$  at higher fields.

The strong enhancement in the transition temperature near the saturation field arises from quantum critical fluctuations there and the nature of the fluctuations strongly restricts symmetry of the Cooper pairs. Analyzing the fluctuations near the saturation field, we find that the exchanging magnetic fluctuations between two electrons (Cooper pair) leads to electron spin flipping. Combining the fact that the Zeeman effects favor the equal-spin pairs and now the spin is not conserved in the presence of the transverse field, the dominant superconducting order parameter is a linear combination of the two equal-spin pairing states. This state is completely different from that in the low field superconducting state, where only one of the equal-spin pairing states is realized due to the strong Zeeman effects by the ferromagnetism.

The phase diagram we have determined is qualitatively consistent with that in URhGe. Experimental determination of the superconducting order parameters near the saturation field is an interesting subject in the future progress for understanding the ferromagnetic superconductivity in URhGe. For more quantitative analyses, it is important to include longitudinal spin fluctuations, which have been observed in UCoGe. Such longitudinal fluctuations would play an important role for realizing meta-magnetic behaviors near the saturation field in URhGe.

#### Reference

[1] K. Hattori and H. Tsunetsugu, Phys. Rev. B 87, 064501 (2013).

#### Authors

K. Hattori and H. Tsunetsugu

## Development of Novel First-Principles Methods for Material Research

### Sugino Group

The first-principles computational methods have enabled, with increasing precision, to elucidate properties of matters starting from the microscopic quantum principles only. This was strongly driven by the development of supercomputers and the computational theory, *e.g.*, density functional theory (DFT) and Hartree-Fock. Those theories have already matured and great many efforts are now made toward the development of post-DFT theory and the extension of the frontier of DFT applications. Towards the goal, our group has made three important steps. The first one is the development of a post-DFT scheme, which is based on the tensor compression technology to compactly represent the many-body wave function. A graduate course student, Wataru Uemura, showed that the canonical decomposition algorithm indeed greatly facilitates handling of the wave function that appears in the full configuration interaction (CI) scheme. The developed scheme [1], called symmetric tensor decomposition (STD), is considered make the full CI a method of choice for the molecular and some of the condensed matter researches.

The use of the tensor compression technology itself is not new, but was established as a powerful method to handle one-dimensional spin and Hubbard systems some years ago. The STD-CI, however, applied the technology to the conventional molecular orbital theory and, with algorithmic improvements, has greatly reduced the memory and the computational time requirement. It is also anticipated that, by combining STD-CI with the tensor network theory developed in the spin physics, extended systems will become the target of study. Despite the improved efficiency, the computational time is yet prohibitively large even for medium-sized molecules, but is expected to become tractable by the next-generation supercomputers because of its excellent parallelizability.

Towards the study of electronically excited states, the research associate, Yoshifumi Noguchi parallelized the code for many-body perturbation theory, or a post-DFT theory, for the K-computer and the ISSP supercomputer. The excited-states of a molecule containing up 100 atoms, such as fullerenes, has become the target of study [2]. By combining with the DFT-based schemes [3], we are advancing the method for excited-state research.

Our group regards the solid-liquid interface is the important application field of DFT. We are particularly interested

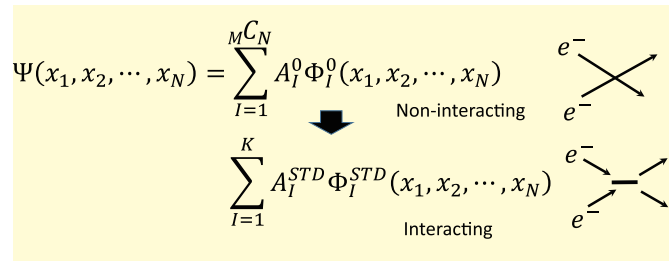


Fig.1: An electronic wave function has been traditionally expanded by non-interacting terms ( $\Phi_I^0$ ) in the configuration interaction (above). The series can be greatly shortened when expanded by interacting ones (below). The tensor decomposition provides a practical way to construct a maximally compact series, allowing thereby accurate numerical handling of the wave function. Using this novel algorithm, or STD-CI, we are developing a code for electronic structure calculation to be used in the next-generation supercomputer.

in explaining the energy conversion mechanism as typified by the fuel-cell reactions. The major object of the fuel-cell science is to relate the bias potential with the electrocatalytic reactions, which has been hampered by the difficulty of applying the bias potential to the interface. Important algorithmic improvements were made by the collaboration with research group in AIST to keep applying the bias potential throughout the DFT-based molecular dynamic simulation [4]. Those methods are now used for the large-scale simulations on K-computer.

#### References

- [1] W. Uemura and O. Sugino, Phys. Rev. Lett. **109**, 253001 (2012).
- [2] Y. Noguchi, O. Sugino *et al.*, J. Chem. Phys. **137**, 24306 (2012).
- [3] T. Tsukagoshi *et al.*, Phys. Rev. B **87**, 35421 (2012); Phys. Rev. A **86**, 64501 (2012).
- [4] N. Bonnet *et al.*, Phys. Rev. Lett. **109**, 266101 (2012).

#### Authors

O. Sugino, Y. Noguchi, N. Bonnet, T. Tsukagoshi, and W. Uemura

## Relaxor Behavior and Morphotropic Phase Boundary in a Simple Model

### Kato Group

Ferroelectric relaxors made from perovskite oxides ( $\text{ABO}_3$ ) have attracted much interest because of their characteristic dielectric properties suitable for application. The common feature of perovskite-type relaxors is intrinsic randomness due to compositional disorder. It is well known that structural phase transition induced by change in composition plays a special role for obtaining excellent dielectric properties; the region near this phase transition is called the morphotropic phase boundary (MPB).

The origin of large dielectric response at the MPB was discussed within the Landau-Ginzburg-Devonshire (LGD) theory. The LGD theory is, however, not satisfactory to describe the whole properties of relaxors since it treats only spatially-averaged quantities. In particular, important information on spatial profiles of electric polarization such as domain structure and spatial inhomogeneity due to compositional disorder cannot be discussed by the LGD theory.

In order to understand physics near the MPB, we have performed large-scale Monte Carlo simulation [1] to a simplified dipole model on a square lattice given as

$$\mathcal{H} = \sum_{i < j} \left[ \frac{\mu_i \cdot \mu_j}{r_{ij}^3} - 3 \frac{(\mu_i \cdot r_{ij})(\mu_j \cdot r_{ij})}{r_{ij}^5} \right].$$

Here,  $\mu_i$  is a three-dimensional vector representing an electric polarization caused by the ionic displacement at site  $i$ , and  $r_{ij}$  is a displacement vector from site  $i$  to  $j$ . In order to represent intrinsic compositional randomness at B-site in perovskite oxides, we divide the square lattice into two sub-lattices, A and B as shown in the inset of Fig. 1(a), and assume that magnitude of the A-site dipole moments is fixed as unity ( $\mu_A = 1$ ), whereas that of the B-site dipole moments has spatial distribution. The magnitude of the B-site moment is chosen randomly as  $\mu_B = \max(0.8-0.1n, 0)$ , where  $n$  is an integer-valued random variable following the Poisson distribution  $P(n) = \lambda^n \exp(-\lambda)/n!$ . We have performed Monte Carlo calculation by using efficient O( $N$ ) algorithm optimized for long-range interaction [2].

In Fig. 1(a), we show real part of calculated dielectric susceptibilities as a function of the temperature  $T$ . The

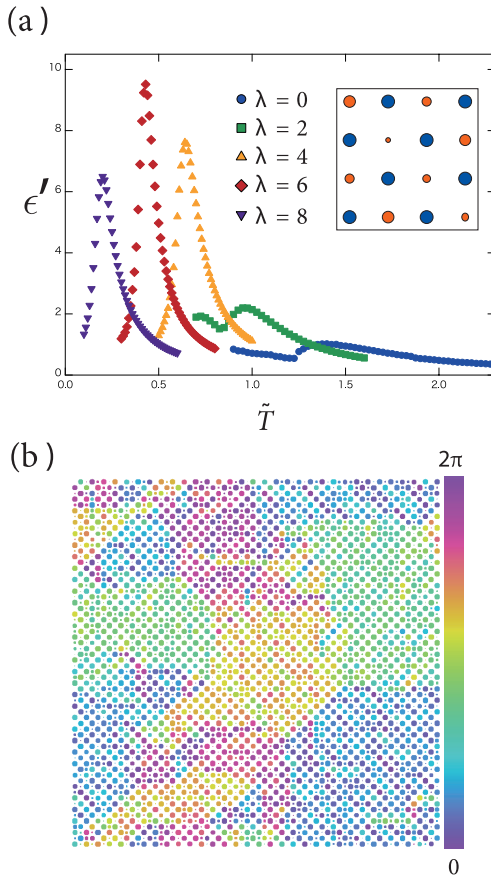


Fig. 1. (a) Plot of real part of dielectric susceptibilities per site. Data are horizontally shifted for each value of  $\lambda$ . (Inset) Blue and red circles indicate A- and B-sublattice on a square lattice. (b) A snapshot of dipole configurations for  $\lambda=6$ . Sizes of radii represent sizes of projected dipole moments, and colors of circles indicate directions of dipole moments.

peak of the dielectric susceptibility is well suppressed for small  $\lambda$ , whereas it rapidly grows with increasing  $\lambda$ . The maximum value becomes largest at an optimum value  $\lambda=5-6$ , and is reduced for larger value of  $\lambda$ . These features well resemble the behavior of the dielectric response near MPB in perovskite oxides, identifying  $\lambda=5-6$  to be the MPB.

To examine mechanism of emerging of the maximum, a snapshot at  $\lambda=6$  is shown in Fig. 1(b). We observe meso-scale ferroelectric domain, whose size becomes significantly large near  $\lambda=5-6$ . This remarkable enhancement of correlation length for ferroelectric ordering, indicated from the snapshot, is due to phase competition. For small  $\lambda$ , anti-ferroelectric phase is stabilized at low temperatures, whereas relaxor ferroelectric phase is realized for large  $\lambda$ . Direction of polarization is diagonal in the former phase, and is along neighboring sites in the latter phase. As a result, the easy-axis potential is mixture of the ones of these two phases near the MPB ( $\lambda=5-6$ ). The resulting mixed potential forms the dimple at the bottom of a wine bottle, and it makes dipoles easy to rotate. This result indicates that *local* polarization rotation under suppressed anisotropy makes domain wall *flexible* to external field, leading to huge dielectric response.

In summary, we proposed a simple dipole model, and executed Monte Carlo simulations to it. We showed that there appears a boundary ferroelectric phase between two phases, and that it has large ferroelectric domains with flexible walls. Our result near the MPB can be related to recent experiments by neutron scattering [3] and transmission electron microscopy [4].

## References

- [1] Y. Tomita and T. Kato, J. Phys. Soc. Jpn. **82**, 063002 (2013).
- [2] K. Fukui and S. Todo, J. Comp. Phys. **228**, 2629 (2009).
- [3] M. Matsuura, K. Hirota, P. M. Gehring, Z.-G. Ye, W. Chen, and G. Shirane, Phys. Rev. B **74**, 144107 (2006).
- [4] K. Kurushima and S. Mori, Materials Science and Engineering **18**, 092015 (2011).

## Authors

Y. Tomita<sup>a</sup> and T. Kato  
<sup>a</sup>Shibaura Institute of Technology

---Division of Nanoscale Science---

## Corbino Thermopower of Quantum Hall Systems

Iye Group

Thermopower is known to be a sensitive probe to investigate properties of electron systems, owing to its direct access to the energy derivative of the density of states (DOS) and to the entropy of the systems. It has been predicted [1, 2] that the radial thermopower  $S_{rr}$  measured in the Corbino geometry (Fig. 1b) exhibits behaviors qualitatively different from the longitudinal thermopower  $S_{xx}$  measured in the Hall-bar geometry in the quantum Hall (QH) systems. Notably, in the QH plateau regions where the longitudinal conductivity  $\sigma_{xx}=\sigma_{rr}$  vanishes,  $S_{xx}$  also vanishes, whereas  $S_{rr}$  is expected to take large values changing sign at the center of the QH plateau. The measurement of  $S_{rr}$  thus provides us with a unique opportunity to probe the entropy of the system in the QH plateau regions [2]. The measurement of thermopower in the QH systems, however, has predominantly been performed on the Hall-bar geometry. In the present study, we make measurements of the diffusion thermopower  $S_{rr}$  in the Corbino geometry [3].

Thermopower generally contains contributions from two distinct mechanisms: diffusion and phonon drag. In the QH systems embedded in GaAs/AlGaAs wafers, it is well known that the latter contribution outweighs the former by orders of magnitude, if the temperature gradient is introduced by an external heater. The high sensitivity to the DOS and entropy, however, is expected only for the former. In order to measure the diffusion contribution selectively, we employ microwave-heating technique [4] (Fig. 1a) in the present study; microwaves injected into the coplanar wave guide (CPW) placed on the surface of the wafer capacitively couple with the two-dimensional electron gas (2DEG) beneath the slots of the CPW and locally heats the electrons. The lattice tempera-

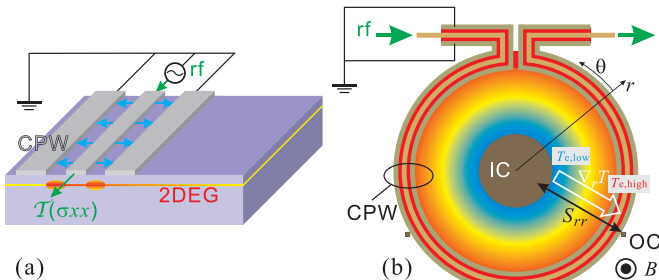


Fig. 1. Schematic diagrams of (a) coplanar wave guide (CPW) used in the microwave-heating technique and (b) Corbino device to measure diffusion thermopower  $S_{rr}$ . IC: inner contact. OC: outer contact. The microwaves (rf) propagating through the CPW placed on the surface are partially absorbed by the two-dimensional electron gas (2DEG) underlying the slot of the CPW and heats the electrons. In the Corbino device, electrons near the outer periphery of the disk are heated by the CPW, generating the concentric temperature gradient toward IC.

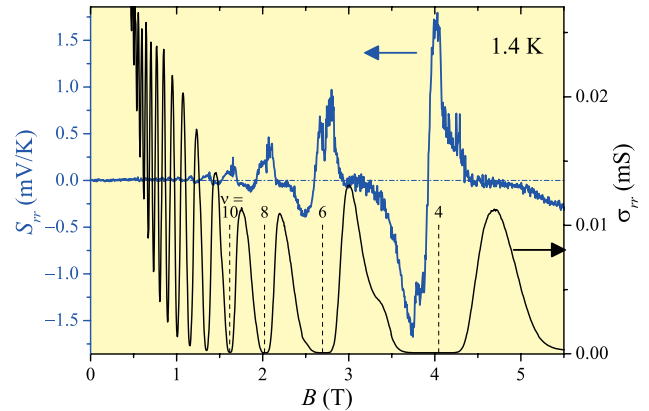


Fig. 2. Thermopower  $S_{rr}$  (left axis) and the conductivity  $\sigma_{rr}$  (right axis) measured in the Corbino device. Vertical dashed lines indicate the positions of the center of the QH plateau (exact even integer fillings  $v$ ).

ture remains intact, eliminating the phonon-drag contribution. As depicted in Fig. 1b, we install CPW along the outer periphery of a Corbino disk, which introduces radial temperature gradient toward the center electrode, leading to the radial thermopower  $S_{rr}$ .

The measured  $S_{rr}$  is plotted in Fig. 2 along with  $\sigma_{rr}$  obtained in the same Corbino device. As can be seen in the figure,  $S_{rr}$  takes large values ( $\sim \pm 1$  meV/K) in the regions where  $\sigma_{rr} = 0$ , alternating the sign at exact even integer fillings marked by vertical dashed lines, in accordance with the theoretical prediction mentioned above. Noting that  $S_{rr}$  represents entropy per carrier [2], large values of  $|S_{rr}|$  can be understood as reflecting the fact that only small numbers of thermally activated carriers are available in the QH plateau regions. The positive (negative) sign of  $S_{rr}$  indicates that the carriers are hole-like (electron-like) for the fillings  $v$  just below (above) integer values.

## References

- [1] H. van Zalinge, R. W. van der Heijden, and J. H. Wolter, Phys. Rev. B **67**, 165311 (2003).
- [2] Y. Barlas and K. Yang, Phys. Rev. B **85**, 195107 (2012).
- [3] S. Kobayakawa, A. Endo, and Y. Iye, J. Phys. Soc. Jpn. **82**, 053702 (2013).
- [4] A. Endo, T. Kajioka, and Y. Iye, J. Phys. Soc. Jpn. **82**, 054710 (2013).

## Authors

S. Kobayakawa, A. Endo, and Y. Iye

## Switching of Andreev Current with Spin-Hall Effect

Katsumoto Group

Two-dimensional electron gas (2DEG) in InAs quantum well has been often adopted as a material for middle layers in Superconductor-Normal conductor-Superconductor (SNS) sandwiches due to its low Schottky barrier to metals. At the same time it is well-known that the spin-orbit interaction (SOI) is generally strong in such materials with narrow band gaps and InAs 2DEG actually shows spin-interference phenomena due to strong Rashba-type SOI. The spin Hall effect originates from the SOI draws apart a spin up-down pair of electrons to form a Cooper pair, thus is supposed to work against the Andreev reflection, and to affect the SNS transport or the Andreev bound states (ABSs) formed in the normal layer.

Here we report suppression of electric current enhanced by Andreev reflection with transverse current flow, which breaks the time-reversal symmetry in two-dimensional system (2DES) of InAs. The inset of Fig.1 schematically shows the sample structure, in which a 200nm wide InAs 2DES stripe is sandwiched by two Nb electrodes. The sample was cooled down to 0.5K. During the electric measurement, we kept the crossing point of Nb and InAs 2DES at the ground level. In order for that, we formed circuits for sweeping the potentials of the four terminals assuming Ohmic contact resistances.

At zero magnetic field and with no transverse current, the differential conductance oscillates with the source-drain voltage  $V_{sd}$  making a large peak structure at the origin. The characteristic lineshape can be interpreted with assuming the formation of ABSs as follows. The zero-bias peak reflects the resonance between the two Fermi levels of superconducting electrodes via the virtual tunneling through ABSs while the two side peaks are direct resonances between one of the superconductors and an ABS. Because the mean free path of InAs 2DES exceeds the width of the 2DES strip, the transport between the two Nb electrodes should be ballistic, that is, ABSs should be formed.

In Fig.1(a) we show the response to the magnetic field, in which the structure is squeezed to the origin and disappears at 0.75T. This behavior manifests that the structure is superconductivity origin and we can explain it with considering some kind of interference effect. Because the additional phase due to the voltage accumulates for Andreev type (electron-hole) shuttling, the Aharonov-Bohm (AB) phase should shift the positions of ABSs. Figure 1(b) shows

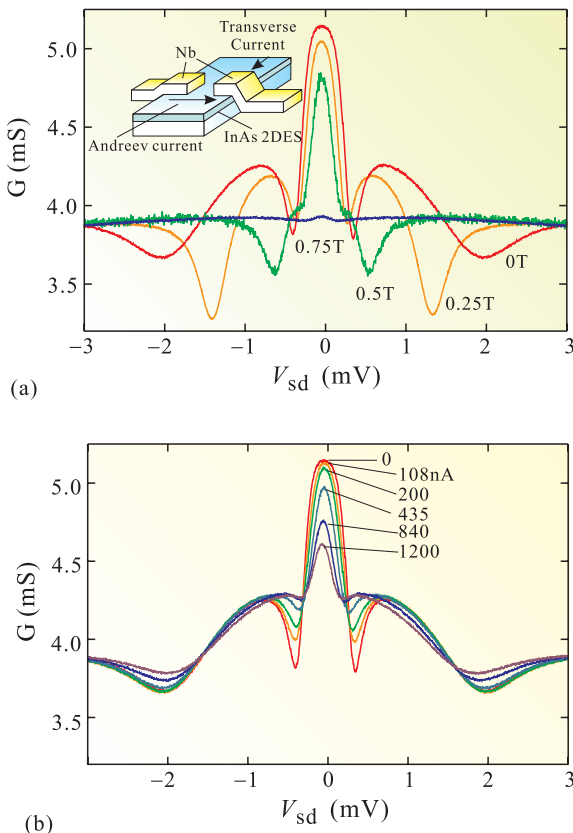


Fig. 1. (a) Differential conductance of Nb-InAs-Nb SNS junction at 0.5K as a function of the source-drain bias voltage. The parameter is the external magnetic field perpendicular to the sample. The inset shows schematic view of the sample. (b) The same measurements as those in (a) under zero magnetic field with transverse currents through the InAs strip from zero to 1.2 $\mu$ A.

the differential conductance ( $G$ ) again as a function of  $V_{sd}$  with the transverse currents through the InAs 2DES strip from 108 nA to 1.2  $\mu$ A. The transverse current also strongly diminishes the  $G$ - $V_{sd}$  structure. The difference between the response to the magnetic field and that to the transverse current is apparent. This suggests that the latter comes not from the orbital effect and that the spin-Hall effect induced by the transverse current reduces the formation of ABSs.

#### Reference

[1] Y. Takahashi, Y. Hashimoto, Y. Iye, and S. Katsumoto, J. Cryst. Growth, published online: <http://www.sciencedirect.com/science/article/pii/S0022024813000705>.

#### Authors

S. Katsumoto, T. Nakamura, and Y. Hashimoto

## A Novel Method to Verify Spin Diffusion Length

### Otani and Kato Groups

Spin relaxation and spin dephasing are the central issues in fields of quantum information and spintronics as they determine how far an electron can transfer spin information, i.e., the spin diffusion length. The spin diffusion length is thus an essential parameter in terms of application in future spintronics devices. However, there is no well-established method for obtaining this length; values reported so far differ greatly depending on the experimental method employed, the number of variables involved in the definition of the spin diffusion length and so on. Since the spin diffusion length determines the spin Hall angle, which is one of the most important physical quantities in spintronics, it is of great importance to evaluate this length correctly.

In a conventional method, a lateral spin valve structure where a weak spin-orbit (SO) material such as Cu is bridged by two ferromagnets is used to determine the spin diffusion length. On the other hand, this conventional method cannot be applied to a strong SO material such as Pt, since the spin diffusion length is in general of the order of nanometers. One of the ways to obtain such a short spin diffusion length is to use the spin absorption technique as shown in Fig. 1(a) [1]. However, there was a big debate about how to evaluate the spin diffusion length of a strong SO material [2] because there are several parameters that determine the spin diffusion length, which hinders straightforward evaluation.

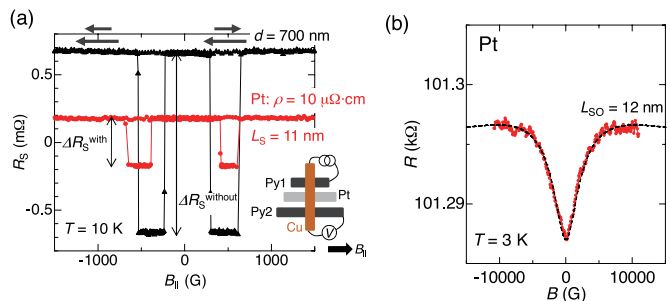


Fig. 1. (a) Nonlocal spin valve (NLSV) signal with a 20 nm thick Pt wire ( $\Delta R_S^{with}$ ) in between two Permalloy (Py) wires. As a reference signal, we also plot the NLSV signal without the Pt wire ( $\Delta R_S^{without}$ ). The magnetic field is applied parallel to the Py wires. From the ratio of  $\Delta R_S^{with}/\Delta R_S^{without}$ , the spin diffusion length of Pt can be evaluated ( $L_S = 11 \pm 2$  nm). A pair of arrows on the top indicates the magnetizations of Py1 and Py2. The inset shows the schematic of our lateral spin valve device. (b) WAL curve of a 20 nm thick Pt wire measured at  $T = 3$  K. In this case, the magnetic field is applied perpendicular to the plane. The broken line is the best fit of Hikami-Larkin-Nagaoka formula. From the fitting, the SO length of Pt can be obtained ( $L_{SO} = 12 \pm 3$  nm).

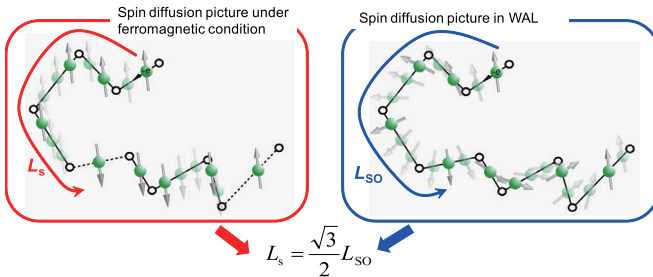


Fig. 2. Spin diffusion lengths measured with ferromagnets ( $L_s$ ; left) and obtained from WAL measurement ( $L_{so}$ ; right). The relation of the two length scales ( $L_s = \sqrt{3}/2 L_{so}$ ) has been experimentally verified.

Otani group in collaboration with Kato group have discovered a new way to evaluate the spin diffusion length [1]. In the new method, the spin diffusion length can be evaluated just by measuring very precisely the resistance of a SO material (see Fig. 1(b)). In metals, electrons are weakly localized at temperatures approaching absolute zero. When there is a finite SO interaction, the weak localization changes into weak antilocalization (WAL) and the magnetoresistance strongly depends on the SO interaction. In the present work, we focused on this dependency and obtained the spin diffusion lengths of several materials such as Cu, Ag and Pt. The values obtained with the new method are quantitatively consistent with those from the conventional methods. Since the new method reduces the number of variables involved in determining spin diffusion length, a more accurate value can be calculated. In addition, it has been shown theoretically that the spin diffusion length in a localized state and under ferromagnetic conditions varies slightly (by a factor of  $\sqrt{3}/2$ ). We have experimentally verified for the first time the relationship between the spin diffusion length in a localized state and under ferromagnetic conditions (see Fig. 2). Thanks to these results, a vigorous debate on the spin diffusion length can be concluded and this new method will play an important role in the fields of quantum information and spintronics.

#### Reference

- [1] Y. Niimi, D. H. Wei, H. Idzuchi, T. Wakamura, T. Kato, and Y. Otani, Phys. Rev. Lett. **110**, 016805 (2013).
- [2] L. Liu, R. A. Buhrman, and D. C. Ralph, arXiv:1111.3702.

#### Authors

- Y. Niimi, D. H. Wei, H. Idzuchi, T. Wakamura, T. Kato, and Y. Otani

## Bias-Dependent Atomic STM Images and Electronic Structure at Au-Adsorbed Ge(111) Surface

Komori Group

The Au-adsorbed Ge(111) surface has two surface metallic bands with hexagonal Fermi surfaces [1]. One band is electron-like and the other is hole-like. The former band is anisotropically split and spin-polarized owing to strong spin-orbit interaction at the surface. These features have been studied by angle-resolved photoemission spectroscopy (ARPES). Figure 1(a) shows the ARPES intensity map along  $\Gamma_0 - M - \Gamma_1$  line for the surface with 0.9 ML of Au on average. The observed electronic states including the surface bands ( $S_1$ ,  $S_2$  and  $S_5$ ) are qualitatively consistent with the bands calculated for an optimized conjugate honeycomb-

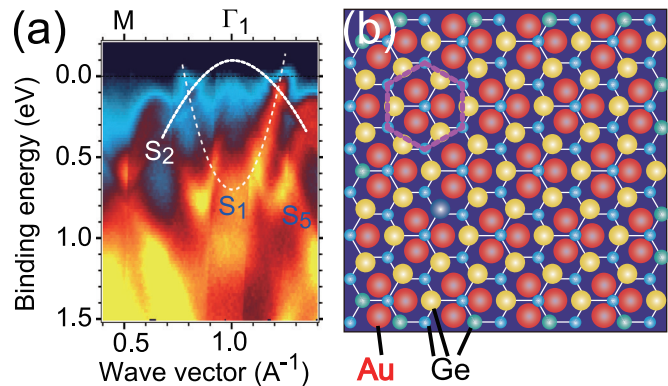


Fig. 1. (a) ARPES intensity map showing the band structure of the Au-adsorbed the Ge(111) surface. Three surface bands  $S_1$ ,  $S_2$  and  $S_5$  are seen, and white dashed lines are guides to the eye for the  $S_1$  and  $S_2$  bands. (b) Schematic top-view CHTC model for the Au-adsorbed Ge(111) surface. The white hexagonal lattice indicates the subsurface bilayer Ge lattice, the small blue balls the lower Ge atoms of the bilayer, small green the upper Ge atoms of the bilayer, yellow the surface Ge atoms, and red the surface Au atoms. Three adjacent Au atoms make an Au trimer, which is imaged as a single protrusion in Fig. 2(a). Centers of three adjacent Ge atoms are imaged as protrusions in Fig. 2(b), and make a honeycomb pattern, which is indicated as the magenta hexagon.

chained-trimer (CHCT) structure model shown in Fig. 1(b) [2]. However, there have been two discrepancies between the experiments and theories; the STM image at low bias voltage ( $V_{sb}$ ) and the bottom energy of the  $S_1$  band. In the present study, we clarify how these are solved by considering the surface electronic structure and the doping by triangular nanoclusters observed on the surface.

Figure 2 shows bias-dependent atomic STM images. The images were observed at 80 K for the surface with 1.2 ML of Au atoms on average. The STM image for  $V_{sb} = 2.0$  V (Fig. 1(a)) shows a triangle lattice pattern with a triangular nanocluster. For  $V_{sb} = 0.1$  V (Fig. 1(b)), a honeycomb pattern appeared on the same surface area, and the position of the triangular nanocluster was imaged as a dented area. The triangle lattice is consistent with the arrangement of the Au trimers on the surface in the CHCT model shown in Fig.

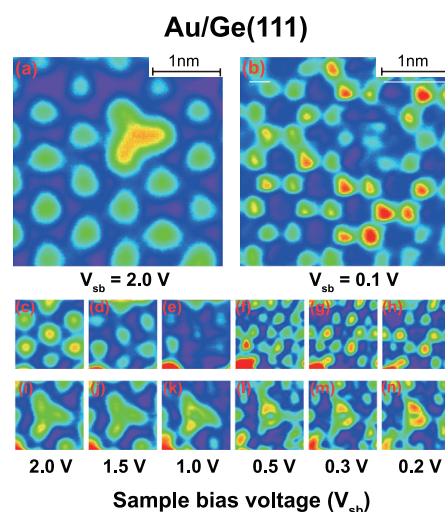


Fig. 2. STM images of the Au-adsorbed Ge(001) surface showing sample-bias-voltage ( $V_{sb}$ ) dependence. Triangle lattice pattern in (a) is attributed to the arrangement of the surface Au trimers. (See Fig. 1(b)). In (b), atomic protrusions arrange in a honeycomb pattern. The same area is imaged in (a) and (b). A triangular nanocluster is seen as a protrusion in (a) while it is imaged as a dented area in (b). The precise bias dependence of the lattice pattern and the triangular nanocluster is shown in (c-h) and (i-n). Both the triangle and honeycomb patterns coexist for  $V_{sb} = 0.5$  V as in (f). The triangular nanocluster becomes thin with decreasing  $V_{sb}$ .

1(b) whereas the honeycomb pattern could not be attributed to any arrangement of the surface Au and Ge atoms in the model. Bias-dependent STM images shown in Figs. 2(c-h), and 2(i-n) indicate gradual change of the lattice pattern and the triangular nanocluster, respectively.

It was theoretically shown that the surface Au trimers of the CHCT model make the electron-like ( $S_1$ ) band. The hole-like ( $S_2$ ) band, on the other hand, originates from the surface and subsurface Ge atoms. The energy maximum of the  $S_2$  band is 0.1 eV above Fermi energy. Consequently, the local density of states around the surface Ge atoms can be high at the top energy of the  $S_2$  band. This causes a honeycomb lattice pattern of the protrusions due to the surface Ge atoms in the STM images as observed for  $V_{sb} < 0.3$  V. The bottom of the  $S_1$  band decreases with increasing the surface density of the triangular nanocluster. It plays a role of the dopant selective to the  $S_1$  band although its atomic structure is unknown [3].

#### References

- [1] K. Nakatsuji *et. al.*, Phys. Rev. B **80**, 081406 (2009).
- [2] K. Nakatsuji *et. al.*, Phys. Rev. B **84**, 035436 (2011).
- [3] K. Nakatsuji *et. al.*, J. Phys. Condens. Matter **25**, 045007 (2013).

#### Authors

K. Nakatsuji, Y. Motomura, R. Nikura, and F. Komori

## Development of Versatile Nanoscale Potentiometry for Visualizing Distribution of Electrical Resistance

Hasegawa Group

Scanning tunneling microscopy (STM) has been utilized for imaging atomic structure of surfaces. Combined with a function of tunneling spectroscopy, the probe microscopy can also visualize spatial distribution of various properties in nanoscale; superconductivity has been detected and visualized through the observation of the superconducting gap. A spin-polarized probe tip picks up signals of local magnetization, and inelastic tunneling provides the energy of spin flipping and transition between spin states of atomic and nanosize systems. Here, we introduce another unique function of STM; mapping of electrical potential and resistance in nanometer-scale spatial resolution.

The method called scanning tunneling potentiometry enables us to observe spatial distribution of the potential of a sample surface under current flow across the sample, as well as its topographic STM image. Under current flow, which is 1 ~ 2 mA in the present case, the potential or the Fermi level changes locally at the places where electrical resistance there. Figure 1 shows an example of the topographic and potential images taken simultaneously on a 2-mm-wide and 2-nm-thick Au thin film. As shown in the topograph, Au grains whose size is 10 to 30 nm are randomly distributed. The potential image, however, clearly reveals steps in the potential, which provide direct evidence of significant resistance there. The sites of the drops exactly correspond to boundaries between the Au grains, as proved by a comparison of the two images. Not all domain boundaries, however, induce the potential drop, although the boundaries that induce the potential drops do not show any structural differences discernible in the STM image from those that do not induce the drops. We confirmed that the

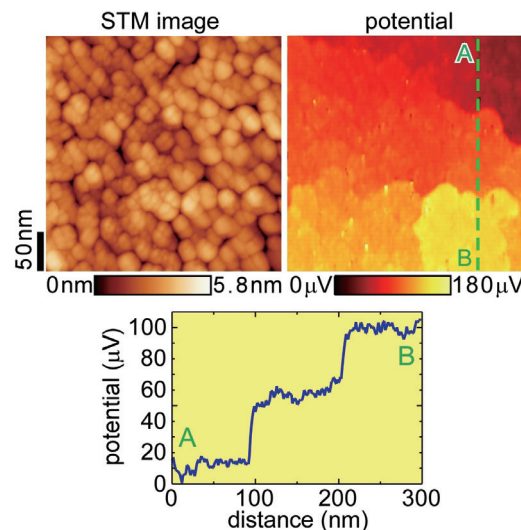


Fig. 1. STM image of a 2-nm-thick Au thin film and its potential mapping taken simultaneously under current flow (1~2 mA) from the bottom to the top of the images. A cross-sectional plot of the potential indicates that potential drops, which correspond to electrical resistance, occurs at grain boundaries and that the potential can be measured with a resolution of  $\sim 5 \mu\text{V}$ .

observed drops are really due to the electrical potential by taking the images under the reversed current flow across the sample; the direction of the potential drops is also reversed with the reversed current. The reversed potential image also indicates that the sites and magnitude of the potential drops do not change significantly in the both directions of the current flow.

The magnitude of the potential drops can be estimated as  $\sim 40 \mu\text{V}$  from the cross-sectional plot shown in Fig. 1(c). The plot also indicates that the noise level of the potential is  $\sim 5 \mu\text{V}$  even at room temperature. The resolution is quite high compared that of other STM-related potential measurement methods, such as Kelvin probe force microscopy, with which we detected interatomic charge transfer [1], and the method of measuring energy levels of electronic states that was used for visualizing the Friedel oscillation [2]. The reason of the high resolution is because of the zero-balance method used in the potential measurement; the potential is measured from the voltage applied on the sample to make the tunneling current zero.

One drawback is that the method can only be applied to metallic samples; in the case of semiconducting samples, the tunneling current is zero within the band gap and therefore the bias voltage that makes the tunneling current zero cannot be determined with high energy sensitivity. In this work, we have developed a new method with which one can take a potential mapping on semiconducting samples [3], which will obviously extend versatility of this technique.

We are applying the method to study potential profiles on surface conductive layers, which are the ultimate two-dimensional electron systems. Superconductivity even on one-monolayer-metal-induced reconstructed surfaces was reported. Our study will reveal roles of various structural defects on the (super-) conductance in real space. By using a spin-polarized tip, one can also detect spin current since the dispersionless current is caused by the potential difference between the two spin directions. We expect that various spin relaxation processes will be identified in real space and attributed to local structures using this method.

## References

- [1] T. Eguchi, *et al.*, Phys. Rev. Lett. **93**, 266102 (2004).
- [2] M. Ono, *et al.*, Phys. Rev. Lett. **96**, 016801 (2006).
- [3] M. Hamada and Y. Hasegawa, Jpn. J. Appl. Phys. **51**, 125202 (2012).

## Authors

M. Hamada and Y. Hasegawa

## Oxide Photocatalysts

Lippmaa Group

Perovskite-type titanates have been proposed as potentially efficient photocatalytic energy conversion materials that can absorb visible sunlight and directly transfer the formed photocarriers to liquid water, thereby generating hydrogen gas. Despite the potential for efficient, cheap, and sustainable energy conversion, photocatalytic materials have so far not reached practical solar light collection efficiencies. The main reason appears to be the high recombination rate of generated photocarriers, which means that the energy of the sunlight is mostly spent on generating heat, rather than splitting water. The purpose of this work was to determine the electronic structure of Rh-doped SrTiO<sub>3</sub>, which is known to be a moderately efficient hydrogen-evolution photocatalyst.

For efficient transfer of photoelectrons from a bulk photocatalyst to water, it is necessary to have a semiconductor with a conduction band located well above the reduction potential of water, while the band gap should be close to 2 eV for the best energy harvesting efficiency. Pure SrTiO<sub>3</sub> is a wide-gap semiconductor that satisfies the conduction band alignment requirement with water, but it is transparent for visible light and only absorbs sunlight in the ultraviolet part of the spectrum, above the band gap energy of 3.2 eV. Rhodium doping of the SrTiO<sub>3</sub> host semiconductor appears to be quite special, in that it creates deep impurity levels either around the mid-gap region of SrTiO<sub>3</sub> or close to the top of the valence band without affecting the location of the conduction band edge. Electrochemical measurements under visible light show an apparent *p*-type photocathode behavior, which is quite unusual for typically *n*-type SrTiO<sub>3</sub>. In this work, we have used a combination of x-ray photoelectron spectroscopy (XPS) at Photon Factory beamline 13A and x-ray absorption (XAS) and emission (XES) spectroscopy at the undulator beamline BL07LSU in SPring-8.

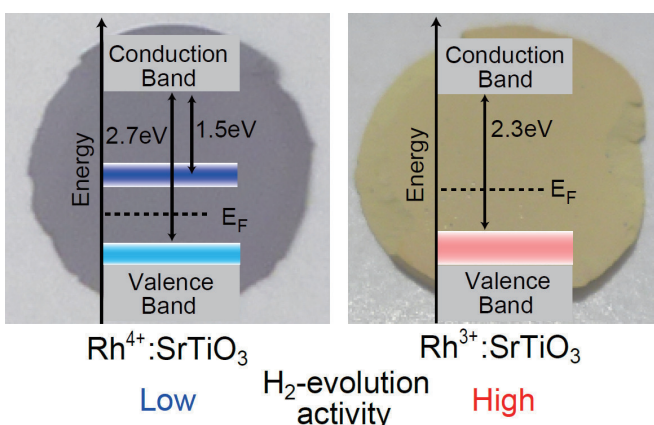


Fig. 1. Photographs of Rh<sup>4+</sup>:SrTiO<sub>3</sub> and Rh<sup>3+</sup>:SrTiO<sub>3</sub> pellets showing the different colors and the Rh in-gap state locations relative to the valence and conduction band edges of SrTiO<sub>3</sub>. The yellow Rh<sup>3+</sup>:SrTiO<sub>3</sub> is photocatalytically more efficient due to the lack of a mid-gap recombination state.

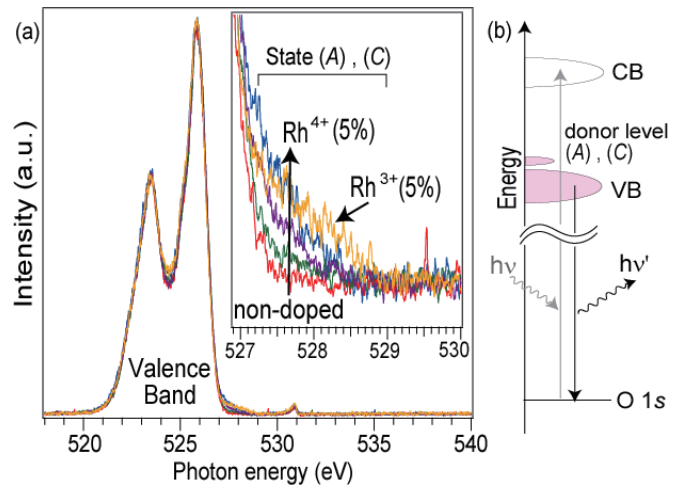


Fig. 2. (a) X-ray emission spectra of various Rh-doped SrTiO<sub>3</sub> samples showing the presence of an occupied Rh state close to the top of the valence band of SrTiO<sub>3</sub>. (b) Illustration of the XES process and the location of the Rh donor levels just above the SrTiO<sub>3</sub> valence band edge.

The XPS experiments were used to investigate the violet-to-yellow color change reaction that occurs when Rh:SrTiO<sub>3</sub> is reduced, typically during the initial induction period of an electrochemical reaction. SrTiO<sub>3</sub> thin films with several different Rh doping levels were grown at various temperatures and ambient oxygen pressures. The Rh 3d XPS profile analysis showed that the color shift is caused by a change in the Rh impurity valence, with Rh<sup>4+</sup>:SrTiO<sub>3</sub> being violet and Rh<sup>3+</sup>:SrTiO<sub>3</sub> yellow [1]. Significant variations were also observed in the Rh content at the catalyst surface due to evaporative loss of Rh at high crystal growth temperatures.

A more detailed analysis of the in-gap energy levels was undertaken by XAS and XES analysis of powder samples. The XAS analysis, which probes unoccupied states, was used to show that a mid-gap unoccupied state appears only in samples containing the Rh<sup>4+</sup> valence state, as illustrated in Fig. 1. Reduced Rh<sup>3+</sup>:SrTiO<sub>3</sub> powders did not show a mid-gap state. Both Rh valence states lead to the appearance of an occupied impurity level close to the top of the valence band, as shown by XES spectra in Fig. 2. In addition to an increase of spectral weight with Rh doping just above the valence band top, a shift was observed in the locations of the Rh<sup>4+</sup> and Rh<sup>3+</sup> impurity levels. A conclusion of the analysis was that the Rh<sup>3+</sup>:SrTiO<sub>3</sub> material shows higher photocatalytic activity due to the lack of a mid-gap unoccupied energy level that would lead to rapid photocarrier recombination. However, the photogenerated charge collection efficiency is limited by the lack of strong hybridization between the deep Rh levels and the O<sub>2p</sub> character valence band of SrTiO<sub>3</sub>.

## References

- [1] S. Kawasaki, K. Nakatsuji, J. Yoshinobu, F. Komori, R. Takahashi, M. Lippmaa, K. Mase, and A. Kudo, Appl. Phys. Lett. **101**, 033910 (2012).
- [2] S. Kawasaki, K. Akagi, K. Nakatsuji, S. Yamamoto, I. Matsuda, Y. Harada, J. Yoshinobu, F. Komori, R. Takahashi, M. Lippmaa, C. Sakai, H. Niwa, M. Oshima, K. Iwashina, and A. Kudo, J. Phys. Chem. C **116**, 24445 (2012).

## Authors:

S. Kawasaki, K. Nakatsuji, S. Yamamoto, I. Matsuda, Y. Harada, J. Yoshinobu, F. Komori, R. Takahashi, M. Lippmaa, K. Akagi<sup>a</sup>, C. Sakai<sup>b</sup>, H. Niwa<sup>b</sup>, M. Oshima<sup>b</sup>, K. Mase<sup>c</sup>, K. Iwashina<sup>d</sup>, and A. Kudo<sup>d</sup>.

<sup>a</sup>Tohoku University

<sup>b</sup>Department of Applied Chemistry, University of Tokyo

<sup>c</sup>High Energy Accelerator Research Organization

<sup>d</sup>Tokyo University of Science

# Pressure-Induced Heavy Fermion Superconductivity in the Nonmagnetic Quadrupolar System $\text{PrTi}_2\text{Al}_{20}$

Uwatoko and Nakatsuji Groups

Unconventional superconductivity (SC) with a variety of exotic characters such as anisotropic superconducting gap, large critical field and effective mass, reentrant SC, FFLO SC, etc. has attracted much attention in condensed matter physics. Since most of these unconventional superconductors have been found near a magnetic quantum critical point (QCP), where the magnetic ordering temperature is suppressed to zero due to the Kondo effect, the interesting question is what would happen near the QCP of orbital order. Although, there have been some theoretical suggestions that orbital fluctuations play an important role in iron based superconductors, it is hard to study experimentally because orbital degree of freedom is strongly coupled with spin and charge degrees of freedom in  $d$ -electron compounds. In contrast, pure orbital degree of freedom sometimes appears as a quadrupole moment in  $f$ -electron compounds such as nonmagnetic  $\Gamma_3$  state in cubic Pr or U based compounds

The cubic  $\Gamma_3$  compound  $\text{PrTi}_2\text{Al}_{20}$  has demonstrated the interplay of a ferroquadrupole order at  $T_Q = 2 \text{ K}$  and Kondo effect through the strong  $c-f$  hybridization [1]. Furthermore, it exhibits SC at  $T_{\text{SC}} = 0.2 \text{ K}$  with the associated enhanced effective mass  $\sim 16 m_0$  [2]. Here we report the discovery of a pressure-induced heavy fermion superconductivity in a nonmagnetic orbital ordering system  $\text{PrTi}_2\text{Al}_{20}$ . In particular, we found that the transition temperature and the effective mass associated with the superconductivity are dramatically enhanced to more than  $100 m_0$  as the system approaches the putative quantum critical point of the orbital order [3].

Figure 1(a) shows the temperature dependence of the magnetic resistivity  $\rho_{\text{mag}}$  measured under various pressures. At high temperatures, the  $T_{\text{max}}$  due to the magnetic Kondo

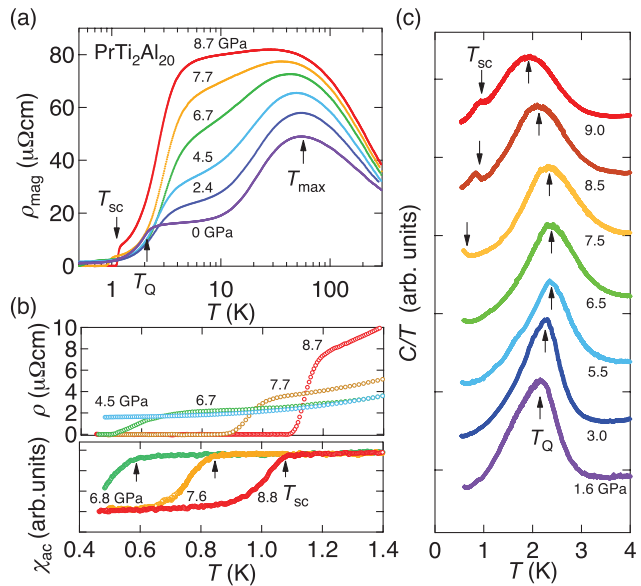


Fig. 1. (a) Magnetic part of the resistivity,  $\rho_{\text{mag}}$ , versus the logarithm of the temperature under various pressures. Here,  $\rho_{\text{mag}}$  is obtained by subtracting the resistivity of  $\text{LaTi}_2\text{Al}_{20}$  obtained under ambient pressure from that of  $\text{PrTi}_2\text{Al}_{20}$ . (b) Temperature dependence of the resistivity and the ac magnetic susceptibility at low temperatures. A large diamagnetic signal due to the SC transition is observed at a lower temperature, which corresponds to nearly 60% superconducting shielding, estimated by comparing to the diamagnetic signal of lead with almost the same size as the sample of  $\text{PrTi}_2\text{Al}_{20}$ . (c) Temperature dependence of the ac specific heat divided by temperature for different pressures. The curves are shifted vertically for clarity.

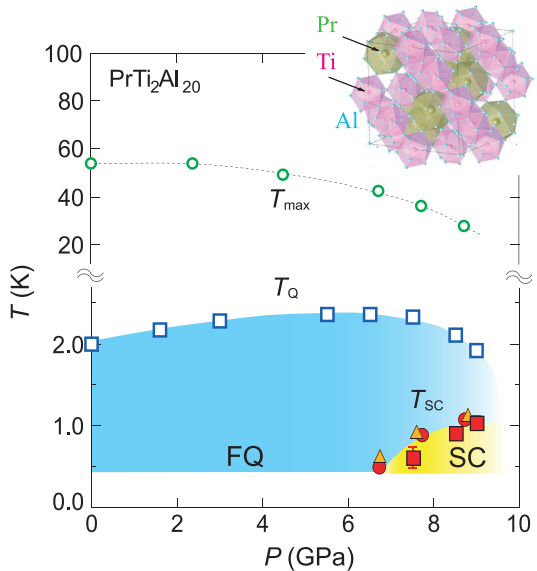


Fig. 2. Open circles and squares represent the position of  $T_{\text{max}}$  determined from the maximum in the temperature dependence of the resistivity and the ferroquadrupole ordering temperature  $T_Q$ , respectively. The SC transition temperatures  $T_{\text{SC}}$  are deduced from the temperature dependence of the resistivity (closed circles), the ac magnetic susceptibility (closed triangles), and the ac specific heat (closed squares), respectively. The FQ phase is indicated by a blue shaded region. The SC phase is indicated by a yellow shaded region. The inset shows the cubic crystal structure of  $\text{PrTi}_2\text{Al}_{20}$ . Cages made by  $\text{PrAl}_{16}$  and  $\text{TiAl}_{12}$  are indicated in green (larger cages) and purple (smaller cages), respectively.

effect using the excited magnetic CEF levels decreases with pressure, suggesting that pressure slightly reduces the CEF splitting. At lower temperatures, the quadrupole ordering temperature  $T_Q = 2 \text{ K}$  at ambient pressure can be traced as a sharp resistivity drop up to  $P = 4.5 \text{ GPa}$  and shows a slight increase with pressure. Surprisingly, above  $6.7 \text{ GPa}$ , another anomaly was observed at lower temperatures. The resistivity shows an abrupt drop to zero at  $0.7 \text{ K}$  at  $6.7 \text{ GPa}$ , indicating the onset of superconductivity. With further increasing pressure, the resistivity drop becomes sharper, and temperature of zero resistance increases up to  $1.1 \text{ K}$  at  $P = 8.7 \text{ GPa}$ . The observation of a large diamagnetic response in the ac magnetic susceptibility at almost the same temperature as the onset of the zero resistance state indicates that pressure-induced superconductivity is of bulk origin (Fig. 1(b)). To further elucidate the interplay between the superconductivity and ferroquadrupole order, we measured the specific heat under pressure (Fig. 1(c)). At  $1.6 \text{ GPa}$ , the specific heat divided by temperature  $C/T$  shows a peak due to the quadrupole ordering at  $T_Q \sim 2 \text{ K}$ . With increasing the pressure,  $T_Q$  monotonically goes up to  $P = 5.5 \text{ GPa}$ , however, further increase of the pressure starts broadening and shifting the transition to a lower temperature and instead induces a well-defined subsequent anomaly on cooling associated with the superconducting transition. The superconducting anomaly appears at the temperature in full agreement with those found in the resistivity and ac magnetic susceptibility measurements, providing further evidence for the bulk superconductivity. Pressure-induced evolution of ferroquadrupolar and superconducting phases of  $\text{PrTi}_2\text{Al}_{20}$  is summarized in the temperature-pressure phase diagram (Fig. 2). After peaking at  $P = 6 \text{ GPa}$ , the ferroquadrupole ordering temperature becomes suppressed with significant broadening, indicating the presence of the associated QCP.

At  $8.7 \text{ GPa}$ , a critical magnetic field  $B_{\text{c}2}$  is estimated to be more than  $3 \text{ T}$ , which is the highest value among Pr-based heavy fermion superconductors and similar to the case found in the Ce-based heavy fermion superconductors. Our results

suggest a generic phase diagram hosting unconventional superconductivity on the border of orbital order, paving a new path for further research on novel quantum criticality and superconductivity due to orbital fluctuations.

#### References

- [1] A. Sakai and S. Nakatsuji, J. Phys. Soc. Jpn. **80**, 063701 (2011).
- [2] A. Sakai, K. Kuga, and S. Nakatsuji, J. Phys. Soc. Jpn. **81**, 083702 (2012).
- [3] K. Matsubayashi, T. Tanaka, A. Sakai, S. Nakatsuji, Y. Kubo, and Y. Uwatoko, Phys. Rev. Lett. **109**, 187004 (2012).

#### Authors

K. Matsubayashi, A. Sakai, S. Nakatsuji, Y. Uwatoko, T. Tanaka<sup>a</sup>, and Y. Kubo<sup>a</sup>  
<sup>a</sup>Nihon University

## Surface Magnetotransport in Quantum Hall Ferromagnetic Phase in the Organic Dirac Fermion System

Osada Group

In the 2D massless Dirac fermion systems with charge neutrality, the  $v=0$  quantum Hall (QH) state appears at the high-field quantum limit, resulting from the breaking of four-fold (spin and valley) degeneracy of the  $n=0$  Landau level. Two kinds of  $v=0$  QH states appear depending on the ratio of spin splitting and valley splitting: One is the spin-unpolarized QH insulating phase, and the other is the spin-polarized QH ferromagnetic phase accompanied by the metallic edge state consisting of a pair of  $n=0$  QH edge states with opposite spin and chirality (helical edge state). The high-field ground state is one of the key issues of the physics of the Dirac fermion system. In undoped graphene, it has been believed that the high-field ground state is the QH insulator.

On the other hand, the Q2D Dirac fermion system, in which 2D massless Dirac layers stack with weak interlayer coupling, is realized in a layered organic conductor  $\alpha$ -(BEDT-TTF)<sub>2</sub>I<sub>3</sub> under pressures  $P>1.5$ GPa. We found the experimental evidences that the high-field ground state is the QH ferromagnetic phase (Fig.1(a)) in  $\alpha$ -(BEDT-TTF)<sub>2</sub>I<sub>3</sub>, in contrast to graphene. In  $\alpha$ -(BEDT-TTF)<sub>2</sub>I<sub>3</sub>, the interlayer

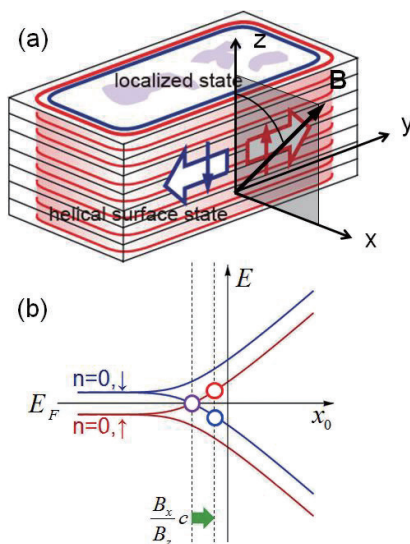


Fig. 1. (a) Helical edge state surrounding the  $v=0$  QH ferromagnet. (b) Edge state dispersion around the layer edge. Interlayer tunneling causes the shift of  $x_0$ .

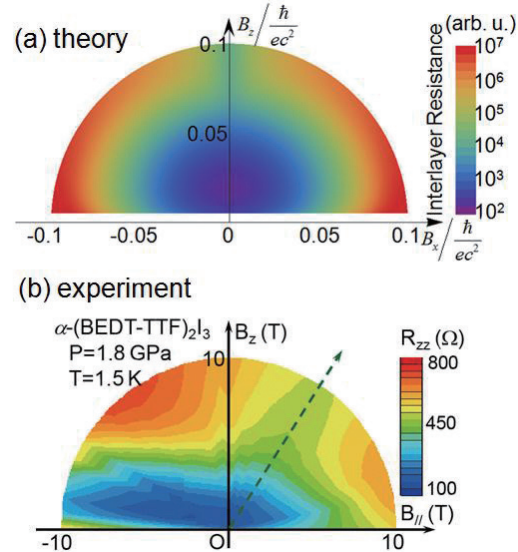


Fig. 2. Interlayer resistance as a function of strength and orientation of magnetic fields. (a) calculation. (b) experiment in  $\alpha$ -(BEDT-TTF)<sub>2</sub>I<sub>3</sub>.

magnetoresistance shows anomalous saturation at high fields. The saturation resistance is scaled not by the sectional area of sample crystals but by sample perimeter. These experimental facts strongly suggest the interlayer surface transport due to the helical edge state on side surfaces of crystals. The existence of the helical edge state directly means the QH ferromagnet.

We have considered the mechanism of interlayer surface transport due to helical edge state. Since the helical edge state is not topologically protected, transport along the helical edge channel must be diffusive due to spin-inversion scattering. So, we can assume that the interlayer tunneling occurs less frequently than the scattering on the single layer edge. In this case, the interlayer surface transport is dominated by the single tunneling process between the edge states on neighboring two layers. The selection rule of this tunneling leads the shift of center coordinate  $x_0$  under finite in-plane magnetic field  $B_x$  as shown in Fig.1(b). Therefore, the interlayer tunneling is allowed only when the magnetic field is parallel to the side surface of the crystal ( $B_x=0$ ).

Figure 2(a) shows the calculated interlayer resistance  $R_{zz}$ , which includes the bulk contribution, as a function of strength and orientation of magnetic fields. We can see that  $R_{zz}$  shows the saturation when the magnetic field is swept in the vertical direction, but shows monotonous increase in other directions. Fig. 2(b) shows the measured interlayer resistance  $R_{zz}$  in  $\alpha$ -(BEDT-TTF)<sub>2</sub>I<sub>3</sub>. The saturation occurs when the magnetic field was parallel to the stacking direction. Observed features are well explained by the calculation. This agreement also indicates the appearance of the QH ferromagnetic phase with the helical edge state in  $\alpha$ -(BEDT-TTF)<sub>2</sub>I<sub>3</sub>.

#### Authors

T. Osada, M. Sato, T. Konoike, and K. Uchida

# Mn<sup>3+</sup>/Mn<sup>4+</sup> Charge Order Driven by K-Vacancy Order in Mn-Hollandite

Y. Ueda Group

Hollandite type oxides, K<sub>2</sub>M<sub>8</sub>O<sub>16</sub> with a mixed valence of M<sup>3+</sup>/M<sup>4+</sup> = 1/3 have intensively investigated, expecting novel itinerant properties such as metal-insulator (MI) transition, charge order and so on. Actually, K<sub>2</sub>V<sub>8</sub>O<sub>16</sub> was found to undergo the metal-insulator transition at 170K, accompanied by the structural transition and charge order [1, 2]. A very rare ferromagnetic MI transition was discovered in K<sub>2</sub>Cr<sub>8</sub>O<sub>16</sub> [3]. This MI transition is caused by a Peierls instability in the quasi-one-dimensional column structure made of four coupled Cr-O chains running in the *c*-direction, leading to the formation of tetramers of Cr ions below the transition temperature [4].

The crystal structure consists of the M<sub>8</sub>O<sub>16</sub>-framework and K-cations. The M<sub>8</sub>O<sub>16</sub>-framework is constructed from the double-chains (zigzag-chains) formed by sharing the edges of MO<sub>6</sub> octahedra. The M<sub>8</sub>O<sub>16</sub>-framework has rectangular tubes surrounded by four double-chains, and K-cations occupy the sites within each rectangular tube and act as electron donor.

K<sub>x</sub>Mn<sub>8</sub>O<sub>16</sub> was prepared by high-pressure synthesis using a cubic anvil press [5]. Unfortunately Mn-hollandite was obtained only in K-deficient form. The maximum K-composition is *x*=1.6, in which K-vacancy molar fraction is 1/5 and Mn<sup>3+</sup> molar fraction is also the same 1/5. K<sub>1.6</sub>Mn<sub>8</sub>O<sub>16</sub> is not a metal and a canted antiferromagnet with Néel temperature of 50 K. Resistivity well obeys a one-dimensional variable range hopping manner. K<sub>1.6</sub>Mn<sub>8</sub>O<sub>16</sub> shows successive structural transitions of tetragonal to monoclinic at 370 K and monoclinic to monoclinic at 250 K. The superlattice reflections with five-fold periodicity along the *b*-axis (tunnel direction) as shown in Fig. 1, are observed by electron diffraction of TEM (transmission electron microscope) below 250 K. Such a five-fold periodicity is consistent with the fraction of K-vacancies, 0.4/2=1/5, suggesting vacancy-ordering at 250 K. At room temperature, similar but rather diffusive super-reflections are observed. These results suggest that in K<sub>1.6</sub>Mn<sub>8</sub>O<sub>16</sub>, the charge differentiation into Mn<sup>3+</sup> and Mn<sup>4+</sup> occurs even at higher temperature than at least 370 K and a short range order of K-vacancies progresses below 370 K, followed by a sudden long range order at 250 K. Such charge differentiation in K<sub>1.6</sub>Mn<sub>8</sub>O<sub>16</sub> could be due to K-deficiency, because the fraction of Mn<sup>3+</sup> is 1/5 which coincides with

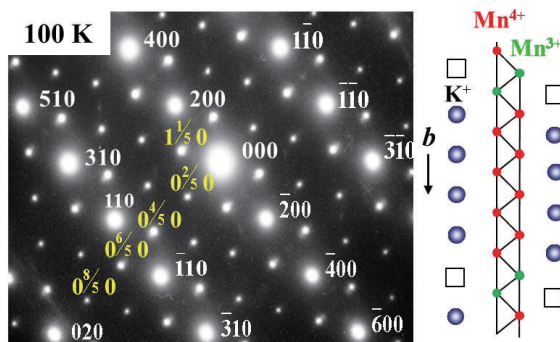


Fig. 1. Electron diffraction pattern observed at 100 K and schematic illustration of charge order between Mn<sup>4+</sup> and Mn<sup>3+</sup> for K<sub>1.6</sub>Mn<sub>8</sub>O<sub>16</sub>. The electron beam incidence is along the [001] direction of the monoclinic lattice. The superlattice reflections with five-fold periodicity along the *b*-axis (tunnel direction) are clearly observed, indicating K-vacancies ordering. The extra electrons are trapped by Mn ions adjacent to K-vacancies, leading to charge order between Mn<sup>4+</sup> and Mn<sup>3+</sup>.

the fraction of K-vacancies. Namely, extra e<sub>g</sub>-electrons are trapped at Mn ions close to K-vacancies, giving rise to Mn<sup>3+</sup> ions, namely an ordering between Mn<sup>3+</sup> and Mn<sup>4+</sup> takes place in cooperation with K-vacancy ordering. An origin for K-deficiency in hollandite manganese oxide could be in its rather shorter *b*-axis compared with those of K<sub>2</sub>M<sub>8</sub>O<sub>16</sub> (*M* = Ti, V, Cr). The electrostatic repulsion between K<sup>+</sup> ions in the tunnel would not allow the full occupancy of K-sites. Much higher pressure would be necessary for the synthesis of the stoichiometric K<sub>2</sub>Mn<sub>8</sub>O<sub>16</sub>.

## References

- [1] M. Isobe, S. Koishi, N. Kouno, J. Yamaura, T. Yamauchi, H. Ueda, H. Gotou, T. Yagi, and Y. Ueda, J. Phys. Soc. Jpn. **75**, 073801 (2006).
- [2] A. C. Komarek, M. Isobe, J. Hemberger, D. Meier, T. Lorenz, D. Trots, A. Cervellino, M. T. Fernández-Díaz, Y. Ueda, and M. Braden, Phys. Rev. Lett. **107**, 027201 (2011).
- [3] K. Hasegawa, M. Isobe, T. Yamauchi, H. Ueda, J-I. Yamaura, H. Gotou, T. Yagi, H. Sato, and Y. Ueda, Phys. Rev. Lett. **103**, 146403 (2009).
- [4] T. Toriyama, A. Nakao, H. Nakao, Y. Murakami, K. Hasegawa, M. Isobe, Y. Ueda, A. V. Ushakov, D. I. Khomskii, S. V. Streltsov, T. Konishi, and Y. Ohta, Phys. Rev. Lett. **107**, 266402 (2011).
- [5] T. Kuwabara, M. Isobe, H. Gotoh, T. Yagi, D. Nishio-Hamane, and Y. Ueda, J. Phys. Soc. Jpn. **81**, 104701 (2012).

## Authors

M. Isobe, H. Gotoh, D. Nishio-Hamane, and Y. Ueda

# Interlayer Switching of Reduction in Layered Bi-V Oxide

Y. Ueda Group

The pseudo binary oxide system Bi<sub>2</sub>O<sub>3</sub>-V<sub>2</sub>O<sub>5</sub> has received considerable interest due to its wide structural diversity and rich functional properties. Of particular interest is Aurivillius phase Bi<sub>4</sub>V<sub>2</sub>O<sub>11</sub> which is found exhibiting remarkably high oxygen anionic mobility. Such a function promises serious potential applications in many important areas, *e.g.* solid oxide fuel/electrolysis cells and oxygen sensors. The crystal structure of idealized Bi<sub>4</sub>V<sub>2</sub>O<sub>11</sub> is built up from infinite (Bi<sub>2</sub>O<sub>2</sub>)<sup>2+</sup> sheets sandwiched between oxygen deficient VO<sub>4.4</sub> perovskite slabs (V-O layer). Intrinsic oxygen vacancies ( $\Delta = 0.5$ ) in the V-O layer, which is normally believed to enable high oxide ion conductivity, are located in both apical and equatorial sites of VO<sub>6</sub> octahedra randomly. Such a description represents a

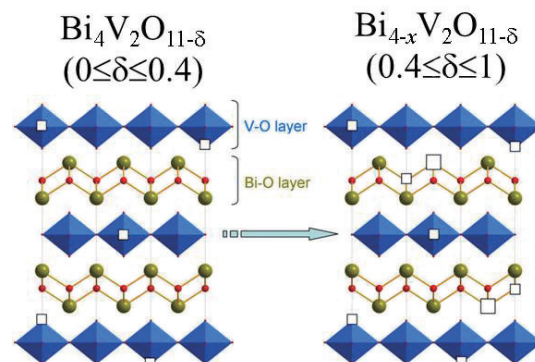


Fig. 1. Interlayer Switching of Reduction from V-O layers to Bi-O layers in Layered Oxide, Bi<sub>4</sub>V<sub>2</sub>O<sub>11-δ</sub> (0 ≤ δ ≤ 1). With increasing oxygen deficiency in Bi<sub>4</sub>V<sub>2</sub>O<sub>11-δ</sub>, the reduction of Bi<sub>4</sub>V<sub>2</sub>O<sub>11-δ</sub> first proceeds in the V-O layers, but beyond δ=0.4, suddenly switched to the Bi-O layers by precipitation of metallic bismuth, retaining a molar ratio of V<sup>4+</sup>/V<sup>5+</sup> = 2/3, namely the relation between bismuth and oxygen deficiencies is expressed as x = 2δ/3 - 4/15 in Bi<sub>4-x</sub>V<sub>2</sub>O<sub>11-δ</sub> (0.4 ≤ δ ≤ 1).

widely accepted prototype structure for the high temperature  $\gamma$ -phase. With decreasing temperature,  $\text{Bi}_4\text{V}_2\text{O}_{11}$  undergoes two consecutive and reversible phase transitions,  $\gamma \rightarrow \beta$  and  $\beta \rightarrow \alpha$  at 553 and 386 °C, respectively, due to the long range oxygen vacancy ordering process.

The oxygen-vacancy-disordered  $\gamma$ -phase reminds us that there might exist a rich phase diagram in the oxygen deficient system where a wealth of unknown phases would be expected. Moreover,  $\text{Bi}_4\text{V}_2\text{O}_{11-\delta}$  is of particular interest as the two-dimensional square lattice enables Aurivillius a favoured structure carrier of novel quantum properties. A full phase diagram for the  $\text{Bi}_4\text{V}_2\text{O}_{11-\delta}$  ( $0 \leq \delta \leq 1$ ) system was built for the first time by examining the whole spectrum of composition [1]. One structure ( $\alpha$ -phase) related to the established  $\text{Bi}_4\text{V}_2\text{O}_{11}$  phase survives in a very narrow  $\delta$  range ( $\approx 0.1$ ) whereas the other structure type (A-type) with its parent phase  $\text{Bi}_4\text{V}_2\text{O}_{10.6}$  shows unusual robustness from  $\delta=0.4$  until  $\delta=1$  ( $0.1 < \delta < 0.4$ : two phase mixture). Surprisingly, the decreasing oxygen stoichiometry in this structural region is found to be accommodated not by lowering the valence of vanadium as would be expected, but instead by reducing bismuth. It means the Bi site is favored over the V site upon reduction. This conclusion was further strengthened by the measurements of magnetic susceptibility over different compositions. All samples ( $0.4 \leq \delta \leq 1$ ) show the similar behavior that is characteristic of a one dimensional  $S = \frac{1}{2}$  antiferromagnetic Heisenberg chain model. The rigid V-O unit shared by all compositions between  $\delta=0.4$  and 1 is thus responsible for the robustness of the second type structure in the current phase diagram. *In situ* XRD investigations as a function of temperature provided strong evidence for the existence of three allotropic forms, which are  $\alpha$ ,  $\beta$  and  $\gamma$  for the  $\text{Bi}_4\text{V}_2\text{O}_{11}$  type and A, B and  $\gamma$  for the  $\text{Bi}_4\text{V}_2\text{O}_{10.6}$  type. When heated to 570°C or higher temperature, all compositions become uniform by forming the same tetragonal  $\gamma$  phase.

These results means that the reduction of  $\text{Bi}_4\text{V}_2\text{O}_{11-\delta}$  first proceeds in the V-O layer, but beyond  $\delta=0.4$ , suddenly switched to the Bi-O layer by precipitation of metallic bismuth, retaining a molar ratio of  $\text{V}^{4+}/\text{V}^{5+} = 2/3$ , namely the relation between bismuth and oxygen deficiencies is expressed as  $x = 2\delta/3 - 4/15$  in  $\text{Bi}_{4-x}\text{V}_2\text{O}_{11-\delta}$  ( $0.4 \leq \delta \leq 1$ ).

With a larger amount of intrinsic disordered oxygen vacancies,  $\gamma$ - $\text{Bi}_4\text{V}_2\text{O}_{11-\delta}$  phases, particularly  $\gamma$ - $\text{Bi}_{3.6}\text{V}_2\text{O}_{10}$  hold great potentials in offering optimized ionic conductivity. On the other hand, given the interesting defect chemistry and electromagnetic properties, this oxygen deficient system provides a very unique opportunity for the study at the interplay between structure and property.

#### Reference

[1] Y. Zhang and Y. Ueda, Inorganic Chemistry **52**, 5206 (2013).

#### Authors

Y. Zhang and Y. Ueda

## A High-Resolution Detector Installed on a Focusing Small-Angle Neutron Scattering Spectrometer (SANS-U)

### Shibayama Group

The small-angle neutron scattering (SANS) spectrometer SANS-U, owned by ISSP, is installed on the C1-2 cold neutron beamline of the research reactor (JRR-3) at the Japan Atomic Energy Agency (JAEA), Tokai, Japan. Recently, SANS-U was upgraded from a pinhole SANS (PSANS) spectrometer to a focusing SANS (FSANS) spectrometer by installation of a stack of 55  $\text{MgF}_2$  lenses and a high-resolution position-sensitive detector (HR-PSD)[1]. Through this upgrade, the accessible low  $Q$ -limit ( $Q_{\min}$ ) was expanded to the order of  $10^{-4} \text{ \AA}^{-1}$ , where  $Q$  is the magnitude of the scattering vector, defined by  $Q = (4\pi/\lambda) \sin\theta$  (where  $\lambda$  and  $2\theta$  are the wavelength and the scattering angle, respectively). Observation of a scattering profile in this  $Q$ -range by means of an FSANS requires a longer measurement time longer than that of conventional PSANS. Consequently, measurement time for FSANS experiments usually has a higher proportion of total user machine time. Therefore, it is desirable to improve the experimental efficiency of FSANS measurements. In case of cold neutrons,  $\text{ZnS}/^6\text{LiF}$  scintillation detectors are known for lower detection efficiency compared with the conventional  $^3\text{He}$  detectors. Therefore, to improve the HR-PSD, we attempted to increase the detection efficiency of the  $\text{ZnS}/^6\text{LiF}$  scintillator by maintaining a high spatial resolution and a low background.

In order to increase the performance of a  $\text{ZnS}/^6\text{LiF}$  scintillator for high-resolution detection of cold neutrons, we determined optimum thickness of the  $\text{ZnS}/^6\text{LiF}$  scintillator. We also examined the characteristics of the HR-PSD with the optimized scintillator, and performed FSANS measurements in order to compare the performances with a commercial scintillator. Figure 1 shows the HR-PSD installed inside the flight-tube of the SANS-U spectrometer. Note that the HR-PSD consists of a cross-wired position-sensitive photomultiplier tube (PSPMT) combined with a  $\text{ZnS}/^6\text{LiF}$  scintillator. According to the specifications of the PSPMT, the size of the effective area of the PMT and its spatial resolution are about  $\phi 100$  mm and 0.45 mm, respectively. The HR-PSD packed in an Al vessel was mounted on an X-Z movable bench in front of the main  $^3\text{He}$ -PSD. Figure 2(a) shows the total count of neutrons depending on scintillator thickness. By increasing the thickness from 0.180 to 0.433 mm, the total count increased remarkably from  $1.23 \times 10^5$  to  $3.18 \times$

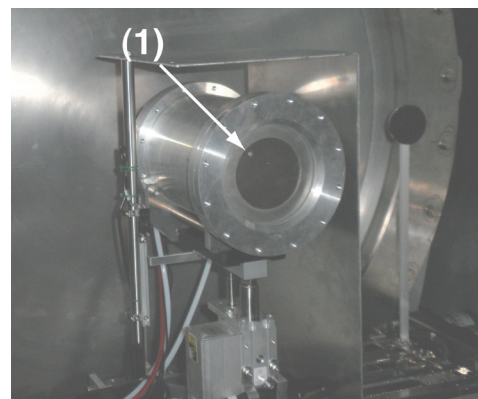
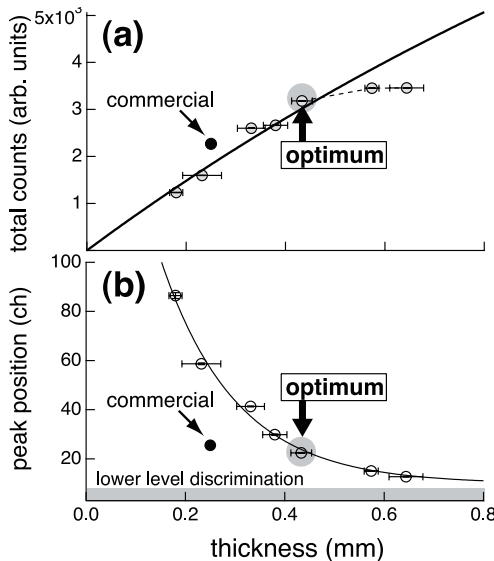


Fig. 1. Photograph of the high-resolution position sensitive detector (HR-PSD) in the flight tube of the SANS-U spectrometer. (1) The position of the fixed beam-stopper (Cd;  $\phi 4$  mm). The details of the HR-PSD are described in another recent publication. [1]



## Glass Transition of Hydrogen Atoms in Palladium Lattice

Yamamuro Group

Palladium hydride ( $\text{PdH}_x$ ) is the most popular metal hydride which has been investigated by many physicists and chemists. It has been remarked also from industrial points of view, e.g., hydrogen storage, filters, sensors, catalysts, etc. Figure 1 shows the adsorption isotherm of the Pd and hydrogen gas system [1]. On adsorption, a hydrogen molecule ( $\text{H}_2$ ) dissociates into two hydrogen atoms (2H). It is known that the  $\alpha$  phase appears in a lower concentration ( $x$ ) region while the  $\beta$  phase in a higher  $x$  region. In the intermediate region (dome-like area of Fig. 1), the  $\alpha$  and  $\beta$  phases coexist and pressure becomes constant according to the Gibbs phase rule. Above the critical point (2.0 MPa, 259°C), one cannot distinguish the  $\alpha$  and  $\beta$  phases. Both  $\alpha$  and  $\beta$  phases have an fcc structure. Most of the H atoms are located at the octahedral sites in the  $\beta$  phase, while the positions of the H atoms are not known in the  $\alpha$  phase. The volume of the  $\beta$  phase is 11% larger than that of the  $\alpha$  phase. There are still many unsolved interesting problems in  $\text{PdH}_x$ , e.g., superconductivity at a higher  $x$  region, a surface ferromagnetic phenomenon, etc. The present work is associated with a mysterious phenomenon called “50 K anomaly”. We have measured the heat capacity of the  $\beta$  phase with various  $x$  using an adiabatic calorimeter which was modified for *in situ* introduction of hydrogen gas into the sample cell.

Figure 2 shows the heat capacities of  $\text{PdH}_x$  ( $x = 0.638, 0.725, 0.782, 0.829$ ). For all of the samples, a heat capacity anomaly appeared around 50 K as expected from the previous work [2, 3]. We have fitted the data at temperatures lower than the anomaly to the function,

$$C_p = C(\text{Debye}) + C(\text{Einstein}) + \gamma T, \quad (1)$$

where the first and second terms correspond to the acoustic and optical vibrations, respectively and the third term represents the electronic heat capacity. It was revealed that  $C(\text{Einstein})$  does not contribute in this temperature range since the mass of an H atom is much smaller than that of a Pd atom. The coefficient  $\gamma$  was determined not by the fitting but by the interpolation for the previous heat capacity data at very low temperatures [4]. The fitting was satisfactory for all samples as shown in Fig. 2. The Debye temperature  $\theta_D$  determined by the fitting is 246 K, being mostly independent from  $x$  in the  $\beta$  phase. This value is smaller than that of pure Pd ( $\theta_D = 276$  K), meaning that the Pd lattice is

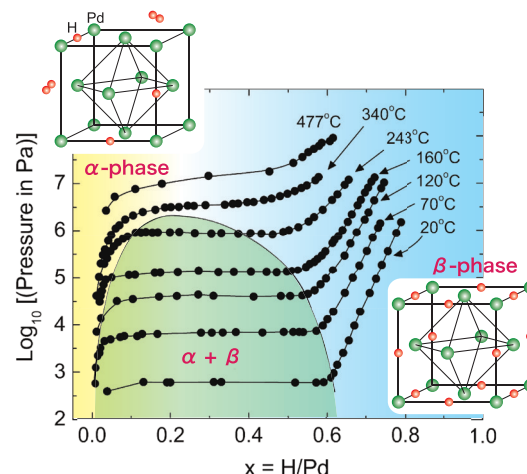


Fig. 1. Adsorption isotherms of Pd-H system and schematic structure of the  $\alpha$  and  $\beta$  phases of  $\text{PdH}_x$ .

Fig. 2. Scintillator thickness dependences of (a) total count, and (b) peak position on a pulse-height spectrum for the  $\text{ZnS}/^6\text{LiF}$  scintillator developed by Katagiri et al. [2]

$10^5$ . In contrast, the total count increased slightly from  $3.18 \times 10^5$  to  $3.46 \times 10^5$  when the scintillator thickness increased from 0.433 to 0.640 mm. Figure 2(b) shows the peak position of the pulse height spectra for varying scintillator thicknesses. The peak position for a commercial scintillator was estimated to be 25.54 ch. A low peak position generally leads to a decrease in counting stability because of difficulty in electrical discrimination, whereas higher values of peak positions are suitable for count stability. Hence, a trade-off exists between the total count and peak position. On the basis of the results of the total count and peak position for varying scintillator thickness, we determined optimum thickness. The requirements for the HR-PSD were as follows: (i) high detection efficiency and (ii) peak position approximately equal to that of the commercial scintillator. Accordingly, the optimum scintillator thickness was determined to be 0.433 mm. The beam intensities obtained using the optimum  $\text{ZnS}/^6\text{LiF}$  scintillator were 1.39 times higher than those obtained using the commercial scintillator, which is consistent with the results of pulsed height measurements for comparison.

In conclusion, the total count of direct focused beam intensity was 1.39 times that of the commercial scintillator while maintaining both  $Q$ -resolution and the background count at the same level. This optimization resulted in a significant improvement in the experimental efficiency of the FSANS experiments.[3]

### References

- [1] H. Iwase, H. Endo, M. Katagiri, and M. Shibayama, *M. J. Appl. Cryst.* **44**, 558 (2011).
- [2] M. Katagiri, K. Sakasai, M. Matsubayashi, T. Nakamura, Y. Kondo, Y. Chujo, H. Nanto, and T. Kojima, *Nucl. Instrum. Methods A* **529**, 274 (2004).
- [3] H. Iwase, M. Katagiri, and M. Shibayama, *M. J. Appl. Cryst.* **45**, 507 (2012).

### Authors

H. Iwase, M. Katagiri<sup>a</sup>, and M. Shibayama  
<sup>a</sup>Japan Atomic Energy Agency

# Spin Nematic Interaction in Square-Lattice Antiferromagnet $\text{Ba}_2\text{CoGe}_2\text{O}_7$

Masuda Group

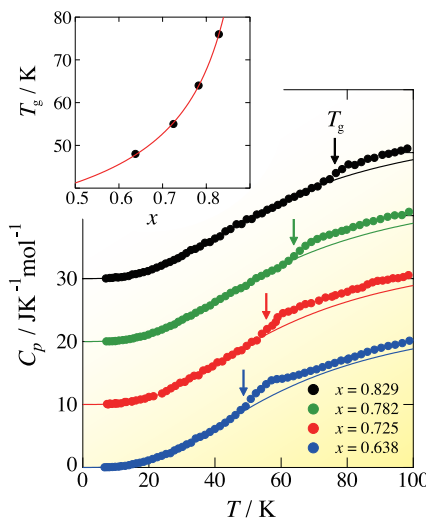


Fig. 2. Heat capacities of  $\text{PdH}_x$  ( $x = 0.638, 0.725, 0.782, 0.829$ ). The arrows represent the glass transition temperatures  $T_g$ 's whose  $x$  dependence is shown in the inset. The curves in the  $C_p$  and  $T_g$  figures represent the results of the fittings to Eqs. (1) and (2), respectively. See text for the details.

softened by accommodating H atoms. In the previous studies [2, 3], the 50 K anomaly was treated as a  $C_p$  peak. From the precise analysis, however, it was found that this is a step-like anomaly. We also found that an exothermic, followed by endothermic, phenomenon appeared around the anomaly. Taking its temperature dependence and annealing effect into consideration, we conclude that the 50 K anomaly of  $\text{PdH}_x$  is not a phase transition but a glass transition that is a freezing phenomenon of the H atoms positionally disordered among the octahedral sites. This conclusion is supported by the previous NMR [5], mechanical [6], thermal relaxation [7] studies which show that the relaxation time of the jump motion of the H atoms reaches 1000 s (the time-scale of the glass transition) around 50 K.

Figure 2 demonstrates that the glass transition temperature  $T_g$  strongly depends on  $x$ . By assuming that the jump rate of the H atoms is proportional to the number of vacant sites and the Arrhenius relation is valid in this region, we derived the following equation,

$$T_g = \Delta E / [\ln(1 - x) + A]. \quad (2)$$

where  $\Delta E$  is the activation energy and  $A$  is a constant. The  $x$  dependence of  $T_g$  is reproduced well as shown the inset of Fig. 2.

We are now planning to measure the heat capacity of the  $\text{PdD}_x$  sample with expectation of isotope effects on the 50 K anomaly. It is possible to observe an ordering transition of the D atoms since the previous neutron diffraction works using  $\text{PdD}_x$  samples suggest some sort of ordering of the D atoms below 50 K.

## References

- [1] F. D. Manchester, Phase Diagrams of Binary Hydrogen Alloys, p.158 (2000).
- [2] D. M. Nace and G. J. Aston, J. Am. Chem. Soc. **79**, 3627 (1957).
- [3] H. Araki, M. Nakamura, S. Harada, T. Obata, N. Mikhin, V. Syvokon, and M. Kubota, J. Low Temp. Phys. **134**, 1145 (2004).
- [4] C. A. Mackiet and A. I. Schindler, Phys. Rev. **146**, 463 (1966).
- [5] D. A. Cornell and E. F. W. Seymour, J. Less-Common Met. **39**, 43 (1975).
- [6] J. K. Jacobs, C. R. Brown, V. S. Pavlov, and F. D. Manchester, J. Phys. F: Metal Phys. **6**, 2219 (1976).
- [7] J. K. Jacobs and F. D. Manchester, J. Phys. F: Metal Phys. **7**, 23 (1977).

## Authors

H. Akiba, M. Kofu, H. Kobayashi<sup>a</sup>, H. Kitagawa<sup>a</sup>, and O. Yamamuro  
<sup>a</sup>Kyoto University

The interaction between magnetic moments has been well known even before the establishment of quantum dynamics and the pioneering research on various types of the magnetic correlations by P. Curie is the basis of modern magnetism. Recently the correlation of the higher order of the spin operator has attracted theoretical interest in terms of hidden order in spin disordered state [1] but the direct experimental probe to identify the correlation is absent. Meanwhile in multiferroic compound that exhibits spontaneous order both in magnetism and dielectricity, the electric polarization is expressed by second order tenors of the spin operators [2], and the spin nematic operator comes to visible. In this fiscal year we demonstrate the existence of the spin nematic interaction in an easy-plane type antiferromagnet  $\text{Ba}_2\text{CoGe}_2\text{O}_7$  [3, 4] by exploring the magnetic anisotropy and spin dynamics. Combination of neutron scattering and magnetization measurements reveals that the dominant origin of the observed in-plane anisotropy is the ferro-type interaction of spin nematic operator instead of conventional single-ion anisotropy. The structure of the spontaneous polarization [10] is consistent with the ferro-type order of the nematic operators. The introduction of the spin nematic interaction is useful to understand the physics of spin and electric dipole in multiferroic compounds.

The crystal structure of  $\text{Ba}_2\text{CoGe}_2\text{O}_7$  is schematized in Fig. 1a. The compound exhibits antiferromagnetic transition at  $T_N=6.7$  K and a staggered antiferromagnetic structure in the (001) plane was identified [3]. Below  $T_N$ , a ferroelectric polarization is simultaneously induced [4]. Inelastic neutron scattering spectrum and magnetization measurements are shown in Figs. 1c and d, respectively. In the former clear anisotropy gap of about 0.12 meV is observed at the antiferromagnetic zone center  $Q = (100)$ . In the derivative of magnetization curve, a peak due to spin flop is observed at

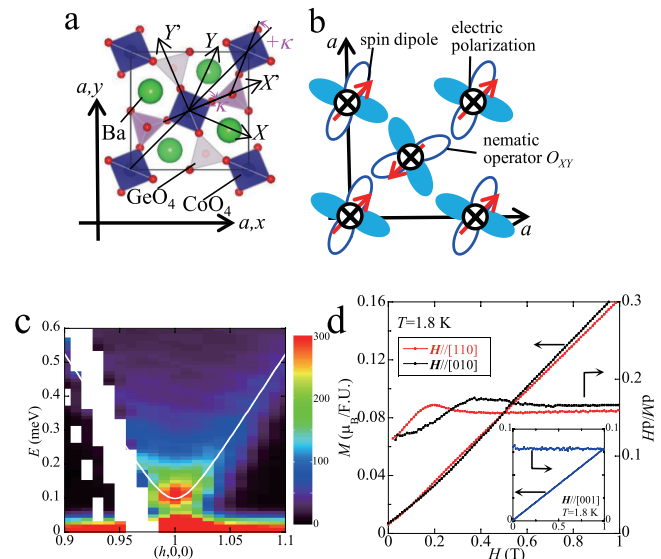


Fig. 1. a, Crystal structure of  $\text{Ba}_2\text{CoGe}_2\text{O}_7$ . b, Structures of spin dipoles, spin nematic operator  $O_{XY}$ , and electric polarizations in  $\text{Ba}_2\text{CoGe}_2\text{O}_7$ . Red arrows are spin dipoles and open circles with crosses and small filled circles indicate the directions of electric polarization calculated by using the relation between spin nematic operator and electric polarization. Two-tone clovers are nematic operators. c, Inelastic neutron scattering spectrum. d, Bulk magnetization  $M$  and the derivative by field  $dM/dH$  in field along [110], [010], and [001] at  $T = 1.8$  K.

the field  $H \sim 0.2$  T in  $H // [110]$ , the spin flop field increases in  $H // [100]$ , and no spin flop is observed in  $H // [001]$ . The results mean that the magnetic easy axis is along the [110] direction. Meanwhile, the point symmetry of  $\text{CoO}_4$  tetrahedron,  $D_{2d}$ , does not allow the magnetic anisotropy along  $\langle 110 \rangle$  as far as single ion anisotropy and two-spin exchange anisotropy are considered. Thus the anisotropy is ascribed to the interaction of higher order of spin operator. Symmetry consideration leads to the relation between the electric polarization and the spin nematic operator,  $P^X = -K_{ab}O_{YZ}$ ,  $P^Y = -K_{ab}O_{ZX}$ , and  $P^Z = -K_cO_{XY}$ , where  $X$ ,  $Y$ , and  $Z$  are the local coordinates on  $\text{CoO}_4$  tetrahedron as shown in Fig. 1a. Among these  $O_{YZ}$  and  $O_{ZX}$  are irrelevant to the anisotropy since the  $Z$  component of spin dipole is zero in the spin structure [3]. Hence we consider the nematic Hamiltonian  $H_p = -J_p K_c^2 \sum_{i,j} O_{XY}(i)O_{XY}(j)$ . Calculation of the classical energy including antiferromagnetic spin interaction and ferro-type nematic interaction between  $O_{XY}$  operators leads the ground state to the staggered spin structure along  $\langle 110 \rangle$  direction. The ferro-type nematic correlation depicted in Fig. 1b is consistent with the ferroelectric polarization along  $Z$  direction previously reported [4]. Both neutron spectrum and bulk magnetization are quantitatively explained by extended spin-wave calculation based on Hamiltonian including the ferro-type nematic interaction.

#### References

- [1] A. F. Andreev and I. A. Grishchuk, Sov. Phys. JETP **60**, 267 (2984).
- [2] H. Katsura, N. Nagaosa, and A.V. Balatsky, Phys. Rev. Lett. **95**, 057205 (2005).
- [3] A. Zheludev *et al.*, B. Phys. Rev. B **68**, 024428 (2003).
- [4] H. Murakawa *et al.*, Y. Phys. Rev. Lett. **105**, 137202 (2010).

#### Authors

M. Soda, T. Masuda, M. Matsumoto<sup>a</sup>, M. Mansson<sup>b</sup>, S. Ohira-Kawamura<sup>c</sup>, and K. Nakajima<sup>c</sup>  
<sup>a</sup>The Shizuoka University  
<sup>b</sup>Tokyo Paul Sherrer Institute  
<sup>c</sup>J-PARC

---International MegaGauss Science Laboratory-----

## Determination of Entropies by Measurements of Magneto-Caloric Effects in Pulsed Magnetic Fields

Tokunaga and Katsumoto Groups

Existence of highly degenerated ground states, *e.g.* in frustrated magnets, results in the emergence of various non-trivial physical phenomena. Such degeneracy involves significant residual entropy at low temperatures, whereas its direct determination is not easily achieved. Our measurement system of the magneto-caloric effects (MCEs) in pulsed high magnetic fields provides unique opportunity to study the residual entropies. Fast field-sweep rates in the pulsed fields enable us to realize effectively adiabatic conditions in the magnetization processes, and hence, accurate evaluation of the entropies in wide range of magnetic fields up to 55 T.

With using our system, we measured the MCEs in  $\text{Gd}_3\text{Ga}_5\text{O}_{12}$  (GGG) [1], which does not show long-range order of Gd moments down to 25 mK owing to geometrical spin frustration. Through the measurements of magnetoresistance in calibrated resistive film thermometers grown on top of the sample surfaces, we successfully monitored the instantaneous change in the sample temperature in duration of the pulsed fields ( $\sim 36$  ms). The solid lines in Fig. 1 show the field dependence of the temperature of GGG. The revers-

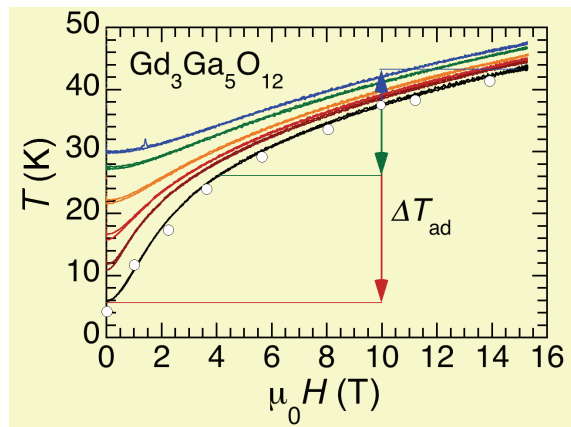


Fig. 1. Magnetic field dependence of the temperature of  $\text{Gd}_3\text{Ga}_5\text{O}_{12}$  measured in pulsed magnetic fields. Open circles represent the reported results derived from the analyses of the magnetization curve measured in the quasi-adiabatic condition [2]. The inset shows a schematic illustration of the film thermometer grown on the sample.

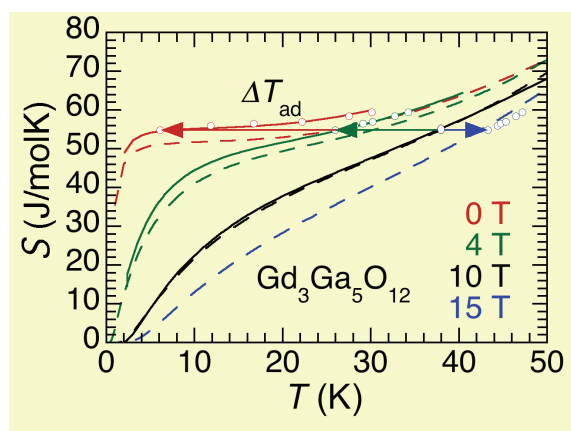


Fig. 2. Temperature dependence of the entropy of  $\text{Gd}_3\text{Ga}_5\text{O}_{12}$  at several magnetic fields. The open circles were determined by the horizontal shift of the standard  $S$ - $T$  curve at 10 T by the amount of  $\Delta T_{ad}$  in the measurements of the MCEs. The solid lines were evaluated by numerical integration of the heat capacity data at various fields. The dashed lines are calculated  $S$ - $T$  curves based on a simple crystal field model [3].

ible profiles indicate that the heat exchange to the thermal bath and the delay in the response of the thermometer are negligibly small. In addition, the present results show reasonable agreement with the preceding results [2] (open circles) indicating the quantitative validity of the present system.

From these data, we can evaluate the entropy ( $S$ ) as a function of temperature ( $T$ ) for various fields. First, we determined the standard  $S$ - $T$  curve by integrating the data of specific heat ( $C$ ) at 10 T, where the residual entropy seems to be negligible at the lowest temperature for the specific heat measurement (2 K). Then the  $S$ - $T$  curves at different fields (open circles) were determined by horizontal shift by  $\Delta T_{ad}$  determined by measurements of MCEs as shown by the arrows in Figs. 1 and 2. The solid lines in Fig. 2 are the  $S$ - $T$  curves evaluated by numerical integration of the specific heat data, in which the amounts of the residual entropies, i.e. the vertical offsets, were determined so as to match with the MCE results. The result reveals the failure of the simple estimation of the entropy by a simple crystal field model (dashed lines), while this discrepancy cannot be resolved by the  $C$ - $T$  curves in this temperature range.

#### References

- [1] T. Kihara *et al.*, submitted to Rev. Sci. Instrum.
- [2] R. Z. Levitin *et al.*, J. Magn. Magn. Mater. **170**, 223 (1997).
- [3] W. Dai, E. Gmelin, and R. Kremer, J. Phys. D: Appl. Phys. **21**, 628 (1988).

**Authors**

T. Kihara, Y. Kohama, Y. Hashimoto, S. Katsumoto, and M. Tokunaga

## Exotic spin states in $\text{SrCu}_2(\text{BO}_3)_2$ at Megagauss Magnetic Fields

**Y. Matsuda and Takeyama Groups**

Quantum spin frustration induces interesting magnetic states in matters. A orthogonal dimer spin system  $\text{SrCu}_2(\text{BO}_3)_2$  exhibits fascinating phenomena due to the frustration [1]. The crystal lattice is topologically equivalent to the Shastry-Sutherland (SS) lattice. The nearest neighbor ( $NN$ )  $S=1/2$  spins of Cu ions are antiferromagnetically coupled and form the singlet dimer through the exchange interaction  $J$ . Since the inter dimer exchange interaction  $J'$  between the next nearest neighbor ( $NNN$ ) Cu ions is antiferromagnetic as well, the orthogonal configuration makes the quantum frustration. The multiple magnetization plateaux found in high magnetic fields have attracted significant attention as the exotic phenomena. [1, 2] The distinct  $1/8$ ,  $1/4$ , and  $1/3$  plateaux were observed in the magnetization process and the existence of the long predicted  $1/2$  plateau was reported by the magnetostriction measurement [3]. However, the whole  $1/2$  plateau phase was not unveiled yet because of the technical upper limit of the magnetic field 100 T. Moreover, high-field spin states in the SS lattice are theoretically suggested to exhibit the exotic states such as the supersolid state between the  $1/3$  and  $1/2$  plateaux and that above the  $1/2$  plateau [4]. The quantum spin state when the density of the triplet state becomes high in the SS lattice has never been uncovered yet.

In the present work, we have investigated the spin states of  $\text{SrCu}_2(\text{BO}_3)_2$  by the magnetization measurement up to 109 T using the single-turn coil method. The distinct  $1/2$  magnetization plateau phase has been observed in the field range from 84 to 108 T. A sharp magnetization increase at the end of the  $1/2$  plateau suggests the possible phase transition to the supersolid phase.

Figure 1 shows the magnetization ( $M$ ) and the magnetic field derivative of the magnetization ( $dM/dH$ ) as a function of magnetic field. Distinct peak structures are observed in the  $dM/dH$  curve, indicating the stepwise increase in the magne-

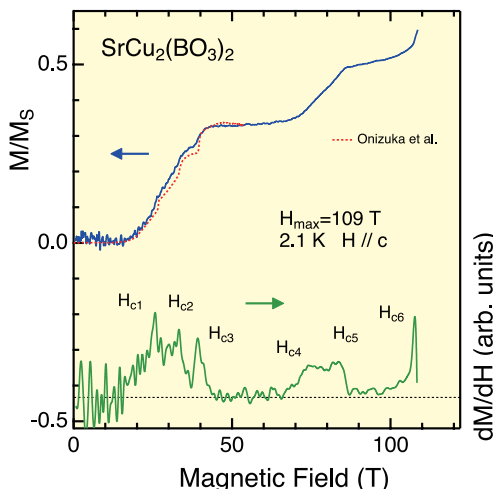


Fig. 1. A magnetization curve at 2.1 K up to 109 T. Applied field is parallel to the  $c$ -axis of the crystal. The magnetic field derivative of the magnetization ( $dM/dH$ ) curve is also shown as a function of magnetic field. The dotted curve is the magnetization curve reported previously. (Ref.[2])

tization at critical magnetic fields ( $H_{cn}$ ,  $n=1\sim 6$ ). By comparison with the magnetization curve in the previous report [2],  $H_{c1}\sim H_{c3}$  correspond to the boundaries of  $1/8$ ,  $1/4$  and  $1/3$  plateau phase. The broad double-peak structure comprised of  $H_{c4}$  and  $H_{c5}$  may suggest that there is an exotic phase between the  $1/3$  and  $1/2$  plateau phase.  $H_{c5}$  and  $H_{c6}$  clarify the whole region of  $1/2$  plateau. The finite slope observed at the  $1/2$  plateau phase can be caused by the thermal excitation. The exotic spin states in the SS lattice will be clarified with a help of detailed theoretical calculations. Such collaboration work is now in progress.

**References**

- [1] H. Kageyama, K. Yoshimura, R. Stern, N. Mushnikov, K. Onizuka, M. Kato, K. Kosuge, C. Slichter, T. Goto, and Y. Ueda, Phys. Rev. Lett. **82**, 3168 (1999).
- [2] K. Onizuka, H. Kageyama, Y. Narumi, K. Kindo, Y. Ueda, and T. Goto, J. Phys. Soc. Jpn. **69**, 1016 (2000).
- [3] M. Jaime, R. Daou, S. A. Crooker, F. Weickert, A. Uchida, A. E. Feiguine, C. D. Batista, H. A. Dabkowska, and B. D. Gaulin, PNAS **109**, 12404 (2012).
- [4] J. Lou, T. Suzuki, K. Harada, and N. Kawashima, arXiv:1212.1999v1 (2012).

**Authors**Y. H. Matsuda, N. Abe, S. Takeyama, and H. Kageyama<sup>a</sup><sup>a</sup>Kyoto University

---Laser and Synchrotron Research Center/  
Synchrotron Radiation Laboratory-----

## Terahertz Time Domain Observation of Rotational Type Spin Reorientation Transition

**Suemoto Group**

Ultrafast coherent excitation of spins is one of the promising technologies for developments in spintronics and information processing. Such ultrafast control of the spin systems are often studied with pump and probe measurement using femtosecond visible laser [1]. Because these methods use indirect excitations of the spins that occur as a result of dielectric interaction with optical pulses, quite large amount of optical energy, typically 10 microjoule per pulse is required for pumping the spins. For this reason, unwanted electronic excitation and heating occurs. Instead, by using the terahertz pulses, spin precession motion can be excited directly through magnetic interaction between the terahertz magnetic component and the spin system [2, 3]. As described in Fig. 1, magnetic field component of the THz pulse instantaneously tilts the spins from their equilibrium orientation,

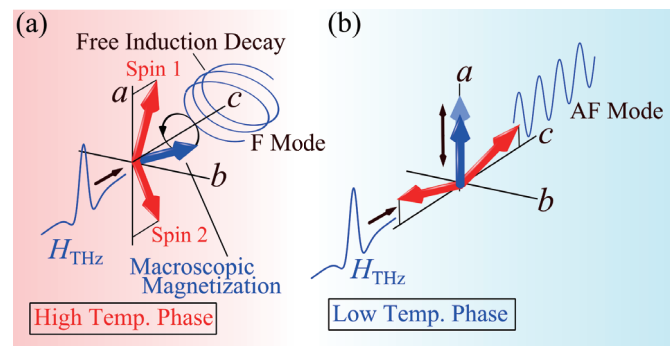


Fig. 1. Illustration of ultrafast spin precession excitation with the magnetic field component of THz pulse parallel to the  $a$ -axis for (a) high temperature phase of  $\text{ErFe}_3$ , and (b) low temperature phase. In the high temperature phase, elliptically polarized emission from F mode resonance is observed. On the other hand, linearly polarized AF mode emission is observed in the low temperature phase. For the ease to see, the precessions of the individual  $\text{Fe}^{3+}$  spins 1 and 2 (red arrows) are omitted from the figures.

causing the spins to precess around the effective magnetic field. Such motion of spins emits radiation which can be observed as free induction decay signal. With this technique, spin precession can be excited and observed simultaneously with a femtojoule terahertz pulse, which enables us to ignore the heating effect. In addition, owing to the low photon energy of the terahertz pulse, unwanted electronic excitation can be avoided.

Weak ferromagnet  $\text{ErFeO}_3$ , which belongs to the rare earth orthoferrites known to have two magnetic resonance modes (Ferromagnetic mode and Antiferromagnetic mode) in sub-THz region [3], shows temperature induced spin reorientation transition. In this phase transition, the easy axis of the  $\text{Fe}^{3+}$  spins show 90 degree rotation. In the temperature range higher than 96 K (high temperature phase), the  $\text{Fe}^{3+}$  spins align antiferromagnetically toward the  $a$ -axis with a  $c$ -axis parallel macroscopic magnetization resulting from the canting of the spins (Fig. 1 (a)). At 87 K or lower (low temperature phase), the easy axis of the  $\text{Fe}^{3+}$  spins and the magnetization become parallel to the  $c$ -axis and  $a$ -axis, respectively (Fig. 1(b)).

Here, by focusing on the two magnetic resonance modes, we devised methods to observe the spin reorientation through THz time domain spectroscopy (TDS) and demonstrated this method with  $\text{ErFeO}_3$  [4]. The measurement was performed with a sintered pellet sample and a single crystal with a (001) surface. The temperature dependence of the two resonant frequencies is shown in Fig. 2(a). It shows that the F mode frequency drops significantly around the reorientation temperature. The spectra of radiation emitted from the spin precession excited with THz magnetic field parallel to  $a$ -axis shows that the frequency of the emission changes significantly between high temperature phase and low temperature phase (Fig. 2(b)). Comparing this with Fig. 2(a), it can be seen that the resonant frequency equals to F mode frequency for 250 K and AF mode for 70 K. Such switching of the excited mode can be explained by rotation of the easy axis due to the spin reorientation (Figs. 1(a) and (b)) and therefore, we have shown that spin reorientation can be detected through THz TDS measurement. To the best of our knowledge, this is the first observation of such phase transitions with THz time domain measurement. When observing this behavior in the temporal waveforms, half-cycle of the precession is sufficient for distinguishing F and AF modes. Thus, by focusing on the existence of the AF mode, the phase of the spin configuration can be determined with a resolution of 0.67 ps. Therefore, this method offers ability to detect spin reorientation with picosecond time resolution and it

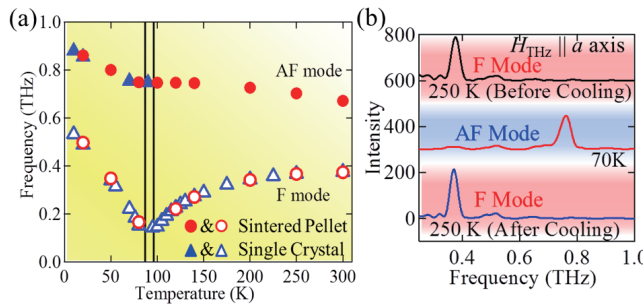


Fig. 2. (a) Temperature dependence of F and AF mode resonant frequencies in  $\text{ErFeO}_3$ . Circle markers show frequencies obtained with the sintered pellet, and triangle markers show frequencies in a single crystal sample with (001) surface. Two vertical lines indicate higher and lower transition temperatures at 96 K and 87 K. (b) Intensity spectra of oscillatory components obtained with  $H_{\text{THz}} \parallel a$ -axis THz pulse excitation.

is expected to open the doorway for studying dynamics of ultrafast spin reorientation.

## References

- [1] A. Kirilyuk, A. V. Kimel, and T. Rasing, Rev. Mod. Phys. **82**, 2731 (2010).
- [2] M. Nakajima, A. Namai, S. Ohkoshi, and T. Suemoto, Opt. Exp. **18**, 18260 (2010).
- [3] K. Yamaguchi, M. Nakajima, and T. Suemoto, Phys. Rev. Lett. **105**, 237201 (2010).
- [4] K. Yamaguchi, T. Kurihara, Y. Minami, M. Nakajima, and T. Suemoto, Phys. Rev. Lett. **110**, 137204 (2013).

## Authors

K. Yamaguchi, T. Kurihara, Y. Minami, M. Nakajima, and T. Suemoto

## Firefly Bioluminescence Affected by Temperatures and Metal Ions

### Akiyama Group

Firefly bioluminescence has attracted great interest among various research fields. The mechanisms of very high quantum yield and condition-sensitive color change of the bioluminescence are long standing issues of basic biochemistry and biophysics, and applications of the bioluminescence such as food hygiene inspection, DNA sequencing, bioimaging, cancer diagnosis, and immunoassay, are under intensive developments and some of them are commercially available. Quantitative study of the bioluminescence is crucially important for both basic research and application, but still very rare [1, 2].

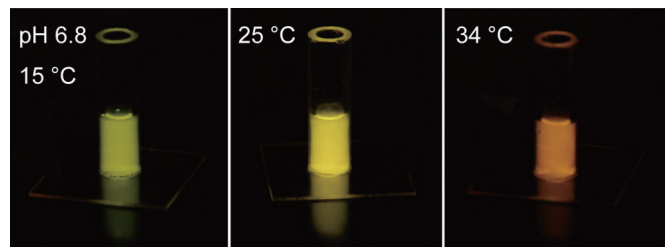


Fig. 1. Picture of temperature-sensitive color change of bioluminescence of North-American Firefly (*Photinus pyralis*) at pH 6.8 in home-made acrylic tube cell placed on an aluminum sheet.

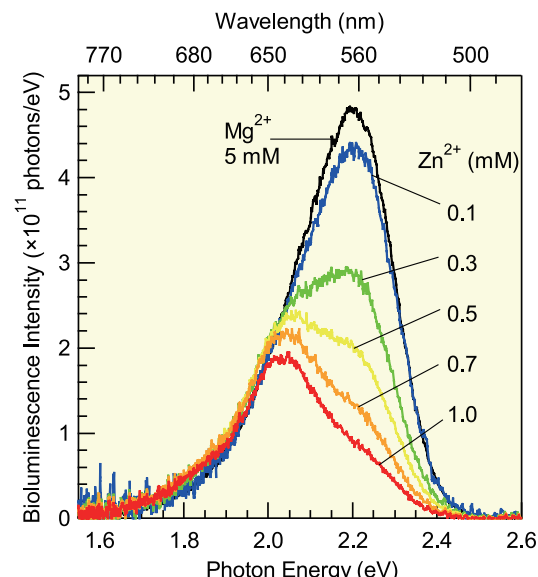


Fig. 2. Time-integrated total photon flux spectra of bioluminescence of North-American Firefly with various zinc-ion densities. Black line shows data with magnesium ion, whose density did not change the spectra significantly, as a reference.

We measured total-photon flux of firefly bioluminescence in various reaction conditions such as temperature, pH, and bivalent metal density quantitatively. All quantitative spectra were very well reproduced by three Gaussian components, which peaked at 1.9 (red), 2.0 (orange), and 2.2 (green) eV. The positions and widths of the components were insensitive to reaction conditions. Firefly bioluminescence changed its color from yellow-green to yellow, then to orange with increasing temperature as shown in Fig. 1. Quantitative analysis revealed that the color change solely owing to decrease of intensity of the green Gaussian component with increasing temperature. Very similar color change was observed with increasing bivalent metal ion density as shown in Fig. 2. The observed similarity of color change is useful for detailed basic study such as comparisons with quantum-chemistry calculations and the robustness of the luminescence below 2.0 eV can be advantageous as a standard yield for future applications of quantitative measurement of bioluminescence.

#### References

- [1] Y. Ando *et al.*, *Nature Photonics*. **2**, 44 (2008).
- [2] Y. Wang *et al.*, *Photochemistry and Photobiology* **87**, 846 (2011).

#### Authors

- T. Mochizuki, Y. Wang<sup>a</sup>, M. Hiyama, H. Akiyama, H. Kubota<sup>b</sup>, K. Terakado<sup>c</sup>, T. Nakatsu<sup>c</sup>  
<sup>a</sup>Chinese Academy of Science, China  
<sup>b</sup>ATTO Corporation  
<sup>c</sup>Kyoto University

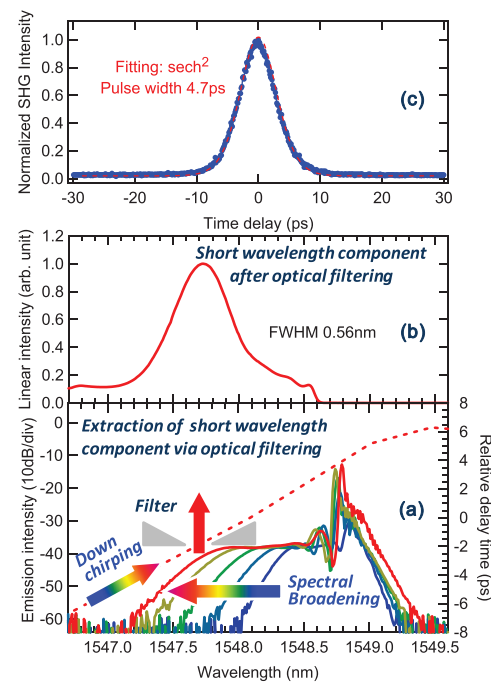


Fig. 1. (a) Lasing spectra of a single-mode DFB-LD at room temperature with various current densities, showing the significant spectral broadening towards short wavelength side with increasing current density. Dashed line shows the down chirp during gain switching of the DFB-LD with the highest excitation density. (b) Spectrum of the short wavelength component after spectral filtering of the one with the highest excitation in (a). The FWHM of the peak is measured to be 0.56 nm. (c) The autocorrelation trace of the spectrally filtered short wavelength component. Fitting result shows that the pulse has a  $\text{sech}^2$  shape with a pulse width of 4.7 ps. The time-bandwidth product (0.33) of the obtained short pulse demonstrates that the obtained short pulses at short-wavelength side are Fourier-transform-limited pulses.

#### References

- [1] H. Yokoyama, *et al.*, *Opt. Express* **14**, 3467 (2006).
- [2] S. Q. Chen, *et al.*, *Jpn. J. Appl. Phys.* **51**, 098001 (2012).
- [3] S. Q. Chen, *et al.*, *Appl. Phys. Lett.* **101**, 191108 (2012).
- [4] S. Q. Chen, *et al.*, *Opt. Express* **21**, 7570 (2013).
- [5] S. Q. Chen, *et al.*, *Opt. Express* **20**, 24843 (2012).
- [6] S. Q. Chen, *et al.*, *Opt. Express* **21**, 10597 (2013).

#### Authors

- S. Q. Chen, M. Yoshita, T. Ito, T. Mochizuki, C. Kim, H. Akiyama, A. Sato<sup>a</sup>, and H. Yokoyama<sup>a</sup>  
<sup>a</sup>Tohoku University

## Direct Short-Pulse Generation from Gain-Switched Semiconductor Lasers

### Akiyama Group

The compact, inexpensive, and easy-to-operate gain-switched semiconductor lasers have wide potential applications as pulse light sources in industries and medical treatments [1]. However, it was very difficult to obtain short pulses with duration shorter than 10 ps through gain-switching technique. We investigated gain-switching dynamics in various semiconductor lasers [2-4], and successfully achieved Fourier-transform limited picosecond optical pulses via spectral filtering technique from gain-switched semiconductor lasers [5, 6].

Excitation-power-dependent lasing spectra from a gain-switched distributed feedback (DFB) laser diode (LD) driven by pulsed current injection with duration of nanosecond are shown in Fig. 1(a). The spectral broadening as well as the down chirping (shown as the dashed line in Fig. 1(a)) on short wavelength side are typical phenomena reflecting the large variation of carrier density during pulse generation by gain switching [6], which in turn is an important reason that results in the broadening of the gain-switched output pulses. By utilizing spectral filtering technique to extract the transient short wavelength components (Fig. 1(b)) in the lasing spectra, we have successfully generated Fourier-transform limited 4.7-ps short pulses (Fig. 1(c)) from a gain-switched DFB-LD. The present technique provides a simple and practical method for short pulse generation and brings new insights for ultrafast nonlinear dynamics producing picosecond optical pulses by gain switching.

# Highlights of Joint Research

## Supercomputer Center

The Supercomputer Center (SCC) is a part of the Materials Design and Characterization Laboratory (MDCL) of ISSP. Its mission is to serve the whole community of computational condensed-matter physics of Japan providing it with high performance computing environment. In particular, the SCC selectively promotes and supports large-scale computations. For this purpose, the SCC invites proposals for supercomputer-aided research projects and hosts the Steering Committee, as mentioned below, that evaluates the proposals.

The ISSP supercomputer system consists of two subsystems: System A, which is intended for a parallel computation with relatively smaller number of nodes connected tightly, and System B, which is intended for more nodes with relatively loose connections. In July, 2010, the SCC replaced the two supercomputer subsystems. The current system B is SGI Altix ICE 8400EX, which consists of 30 racks or 15360 cores whereas the system A is NEC SX-9, which consists of 4 nodes or 64 cpus. They have in total 200 TFlops.

The hardware administration is not the only function of the SCC. The ISSP started hosting Computational Materials Science Initiative (CMSI), a new activity of promoting materials science study with next-generation parallel supercomputing. This activity is financially supported by the MEXT HPCI strategic program. In CMSI, a number of major Japanese research institutes in various branches of materials science are involved. The SCC supports the activities of CMSI as its major mission.

System C - FUJITSU PRIMEHPC FX10 has just been installed in April, 2013. It is highly compatible with K computer, the largest supercomputer in Japan. System C consists of 384 nodes, and each node has 1 SPARC64<sup>TM</sup> IXfx CPU (16 cores) and 32 GB of memory. The total system achieves 90.8 TFlops theoretical peak performance.

Class	Max/Min Points	Application	Number of Projects	Total Points			
				Applied		Approved	
				System A	System B	System A	System B
A	<100	any time	3	10	290	10	290
B	<2k	twice a year	49	14.5k	40.8k	14.1k	29.5k
C	<20k	twice a year	121	448.8k	919.4k	422.3k	406.5k
D	<20k	any time	11	0	94.0k	0	53.0k
E	<30k	twice a year	21	-	597.0k	-	286.0k
S	>10k	twice a year	0	0	0	0	0
CMSI				-	-	-	151.6k
Total			205	463.3k	1,651.5k	436.4k	926.9k

Table 1. Research projects approved in 2012

The maximum points allotted to the project of each class are the sum of the points for the two systems; Computation for 1 CPU•hour corresponds to 0.6 and 0.02 points for System-A and System-B, respectively.

All staff members of universities or public research institutes in Japan are invited to propose research projects (called User Program). The proposals are evaluated by the Steering Committee of SCC. Pre-reviewing is done by the Supercomputer Project Advisory Committee. In school year 2012 totally 205 projects were approved. The total points applied and approved are listed on Table 1 below.

The research projects are roughly classified into the following three (the number of projects approved):

First-Principles Calculation of Materials Properties (94)  
Strongly Correlated Quantum Systems (53)  
Cooperative Phenomena in Complex, Macroscopic Systems (58)

Projects in all three categories involve both methodology of computation and its applications. The results of the projects are reported in 'Activity Report 2012' of the SCC. Every year 3-4 projects are selected for "invited papers" and published at the beginning of the Activity Report. In the Activity Report 2012, the following three invited papers are included:

"First-Principles X-ray Photoelectron Spectroscopy Calculation on Defects in Semiconductors",  
Jun TAMAUCHI, Yoshihide YOSHIMOTO, and Yuji SUWA  
"Topological Hall Effect in Spatially Inhomogeneous Systems",  
Masafumi UDAGAWA  
"Huge-Scale Molecular Study of Multi-Bubble Nuclei",  
Hirosi WATANABE and Nobuyasu ITO

## Neutron Science Laboratory

The Neutron Science Laboratory (NSL) has been playing a central role in neutron scattering activities in Japan since 1961 by performing its own research programs as well as providing a strong General User Program with the university-owned various neutron scattering spectrometers installed at the JRR-3 (20MW) operated by Japan Atomic Energy Agency (JAEA) in Tokai (Fig. 1). In 2003, the Neutron Scattering Laboratory was reorganized as the Neutron Science Laboratory to further promote the neutron science with use of the instruments in JRR-3. Under the General User Program supported by NSL, 14 university-group-owned spectrometers in the JRR-3 reactor are available for a wide scope of researches on material science, and proposals close to 300 are submitted each year, and the number of visiting users under this program reaches over 6000 person-day/year. In 2009, NSL and Neutron Science Laboratory (KENS), High Energy Accelerator Research Organization (KEK) built a chopper spectrometer, High Resolution Chopper Spectrometer, HRC, at the beam line BL12 of MLF/J-PARC



**Fig. 1.** The reactor of JRR-3. The eight neutron scattering instruments are attached to the horizontal beam tubes in the reactor experimental hall. Two thermal and three cold guides are extracted from the reactor core towards the guide hall to the left.

(Materials and Life Science Experimental Facility, J-PARC). HRC covers a wide energy and Q-range ( $10\mu\text{eV} < \hbar\omega < 2\text{eV}$  and  $0.02\text{\AA}^{-1} < Q < 50\text{\AA}^{-1}$ ), and therefore becomes complementary to the existing inelastic spectrometers at JRR-3. HRC started to accept general users through the J-PARC proposal system in FY2011.

Triple axis spectrometers, HRC, and a high resolution powder diffractometer are utilized for a conventional solid state physics and a variety of research fields on hard-condensed matter, while in the field of soft-condensed matter science, researches are mostly carried out by using the small angle neutron scattering (SANS-U) and/or neutron spin echo (NSE) instruments. The upgraded time-of-flight (TOF) inelastic scattering spectrometer, AGNES, is also available through the ISSP-NSL user program.

On March 11, 2011, a great earthquake with Magnitude 9.0 hit North East Coast of Japan. Fortunately, JRR-3 was under regular inspection and no serious accidents or damages were reported. However, the lifeline of Tokai Village area was lost for more than two weeks, and it took more than two months before damage inspection of JRR-3 could be started. As of May of 2013, JRR-3 has not restarted yet. General User Program of 2012 was cancelled and that of 2013 has been suspended so far. In order to compensate the loss of the activity of NSL, a number of proposals accepted in 2011



**Fig. 2.** The U.S.-Japan spectrometer, CTAX, installed at the cold guide line CG4, High Flux Isotope Reactor (HFIR), in Oak Ridge National Laboratory. Members who contributed the relocation project of the U.S.-Japan spectrometer celebrates the completion of the project in October 2010.)

and 2012 were transferred to overseas thanks to kind offer from the major facilities, namely, ORNL, ILL, ANSTO, and HANARO.

Research topics in FY2012 cover Hydrogen release from Li alanates originates in molecular lattice instability (6G: TOPAN T1-3:HERMES), Direct observation of antiferromagnetic ordering in s electrons confined in regular nanospace of sodalite (5G:PONTA), Structural analysis of high performance ion-gel comprising tetra-PEG networks (SANS-U), Neutron scattering studies of Ti-Cr-V bcc alloy with the residual hydrogen and deuterium (AGNES). In addition, there are a variety of activities on fundamental physics, neutron beam optics, developments of neutron scattering techniques.

The NSL also operates the U.S.-Japan Cooperative Program on neutron scattering, providing further research opportunities for material scientists who utilize the neutron scattering technique for their research interests. In 2010, relocation of the U.S.-Japan triple-axis spectrometer, CTAX, was completed, and it is now open to users (Fig. 2). <http://neutrons.ornl.gov/instruments/HFIR/CG4C/>

The activity report on Neutron Scattering Research in FY2011 is given in NSL-ISSP Activity Report vol. 18 (2011), which can be downloaded from the following URL, [http://quasi.issp.u-tokyo.ac.jp/actrep/actrep-18-2011/index-rep\\_vol18.html](http://quasi.issp.u-tokyo.ac.jp/actrep/actrep-18-2011/index-rep_vol18.html)

The list of publication is also given at, ([http://quasi.issp.u-tokyo.ac.jp/actrep/actrep-18-2011/index-pub\\_vol18.html](http://quasi.issp.u-tokyo.ac.jp/actrep/actrep-18-2011/index-pub_vol18.html)).

## International MegaGauss Science Laboratory

The objective of this laboratory (Fig.1) is to study the physical properties of solid-state materials (such as semiconductors, magnetic materials, metals, insulators, superconducting materials) under ultra-high magnetic field conditions. Such a high magnetic field is also used for controlling the new material phase and functions. Our pulse magnets, at moment, can generate up to 87 Tesla (T) in a non-destructive manner, and from 100 up to 730 T (the world strongest as an in-door record) by destructive methods.

They are open to scientists both from Japan and from overseas, especially from Asian countries, and many fruitful results are expected to come out not only from collaborative research but also from our in-house activities. One of



**Fig. 1.** Signboard at the entrance of the IMGSL.



Fig. 2. The building for the flywheel generator (left hand side) and a long-pulse magnet station (right hand side). The flywheel giant DC generator is 350 ton in weight and 5 m high (bottom). The generator, capable of a 51 MW output power with the 210 MJ energy storage, is planned to energize the long-pulse magnet generating 100 T without destruction.

our ultimate goals is to provide the scientific users as our joint research with magnets capable of a 100 T, millisecond pulses in a non-destructive mode, and to offer versatile precision physical measurements. The available measuring techniques now include magneto-optical measurements, cyclotron resonance, spin resonance, magnetization and transport measurements.

Our interests cover quantum phase transitions (QPT) induced by high magnetic fields. Field-induced QPT has been explored in various materials such as quantum spin systems, strongly correlated electron systems and other magnetic materials. Non-destructive strong pulse magnets are expected to provide us with reliable and precise solid state physics measurements. The number of collaborative groups for the research is over 50 in the year of 2012.

A 210 MJ flywheel generator (Fig.2) which is the world's largest DC power supply has been installed in the newly built

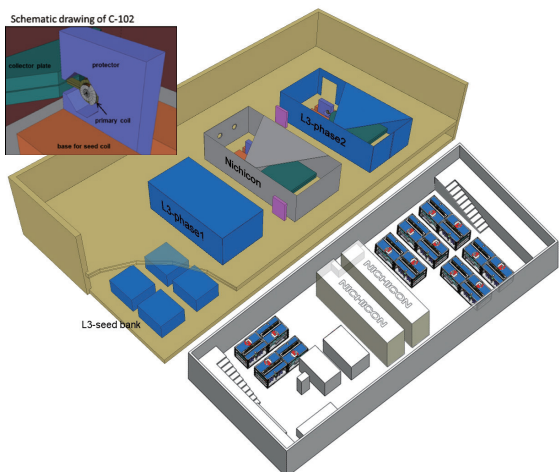


Fig. 3. (Build. C) The building for the electro-magnetic flux compression, generating over 700 T. 1000 T project started since 2010, and finally condenser banks of 9 MJ (5 MJ + 2 MJ + 2 MJ) as a main system with the 2 MJ sub bank system for the seed field will be installed, and will be completed in the year of 2013.

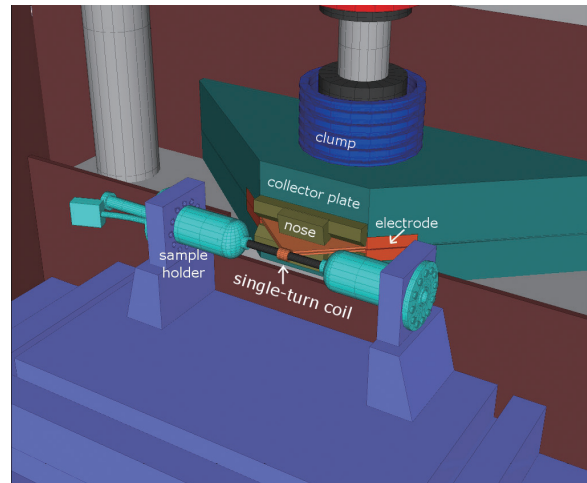


Fig. 4. Schematic picture of the H-type single-turn coil equipped with a 50 kV, 200 kJ fast operating pulse-power system, capable of generating 300 T within 3 mm bore coil.

DC flywheel generator station at our institute. The generator, once used for Toroidal magnet coil in JFT-2M (JAERI Fusion Torus-2M) Tokamak nuclear fusion testing device, is now renewed as a power supply for the pulse magnets. The construction of the magnet service station has also been accomplished. The magnet technologies are intensively devoted to the quasi-steady long pulse magnet (of order of 1-10 sec) energized by the giant DC power supply, and also used for the outer-magnet coil to realize a 100 T nondestructive magnet.

Developments of our destructive magnets are currently in progress. The ultra-high magnetic fields are obtained in a microsecond time scale. The electromagnetic flux compression (EMFC) system is equipped with a 5 MJ condenser bank and its seed coils with a 1.5 MJ condenser bank. The protector chamber and iron block protectors were refined against stronger explosion than before to be endurable against explosion by a full injection of 5 MJ. By devising copper lined primary coil, we could improve energy transfer efficiency from the primary coil to the liner kinetic energy compressing the magnetic flux. The seed field coils providing the initial magnetic flux are also newly designed and the maximum magnetic field was increased from 3.2 T to over 4.4 T at the position of the primary coil. These efforts led us to obtain the maximum magnetic field of 730 T by a 4 MJ injection of the EMFC recognized as a renewal of the world record as an indoor experiment. We have started a new project of the EMFC aiming at achieving 1000 T and its application to the materials science, financed by the ministry of education, culture, sports, science and technology in the fiscal year of 2010 and 2011 (Fig.3).

As an easy access to the megagauss science and technology, we have the single-turn coil (STC) system capable of generating the fields of up to 300 T by a fast-capacitor of 200 kJ. We have two STC systems, one is a horizontal type (H-type, Fig.4) and the other is a vertical type (V-type). Various kinds of laser spectroscopy experiments such as the cyclotron resonance and the Faraday rotation using the H-type STC are available. On the other hand, for very-low temperature experiments, a combination of the V-type STC and a liquid helium bath cryostat is very useful; the precise magnetization measurements at 2.5 K can be performed up to 120 T.

	Alias	Type	B <sub>max</sub>	Pulse width Bore	Power source	Applications	Others
Building C Room 101-113	Electro- Magnetic Flux Compression	destructive	730 T	$\mu$ s 10 mm	5 MJ, 40kV	Magneto-Optical Magnetization	5 K – Room temperature
	Horizontal Single-Turn Coil	destructive	300 T 200 T	$\mu$ s 5 mm 10 mm	0.2 MJ, 50 kV	Magneto-Optical measurements Magnetization	5 K – 400 K
	Vertical Single-Turn Coil	destructive	300 T 200 T	$\mu$ s 5 mm 10 mm	0.2 MJ, 40 kV	Magneto-Optical Magnetization	2 K – Room temperature
Building C Room 114-120	Mid-Pulse Magnet	Non-destructive	60 T  70 T	40 ms 18 mm  40 ms 10 mm	0.9 MJ, 10 kV	Magneto-Optical measurements Magnetization Magneto-Transport Hall resistance Polarization Magneto-Striction Magneto-Imaging Torque Magneto- Calorimetry Heat Capacity	Independent Experiment in 5 site  Lowest temperature 0.1 K
Building C Room 121	PPMS	Steady State	14 T			Resistance Heat Capacity	Down to 0.3 K
	MPMS	Steady State	7 T			Magnetization	
Building K	Short-Pulse magnet	Non-destructive	87 T (2-stage pulse)  85 T	5 ms 10 mm  5 ms 18 mm	0.5 MJ, 20 kV	Magnetization Magneto-Transport	2K – Room temperature
	Long-Pulse magnet	Non-destructive	30 T	0.5 s 30 mm	210 MJ, 2.7 kV	Resistance Magneto-Calorimetry	2K – Room temperature

Table 1. Available Pulse Magnets, Specifications

## Center of Computational Materials Science

K-computer at Kobe won the title of the world's fastest computer at TOP500 ranking announced at International Supercomputing Conference (ISC) 11. Though it is in the 3rd place in the list as of today, it is still providing the Japanese scientific community with an incomparable amount of computational resources. With the advancement of hardware and software technologies, large-scale numerical calculations have been making important contributions to materials science and will have even greater impact on the field in the near future. Center of Computational Materials Science (CCMS) was founded as a specialized research center for promoting computer-aided materials science with massively parallel computation using K-computer. This center also functions as the headquarters of Computational Materials Science Initiative (CMSI), which is an inter-institutional organization for computational science of a broad range of disciplines, including molecular science, quantum chemistry, biological materials, and solid state physics. ISSP made contracts with 9 universities and 2 national institutes for supporting the activities of CMSI in which nearly 100 research groups are involved. The main purpose of CMSI is to establish a new community of computational science in which researchers from different backgrounds work together on grand challenge problems, thereby developing computational infrastructures (new algorithms, coding styles, standard software packages, etc) and inspire young scientists.

A branch office of CCMS was also established in the RIKEN AICS building on the Port Island Kobe, where K-computer is located, for supporting CMSI researchers getting together at Kobe to fine-tune various applications software for K-computer. It also helps developing better contact with staff members of RIKEN, the operating institute of K-computer. Another mission of the Kobe branch of CCMS is exchanging ideas and techniques with researchers from other fields of computer science. (There are 5 major



Fig. 1. K-Computer



Fig. 2. Summer School in Zao

fields in the HPCI strategic program of MEXT, “biology”, “materials and energy” (our field), “seismology, oceanography and meteorology”, “industrial applications”, and “high-energy physics and cosmology”).

The following is the selected list of meetings organized by CMSI and CCMS in SY2012:

- “K-Computer Users' Forum”  
(May 10/2012, Kobe)
- “Joint-Meeting between Field 2 and 5”  
(May 30/2012 Kashiwa)
- “Material Simulation in Petaflops Era (MASP) 2012”  
(June 25-July 13/2012, Kashiwa)
- “Workshop: Programming Techniques for K-Computer”  
(July 17-19/2012, Kakegawa)
- “Summer School: New Materials and New Quantum States”  
(Aug. 20/2012, Zao)
- “RSC-CMSI Joint Symposium: Multi-scale Structures Research” (Sep. 15/2012, Hyogo)
- “CMSI Symposium”  
(Dec. 03-05/2012, Okazaki)
- “Interdisciplinary Workshop on Numerical Methods for Many-Body Correlations” (Feb. 05-06/2013, Hongo)
- “CMSI Kobe Hands-On: FMO Tutorial”  
(Feb. 07/2013, Kobe)
- “Workshop on Synchrotron Radiation and Computational Physics” (Feb. 14/2013, Hongo)
- “Workshop: Programming Techniques for K-Computer”  
(Feb. 14-16/2013, Kanazawa)
- “Symposium: Visualization of Materials Science”  
(Mar. 05/2013, Akihabara)
- “CMSI Kobe Hands-On: ALPS Tutorial”  
(Mar. 06/2013, Kobe)
- “CMSI Kobe Hands-On: xTAPP Tutorial”  
(April 23/2013, Kobe)

## Synchrotron Radiation Laboratory

The Synchrotron Radiation Laboratory (SRL) was established in 1975 as a research division dedicated to solid state physics using synchrotron radiation (SR). In 1989, SRL started to hold the Tsukuba branch, a branch laboratory in the Photon Factory (PF), High Energy Accelerator Research Organization (KEK). SRL maintains a Revolver undulator, two beamlines and three experimental stations; BL-18A for angle-resolved photoemission spectroscopy with SCIENTA electron analyzer, while undulator beamline BL-19A and BL-19B, for spin- and angle-resolved photoelectron spectroscopy (SARPES) and soft X-ray emission spectroscopy experiments, respectively. Recently, a high-yield spin detector, using very low energy electron diffraction, was developed at BL-19A. SAPRES measurements have now been performed with high-resolution and the experiments at the beamline have become important for exciting topics of surface/solid state physics such as topological insulators and ferromagnetic nanofilms.

The SRL staffs have joined the Materials Research Division of the Synchrotron Radiation Research Organization (SRRO) of the University of Tokyo and they have played essential role in constructing a new high brilliant soft X-ray beamline, BL07LSU, in SPring-8. The light source is the polarization-controlled 25-m long soft X-ray undulator. The monochromator is equipped with varied-line-spacing plain grating, which covers the photon energy range from 250 eV to 2 keV. At the end of the beamline, four experimental stations have been developed for frontier spectroscopy researches: the three-dimensional (3D) nano-ESCA station, the soft X-ray emission spectroscopy (XES) station, the time-resolved soft X-ray spectroscopy (TR-SX) station, and the free-port station for any experimental apparatus.



Fig. 1. 3D nano ESCA at SPring-8 BL07LSU



Fig. 2. XES station at SPring-8 BL07LSU

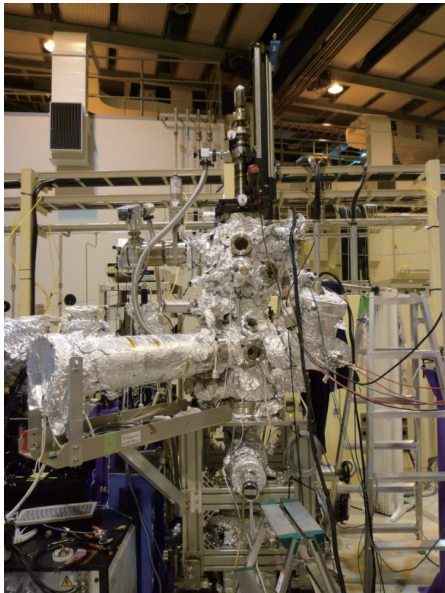


Fig. 3. TR-SX station at SPring-8 BL07LSU

The beamline construction was completed in 2009 and SRL established the Harima branch laboratory in SPring-8. The four end-stations have now been opened fully to outside users. In 2012, 110 researchers made their experiments during the SPring-8 operation time of 4000 hours.

Members of SRL have devoted themselves in serving users with technical supports and they have also carried out their own research works on advanced solid state spectroscopy. At SPring-8 BL07LSU, for example, the staffs have achieved the high performance at their stations: the 3D nano-ESCA reaches the spatial resolution of 70 nm, the XES station obtains spectra with energy resolving power  $E/\Delta E$  larger than 10,000, and the TR-SX makes the laser -pump and SR-probe method with the time-resolution of 50 ps which corresponds to the SR pulse-width.

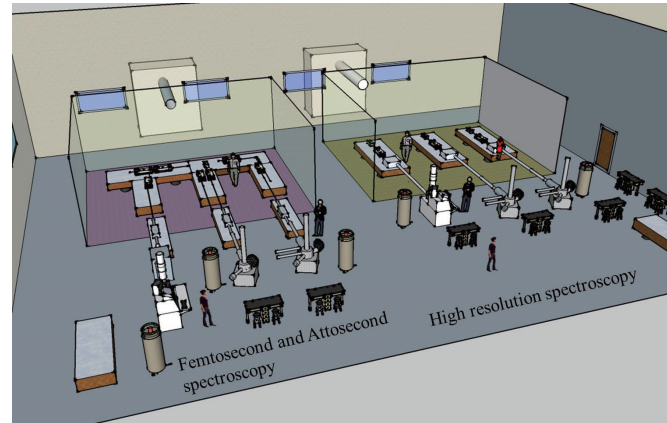


Fig. 2. Image of laser activities in Building E

time-resolved, spin-resolved spectroscopy, diffraction, light scattering, imaging, microscopy and fluorescence spectroscopy, by new coherent light sources based on laser and synchrotron radiation technology over a wide spectrum range from terahertz to soft X-ray. In LASOR center, a variety of materials sciences, such as semiconductors, strongly-correlated materials, molecular materials, surface and interfaces, and bio-materials, are studied using advanced light sources and advanced spectroscopy. Another aim of LASOR center is to promote the collaboration between the advanced photon sciences and materials sciences. Most of the research activities on the development of new lasers with an extreme performance and the application to material science are studied in specially designed Buildings D and E with large clean rooms and the isolated floor in Kashiwa Campus. On the other hand, the experiments utilizing the synchrotron radiation are performed at beamline BL07LSU in SPring-8 (Hyogo) by Synchrotron Radiation Laboratory in LASOR center.

## Laser and Synchrotron Research Center

Laser and Synchrotron Research (LASOR) Center started from October, 2012. LASOR center consists of extreme laser groups and Synchrotron Radiation Laboratory. LASOR center develops new lasers with extreme performance of ultra-precise, high intensity and ultra-short pulse lasers, and the cutting edge synchrotron radiation beamline in soft X-ray region. LASOR center is responsible for the advanced spectroscopy, such as ultra-high resolution photoemission,



Fig. 1. Open ceremony of LASOR center

# Unconventional Magnetic and Thermodynamic Properties of $S = 1/2$ Spin Ladder with Ferromagnetic Legs

H. Yamaguchi and T. Sakakibara

Spin-ladder systems have been investigated both theoretically and experimentally in relation in particular to field-induced quantum phase transitions and high- $T_c$  superconductivity. Among these systems, antiferromagnetic (AFM) two-leg spin ladders, which have AFM rung and leg interactions, have been most extensively studied and have turned out to show attractive behaviors originating from their strong quantum fluctuations. By contrast, a spin ladder with ferromagnetic (FM) leg interactions, which can be viewed as antiferromagnetically coupled FM chains, has not been realized experimentally. Its ground state and the magnetic behavior have been discussed extensively from a theoretical point of view as an example of complicated quantum spin systems. The experimental verification of these properties is thus quite significant for studies on complicated quantum behavior unsuspected in conventional spin systems.

Here, we report the first model compound of an  $S = 1/2$  two-leg spin ladder with FM leg interaction [1]. We have succeeded in synthesizing a new verdazyl radical 3-Cl-4-F-V [3-(3-chloro-4-fluorophenyl)-1,5-diphenylverdazyl] and solved its crystal structure. The *ab initio* molecular orbital (MO) calculation indicated the formation of an  $S = 1/2$  two-leg spin ladder with FM leg and AFM rung interactions. The experimental results of magnetic susceptibility, magnetization curve, and specific heat were successfully explained as the expected spin-ladder model by using the quantum Monte Carlo method.

Figures 1(a) and 1(b) show the low-temperature region of the magnetic susceptibility and magnetic specific heat in various magnetic fields, respectively. At higher magnetic fields, we observed extrema of the magnetic susceptibility, which appear almost symmetrically with respect to the curve at 3.0 T. Regarding the magnetic specific heat, the anomaly observed at zero field splits into two peaks above 1.5 T, as shown in Fig. 1(b). Figure 2 shows the temperature-field phase diagram obtained from those specific temperatures. The transition point shifts toward the high-temperature region with an increasing magnetic field up to 3.0 T. This type of phase boundary shape is often associated with the field-induced phase transition in a gapped spin system. Since

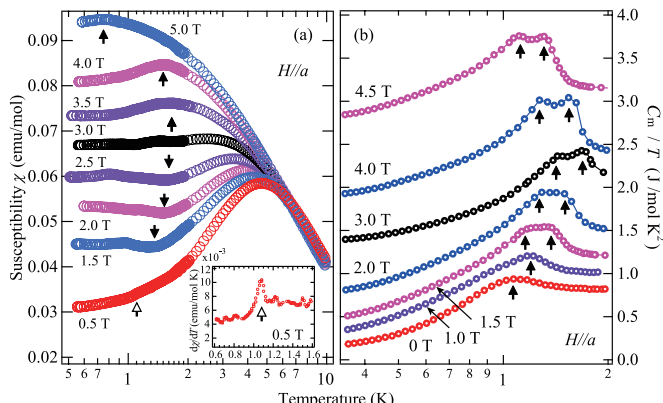


Fig. 1. Temperature dependence of (a) the magnetic susceptibility and (b)  $C_m/T$  of 3-Cl-4-F-V in various magnetic fields for  $H//a$ . The arrows indicate the phase transition temperatures. For clarity,  $C_m/T$  for 1.0, 1.5, 2.0, 3.0, 4.0, and 4.5 T have been shifted up by 0.2, 0.4, 0.7, 1.3, 1.7, and  $2.5 \text{ J} \cdot \text{mol}^{-1} \cdot \text{K}^{-1}$ , respectively. The inset shows the temperature derivative of the magnetic susceptibility at 0.5 T.

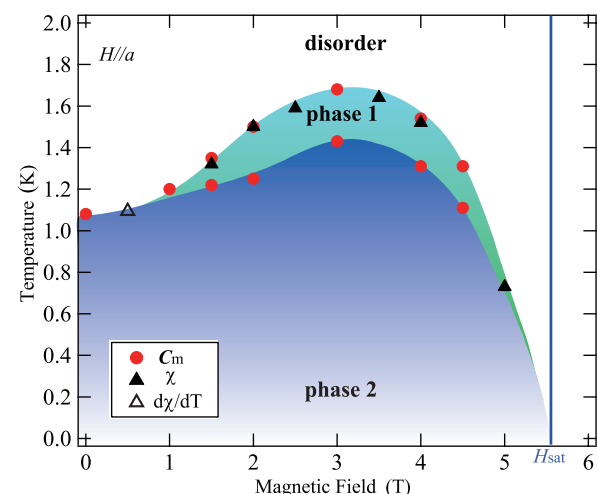


Fig. 2. Magnetic field versus temperature phase diagram of 3-Cl-4-F-V for  $H//a$ . The closed circles, closed triangles, and open triangle indicate the transition temperatures determined from the magnetic specific heat, the magnetic susceptibility, and its temperature derivative, respectively. The solid vertical line indicates the saturation field.

the expected small energy gap of 1.06 K is considered to disappear owing to the weak interladder interactions, the present system must be in the vicinity of the quantum critical point between the gapped rung-singlet and the gapless ordered phases. Considering the magnetic specific heat, we should take into account the possibility of successive phase transitions, which is often induced by large magnetic anisotropy and/or noncollinear magnetic structure. Since organic radical systems have negligibly weak magnetic anisotropy, we can suggest the possibility of noncollinear magnetic structure induced by frustration. The MO calculation indicated that there are three kinds of possible small interladder interactions. These three interactions can form frustrated lattices, and then a noncollinear magnetic structure will appear. This unexpected field-induced successive phase transition possibly originates from the interplay of low dimensionality and frustration. The present results will stimulate studies on spin ladder with FM interactions and unconventional behavior of the complicated quantum spin systems.

## Reference

- [1] H. Yamaguchi, K. Iwase, T. Ono, T. Shimokawa, H. Nakano, Y. Shimura, N. Kase, S. Kittaka, T. Sakakibara, T. Kawakami, and Y. Hosokoshi, Phys. Rev. Lett. **110**, 157205 (2013).

## Authors

H. Yamaguchi<sup>a</sup>, K. Iwase<sup>a</sup>, T. Ono<sup>a</sup>, T. Shimokawa<sup>b</sup>, H. Nakano<sup>c</sup>, Y. Shimura<sup>d</sup>, N. Kase<sup>d</sup>, S. Kittaka<sup>d</sup>, T. Sakakibara<sup>d</sup>, T. Kawakami<sup>c</sup>, and Y. Hosokoshi<sup>a</sup>

<sup>a</sup>Osaka Prefecture University

<sup>b</sup>Kobe University

<sup>c</sup>University of Hyogo

<sup>d</sup>Osaka University

## Axion Electrodynamics and Condensed Matter

H. Ooguri and M. Oshikawa

Condensed matter physics and high-energy physics deal with phenomena at very different scales. Nevertheless, surprisingly often we encounter similar mathematical structures in these two different subfields of physics. Indeed, those encounters have been very fruitful for new devel-

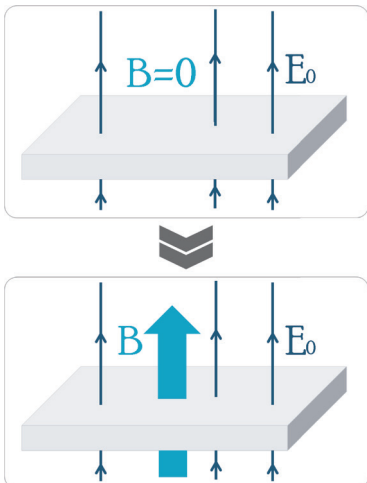


Fig. 1. The phase transition of the “axion” field takes place under an applied electric field  $E_0$  above the critical value. It results in a spontaneous generation of magnetic field, even though no magnetic field is applied externally. (Figure drawn by Euan McKay and Azusa Minamizaki, reprinted from Todai Research Editor’s Choice: <http://www.u-tokyo.ac.jp/en/todai-research/editors-choice/theory-of-undiscovered-elementary-particle-applied-to-topological-insulator/>)

opments in physics: notable examples include Nambu’s development of spontaneous symmetry breaking in field theory with a hint from superconductivity, and Wilson’s renormalization group unifying critical phenomena and field theory. Very recently, application of AdS/CFT correspondence to condensed matter is actively pursued. The foundation of IPMU (Institute for Physics and Mathematics of the Universe, now Kavli IPMU) in 2007 and opening of its building next to ISSP in 2010 provides a great opportunity for ISSP. In 2010, IPMU and ISSP co-hosted a workshop “Condensed Matter Physics Meets High-Energy Physics” to stimulate exchanges between the two fields.

Here we report on a recent joint research [1] between the two institutes. “Axion” is a hypothetical elementary particle, which has not yet been detected experimentally, but could be a key to solve mysteries in high-energy physics and cosmology. Recently, instability of axion field in the presence of strong electric field has been pointed out in high-energy physics. While the original axion as an elementary particle would not directly appear in condensed matter, it was pointed out [2] that doping of magnetic ions to a topological insulator results in fluctuating magnetic moments, which could be described by a similar field theory as the one of axions. We investigated the instability of the “axion” field in the condensed matter realization. It also led to a understanding of the physical mechanism of the instability, and to the clarification of the final state reached as a result of the instability. Above a critical electric field, magnetic field is spontaneously generated, and the excess electric field is screened by the effective surface charge induced by the deformation of the “axion” field and the magnetic field.

#### References

- [1] H. Ooguri and M. Oshikawa, Phys. Rev. Lett. **108**, 161803 (2012).
- [2] R. Li, J. Wang, X.-L. Qi, and S.-C. Zhang, Nature Phys. **6**, 284 (2010).

#### Authors

H. Ooguri<sup>a</sup> and M. Oshikawa  
<sup>a</sup>Kavli IPMU and California Institute of Technology

## Band-Gapped Graphene Nanoribbons Made by Molecular Beam Epitaxy

S. Tanaka and F. Komori

Graphene nanoribbons (GNRs) are attracting much attention in solid state physics and nanoelectronic applications, where the band-gap opening or modification of the electronic structure at K-points is a central interest. The electronic structure at K-points in GNRs has been theoretically shown to depend on the type of edge geometry: armchair or zigzag [1]. Semiconducting characteristics are expected in the case of armchair edges owing to the band-gap opening at K-points. As the width of GNRs is reduced, the gap is increased by both electron confinement and edge effects. However, realization of GNRs with atomically well-defined edges and providing experimental evidences of the gap opening at K-points remain challenging. Here we demonstrate a new approach for producing a dense array of aligned GNRs on unique SiC surfaces [2] as templates via molecular beam epitaxy (MBE), and show band-gap openings at K-points visualized by angle-resolved photoemission spectroscopy (ARPES) [3].

In the present study, we used an off-axis SiC substrate (Si-face, 4° off toward [1-100]), and first prepared a self-ordered periodic structure consisting of pairs of a (0001) basal plane terrace and a (1-10n) nanofacet ( $n = 35\sim37$ ) with a characteristic periodicity of ~ 20 nm by H<sub>2</sub> gas etching [2]. A typical atomic-force-microscopy (AFM) image of the substrate and a model are shown in Fig. 1. After cleaning the surface of the substrate under Si flux at 1050°C, a carbon mono-atomic layer with  $(6\sqrt{3}\times6\sqrt{3})R30^\circ$  registry was grown exclusively on the SiC terrace by MBE. Finally, the samples were exposed to H<sub>2</sub> gas at 600°C for 1 h to transform the carbon layer into quasi-free-standing graphene by hydrogen intercalation. The GNRs thus made have armchair edges parallel to the step edge of the substrate. Quality of the graphene was evaluated by AFM, scanning tunneling microscopy, reflection high-energy electron diffraction, low-energy electron diffraction, and Raman spectroscopy.

Figure 2(a) shows the ARPES result along the  $\Gamma$ -K-M lines of the graphene surface Brillouin zone. The measured  $\Gamma$ -K-M direction in k-space corresponds to the [1-100] direction in real space, which is perpendicular to the edges of the GNRs. A conduction band is invisible, and the valence band is folded at the K-point area, as shown in Fig. 2(b). No states are detected at the K-point between the Fermi energy ( $E_F$ ) and top of the valence band, which is 0.14 eV below  $E_F$ .

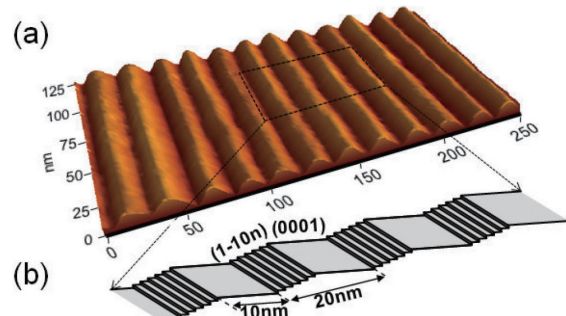


Fig. 1. (a) An AFM 3-dimensional view of the vicinal SiC(0001) surface after hydrogen etching, showing a periodic array of terrace and facet structure. (b) A schematic drawing of the SiC surface in (a). This was derived from high-resolution transmission electron microscopy images. Each pair of array consists of the (0001) terrace and (1-10n) facet, and is ordered with the periodic distance of ~ 20 nm. Here,  $n = 37$ . The width of each (0001) terrace is ~ 10 nm.

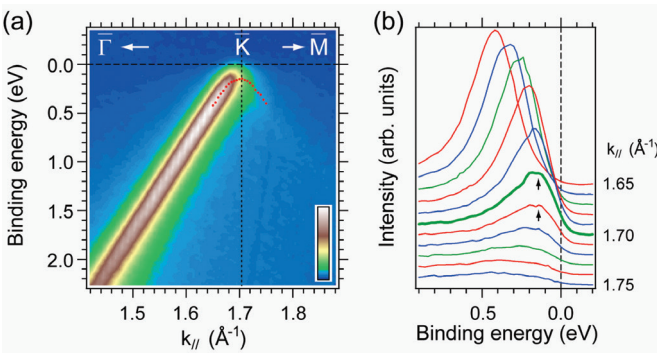


Fig. 2. Intensity map (a) and energy distribution curves (EDCs) (b) of the ARPES spectra around the K-point for the GNRs on the vicinal SiC(0001) substrate. The spectra are taken along the  $\Gamma$ -K-M line. The EDCs show the folding of the valence band at the K-point below  $E_F$ . The red dots in (a) indicate the positions of the EDC peaks and represent band dispersion around the K-point. The intensity map indicates a linear dispersion, which is consistent with the valence band of single-layer graphene.

The band-gap value can be more than 0.28 eV if we assume a slight p-type doping in the sample as in the case of the hydrogen-intercalated graphene on SiC(0001). This value is consistent with the theoretical estimation for the GNR with the width of 10 nm.

#### References

- [1] K. Nakada *et. al.*, Phys. Rev. B **54**, 17954 (1996).
- [2] H. Nakagawa *et. al.*, Phys. Rev. Lett. **91**, 226107 (2003).
- [3] T. Kajiwara *et. al.*, B **87**, 121407(R) (2013).

#### Authors

T. Kajiwara<sup>a</sup>, Y. Nakamori<sup>a</sup>, A. Visikovskiy<sup>a</sup>, T. Iimori, F. Komori, K. Nakatsuji<sup>b</sup>, K. Mase<sup>c</sup>, and S. Tanaka<sup>a</sup>

<sup>a</sup>Kyushu University

<sup>b</sup>Tokyo Institute of Technology

<sup>c</sup>High Energy Accelerator Research Organization

## Spin Filtering in Oxide Tunnel Junctions

I. Ohkubo, T. Harada, and M. Lippmaa

The operation of conventional functional tunnel devices, such as tunnel magnetoresistance junctions or Josephson junctions, is derived from the physical properties of the electrode materials, such as soft ferromagnets or superconductors. The tunnel barrier is usually a passive element in a junction, simply providing a suitable separation between

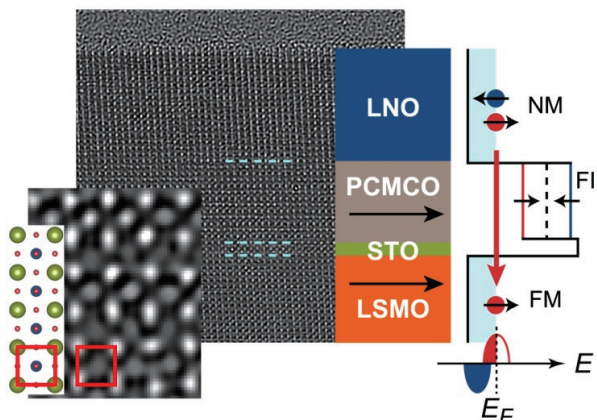


Fig. 1. Cross-sectional electron microscope image and a schematic diagram of a spin-filter tunnel junction consisting of normal metal (NM)  $\text{LaNiO}_3$  (LNO) injection electrode, a  $\text{Pr}_{0.8}\text{Ca}_{0.2}\text{Mn}_{1-y}\text{Co}_y\text{O}_3$  (PCMCO) tunnel barrier, a  $\text{SrTiO}_3$  (STO) spacer, and a ferromagnetic (FM) spin detector  $\text{La}_{0.6}\text{Sr}_{0.4}\text{MnO}_3$  (LSMO).

the functional electrodes. The appearance of a ferromagnetic insulator state in mixed-valent manganites opens a possibility to construct a different type of junction, where the electrodes are passive and the functional element is the tunnel barrier itself. The junctions developed in this project contain tunnel barriers made of 10 to 12 unit cells of  $\text{Pr}_{0.8}\text{Ca}_{0.2}\text{Mn}_{1-y}\text{Co}_y\text{O}_3$  [1]. The ferromagnetic insulating state can be achieved by a suitable Pr/Ca ratio, while the saturation magnetization can be adjusted by Co doping. The electrodes of the junctions were made of a normal metal  $\text{LaNiO}_3$  and a ferromagnetic metal  $\text{La}_{0.6}\text{Sr}_{0.4}\text{MnO}_3$ , as illustrated in Fig. 1. Electrons tunneling from the  $\text{LaNiO}_3$  electrode to the  $\text{La}_{0.6}\text{Sr}_{0.4}\text{MnO}_3$  side see different barrier heights, depending on spin state, due to an exchange splitting in the magnetic barrier layer. The spin injection rate into the ferromagnetic  $\text{La}_{0.6}\text{Sr}_{0.4}\text{MnO}_3$  electrode is thus different for spin-up and spin-down electrons.

The  $\text{La}_{0.6}\text{Sr}_{0.4}\text{MnO}_3$  layer in the junction works not only as a metallic electrode but also as a built-in ferromagnetic spin detector. Due to strong spin polarization in  $\text{La}_{0.6}\text{Sr}_{0.4}\text{MnO}_3$ , a spin-filtered tunneling current can only flow through the device when the magnetization directions in the ferromagnetic barrier and electrode layers are parallel. The efficiency of the tunnel barrier spin filter can therefore be determined easily by measuring the junction resistance as a function of an applied magnetic field (Fig. 2). Such a plot shows high resistance when the applied field has just changed sign and the magnetically soft  $\text{La}_{0.6}\text{Sr}_{0.4}\text{MnO}_3$  electrode layer magnetization has flipped antiparallel to the tunnel barrier layer. Above the coercive field of the barrier layer, at an applied field of about 200 mT, the whole device magnetizes in the same direction and the total resistance drops sharply. The magnetoresistance ratio of over 100% is among the largest seen for any spin-filter junction.

Spin-filter junctions have several interesting uses, the most important being an efficient spin injector for semiconducting spintronic devices. Since the material in contact with a semiconductor is insulating, a spin-filter tunnel junction injector does not suffer from an impedance mismatch that occurs when a ferromagnetic metallic electrode is used as a spin-polarized current source in a semiconductor device. Analysis of spin filter efficiencies and inelastic electron tunneling spectroscopy showed that the choice of the normal metal electrode material is important in achieving efficient spin injection [2]. The use of a perovskite-type  $\text{LaNiO}_3$  electrode that was lattice matched (Fig. 1) with the insulator layer greatly increased the magnetoresistance ratio of the junctions, indicating improved spin filtering contrast. An approximate matching of the Fermi surface shapes

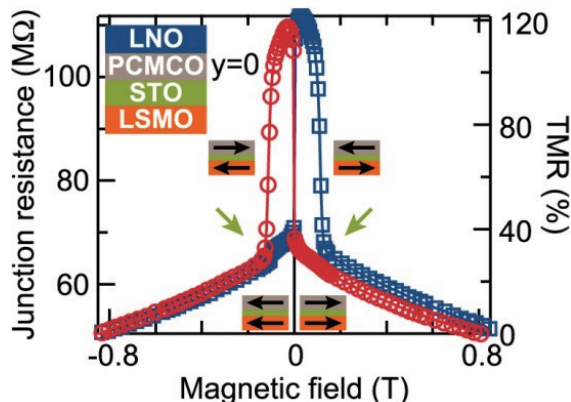


Fig. 2. Tunnel magnetoresistance response of a spin-filter tunnel junction at 4 K, showing a resistance switching ratio of over 100%.

of the electrode materials appeared to reduce scattering of tunneling electrons, further improving the spin filter efficiency.

## References

- [1] T. Harada, I. Ohkubo, M. Lippmaa, Y. Sakurai, Y. Matsumoto, S. Muto, H. Koinuma, and M. Oshima, *Adv. Funct. Mater.* **22**, 4471 (2012).
- [2] T. Harada, I. Ohkubo, M. Lippmaa, Y. Sakurai, Y. Matsumoto, S. Muto, H. Koinuma, and M. Oshima, *Phys. Rev. Lett.* **109**, 076602 (2012).

## Authors

- T. Harada, I. Ohkubo<sup>a,b</sup>, M. Lippmaa, Y. Sakurai<sup>b</sup>, Y. Matsumoto<sup>c</sup>, S. Muto<sup>d</sup>, H. Koinuma<sup>e,f</sup> and M. Oshima<sup>b</sup>
- <sup>a</sup>National Institute for Materials Science  
<sup>b</sup>Department of Applied Chemistry, University of Tokyo  
<sup>c</sup>Tokyo Institute of Technology  
<sup>d</sup>Nagoya University  
<sup>e</sup>Graduate School of Frontier Sciences, University of Tokyo  
<sup>f</sup>Pusan National University

## Anisotropy of Upper Critical Field in a One-Dimensional Organic System, $(\text{TMTTF})_2\text{PF}_6$ under High Pressure

M. Kano and M. Itoi

The Bechgaard salt  $(\text{TMTSF})_2\text{PF}_6$  ( $\text{TMTSF}$  = tetramethyltetraselenafulvalene) was the first organic superconductor discovered in 1980 with a superconducting temperature of  $T_c = 0.9$  K (critical pressure,  $P_c = 1.2$  GPa) [1]. Since this discovery, materials based on  $\text{TMTSF}$  and its derivatives, such as  $\text{TMTTF}$  (tetramethyltetraethiofulvalene), the so-called  $(\text{TMTCF})_2\text{X}$  ( $\text{X}$  = monovalent anion) series, have been investigated extensively to search for other superconducting behaviors. They also attracted attention owing to their rich properties such as spin-Peierls (SP), charge-ordering (CO), spin density wave (SDW), and possible unconventional superconductivity (SC) that appear by changing the counter

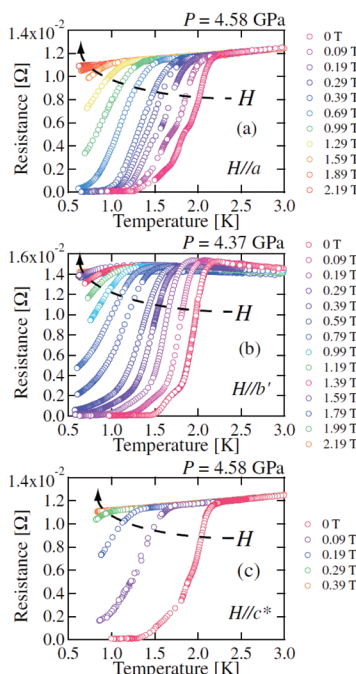


Fig. 1. The temperature-dependent resistivity of  $(\text{TMTTF})_2\text{PF}_6$  was measured up to 7 GPa using a turnbuckle-type diamond anvil cell (DAC) and at magnetic fields of up to 5 T. The applied magnetic fields were (a) parallel to the  $a$ -axis at  $P = 4.58$  GPa, (b)  $b'$ -axis at  $P = 4.37$  GPa and (c)  $c^*$ -axis at  $P = 4.58$  GPa.

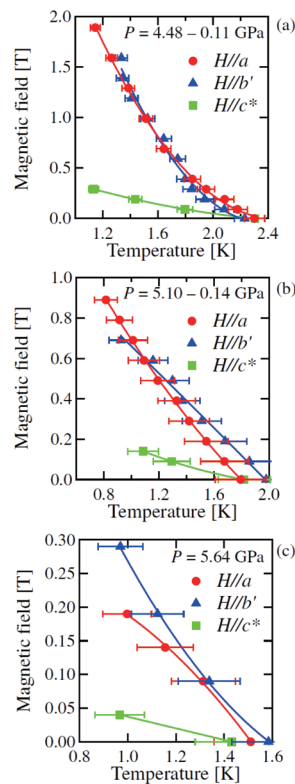


Fig. 2.  $H_{c2}$  curves with applied fields  $H \parallel a$ ,  $H \parallel b'$  and  $H \parallel c^*$  for  $P =$  (a) 4.48, (b) 5.10 and (c) 5.64 GPa obtained by using the onset criterion.

anion or by applying external pressure [2]. Many compounds with  $\text{TMTSF}$  molecules exhibit an SC state at low pressures of approximately 1 GPa, whereas most compounds with  $\text{TMTTF}$  exhibit an SC transition at ultra high pressures, for example,  $P_c = 5$  GPa in  $(\text{TMTTF})_2\text{PF}_6$  [3,4,5]. Taking advantage of the low pressure induced and ambient pressure superconductivity, the characteristic for SC phase has been well studied with  $\text{TMTSF}$  salts, but rarely with  $\text{TMTTF}$  salts owing to the technical difficulty in applying hydrostatic pressure to the fragile organic compounds at low temperatures in magnetic fields. Recently, we have succeeded in resistivity measurement by using a turnbuckle-type Diamond anvil cell (DAC) on  $(\text{TMTTF})_2\text{PF}_6$  under multi-extreme conditions which was previously difficult to achieve [6]. We report on the characteristic superconductivity on  $(\text{TMTTF})_2\text{PF}_6$ .

The resistivity of  $(\text{TMTTF})_2\text{PF}_6$  one-dimensional exhibits strong anisotropy at ambient pressure. In the stacking direction of  $\text{TMTTF}$  molecules ( $a$ -axis), the metal-insulator (M-I) transition was suppressed with increasing external pressure, and the superconductivity was observed in the range of  $P = 4.18$  to  $6.03$  GPa. The highest SC transition temperature is  $T_c = 2.25$  K at  $4.58$  GPa, and no SC transition was observed above  $P = 6.96$  GPa. The presence of zero resistance was confirmed at approximately 1.5 K in the pressure range of  $4.18 \leq P \leq 4.58$  GPa.

Data of resistivity vs temperature at  $P = 4.37$ - $4.58$  GPa with the field along three different axes are shown in Fig. 1, and the temperature dependence of  $H_{c2}$  along the three axes on  $(\text{TMTTF})_2\text{PF}_6$  is described in Fig. 2.

The  $H_{c2}$  has a positive curvature without saturation, which may be attributed to an FFLO state, for a magnetic field along the  $a$  (intra-chain direction) – and  $b'$  (inter-chain direction)- axes at  $T \geq 0.5$  K for  $P = 4.48$  GPa. We also have shown that the upturn feature is suppressed with increasing pressure and the orbital pair breaking mechanism becomes dominant. In further studies of the pair breaking mechanism,

measurement should be conducted at lower temperatures and with more refined pressure control. Our data above  $T = 0.5$  K shows that  $H_{c2}$  slightly exceeds the Pauli paramagnetic limit at  $P = 4.48$  GPa for  $H \parallel a$ .  $H_{c2}$  curves for  $H \parallel a$  and  $H \parallel b'$  lie on top of each other indicating that it has a two-dimensional-like feature, being isotropic within the  $ab'$ -plane. GL coherence lengths were obtained, which are highly anisotropic, for example,  $\xi_a : \xi_b : \xi_c = 5 : 5 : 1$  at  $P = 5.64$  GPa. The interlayer coherence length  $\xi_c$  is much larger than the thickness of the conducting sheet for all pressures, which is  $c/2 \sim 6.5$  Å, where  $c$  is a lattice parameter of  $(\text{TMTTF})_2\text{PF}_6$ . These results revealed that  $(\text{TMTTF})_2\text{PF}_6$  is an anisotropic three-dimensional superconductor.

#### References

- [1] D. Jérôme, A. Mazaud, M. Ribault, and K. Bechgaard, *J. Phys. Lett.* **41**, 95 (1980).
- [2] D. Jérôme, *Science* **252**, 1509 (1991).
- [3] T. Adachi, E. Ojima, K. Kato, H. Kobayashi, T. Miyazaki, M. Tokumoto, and A. Kobayashi, *J. Am. Chem. Soc.* **122**, 3238 (2000).
- [4] D. Jaccard, H. Wilhelm, D. JeÅLrome, J. Moser, C. Carcel, and J. M. Fabre, *J. Phys.: Condens. Matter* **13**, L89 (2001).
- [5] C. Araki, M. Itoi, M. Hedo, Y. Uwatoko, and H. Mori, *J. Phys. Soc. Jpn.* **76**, Suppl. A 198 (2007).
- [6] M. Kano, H. Mori, K. Matsubayashi, M. Itoi, M. Hedo, T. P. Murphy, S. W. Tozer, Y. Uwatoko, and T. Nakamura, *J. phys. Soc. Jpn.* **81**, 024716 (2012).

#### Authors

M. Kano<sup>a</sup>, H. Mori, K. Matsubayashi, M. Itoi<sup>b</sup>, M. Hedo<sup>c</sup>, T. P. Murphy<sup>d</sup>, S. W. Tozer<sup>d</sup>, Y. Uwatoko, and T. Nakamura<sup>e</sup>

<sup>a</sup>Tohoku University

<sup>b</sup>Nihon University

<sup>c</sup>University of the Ryukyu

<sup>d</sup>National High Magnetic Field Laboratory

<sup>e</sup>Institute for Molecular Science

## Topological Hall Effect in Spin Ice Conduction Systems - Application to Exotic Hall Response in $\text{Pr}_2\text{Ir}_2\text{O}_7$ -

M. Udagawa

Topological Hall effect (THE) is a hallmark of modern condensed matter physics. We have addressed the THE in conduction electron systems interacting with spin ice, which is one of the prototypical magnetic states arising from geometrical frustration. This setting is relevant to  $\text{Pr}_2\text{Ir}_2\text{O}_7$ , where conduction electrons due to Ir 5d bands interact with Pr magnetic moments forming spin ice. In this compound, Hall conductivity shows highly non-monotonous and anisotropic behavior [1], while the conventional mechanisms of Hall conductivity lead to monotonously increasing Hall conductivity with magnetic field.

To address this peculiar Hall response, we started with the construction of general theory of THE in spatially inhomogeneous systems. As the simplest case, we considered Ising Kondo lattice model on a kagome lattice with [111]-type easy-axes anisotropy. Through the numerical diagonalization of this model, we found a characteristic crossover with respect to spin-electron coupling,  $J$  (Fig. 1. (a)). For small  $J$ , the Hall conductivity is scaled as  $\propto J^3$ , where real-space spin scalar chirality spanned by three localized spins acts as an independent skew scatterer. On the other hand, for large  $J$ , the Hall conductivity converges to a finite value, where the electron spins are forced to align parallel to the localized moments.

Motivated by the clear identification of  $J^3$  scaling in

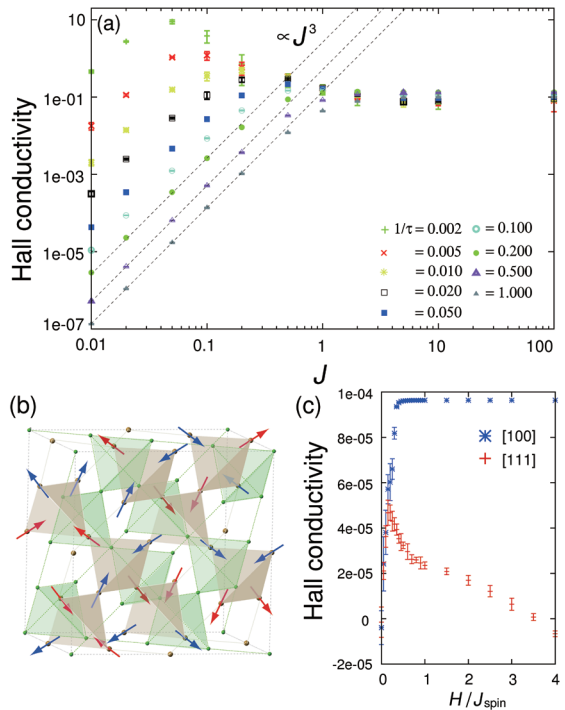


Fig. 1. (a)  $J$  and damping rate dependence of Hall conductivity of the Ising Kondo lattice model on a kagome lattice. Clear  $J^3$  scaling can be observed in a weak-coupling region. (b) Schematic picture of double pyrochlore lattice. On one sublattice (brown), localized moments reside, while on the other (green), conduction electrons are defined. (c) Magnetic field dependence of Hall conductivity in the Ising Kondo lattice model on a double pyrochlore lattice. Steep kink is observed for  $H \parallel [111]$ , signaling the onset of kagome ice correlation.

weak coupling region, we applied the third-order perturbation theory [2] to the Hall conductivity of  $\text{Pr}_2\text{Ir}_2\text{O}_7$ , in which the coupling between conduction electrons and Pr moments arises from superexchange process and is small. To describe this compound, we adopt the Ising-type Kondo lattice model on a double pyrochlore lattice, where conduction electrons defined on one pyrochlore sublattice interact with localized Ising moments residing on the other pyrochlore sublattice (Fig 1. (b)). We calculate Hall conductivity by combining the third-order perturbation theory and Kubo formula.

As a result, we could successfully reproduce the non-monotonic behavior of Hall conductivity (Fig 1. (c)). In particular, for [111] magnetic field, the Hall conductivity shows steep peak at a relatively low field, then decreases, leading to sign reversal. These results well capture the main features of experimental data. One of the main implications of our analysis is that the peak for  $H \parallel [111]$  can be associated with the crossover from zero-field spin ice state to kagome-ice-like state[3]. So far, this peak has been associated with the spin ice (2-in 2-out) to fully saturated state (3-in 1-out and 1-in 2-out)[1,4]. We thank R. Moessner for fruitful discussions.

#### References

- [1] Y. Machida *et al.*, *Phys. Rev. Lett.* **98**, 057203 (2007).
- [2] G. Tatara and H. Kawamura, *J. Phys. Soc. Jpn.* **73**, 2624 (2004).
- [3] M. Udagawa and R. Moessner, submitted to *Phys. Rev. Lett.*
- [4] T. Tomizawa and H. Kontani, *Phys. Rev. B* **82**, 104412 (2010).

#### Author

M. Udagawa  
University of Tokyo

# Direct Observation of Antiferromagnetic Order by Neutron Diffraction of s-Electrons Confined in Regular Nanospace of Sodalite

T. Nakano and M. Matsuura

Various kinds of magnetically ordered state, such as ferromagnetism, antiferromagnetism, and ferrimagnetism, have been found in alkali metal nanoclusters arrayed in regular nanospace of aluminosilicate zeolite crystals. The magnetic properties depend on the zeolite framework structures, the species of alkali element and the electron density of the clusters. They are quite a new class of magnetic materials because the magnetic orderings are realized by the mutual interaction between s-electrons confined in the nanospace and they contain no magnetic elements such as transition metal or rare earth metal. In this article, we report the first direct observation of long-range magnetic ordering of s-electrons by neutron diffraction (ND) [1].

Sodalite is a kind of aluminosilicate zeolites. As shown in Fig. 1 (a), truncated-octahedron-shaped  $\beta$ -cages are arrayed in a body-centered cubic (bcc) structure. The inside diameter of the  $\beta$ -cage is approximately 0.7 nm. The framework  $\text{Al}_3\text{Si}_3\text{O}_{12}$  is negatively charged and three  $\text{Na}^+$  ions are distributed in the cage. By the loading of guest Na atom into sodalite,  $\text{Na}_4^{3+}$  cluster can be formed in the  $\beta$ -cage as shown in Fig. 1 (b). In the cluster, one unpaired s-electron provided by the guest Na atom is shared among four  $\text{Na}^+$  ions and confined in the cage. When the clusters are formed in all the cages, antiferromagnetic (AFM) ordering appears below the Néel temperature of  $T_N = 48$  K because of the exchange interaction between adjacent clusters via the window of the cage. The magnetic phase transition has been confirmed by susceptibility, ESR, NMR,  $\mu$ SR and so on, but there have been no reports on determining the magnetic structure. This might be due to the difficulties originated from the large unit cell and resultant low spin density. In the present study, we prepared approximately 2 grams of powder specimen of Na-loaded sodalite and performed ND experiments for the first time by utilizing the spectrometer PONTA at the JRR-3 at JAEA.

We succeeded in observing the 001 and 111 magnetic Bragg peaks at low temperature. The intensity was nearly three orders of magnitude weaker than that of the 011 nuclear Bragg peak. The temperature dependence of the intensity of 001 peak was well fitted by using a phenomenological equation of the order parameter with a three-dimensional Heisenberg antiferromagnet. The simultaneous observation of 001 and 111 magnetic Bragg peaks is consis-

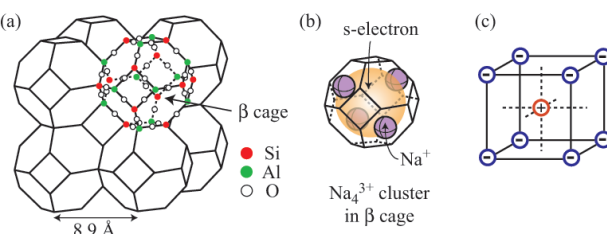


Fig. 1. Schematic illustrations of (a) crystal structure of aluminosilicate sodalite, (b)  $\text{Na}_4^{3+}$  cluster formed in the  $\beta$ -cage, and (c) magnetic structure model of Na clusters in sodalite. The framework of sodalite consists of Si, Al and O covalent-bonding network. The  $\beta$ -cages with an inner diameter of 0.7 nm are arrayed in a bcc structure. In the  $\text{Na}_4^{3+}$  cluster, one unpaired s-electron is shared among four  $\text{Na}^+$  ions and confined in the  $\beta$ -cage. Under the antiferromagnetic ordered state, the electronic spin in the body center cluster and that in the corner cluster are coupled in antiparallel in the bcc lattice.

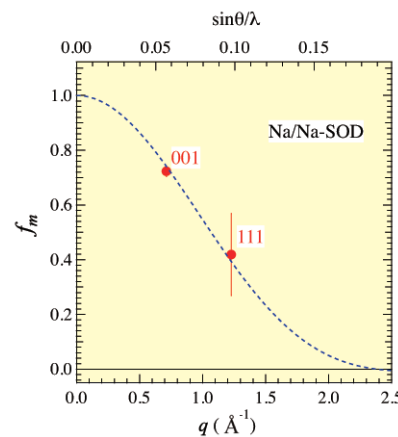


Fig. 2. Magnetic form factor of Na clusters in sodalite for scattering vector  $q$ . The closed circles show experimental results obtained by 001 and 111 magnetic Bragg peaks. The dotted curve shows the form factor evaluated from the 1s wave function in the spherical well potential with the inner diameter of 0.7 nm.

tent with the magnetic structure shown in Fig. 1 (c) where the electronic spin in the body center cluster and that in the corner cluster are antiparallel in the bcc lattice. We also evaluated the magnetic form factor from the ratio of the integrated intensities of the 001 and 111 magnetic Bragg peaks to the 011 nuclear one. The form factor is found to drop very quickly as a function of  $q$  as shown in Fig. 2. The simplest model describing the electron wave function of the cluster is a spherical well potential model with the diameter of the cluster. The dotted curve in Fig. 2 shows the calculated form factor of the 1s wave function confined in the spherical well with the inner diameter of 0.7 nm. The calculation results are in good agreement with the experimental ones. Therefore, it is evident that the s-electron responsible for the AFM order possesses a wave function delocalized over nanometer size in the cluster.

## Reference

- [1] T. Nakano, M. Matsuura, A. Hanazawa, K. Hirota, and Y. Nozue, Phys. Rev. Lett. **109**, 167208 (2012).

## Authors

T. Nakano<sup>a</sup>, M. Matsuura<sup>a,b</sup>, A. Hanazawa<sup>a</sup>, K. Hirota<sup>a</sup>, and Y. Nozue<sup>a</sup>

<sup>a</sup>Osaka University

<sup>b</sup>Present Address: CROSS Tokai

## Marked Change in the Ground State of $\text{CeRu}_2\text{Al}_{10}$ Induced by Small Amount of Rh Substitution

M. Sera, T. Nishioka, and K. Kindo

The recently discovered Kondo semiconductor  $\text{CeT}_2\text{Al}_{10}$  ( $T = \text{Ru, Os, Fe}$ ) has attracted much attention because of their unusual ground states. Among many Kondo semiconductors,  $\text{CeRu}_2\text{Al}_{10}$  and  $\text{CeOs}_2\text{Al}_{10}$  are very rare systems exhibiting antiferromagnetic (AFM) order at  $T_0 \sim 30$  K [1, 2]. As has been revealed by extensive studies up to now, the AFM ordered phases in these two compounds are strange. The AFM moment ( $M_{\text{AF}}$ ) is parallel to the  $c$ -axis, which is not expected from the large anisotropy in magnetic susceptibility ( $\chi_a > \chi_c > \chi_b$ ) in the paramagnetic region. Here,  $\chi_a$  is the magnetic susceptibility along the  $a$ -axis, etc. The transition temperature is relatively high considering

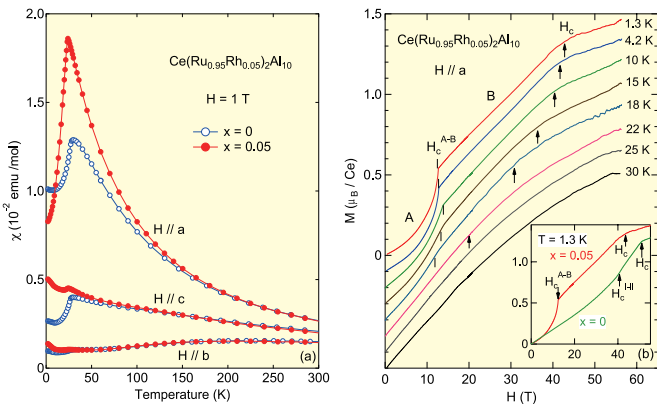


Fig. 1. (a) Temperature dependence of magnetic susceptibility of  $\text{Ce}(\text{Ru}_{1-x}\text{Rh}_x)_2\text{Al}_{10}$  ( $x = 0, 0.05$ ) along the  $a$ -,  $b$ -, and  $c$ -axes measured at 1 T. (b) Magnetization curve of  $\text{Ce}(\text{Ru}_{0.95}\text{Rh}_{0.05})_2\text{Al}_{10}$  under various temperatures for  $H \parallel a$  axis. The inset shows the  $M$ - $H$  curve of  $\text{Ce}(\text{Ru}_{1-x}\text{Rh}_x)_2\text{Al}_{10}$  ( $x = 0, 0.05$ ) at  $T = 1.3$  K for the  $H \parallel a$ -axis.

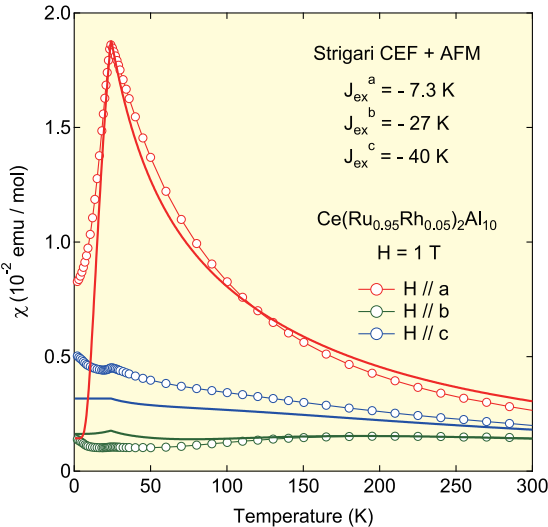


Fig. 2. Temperature dependence of magnetic susceptibility for  $H \parallel a$ -,  $b$ -, and  $c$ -axes at 1 T calculated by mean field calculation using CEF level scheme obtained by Strigari *et al.* The solid lines represent the calculated results with the anisotropic exchange interaction of  $(J_a^{\text{ex}}, J_b^{\text{ex}}, J_c^{\text{ex}}) = (-7.3 \text{ K}, -27 \text{ K}, -40 \text{ K})$ . The symbols are experimental results of  $\text{Ce}(\text{Ru}_{0.95}\text{Rh}_{0.05})_2\text{Al}_{10}$ .

the long distance (5.2 Å) between Ce ions. Although  $T_0$  is high, the ordered moment is as small as  $0.3 \sim 0.4 \mu_B/\text{Ce}$ . In our previous paper, we reported the high field magnetization curve of  $\text{CeRu}_2\text{Al}_{10}$  and  $\text{CeOs}_2\text{Al}_{10}$  for the magnetic field ( $H$ ) along the  $a$ -axis, and proposed that the unusual AFM ordered phase in this system is caused by the large hybridization between the conduction band and the nearly localized 4f shell ( $c-f$  hybridization) along the  $a$ -axis, leading to the AFM order with  $M_{\text{AF}} \parallel c$  [3].

Quite recently, Kobayashi *et al.* have reported the marked change in the magnetic susceptibility of  $\text{CeRu}_2\text{Al}_{10}$  by Rh substitution [ $\text{Ce}(\text{Ru}_{1-x}\text{Rh}_x)_2\text{Al}_{10}$ ,  $x = 0.1, 0.2$ , and  $0.3$ ]. They found in these compounds that, below  $\sim 150$  K down to  $T_0$ ,  $\chi_a$  is strongly enhanced and shows a very large decrease with decreasing temperature after showing a sharp peak at  $T_0$ , and thus suggested a possible AFM order with  $M_{\text{AF}} \parallel a$ . To clarify the origin of the marked change in the ground state by Rh substitution, we studied the magnetic susceptibility and high field magnetization of  $\text{Ce}(\text{Ru}_{0.95}\text{Rh}_{0.05})_2\text{Al}_{10}$ .

Figure 1(a) represents the temperature ( $T$ ) dependence of  $\chi$  of  $\text{Ce}(\text{Ru}_{1-x}\text{Rh}_x)_2\text{Al}_{10}$  ( $x = 0, 0.05$ ) along the  $a$ -,  $b$ -, and  $c$ -axes measured at 1 T. In  $\text{Ce}(\text{Ru}_{0.95}\text{Rh}_{0.05})_2\text{Al}_{10}$ ,  $\chi_a$  shows a large decrease with decreasing temperature after showing a sharp peak at  $T_0 \sim 24$  K and the decrease

in  $\chi_c$  below  $T_0$  observed in  $\text{CeRu}_2\text{Al}_{10}$  originating from  $M_{\text{AF}} \parallel c$  disappears by Rh substitution. These results suggest that the AFM order with  $M_{\text{AF}} \parallel a$  occurs below  $T_0$ . In Fig. 1(b), we show the magnetization ( $M$ ) curves of  $\text{Ce}(\text{Ru}_{0.95}\text{Rh}_{0.05})_2\text{Al}_{10}$  under various temperatures for the  $H \parallel a$ -axis. In  $\text{Ce}(\text{Ru}_{0.95}\text{Rh}_{0.05})_2\text{Al}_{10}$ , at 1.3 K,  $M$  exhibits a spin-flop transition at  $\sim 13$  T.  $M$  at 50 T is  $\sim 1.4 \mu_B/\text{Ce}$ , which is larger than  $\sim 1.3 \mu_B/\text{Ce}$  for  $x = 0$ . This suggests a more localized nature of Ce ions in  $\text{Ce}(\text{Ru}_{0.95}\text{Rh}_{0.05})_2\text{Al}_{10}$  than in  $\text{CeRu}_2\text{Al}_{10}$ . The experimental results were analyzed by mean field calculation for the two-sublattice model using the crystalline electric field (CEF) level scheme obtained by Strigari *et al.* and the anisotropic exchange interaction [4,5]. The calculated results of  $\chi$  along the three crystal axes are shown in Fig. 2.  $\chi_a$  in the paramagnetic region and a sharp peak at  $T_0$  are reproduced well by the calculation.  $\chi_b$  and  $\chi_c$ , which are nearly independent of temperature, are also reproduced. On the basis of both experimental and calculated results, we conclude that, by a small amount of Rh substitution with one extra 4d electron, the large  $c-f$  hybridization along the  $a$ -axis, leading to the unusual ground state of  $\text{CeRu}_2\text{Al}_{10}$ , is markedly suppressed and the Ce ion in a Rh-substituted sample becomes close to the normal localized magnetic ion.

## References

- [1] T. Nishioka *et al.*, J. Phys. Soc. Jpn. **78**, 123705 (2009).
- [2] D. D. Khalyavin *et al.*, Phys. Rev. B **82**, 100405 (2010).
- [3] A. Kondo *et al.*, Phys. Rev. B **83**, 180415 (2011).
- [4] F. Strigari *et al.*, Phys. Rev. B **86**, 081105 (2012).
- [5] K. Kunimori *et al.*, Phys. Rev. B **86**, 245106 (2012).

## Authors

- A. Kondo, K. Kindo, K. Kunimori<sup>a</sup>, H. Nohara<sup>a</sup>, H. Tanida<sup>a</sup>, M. Sera<sup>a</sup>, R. Kobayashi<sup>b</sup>, T. Nishioka<sup>c</sup>, and M. Matsumura<sup>c</sup>  
<sup>a</sup>Hiroshima University  
<sup>b</sup>Japan Atomic Energy Agency  
<sup>c</sup>Kochi University

## Gigantic Negative Magnetoresistance Effects in Pyrochlore Iridates

K. Matsuhira, M. Tokunaga, and M. Wakushima

Since the discovery of high- $T_c$  superconductivity in cuprate materials, physical properties of 3d transition metal oxides have been extensively studied. In this class of materials, strong Coulomb interaction dominates the other

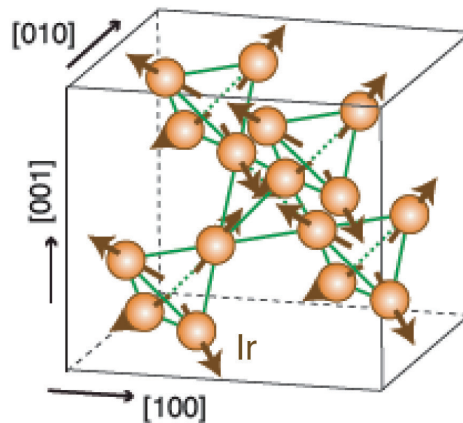


Fig. 1. Schematic illustration of the Ir-sites in the pyrochlore structure. Corner shared tetrahedra form three-dimensional network of the ions. The brown arrows represent the magnetic moments in the Ir ions.

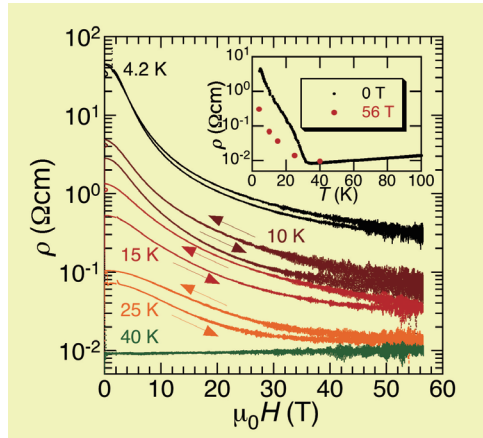


Fig. 2. Longitudinal magnetoresistance of a high-purity poly-crystal of  $\text{Nd}_2\text{Ir}_2\text{O}_7$  [5]. The observed hysteresis can be caused by the change in temperature due to the magneto-caloric effect. Inset shows temperature dependence of the resistance at 0 T and 56 T.

interactions. Various interesting phenomena show up as a result of the interactions between charge carriers and local spins in the orbitals determined by the strong crystal electric fields. On the other hand, 5d transition metal oxides involve strong spin-orbit interaction, and hence, come to attract considerable attention as a playground for novel physics. In particular, rare-earth iridates  $\text{Ln}_2\text{Ir}_2\text{O}_7$  ( $\text{Ln}$ : lanthanoid elements) are one of the attracting materials because of the geometrical frustration in the pyrochlore structure (Fig. 1).

The series of  $\text{Ln}_2\text{Ir}_2\text{O}_7$  with  $\text{Ln} = \text{Nd}, \text{Sm}, \text{Eu}, \text{Gd}, \text{Tb}, \text{Dy}$ , and  $\text{Ho}$  exhibit metal-insulator transition when the Ir spins order at temperatures between 33 K and 141 K [1, 2]; the Ir moments exhibit the antiferromagnetic ordering with  $q=0$  (all-in/all-out state) shown in Fig. 1 [3, 4]. Thereby, application of sufficiently high magnetic fields to remove the spin order is expected to induce insulator-metal transitions. We studied magnetoresistance on high-purity polycrystals of  $\text{Nd}_2\text{Ir}_2\text{O}_7$  [5] in pulsed high magnetic fields up to 56 T. The results show prominent negative magnetoresistance effects below the metal-insulator transition temperature of 33 K (Fig. 2). The temperature dependence of the resistance at 56 T, however, remains semiconducting as shown in the inset of Fig. 2. This result suggests that the magnetic field of 56 T is insufficient to cause phase transitions in the Ir spin system. Similar behavior is observed when the  $\text{Ln}$  is magnetic, whereas non-magnetic Eu compound shows positive magnetoresistance effect [5]. Therefore, the observed negative magnetoresistance effects can be caused by the reduction of the spin fluctuation in the rare-earth ions and their coupling to the mobile 5d electrons via the  $d$ - $f$  interactions.

#### References

- [1] K. Mastuhira *et al.*, J. Phys. Soc. Jpn. **76**, 043706 (2007).
- [2] K. Mastuhira *et al.*, J. Phys. Soc. Jpn. **80**, 094701 (2011).
- [3] K. Tomiyasu *et al.*, J. Phys. Soc. Jpn. **81**, 034709 (2012).
- [4] H. Sagayama *et al.*, Phys. Rev. B **87**, 100403(R) (2013).
- [5] K. Mastuhira *et al.*, J. Phys. Soc. Jpn. **82**, 023706 (2013).

#### Authors

K. Mastuhira, M. Tokunaga, M. Wakushima, Y. Hinatsu, and S. Takagi

## Cyclotron Resonance Studies in Ferromagnetic Semiconductors

G. A. Khodaparast and Y. H. Matsuda

The carrier-induced ferromagnetism in magnetic III-V semiconductors [1, 2] has opened up several opportunities for device applications, as well as fundamental studies of a material system in which itinerant carriers interact with the localized spins of magnetic impurities. The origin of carrier-induced ferromagnetism is still controversial where reasonable agreement between theory and experiments has been noted for GaMnAs, but in contrast, the observation of  $T_c$  of 10 K for InMnAs films with carrier concentration of  $10^{18}\text{cm}^{-3}$  is inconsistent with theory [3]. Based on theoretical calculations, InMnAs with a hole concentration of  $10^{18}\text{cm}^{-3}$  should have a  $T_c$  of 8 K instead of the experimentally observed 40~90 K [2]. The case for MOVPE grown films is even more complex. Films with a carrier concentration of  $10^{18}\text{cm}^{-3}$  have a  $T_c$  of 330 K and the  $T_c$  is nearly independent of carrier concentration [3]. In order to understand hole mediated ferromagnetism, probing the band structure in these materials are crucial. Cyclotron Resonance (CR) spectroscopy is an extremely powerful tool for the study of electronic states in semiconductors and here we present and compare the experimental and theoretical studies

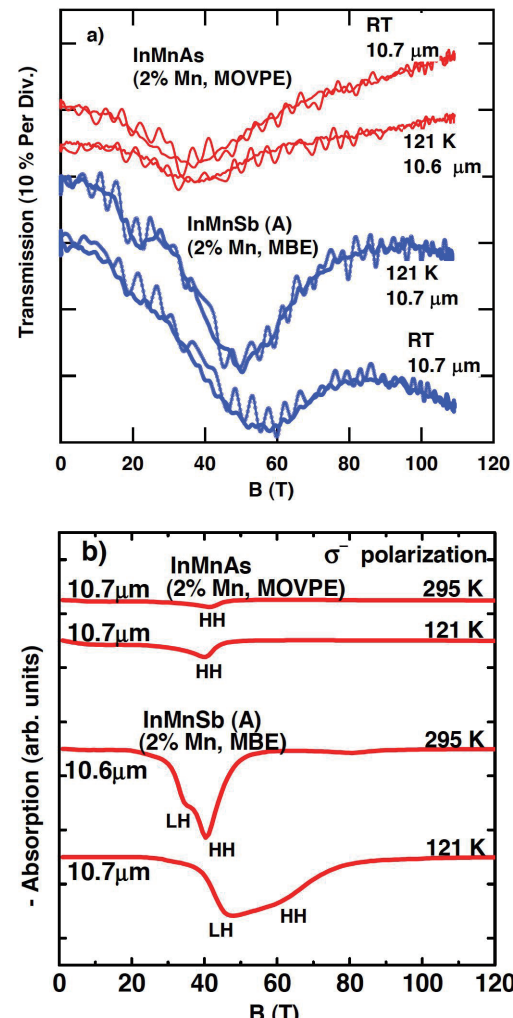


Fig. 1. a) CR spectra for InMnAs and InMnSb films. The CR of InMnSb at 295 K, was measured at 10.6  $\mu\text{m}$ ; whereas, the other three resonances were measured at 10.7  $\mu\text{m}$ . b) Calculated CR spectra for InMnAs and InMnSb comparing to the experimental results in Fig. 1a. The CR resonance in InMnAs originates from a single (HH only) transition; whereas, in InMnSb it arises from multiple (both LH and HH) transitions.

of the magneto-optical properties of p-type  $\text{In}_{1-x}\text{Mn}_x\text{As}$  and  $\text{In}_{1-x}\text{Mn}_x\text{Sb}$  ferromagnetic semiconductors films in ultrahigh magnetic fields oriented along [001].

Since these magnetic semiconductors usually have low carrier mobilities (typically of the order of  $100 \text{ cm}^2/\text{Vs}$ ), a very high magnetic field is necessary to observe CR (i.e.,  $\omega_c\tau > 1$ ) where  $\omega_c$  is the cyclotron frequency. Since CR directly provides the effective masses and scattering times of carriers, we can obtain detailed information on the itinerancy of the carriers while in transport measurements it is normally difficult to deduce the contributions of the mass and scattering time independently. In addition, our observations provide information on the band structure, sp-d exchange parameters ( $\alpha, \beta$ ), and the position of the Fermi level in these material systems. Recently in GaMnAs, the tunability of the Fermi level within the impurity band can be used to control the  $T_c$ .

CR measurements were performed using  $\text{CO}_2$ ,  $\text{H}_2\text{O}$ , and CO lasers, providing laser radiation at 10.6, 10.7, and 16.9 and  $5.53 \mu\text{m}$ . Magnetic fields exceeding 100 T were generated by a single turn coil technique. The external magnetic field was applied along the growth direction and measured by a pick-up coil around the sample, placed inside a continuous flow helium cryostat. Several IR wavelengths were used as the excitation source and the transmitted signal through the sample was collected using a fast liquid-nitrogen-cooled HgCdTe detector.

Figure 1a shows the results of the CR measurements for MBE grown InMnSb (sample A) and MOVPE grown InMnAs with 2% Mn content. The observed cyclotron mass in the InMnSb(A) is larger than that in MOVPE grown InMnAs with similar Mn contents ( $x \sim 0.02$ ). The larger hole density in the InMnSb compared to the InMnAs, can shift the Fermi energy to a much higher level. The cyclotron mass can be enhanced when the resonance transition takes place between the Landau levels with higher indices. The CR of the holes in InMnSb has been observed for the first time and in the case of Fig. 1a, the CR masses are  $0.057m_0$  at room temperature (RT) and  $0.051m_0$  at 121 K. These are much smaller than the band edge HH mass in InSb ( $0.32m_0$ ). The cyclotron mobility,  $\mu_{\text{CR}}$ , was extracted from the width of the resonance peaks. We have  $\mu_{\text{CR}} = 4.8 \times 10^2 \text{ cm}^2/(\text{V s})$  at RT and  $\mu_{\text{CR}} = 6.0 \times 10^2 \text{ cm}^2/(\text{V s})$  at 121 K. Lowering the temperature in InMnSb increased the mobility and reduced the effective mass, where the InMnAs resonance was not affected significantly by lowering the temperature. The CR absorption spectra shown in Fig. 1b, is obtained from the calculated magneto-optical absorption due to transitions between different Landau levels. From Fermi's golden rule, the magneto-optical absorption coefficients at a given photon energy and for a magnetic field perpendicular to the sample can be calculated.

The observed effective mass in the InMnAs studied here is consistent with the heavy hole (HH) mass reported in an earlier CR study of p-type MBE grown InMnAs grown on GaAs [4] but different from the observation reported in InMnAs with the GaSb buffer layer [5]. The MOVPE grown InMnSb structure shows a much higher hole mobility and a factor of 100 less hole carrier density compared to the MBE grown structures.

## References

- [1] H. Munekata, H. Ohno, S. von Molnar, A. Segmuller, L. L. Chang, and L. Esaki, Phys. Rev. Lett. **63**, 1849 (1989).
- [2] T. Schallenberg and H. Munekata, Appl. Phys. Lett. **89**, 042507 (2006).
- [3] N. Rangaraju, Li Pengcheng, and B. W. Wessels, Phys. Rev. B **79**, 205209 (2009).

[4] Y. H. Matsuda, G. A. Khodaparast, M. A. Zudov, J. Kono, Y. Sun, F. V. Kyrychenko, G. D. Sanders, C. J. Stanton, N. Miura, S. Ikeda, Y. Hashimoto, S. Katsumoto, and H. Munekata, Phys. Rev. B **70**, 195211 (2004).

[5] G.A. Khodaparast, J. Kono , Y. H. Matsuda, S. Ikeda , N. Miura, Y. J. Wang, T. Slupinski, A. Oiwa, H. Munekata, Y. Sun, F. V. Kyrychenko, G. D. Sanders, and C. J. Stanton, Physica E **21**, 978 (2004).

## Authors

G. A. Khodaparast<sup>a</sup>, Y. H. Matsuda, T. R. Merritt<sup>a</sup>, H. Saito, S. Takeyama, D. Sahab<sup>b</sup>, G. D. Sanders<sup>b</sup>, C. J. Stanton<sup>b</sup>, C. Feeser<sup>c</sup>, B. Wessels<sup>c</sup>, X. Liu<sup>d</sup>, and J. Furdyna<sup>d</sup>

<sup>a</sup>Virginia Tech

<sup>b</sup>Department of Physics, University of Florida

<sup>c</sup>Northwestern University

<sup>d</sup>University of Notre Dame

## Pulsed Laser Ablation in Supercritical $\text{CO}_2$ for Nanomaterials Synthesis

T. Kato, K. Terashima, and M. Baba

Pulsed laser ablation (PLA) is a versatile technique that allows the fabrication of high-quality thin films in vacuum, and it has also been increasingly used in liquids for the formation and functionalization of nanomaterials. Compared to gases and liquids, PLA in supercritical fluids (SCFs) offers further advantages for materials synthesis because of the favorable thermophysical properties of SCFs. For instance, in SCFs, coagulation of nanomaterials can be avoided because of the possibility to tune the solubility of the synthesized materials. Furthermore, certain thermophysical properties of SCFs, for instance the density fluctuation  $F_D$ , which characterizes the inhomogeneity of the local molecular density, present a local maximum at the critical point.

We have applied PLA in supercritical xenon (scXe) and carbon dioxide (sc $\text{CO}_2$ ) near their critical points to the synthesis of diamondoids, which are  $\text{C}(sp^3)\text{-C}(sp^3)$  hybridized hydrogen-terminated molecules whose cage structures

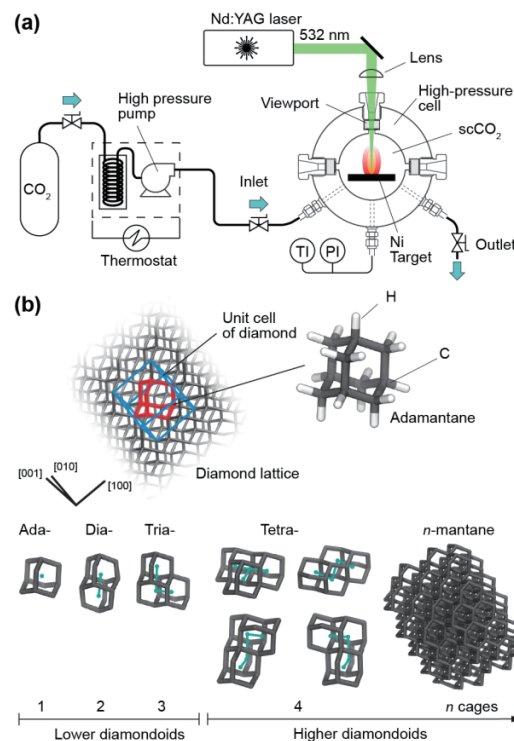


Fig. 1. (a) Schematic of pulsed laser ablation (PLA) in supercritical carbon dioxide (sc $\text{CO}_2$ ). (b) Relation of diamondoids and diamond lattice and molecular structures of lower and higher diamondoids.

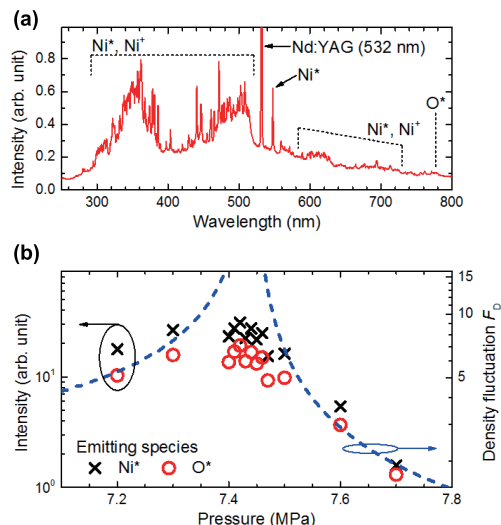


Fig. 2. (a) Optical emission spectrum acquired from PLA in scCO<sub>2</sub> near the critical point (b) variation of emission intensities of Ni<sup>\*</sup> and O<sup>+</sup> atomic lines and density fluctuation  $F_D$  of CO<sub>2</sub> fluid as a function of pressure. [4]

can be superimposed on a diamond lattice [1] (Fig. 1). Despite their promising physical properties and potential for a wide range of applications, the availability of high-order diamondoids is still very limited [2]. Using the first diamond member, adamantane, as a precursor and seed, we succeeded in the synthesis of higher diamondoids that had not been synthesized before, utilizing the dense and highly non-equilibrium reaction field of PLA plasmas in SCFs near the critical point [3].

Our joint group's study now aims to reveal the dynamics of the PLA reaction fields generated in SCFs using spectroscopic diagnostic equipment in the Spectroscopy Section of the Materials Design and Characterization Laboratory, for further improvement of the nanomaterials synthesis. Optical emission spectroscopy (OES) gave us information of target- and solvent-originated excited species in the PLA reaction field. We found that the emission intensities of both Ni (target) and O atoms (originating from the CO<sub>2</sub> solvent) reached local maxima that could be correlated to the change of the density fluctuation  $F_D$  [4] (Fig. 2). This is the first report on the critical anomaly in PLA dynamics in the world. The local maxima of emission intensities are probably due to the enhancement of the plasma excitation and effective quenching resulting from the large  $F_D$ , and it also means that the large number of excited species can contribute to the nanomaterials synthesis near the critical point. These experimental approaches for investigating the PLA dynamics will strongly assist the optimization of PLA nanomaterials synthesis in SCFs.

#### References

- [1] S. Nakahara, S. Stauss, H. Miyazoe, T. Shizuno, M. Suzuki, H. Kataoka, T. Sasaki, and K. Terashima, *Appl. Phys. Express* **3**, 096201 (2010).
- [2] J. E. Dahl, S. C. Liu, and R. M. K. Carlson, *Science* **299**, 96 (2003).
- [3] S. Nakahara, S. Stauss, T. Kato, T. Sasaki, and K. Terashima, *J. Appl. Phys.* **109**, 123304 (2011).
- [4] T. Kato, S. Stauss, S. Kato, K. Urabe, M. Baba, T. Suemoto, and K. Terashima, *Appl. Phys. Lett.* **101**, 224103 (2012).

#### Authors

T. Kato<sup>a</sup>, S. Stauss<sup>a</sup>, S. Kato<sup>a</sup>, S. Himeno<sup>a</sup>, K. Urabe<sup>a</sup>, K. Terashima<sup>a</sup>, M. Baba, and T. Suemoto

<sup>a</sup>Department of Advanced Materials Science, The University of Tokyo

## Development of a Hard Magnetic Ferrite Exhibiting a Gigantic Coercivity and High Frequency Millimeter Wave Rotation

A. Namai and S. Ohkoshi

Magnetic ferrites such as Fe<sub>3</sub>O<sub>4</sub> and Fe<sub>2</sub>O<sub>3</sub> are extensively used because they are inexpensive and chemically stable. However, due to their low magnetocrystalline anisotropies, the coercivity of magnetic ferrites is generally low. The development of magnetic ferrites with a large coercive field ( $H_c$ ) is an important issue because this type of ferrite can be used in various advanced applications.

In this work, we prepared rhodium-substituted  $\epsilon$ -Fe<sub>2</sub>O<sub>3</sub>,  $\epsilon$ -Rh<sub>x</sub>Fe<sub>2-x</sub>O<sub>3</sub> nanomagnets, by a nanoscale chemical synthesis using mesoporous silica as a template. The transmission electron microscope image indicates that the obtained sample is composed of nanoparticles with an average particle size of *ca.* 35 nm. The X-ray diffraction patterns confirmed that the crystal structure is orthorhombic with *Pna*2<sub>1</sub> space group (Fig. 1a). The magnetic hysteresis loops measured at room temperature show that the  $H_c$  value increased with rhodium substitution and  $\epsilon$ -Rh<sub>0.14</sub>Fe<sub>1.86</sub>O<sub>3</sub> exhibits a huge  $H_c$  value of 27 kOe. Furthermore, as shown in Figure 1b, a crystallographically oriented  $\epsilon$ -Rh<sub>0.14</sub>Fe<sub>1.86</sub>O<sub>3</sub> nanomagnet recorded an  $H_c$  value of 31 kOe, which is the largest value among metal-oxide-based magnets and is comparable to those of rare-earth magnets ( $H_c$  values of Sm-Co and Nd-Fe-B magnet are 30 kOe and 25 kOe, respectively). Such a gigantic  $H_c$  value is explained by the following reasons. The particle size in the present series should be sufficiently small to form a single magnetic domain. In addition, the results of the first-principles calculations indicate strong Fe–O hybridization causing a non-zero orbital angular momentum on the Fe ion, which induces a large magnetocrystalline anisotropy. Furthermore, Rh–O–Fe hybridization is observed around the Rh substituted site, which enhances the magnetocrystalline anisotropy through the contribution from the orbital angular momentum on Rh.

Insulating magnetic materials with high magnetic anisotropy is expected to show high-frequency zero-field ferromagnetic resonance (natural resonance). The electromagnetic

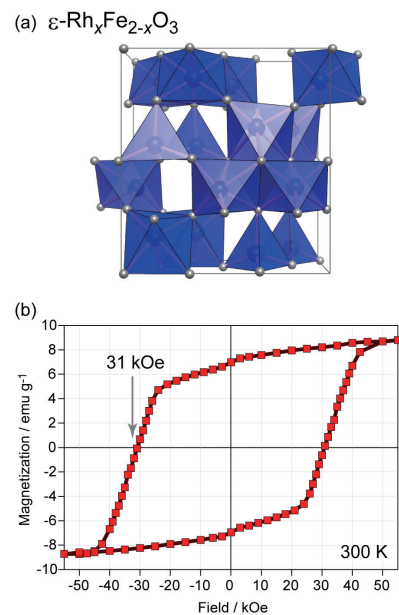
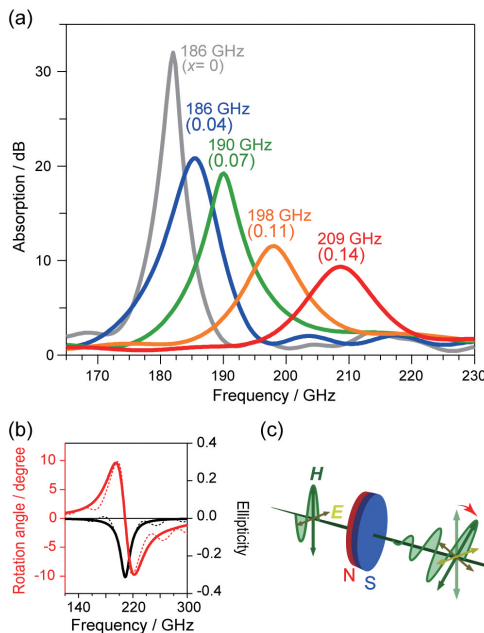


Fig. 1. (a) Crystal structure and (b) magnetic hysteresis of  $\epsilon$ -Rh<sub>x</sub>Fe<sub>2-x</sub>O<sub>3</sub>.



**Fig. 2.** (a) Electromagnetic wave absorption properties of  $\epsilon\text{-Rh}_x\text{Fe}_{2-x}\text{O}_3$  measured by THz-TDS. (b) Rotation angle and ellipticity of the magnetized  $\epsilon\text{-Rh}_{0.14}\text{Fe}_{1.86}\text{O}_3$  pellet. (c) The schematic illustration of millimeter wave rotation.

wave absorption properties of  $\epsilon\text{-Rh}_x\text{Fe}_{2-x}\text{O}_3$  were measured under zero-magnetic field at room temperature using terahertz time domain spectroscopy (THz-TDS). As shown in Figure 2a, resonance frequencies ( $f_r$ ) were observed at 182 GHz ( $x = 0$ ), 186 GHz ( $x = 0.04$ ), 190 GHz ( $x = 0.07$ ), 198 GHz ( $x = 0.11$ ), and 209 GHz ( $x = 0.14$ ). The observed  $f_r$  values are the highest among all magnetic materials. Furthermore, a magnetized  $\epsilon\text{-Rh}_{0.14}\text{Fe}_{1.86}\text{O}_3$  pellet sample exhibited magnetic rotation and ellipticity change of the propagated millimeter wave at 220 GHz, which is caused by gyromagnetic effect (Fig. 2b and 2c).

The gigantic  $H_c$  value has potential to be applied in future high-density magnetic recording media because the large  $H_c$  value enables the particle size to be greatly reduced while maintaining ferromagnetic properties. In addition,  $\epsilon\text{-Rh}_x\text{Fe}_{2-x}\text{O}_3$  exhibits zero-field ferromagnetic resonance up to 209 GHz, and magnetic rotation of the propagated millimeter wave occurs due to an optically induced magnetic dipole transition at 220 GHz. The present material should be useful for high frequency millimeter wave absorbers and rotators (isolators or circulators) since it should restrict electromagnetic interference problems because the frequency of the magnetic rotation corresponds to the highest window of air (220 GHz band), which is the anticipated carrier frequency for next-generation millimeter wave wireless communications.

#### Reference

A. Namai, M. Yoshiyuki, K. Yamada, S. Sakurai, T. Goto, T. Yoshida, T. Miyazaki, M. Nakajima, T. Suemoto, H. Tokoro, and S. Ohkoshi, Nature Communications 3, 1035 (2012). [Nature Materials "Research Highlights" and Nature Japan "Focused Articles"]

#### Authors

A. Namai, M. Yoshiyuki, K. Yamada, S. Sakurai, T. Goto<sup>a</sup>, T. Yoshida<sup>a</sup>, T. Miyazaki<sup>a</sup>, M. Nakajima, T. Suemoto, H. Tokoro, and S. Ohkoshi<sup>a</sup> Dowa Electronics Materials Co., Ltd.

## Biexciton Luminescence from Individual Isoelectronic Traps in Nitrogen δ-Doped GaAs

K. Takamiya, H. Yaguchi, and H. Akiyama

Single photons and entangled photon pairs are expected to play an important role in the field of quantum information science and technology, such as quantum key distribution and quantum computation. Single isoelectronic traps formed by nitrogen–nitrogen (NN) pairs in GaAs are also promising candidates for generating single photons or entangled photon pairs [1-6]. The present paper reports on the observation of biexciton emission from individual isoelectronic traps in nitrogen δ-doped GaAs [7].

The sample used in this study was a nitrogen δ-doped GaAs layer grown on a semi-insulating undoped GaAs (110) substrate by low-pressure metalorganic vapor phase epitaxy. We measured micro-photoluminescence (PL) spectra at 4.2 K using a diode-pumped solid-state laser ( $\lambda=532\text{nm}$ ) as the excitation source to observe the emission from single isoelectronic traps. The spatial and energy resolutions of the micro-PL measurement system used in this study were  $\sim 1\text{ }\mu\text{m}$  and  $\sim 30\text{ }\mu\text{eV}$ , respectively.

Figure 1 shows the excitation-power-dependent micro-PL spectra obtained from an individual isoelectronic trap in nitrogen δ-doped GaAs. As shown in this figure, sharp emission lines with full width at half maximum of about  $30\text{ }\mu\text{eV}$ , which may be restricted by the energy resolution of the measurement system, are seen at 1.444 eV (labeled X) and 1.436 eV (labeled XX). The PL line labeled X is assigned to the excitonic emission due to a NN pair named  $Z_2$  because its photon energy is 1.444 eV. Figure 2 shows the intensity of the PL labeled X and XX as a function of laser power. The intensity of the excitonic emission labeled X increases linearly with increasing laser power while the PL intensity labeled XX clearly shows a quadratic dependence on the laser power under weak excitation conditions. This shows that the emission labeled XX is due to a radiative transition from a biexciton state to an exciton state.

In conclusion, we have observed biexciton luminescence from single isoelectronic traps formed by NN pairs in nitrogen δ-doped GaAs grown on GaAs(110). The biexciton binding energy was found to be 8 meV and almost always constant. Thus, biexciton emission with a highly reproducible photon energy can be easily obtained from single NN pairs in GaAs as in the case of exciton emission. Both the biexciton and exciton emission lines show random polariza-

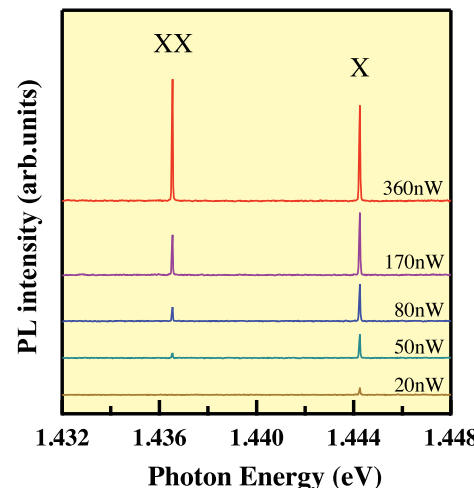


**Fig. 1.** Excitation-power-dependent micro-PL spectra obtained from an individual isoelectronic trap in nitrogen δ-doped GaAs.

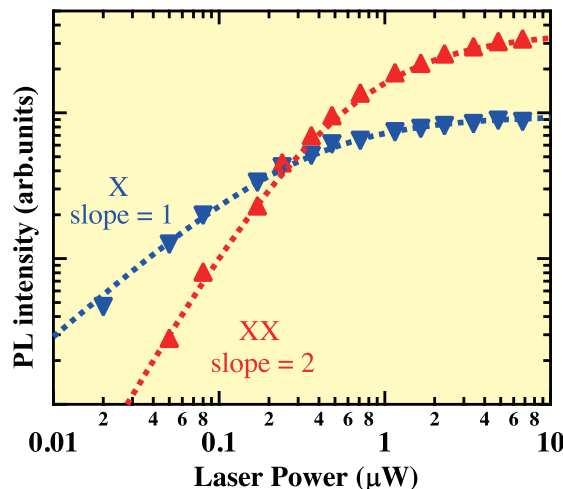


Fig. 2. PL intensity for the X and XX emission lines as a function of laser power.

tion and no fine-structure splitting, which shows promise for the application to polarization-entangled photon pairs.

#### References

- [1] Y. Endo *et al.*, J. Cryst. Growth **298** 73 (2007).
- [2] Y. Endo *et al.*, Physica E **40**, 2110 (2008).
- [3] T. Fukushima *et al.*, Physica E **42**, 2529 (2010).
- [4] H. Yaguchi, Proc. SPIE **7945**, 79452F (2011).
- [5] K. Takamiya *et al.*, Mater. Sci. Forum **706**, 2916 (2012).
- [6] M. Ikezawa *et al.*, Appl. Phys. Lett. **100**, 042106 (2012).
- [7] K. Takamiya *et al.*, Appl. Phys. Express **5**, 111201 (2012).

#### Authors

K. Takamiya<sup>a</sup>, T. Fukushima<sup>a</sup>, S. Yagi<sup>a</sup>, Y. Hijikata<sup>a</sup>, T. Mochizuki, M. Yoshita, H. Akiyama, S. Kuboya<sup>b</sup>, K. Onabe<sup>b</sup>, R. Katayama<sup>c</sup>, and H. Yaguchi<sup>a</sup>

<sup>a</sup>Saitama University

<sup>b</sup>Department of Advanced Materials Science, The University of Tokyo

<sup>c</sup>Tohoku University

# International Conferences and Workshops

## MAterial Simulation in Petaflops era (MASP2012)

June 25 - July 13, 2012  
O. Sugino

With the development of petaflops supercomputers, such as K-computer, the computational condensed matter physics is undergoing a sea change. The stupendous computer power has enabled to handle very large number of parameters, allowing thereby to apply increasingly complex formalisms. While, the massive parallelization severely limits the applicable algorithms. In this context, top level scientists working in this field were invited from all over the world to discuss deeply (taking three weeks) what can be achieved in the petaflops era. The topics included the high-precision many-body theories, density functional theory (DFT) for dynamical phenomena, algorithms for very large scale DFT calculation, and application to solid-liquid interface. Through the lecture of 2-3 hours and the symposium talks, followed by endless informal discussions, the attendees enjoyed the time to deeply think about the future of the computational condensed matter theories.

This event consisted of the workshop (June 25 - July 1st and July 3 - 11), where one or two lectures were given, and the symposium (July 2, and 12 - 13), where the most recent achievement was presented. It was remarkable that some of experimentalists, invited to the symposium, are expecting the future success of joint computational and experimental research, and such comment was given from the field where the joint research had not been so common.

This workshop was financially supported by Computational Materials Science Initiative (CMSI) and ISSP, and the symposium was additionally supported by the Joint Research budget of ISSP. The management of the workshop was performed by Profs. Naoki Kawashima, Hiroshi Noguchi and Yoshifumi Noguchi (ISSP), Shinji Tsuneyuki and Koichi Yamashita (The University of Tokyo), Drs. Yoshiyuki Miyamoto and Minoru Otani (The National Institute of Advanced Industrial Science and Technology) and Drs. Takahisa Ohno and Yoshitaka Tateyama (The National Institute for Materials Science).



# ISSP International Workshop on Coherent Soft X-ray Sciences, and 5th Asian Workshop on Generation and Applications of Coherent XUV and X-ray Radiation (5th AWCXR)

June 27-29, 2012

J. Itatani, Y. Kobayashi, and S. Shin

The joint workshop of the 5th Asian Workshop on Generation and Application of Coherent XUV and X-ray Radiation (5th AWCXR) and the ISSP International Workshop on Coherent Soft X-ray Sciences were held from June 27 to 29, 2012 at the Media Hall, Kashiwanoha Library. The AWCXR workshop is originated from Asian Intense Laser Network. This time, it is jointly held with the ISSP International Workshop on Coherent Soft X-ray Sciences, aiming to envisage the future direction of new light sources such as laser-based high harmonics and XFEL's and their applications.

Because of the rapid progress in ultrafast soft-x-ray sciences, many fields are now getting close to each other. This joint workshop has become an opportunity where various fields (*e.g.*, intense lasers, next-generation synchrotrons, strong-field physics and material sciences) will meet in one place to discuss the future of emerging sciences and technologies. Following are the discussed topics:

- Intense ultrafast lasers
- High harmonic generation and attosecond physics
- VUV frequency comb and their applications
- XFEL and their applications
- Strong field physics and molecular sciences
- Material sciences with short-wavelength light sources

There were 2 tutorials, 35 oral presentations, and 20 poster presentations. There were about 120 participants including those from Korea (6), China (12) and Taiwan (1).

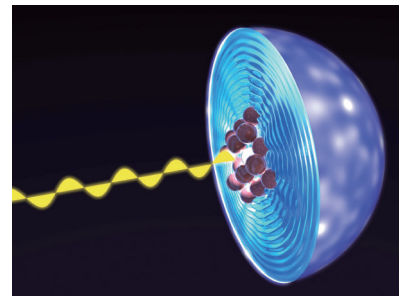


## International Workshop on 3D Atomic Imaging at Nano-Scale Active Sites in Materials

August 6-8, 2012

K. Hayashi, H. Daimon, K. Gohara, T. Takahashi, J. Yoshinobu, Y. Sasaki, K. Ohoyama, and T. Matsushita

“3D atomic imaging” is a quite new keyword as a scope of workshop, symposium or conference, despite of its importance for structural analysis in materials science. Therefore, we planned the ISSP workshop of “3D-AINAS” in order to exchange the ideas about the different analytical techniques aiming at 3D atomic imaging. We invited researchers whose specialities were atomic resolution holography, surface/interface scattering and diffractive imaging, and discussed what is necessary for realizing the ideal 3D atomic imaging. The ISSP workshop was consisted of 16 oral presentations and 23 poster presentations. Two young scientists were awarded in the banquet. Over 70 participants were attended to the workshop, and had a hot discussion during the whole time. At the end of the workshop, we got a consensus that the establishment in the 3D atomic imaging is necessary for revealing roles of the active sites in functional materials. The program is given at <https://sites.google.com/site/3daiworkshop/>.



# ISSP Workshops

## ISSP Workshop: Triple-Axis Spectrometer

April 27, 2012

T. Masuda and H. Yoshizawa

Since the fiscal year of 2010 the neutron scattering laboratory (NSL) started a new system for Instrument and Research Team (IRT) so that the IRT members can effectively use the machine time and they promote scientific activities in a specific theme. The members have produced excellent results in the fields of strongly correlated electron systems, frustrated system, Fe-based superconductor, f-electron system, etc. Then, on 11th March in 2011, the east Japan earthquake attacked neutron facilities and scientists could not perform neutron experiment in Japan. Instead many Japanese scientists had opportunity to conduct their experiments abroad thanks to the aid from foreign facilities including Oak Ridge National Laboratory (ORNL), Australian Nuclear Science and Technology Organization (ANSTO), Korea Academic Energy Research Institute (KAERI), etc. Many proposals of NSL joint research were transferred to these foreign facilities.

The aims of this workshop are to report the situation of the new IRT system and to present the scientific output obtained in the IRT system and in the transferred proposals. Instrumental scientists of six triple-axis spectrometers reported current situation and management of their spectrometers. Outstanding sciences outcomes including multiferroics, Fe-based superconductivity, f-electron systems, etc., were reported by the IRT members and several frequent users. The new IRT system and scientific topics in condensed matter physics were actively discussed by the professionals of triple-axis spectrometer.

## ISSP International Workshop on Coherent Soft X-ray Sciences, and 5th Asian Workshop on Generation and Applications of Coherent XUV and X-ray Radiation (5th AWCXR)

June 27-29, 2012

J. Itatani, Y. Kobayashi, and S. Shin

This ISSP workshop was held as a part of the international workshop of the same title. See the section of “International Conferences and Workshops”.

## MAterial Simulation in Petaflops era (MASP2012)

June 25 - July 13, 2012

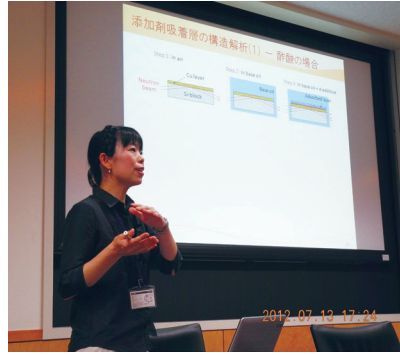
O. Sugino

This ISSP workshop was held as a part of the international workshop of the same title. See the section of “International Conferences and Workshops”.

# ISSP Workshop: Transport and Conversion Processes at Surfaces and Interfaces

July 13 - 14, 2012  
J. Yoshinobu

It becomes more and more important to utilize renewable energies efficiently after the 2011 Great East Japan Earthquake. Fundamental and applied studies towards practical use have been accelerated in the field of material science including artificial photosynthesis, water-splitting photocatalysis, thermoelectric conversion device etc. as well as solar cells. These materials and devices are closely related to the disciplines of new material development, optical properties of condensed matter, electronic states of solids, electrochemistry and so on. In particular, surfaces and interfaces between materials in devices play crucial roles, where various energy conversion and transport processes occur including photo excitation, charge separation, charge transport, energy level alignment, and chemical reactions. The processes at surface and/or interfaces could be rate limiting. In addition, energy dissipation (friction) occurs at interfaces. However, researchers in these fields have been working in different academic communities so far. In order to overcome the compartmentalized academic areas, this ISSP workshop was held; we have shared and exchanged our recent knowledge and idea in different fields. We hope that this workshop would activate the collaboration and joint research in the future.



# ISSP Workshop: Future Mission of Triple-Axis Spectrometer in Research Reactor and Polarized Neutron Scattering

July 23 - 24, 2012  
T. Masuda

Neutron scattering laboratory (NSL) operates triple-axis spectrometers (TAS) installed in research reactor JRR-3 that lead the frontier of neutron science in Japan. Meanwhile J-PARC, in which NSL owns a chopper spectrometer HRC, restarted its operation since December 2011 and now we are in the coexistence era of JRR-3 and J-PARC. In this workshop the future role of the TAS, the flagship of spectrometer in JRR-3, was discussed. As state of arts triple-axis spectrometers, those equipped with multi-detectors that cover wide reciprocal space are of practical use and MACS in NIST and Flatcone in ILL were introduced as successful examples. Meanwhile the important missions for the existing TAS were pointed out; spectrometer for polarized neutron scattering, spectrometer for general purposes from powder diffraction to inelastic neutron scattering on single crystal, and spectrometer for education. Among them polarized inelastic neutron scattering technique is noticed as a potentially powerful one that has not been well developed because of low efficiency of polarizer. Recent progress of polarizer such as supermirror or SEOP can be a breakthrough to realize the efficient inelastic polarized neutron scattering. Relevant research topics in the condensed matter sciences including novel magnetic correlation, precise measurement on spin fluctuations, hybrid mode of magnetic and lattice excitations, and etc. are introduced. Furthermore spin-echo option combined with polarized mode enables very high energy resolution experiment that is useful to the measurement of phonon lifetime, dynamics of Skyrmion lattice, low frequency mode of relaxor, etc. Cryopad option enables three-dimensional polarized neutron analysis and it is used for precise magnetic structure analysis on complex structure. Thus the upgrade of polarization function in TAS is the most important mission. Furthermore, the development of novel types of TAS having multi-detector is also desired. Finally the education for the students in neutron sciences is indispensable to the progress of the field and the TAS, of which the basic is simple, plays important role. Interesting presentations and fruitful discussions were made by 11 speakers and 20 participants.

# International Workshop on 3D Atomic Imaging at Nano-Scale Active Sites in Materials

August 6-8, 2012

K. Hayashi, H. Daimon, K. Gohara, T. Takahashi, J. Yoshinobu, Y. Sasaki, K. Ohoyama, and T. Matsushita

This ISSP workshop was held as a part of the international workshop of the same title. See the section of "International Conferences and Workshops".

## Frontier of Searching for Strongly Correlated Materials

October 22, 2012

Z. Hiroi, H. Kageyama, M. Nohara, and Y. Ueda

The workshop focused on the recent progress in searching for new compounds in the field of the strongly correlated electron systems. Approximately 60 people including 14 invited speakers got together and intensively discussed various classes of materials such as superconductors, frustrated compounds, and heavy fermion compounds. The workshop gave a good opportunity for attendees to understand the present status and to imagine the future prospect of materials research. Moreover, it was helpful in building a community for solid state chemists and physicists.



## Workshop on the Occasion of the Establishment of Laser and Synchrotron Research Center "Frontier of Laser and Synchrotron Joint Research"

November 29-30, 2012

T. Suemoto

Laser spectroscopy and synchrotron radiation (SOR) spectroscopy have made a considerable progress for decades as two independent fields. Recently, these two advanced light sources become to have a large overlap in the wavelength domain from terahertz to soft-X-ray. This workshop aimed at promoting collaboration between these two fields and we invited speakers from both laser and synchrotron communities under common concepts on physics and methodology. On the occasion of the establishment (Oct. 2012) of LASOR (Laser and Synchrotron Research Center) at Institute for Solid State Physics, we organized this workshop.

The sessions included are:

(1) General introduction of the recent activity of LASOR:

Laser sources based on high harmonic generation. High performance undulator at SPring-8.

(2) Time-resolved inner shell spectroscopy:

Chemistry of adsorbed molecules and catalysts. Operand-spectroscopy. Time-resolved inner-shell spectroscopy.

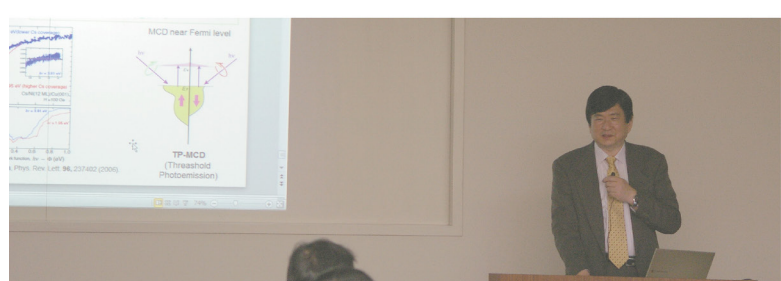
(3) High resolution photoemission spectroscopy (PES):

Application of high resolution PES to new materials including strongly correlated systems, topological insulators etc.

(4) Time-resolved photoemission spectroscopy:

Dynamics of photoinduced phase transitions, excited carriers in semiconductors, etc. Comparison of laser and SOR.

On average, 80 participants were present in every session, and we shared common science irrespective of the light source hardware. We believe that this workshop promote growth of a merged community of materials photon scientists.



# Recent Developments in Computational Condensed Matter Physics

January 10-11, 2013

O. Sugino, N. Kawashima, H. Noguchi, S. Todo, H. Watanabe, S. Kasamatsu, Y. Noguchi, and H. Shiba

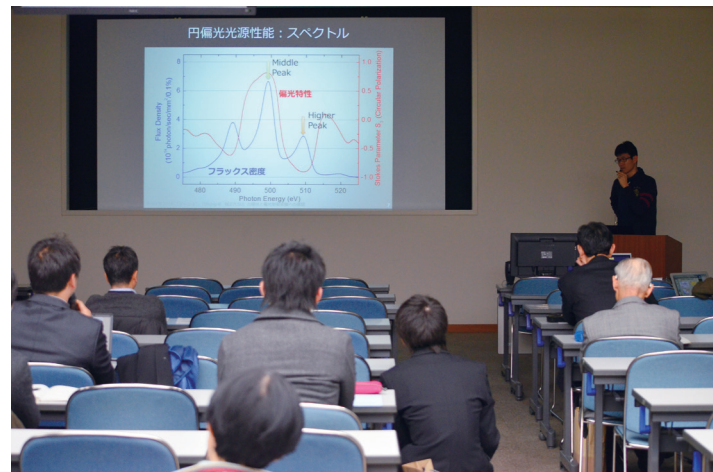
This workshop was held cosponsored by ISSP, CCMS (center of computational material science) of ISSP, and centers of the MEXT project “Research for Advanced Strategic Materials”. The ISSP supercomputing environment is facing sea change by the vast computer resources provided by K-computers (and possibly the exaflops computers of the next decade) and by the responsibility to take part in strategic material design. The ISSP supercomputer itself is going to be reinforced by the system C (Fujitsu FX10) in the coming new fiscal year and will be replaced to novel systems in 2015. In this circumstance, the annual ISSP supercomputer user workshop was enlarged this year to call for attendance of general computational materials scientists. The workshop started by the plenary talk by Prof. Matsuoka, a developer of Tsubame supercomputer, where the role of Graphics Processing Unit (GPU) played in the next generation supercomputers was discussed; Prof. Yoshimoto, on behalf of a committee of the HPCI consortium, discussed possible hardware and software requirements in the exaflops computers. In addition to the fifteen oral presentations given by the heavy users of ISSP supercomputers, four presentations were given on the future strategic research on advanced electronic materials, magnets, catalysts/batteries, and structural materials.

## Development for Polarization-Control Experiments at SPring-8BL07LSU: Present and Future

February 15, 2013

S. Shin, I. Matsuda, Y. Harada, and F. Komori

In the high-brilliance soft X-ray beamline BL07LSU of SPring-8, new proposals for long-term beam-time were approved and the beam-time started last year using three regular end-stations, which were made by the construction teams. The experiments of the short-time proposals have progressed smoothly as well. In parallel, the development for polarization-controlled experiments has been continued. This workshop was held to review the achievements of the proposals submitted this year in this beamline and to discuss the prospects of the polarization-controlled experiments. The number of the participants was over 60. After the summary of the beamline and achievements, the present status of the development for polarized light from the undulator was first reported. Then, the plan of the further developments for the polarization control using new phase-shifters and the application to the experimental studies of material science were proposed and discussed. In the latter half, fruitful and interesting experimental results at the regular end-stations and at the free port were presented. The beamline has been successfully constructed, and is now used for various studies on solid-state physics and materials science related to electronic devises, batteries and catalyses.



# Valence Fluctuations and Quantum Criticality in the Strongly Correlated Electron Systems

February 25, 2013

S. Nakatsuji, M. Takigawa, and Y. H. Matsuda

Quantum critical phenomena in the strongly correlated electron systems have attracted attention for the emergence of the exotic quantum phases such as anomalous metallic phase and anisotropic superconductivity. In this context, the heavy fermion systems have been well-studied since the high-purity single crystal samples are available and the ground state is tunable by magnetic field and pressure in the clean limit. As a result, anisotropic superconductivities and non-Fermi liquid behaviors have been found in various heavy fermion systems near the antiferromagnetic quantum critical point. These studies have been performed in the Kondo lattice systems where the valence of the rare-earth ions has the integer value. In contrast, in the valence fluctuating systems with a moderately high Kondo temperature, no instability of magnetism have been found because of strong screening effect. In recent years, however, the valence fluctuating systems have been found to show physical properties indicating localization of  $4f$  electrons, quantum critical phenomena and the superconductivities. In addition, the experimental results based on the recent developments of microscopic/macrosopic methods imply that these anomalous behaviors are strongly related to the valence fluctuations. Therefore, it was quite timely to organize this workshop to discuss the interesting developments and the future directions.

In spite of a short announcement, a relatively large number of on/off-campus researchers reaching 38 attended this workshop. As the first speaker, Prof. Kazumasa Miyake from Osaka University gave a introductory lecture about the theory of the quantum critical valence fluctuations. Next, based on the results obtained by the various experimental methods, several talks were made to discuss the quantum critical phenomena due to the valence fluctuations in  $\beta$ -YbAlB<sub>4</sub>. Distinct quantum critical behaviors were discussed, which were found under magnetic fields and pressure in the electric/thermal transport properties as well as the thermal bulk properties. It was pointed out that these quantum critical behaviors are clearly different from the typical non-Fermi liquid behaviors observed in the vicinity of the antiferromagnetic quantum critical point. The results of the microscopic measurements including Mossbauer spectroscopy and nuclear magnetic resonance were also reported in detail. Prof. Hisao Kobayashi from University of Hyogo reported slow valence fluctuations estimated from the latest results of the Yb Mossbauer spectroscopy obtained by using Synchrotron Radiation. Prof. Yasuhiro Matsuda at ISSP talked about the recent developments of the valence control by magnetic field. His talk provided an active discussion about the relation between the valence crossover and quantum critical phenomena. The time-resolved photoemission spectroscopy was also introduced as a new tool to measure dynamics of valence fluctuations. Finally, Prof. Hisatomo Harima from Kobe University introduced a new viewpoint to understand anomalous properties and superconductivities in the zigzag lattice. Through this workshop, the future direction was addressed to shed further light on this new quantum criticality.

# 平成24年度 共同利用課題一覧(前期) Joint Research List (2012 First Term)

## 嘱託研究員 (Commission Researcher)

No.	課題名	氏名	所属	Title	Name	Organization
1	超流動 <sup>3</sup> He-B相における表面束縛状態の実験的研究	奥田 雄一	東京工業大学 大学院理工学 研究科	Experimental study of the surface bound state of superfluid <sup>3</sup> He-B	Yuichi Okuda	Tokyo Institute of Technology
2	大規模第一原理計算プログラムSTATEを用いた固液界面の分子動力学シミュレーション	大谷 実	産業技術総合研究所 ナノシステム研究部門	Molecular dynamics simulations of metal-water interface using the large scale simulation tool (STATE)	Minoru Otani	National Institute of Industrial Science and Technology
3	<sup>3</sup> He- <sup>4</sup> He希釈冷凍機を用いた走査トンネル顕微鏡の改良と極低温スピンドル偏極STMの開発	河江 達也	九州大学 大学院工学研究科	Development of very Low-temperature spin-polarized STM with a <sup>3</sup> He- <sup>4</sup> He dilution refrigerator	Tatsuya Kawai	Kyushu University
4	3d遷移金属化合物の圧力下における磁気特性	鹿又 武	東北学院大学 工学総合研究所	Investigation of magnetic properties for 3d transition intermetallic compounds under pressure	Takeshi Kanomata	Tohoku Gakuin University
5	磁化測定装置の開発	名嘉 節	物質・材料研究機構	Development of the magnetometer	Takashi Naka	National Institute for Materials Science
6	NiCrAlを用いた圧力装置の開発	松本 武彦	物質・材料研究機構	The development of the pressure equipment using NiCrAl	Takehiko Matsumoto	National Institute for Materials Science
7	高压下の比熱測定装置の開発	梅原 出	横浜国立大学 工学部	Development of apparatus for specific heat measurements under high pressure	Izuru Umehara	Yokohama National University
8	擬一次元有機物質の圧力下物性研究	糸井 充穂	日本大学 医学部	Study on pressure induced superconductivity of quasi organic conductor	Miho Itoi	Nihon University
9	中性子回折に用いる圧力装置の開発	片野 進	埼玉大学	Developments of high pressure cell for neutron diffraction	Susumu Katano	Saitama University
10	新しい122化合物の単結晶成長の試みと圧力効果	池田 伸一	産業技術総合研究所 ナノエレクトロニクス研究部門	Pressure effect of new materials	Shinichi Ikeda	National Institute of Industrial Science and Technology
11	圧力下NMR測定法に関する開発	藤原 直樹	京都大学 大学院人間・環境学研究科	Development of NMR measurement method under high pressure	Naoki Fujimori	Kyoto University
12	有機伝導体の圧力効果	村田 恵三	大阪市立大学 大学院理学研究科	Effect of pressure on the organic conductor	Keizo Murata	Osaka City University

No.	課題名	氏名	所属	Title	Name	Organization
13	多重極限開連装置の調整	高橋 博樹	日本大学 文理学部	Adjustment of Cubic Anvil Apparatus	Hiroki Takahashi	Nihon University
14	AgPdCu合金圧力セルを用いた磁場中比熱測定	河江 達也	九州大学 大学院工学研究科	Development of pressure cell for specific heat measurements under magnetic field	Tatsuya Kawai	Kyushu University
15	重い電子系物質における圧力下電気抵抗測定	礒田 誠	香川大学 教育学部	Effect of Pressure on the Electrical Resistivity of Heavy Fermi on Compounds	Makoto Isoda	Kagawa University
16	Ce化合物の単結晶試料評価とその圧力効果	藤原 哲也	山口大学 大学院理工学研究科	Effect of Pressure on the Ce Compounds	Tetsuya Fujiwara	Yamaguchi University
17	低温マルチアンビル装置の開発	辺土 正人	琉球大学 理学部	Development of multi-anvil apparatus for low temperature	Masato Hedo	University of the Ryukyus
18	磁性体の圧力効果	巨海 玄道	久留米工業大学	Effect of Pressure on the Magnetic Materials	Gendo Oomi	Kurume Institute of Technology
19	高輝度放射光軟X線を用いた時間分解光電子分光による表面ダイナミクス研究	近藤 寛	慶應義塾大学 理工学部	Study of surface dynamics by time-resolved photoemission spectroscopy with high-brilliant soft x-ray synchrotron radiation	Hirosi Kondoh	Keio University
20	軟X線アンジュレータビームラインの分光光学系の開発研究	雨宮 健太	高エネルギー加速器研究機構 物質構造科学研究所	Research and development of soft X-ray undulator beamline	Kenta Amemiya	High Energy Accelerator Research Institute
21	高輝度光源計画における直入射ビームラインおよびその利用計画の検討	伊藤 健二	高エネルギー加速器研究機構 物質構造科学研究所	Design and case study for the high-resolution atoms- and molecules-spectroscopy beamline at the Super SOR facility	Kenji Ito	High Energy Accelerator Research Institute
22	光電子スピン検出器の開発・研究	奥田 太一	広島大学 放射光科学研究センター	Research and development of a new photoelectron spin detector	Taichi Okuda	Hirosima University
23	光電子顕微鏡による磁性ナノ構造物質の磁化過程	木下 豊彦	高輝度光科学研究所	Magnetization in process of magnetic nano structure by PEEM	Toyohiko Kinoshita	Japan Synchrotron Radiation Institute
24	高輝度極紫外ビームラインの設計・評価	小野 寛太	高エネルギー加速器研究機構 物質構造科学研究所	Design and characterization of brilliance VUV beamline	Kanta Ono	High Energy Accelerator Research Institute
25	高輝度極紫外ビームラインの設計・評価	木村 真一	自然科学研究機構 分子科学研究所	Design and characterization of brilliance VUV beamline	Shinichi Kimura	Institute for Molecular Science
26	高輝度光源ビームラインにおける分光光学系の設計・開発	後藤 後治	高輝度光科学研究所	Design of the new undulator beamline at Spring-8	Syunji Goto	Japan Synchrotron Radiation Institute
27	高輝度光源ビームラインにおける分光光学系の設計・開発	大橋 治彦	高輝度光科学研究所	Design of the new undulator beamline at Spring-8	Haruhiko Ohashi	Japan Synchrotron Radiation Institute
28	強磁場量子ビーム科学のためのハルスマグネットの開発	鳴海 康雄	東北大學	Development of pulse magnets for synchrotron and neutron experiments in pulsed high magnetic fields	Yasuo Narumi	Tohoku University
29	Mn化合物の時間分解光電子分光	大川 万里生	東京理科大学 理学部	Time resolved photoemission on Mn compounds	Mario Okawa	Tokyo University of Science

No.	課題名	氏名	所属	Title	Name	Organization
30	B系超伝導体の角度分解光電子分光	竹内 恒博	名古屋大学 エコトピア科学 研究所	Angle-resolved photoemission study on high Tc cuprate	Tsunehiko Takeuchi	Nagoya University
31	光電子分光法を用いた各種分子性結晶の電子状態の研究及び装置の低温化	木須 孝幸	大阪大学 大学院基礎工 学科研究科	Research on electron state of molecular crystals using photoemission spectroscopy	Takayuki Kisu	Osaka University
32	共鳴逆光電子分光装置の開発	樋口 透	東京理科大学 理学部	Development of resonant inverse photoemission spectroscopy	Tohru Higuchi	Tokyo University of Science
33	重い電子系ラン化合物の高分解能光電子分光	藤森 伸一	日本原子力研 究開発機構 量子ビーム応用 部門	Ultra high resolution photoemission study on heavy fermion uranium compounds	Shinichi Fujimori	Japan Atomic Energy Agency
34	準結晶の高分解能光電子分光	田村 隆治	東京理科大学 基礎工学部	High-resolution photoemission study on quasi crystals	Ryuji Tamura	Tokyo University of Science
35	レーザー光電子分光による酸化物薄膜の研究	津田 後輔	物質・材料研究 機構	Laser-photoemission study on oxide films	Shunsuke Tsuda	National Institute for Materials Science
36	超高空間分解能光電子顕微鏡による磁区構造観察	中川 剛志	自然科学研究 機構	Observation of magnetic domain structures by ultra-high resolution photoemission electron microscopy	Takeshi Nakagawa	Institute for Molecular Science
37	新規開発強相関物質の高分解能光電子分光	小野瀬 佳文	東京大学 大学院工学系 研究科	Ultra-high resolution photoemission spectroscopy on new strongly correlated materials	Yoshinori Onose	The University of Tokyo
38	レーザーPEEMによる磁性体の研究	小野 寛太	高エネルギー加 速器研究機構 物質構造科学 研究室	Study on magnetism by laser PEEM	Kanta Ono	High Energy Accelerator Research Institute
39	酸化バナジウムの高分解能光電子分光	江口 律子	岡山大学 大学院自然科 学研究科	Photoemission study on vanadium oxides	Ritsuko Eguchi	Okayama University
40	有機化合物の光電子分光	金井 要	東京理科大学 理工学部	Photoemission study on organic compounds	Kaname Kanai	Tokyo University of Science
41	鉄ニクタイドの高分解能光電子分光	吉田 鉄平	東京大学 大学院理学系 研究科	Ultra-high resolution photoemission spectroscopy on Fe-based superconductor	Teppei Yoshiida	The University of Tokyo
42	鉄系超伝導体のレーザー光電子分光	下志万 貴博	東京大学 大学院工学系 研究科	Laser-ARPES on Fe superconductor	Takahiro Shinjojima	The University of Tokyo
43	4f電子系物質の高分解能光電子分光	松波 雅治	自然科学研究 機構	Photoemission study on 4f materials	Masaharu Matsunami	Institute for Molecular Science
44	高分解能光電子分光による強相関物質の研究	横谷 尚睦	岡山大学 大学院自然科 学研究科	Ultra-high resolution study on strongly correlated materials	Takayoshi Yokoya	Okayama University
45	高温超伝導体の高分解能光電子分光	藤森 淳	東京大学 大学院理学系 研究科	Ultra-high resolution photoemission spectroscopy on high Tc superconductor	Atsushi Fujimori	The University of Tokyo
46	60-eVレーザーを用いた時間分解光電子分光の開発	石坂 香子	東京大学 大学院工学系 研究科	The development of time-resolved photoemission using 60eV laser	Kyoko Ishizaka	The University of Tokyo

No.	課題名	氏名	所属	Title	Name	Organization
47	小型集中型小角散乱装置の高性能化及びそれにによる応用研究	古坂 道弘	北海道大学 大学院工学研究科	Development of a compact focusing small-angle neutron scattering instrument and application research using the instrument	Michihiro Furusaka	Hokkaido University
48	中性子極小角散乱実験装置のアップグレード	金子 純一	北海道大学 大学院工学研究科	Upgrade of ULS system	Junichi Kaneko	Hokkaido University
49	中性子散乱装置FONDERのアップグレード後の研究計画の実施と共同利用の推進	野田 幸男	東北大学 多元物質科学研究所	Upgrading of neutron diffractometer FONDER and contributing to user collaboration program	Yukio Noda	Tohoku University
50	中性子散乱装置の共同利用・開発による強相関電子系物質の構造物性の研究	岩佐 和晃	東北大学 大学院理学研究科	Structural studies of strongly correlated electron systems by neutron scattering method and instrumental development	Kazuaki Iwasa	Tohoku University
51	中性子4軸回折計FONDERの制御プログラムの改良	木村 宏之	東北大学 多元物質科学研究所	Updating of control program for four circle neutron diffractometer FONDER	Hiroyuki Kimura	Tohoku University
52	中性子散乱装置のアップグレードと共同利用研究の推進	藤田 全基	東北大学 金属材料研究所	Upgrading of the neutron scattering device and promotion of the research and public use	Masaki Fujita	Tohoku University
53	中性子散乱装置のアップグレード後の研究計画の実施と共同利用の推進	大山 研司	東北大学 金属材料研究所	Propelling the inter university research cooperation	Kenji Ohoyama	Tohoku University
54	中性子散乱装置のアップグレード後の研究計画の実施と共同利用の推進	平賀 晴弘	東北大学 金属材料研究所	Implementation of the research plan under the cooperation-use program after upgrading neutron scattering instruments	Haruhiro Hiraka	Tohoku University
55	中性子散乱装置のアップグレード後の研究計画の実施と共同利用の推進	田畑 吉計	京都大学 大学院工学研究科	Progress of the joint research by using the neutron scattering instruments	Yoshikazu Tabata	Kyoto University
56	中性子散乱装置のアップグレード後の研究計画の実施と共同利用の推進	松村 武	広島大学 大学院先端物質科学研究所	Promotion of joint research after the upgrade of neutron scattering instruments	Takeshi Matsumura	Hirosima University
57	J-PARC/MLFとJRR-3共存時代に向けた3軸型中性子散乱装置の高度化	松浦 直人	東北大学 金属材料研究所	Upgrade of 3-axis neutron spectrometer for the oncoming coexistence of J-PARC/MLF and JRR-3	Masato Matsura	Tohoku University
58	中性子分光器を用いた強相関電子系物質の微視的研究	桑原 慶太郎	茨城大学 大学院理工学研究科	Neutron scattering study of strongly correlated electron systems by using neutron triple-axis spectrometers	Keitaro Kuwahara	Ibaraki University
59	高度化した3軸分光器を用いた共同利用の推進と物質科学研究の実施	横山 淳	茨城大学 理学部	Executing user program and study of material science with the advanced triple-axis spectrometers	Makoto Yokoyama	Ibaraki University
60	冷中性子スピン干渉計の応用とMINEビームラインの整備	田崎 誠司	京都大学 大学院工学研究科	Development of cold neutron spin interferometry and improvements of MINE beam line	Seiji Tasaki	Kyoto University
61	膜貫通ペプチドのフリップフロップ誘起能の評価	中野 実	富山大学 大学院医学薬学研究部(薬学)	Induction of Phospholipid Flip-Flop by Transmembrane Peptides	Minoru Nakano	University of Toyama
62	C1-3 ULS極小角散乱装置IRT	杉山 正明	京都大学 原子炉実験所	Development of micro-focusing small-angle neutron scattering spectrometer	Masaaki Sugiyama	Kyoto University
63	集光テスト用小型SANSの開発及び冷中性子反射率計・干渉計のアップグレード	日野 正裕	京都大学 原子炉実験所	Improvement of MIEZE spectrometer and cold neutron reflectometer and interferometer	Masahiro Hino	Kyoto University

No.	課題名	氏名	所属	Title	Name	Organization
64	集光テスト用小型SANSの開発及び冷中性子反射率計・干渉計のアップグレード	北口 雅典	京都大学 原子炉実験所	Improvement of MIEZE spectrometer and cold neutron reflectometer and interferometer	Masaaki Kitaguchi	Kyoto University
65	中性子散乱用高压セルの開発および高压下における中性子散乱実験	藤原 哲也	山口大学 大学院理工学研究科	Neutron scattering experiments under high pressure and development of high pressure cell for neutron scattering	Tetsuya Fujiiwara	Yamaguchi University
66	流动場でのソフトマターの構造変化に関する研究	高橋 良彰	九州大学 先導物質化学研究所	Studies on structural change of soft matter under flow field	Yoshiaki Takahashi	Kyushu University
67	三軸分光器を用いた極端条件下における物質科学研究の実施	阿曾 尚文	琉球大学 理学部	Material science studies under extreme conditions by using triple-axis spectrometers	Naofumi Aso	University of the Ryukyus
68	糖系界面活性剤水溶液のゲル構造におけるラメドメイン構造	川端 康平	首都大学東京 大学院理工学研究科	Lamellar domain structures in the gel structure of a sugar surfactant solution	Youhei Kawabata	Tokyo Metropolitan University
69	中性子散乱研究計画の実施と共同利用の推進	伊藤 晋一	高エネルギー加速器研究機構 仁科加速器センター	Propelling the inter university research cooperation	Shinichi Itoh	High Energy Accelerator Research Institute
70	冷中性子干涉コントロールシステムがびに超精密光学実験の開発研究	大竹 淑恵	理化学研究所	Upgrade the instrument of the ultra-precise optics for cold neutron and research and development of cold neutron interferometer	Yoshie Otake	RIKEN
71	量子臨界物質の極低温磁化測定	柄木 良友	琉球大学 教育学部	Ultra low temperature measurements for quantum critical materials	Yoshitomo Karaki	University of the Ryukyus
72	テラヘルツパルス電磁波によるスピinn秩序の制御の研究	中嶋 誠	千葉大学 理学部	Study of spin order control by pulsed terahertz radiation	Makoto Nakajima	Chiba University
73	高輝度軟X線を利用した強相関物質の電子状態研究	組頭 広志	高エネルギー加速器研究機構 物質構造科学研究所	Study of electronic states in strongly correlated materials with high brilliant soft-Xray	Hiroshi Kumigashira	High Energy Accelerator Research Institute
74	時間分解光電子分光法による光触媒材料のキャラクタライジング研究	小澤 健一	東京工業大学 大学院理工学研究科	Study of carrier dynamics in photocatalysis materials by time-resolved photoemission spectroscopy	Kenichi Ozawa	Tokyo Institute of Technology
75	高輝度軟X線を利用する光電子顕微鏡装置の設計・開発	坂本 一之	千葉大学 大学院融合科学研究中心	Research and designing of a PEEM spectrometer for high brilliance soft X ray.	Kazuyuki Sakamoto	Chiba University
76	二次元表示型スピinn分解光電子エネルギー分析器の開発	大門 寛	奈良先端科学技術大学院大学	Development of 2D display type spin resolved photoelectron energy analyzer.	Hiroshi Daimon	Nara Institute of Science and Technology
77	転X線時間分解分光実験による磁性研究	木村 昭夫	広島大学 大学院理学研究科	Study of magnetic properties by time-resolved soft X-ray spectroscopy	Akio Kimura	Hirosima University
78	超高分解能転X線発光分光による水素吸蔵合金中の水素の波動関数の局在性に関する研究	関場 大一郎	筑波大学	Study on the localization of Wave functions of hydrogen atom in hydrogen storage alloys using ultrahigh resolution soft X-ray emission spectroscopy	Daiichiro Sekiba	University of Tsukuba
79	転X線吸収／発光分光法によるリチウムイオン電池電極材料の電子物性研究	朝倉 大輔	産業技術総合研究所 エネルギー界面技術グループ	Study on the electronic property of electrode materials for Li-ion batteries by soft X-ray absorption/emission spectroscopy	Daisuke Asakura	National Institute of Industrial Science and Technology
80	時間分解光電子分光による重い電子系の研究	関山 明	大阪大学 大学院基礎工学科	Study on heavy Fermion materials by time-resolved Photoemission	Akira Sekiyama	Osaka University

No.	課題名	氏名	所属	Title	Name	Organization
81 究	高分解能光電子分光による酸化バナジウムの研	藤原 秀紀	大阪大学 大学院基礎工 学研究科	Study on vanadium oxides by high resolution Photoemission	Hidegori Fujiwara	Osaka University
82	鉄シリコンの円2色性光電子分光の研究	中村 元彦	奈良教育大学 理科教育講座	Study of circular dichroism of photoemission on FeSi	Motohiko Nakamura	Nara University of Education
83	角度分解光電子分光法による遷移金属酸化物の 表面/界面電子状態の研究	吉松 公平	東京大学 大学院理学系 研究科	Angle-resolved photoemission study of the interfacial states of transition-metal oxides	Kohei Yoshimatsu	The University of Tokyo

一般研究員 (General Researcher)

No.	課題名	氏名	所属	Title	Name	Organization
1	ずれ振動に対する固体ヘリウム4の応答	青木 悠樹	東京工業大学 大学院総合理 工学研究科	Acoustic shear response of solid Helium 4	Yuki Aoki	Tokyo Institute of Technology
2	回転超流動ヘリウム3のテクスチャーダイナミクス の研究	佐々木 豊	京都大学 低温物質科学 研究センター	Texture dynamics of Rotating Superfluid <sup>3</sup> He	Yutaka Sasaki	Kyoto University
3	強相関電子系化合物の秩序相に対する結晶対 称性および軌道還縮退の効果	横山 淳	茨城大学 理学部	Effects of crystal symmetry and orbital degeneracy in ordered states of strongly correlated electron systems	Makoto Yokoyama	Ibaraki University
4	"	中野 優	茨城大学 大学院理工学 研究科	"	Suguru Nakano	Ibaraki University
5	高压合成希土類6,12元化合物の磁化特性	伊賀 文俊	茨城大学 理学部	Magnetic property of rare earth hexa- and dodeca-borides produced by high pressure synthesis	Fumitoshi Iga	Ibaraki University
6	重い電子系超伝導体の対称性決定	町田 一成	岡山大学 大学院自然科 学研究科	Symmetry determination of pairing functions in heavy Fermion superconductors	Kazushige Machida	Okayama University
7	超流動ヘリウム3-A相の新奇量子渦の研究	石川 修六	大阪市立大学 大学院理学研 究科	Study of novel quantum vortex of superfluid <sup>3</sup> He	Osamu Ishikawa	Osaka City University
8	"	國松 貴之	大阪市立大学 大学院理学研 究科	"	Takayuki Kunitatsu	Osaka City University
9	量子スピinn液体Tb <sub>2</sub> Ti <sub>2</sub> O <sub>7</sub> の比熱測定	高津 浩	首都大学東京 大学院理工学 研究科	Specific heat of the quantum spin liquid of Tb <sub>2</sub> Ti <sub>2</sub> O <sub>7</sub>	Hiroshi Takatsu	Tokyo Metropolitan University
10	一次元フラーストレート磁性体におけるネマティック 相間の微視的観測	吉村 一良	京都大学 大学院理学研 究科	Microscopic observation of nematic correlation in one- dimensional frustrated magnets	Kazuyoshi Yoshimura	Kyoto University
11	"	那波 和宏	京都大学 大学院理学研 究科	"	Kazuhiro Nawa	Kyoto University
12	擬二次元磁性体Sr <sub>2</sub> V <sub>2</sub> O <sub>5</sub> における磁気低温相の解 明	吉村 一良	京都大学 大学院理学研 究科	Investigation of a low-temperature magnetic phase in a quasi- two-dimensional magnet Sr <sub>2</sub> V <sub>2</sub> O <sub>5</sub>	Kazuyoshi Yoshimura	Kyoto University

No.	課題名	氏名	所属	Title	Name	Organization
13	擇二次元磁性体Sr <sub>2</sub> VO <sub>4</sub> における磁気低温相の解明	那波 和宏	京都大学 大学院理学研究科	Investigation of a low-temperature magnetic phase in a quasi-two-dimensional magnet Sr <sub>2</sub> VO <sub>4</sub>	Kazuhiko Nawa	Kyoto University
14	磁気トルク測定による有機導体の研究	鳥塚 潔	法政大学 理工学部	Studies on organic molecular conductors by magnetic torque measurements	Kiyoshi Torizuka	Hosei University
15	超高压プレスを用いた新規プロトニクス酸化物のソフト化学的合成法の検討	山口 周	東京大学 大学院工学系研究科	Oxide-Protonics materials synthesis by combined use of soft chemical method and high pressure	Shu Yamaguchi	The University of Tokyo
16	"	三好 正悟	東京大学 大学院工学系研究科	"	Shogo Miyoshi	The University of Tokyo
17	"	田中 和彦	東京大学 大学院工学系研究科	"	Kazuhiro Tanaka	The University of Tokyo
18	溶融亜鉛メッキ合金相の応力誘起変態	山口 周	東京大学 大学院工学系研究科	Stress-induced phase transformation of Fe-Zn alloy formed in hot-dip process	Shu Yamaguchi	The University of Tokyo
19	"	三好 正悟	東京大学 大学院工学系研究科	"	Shogo Miyoshi	The University of Tokyo
20	"	田中 和彦	東京大学 大学院工学系研究科	"	Kazuhiro Tanaka	The University of Tokyo
21	幾何学的フラストレート遍歷電子系における電子相關効果	山下 靖文	日本大学 工学部	Effect of electron correlations in geometrically frustrated itinerant-electron systems	Yasufumi Yamashita	Nihon University
22	機械的応力のシリコン表面化学への影響に関する研究	成島 哲也	自然科学研究機構	Effect on Silicon Surface Chemistry of External Mechanical Stress	Tetsuya Narushima	Institute for Molecular Science
23	銅表面上ナノ構造における非線形発光の時間分解測定	河村 紀一	日本放送協会 放送技術研究所	Time resolved spectroscopy of harmonics from nano-structures on Cu surfaces	Norikazu Kawamura	NHK Science and Technology Research Laboratory
24	エピタキシャルシリセンの低温走査トンネル顕微鏡観察	高村 由起子	北陸先端科学技術大学院大学	Low temperature scanning tunneling microscopy investigations of epitaxial silicene	Yukiko Takamura	Japan Advanced Institute of Science and Technology
25	"	ライナー フリードライバー	北陸先端科学技術大学院大学	"	Rainer Friedlein	Japan Advanced Institute of Science and Technology
26	"	アントワーヌ フロランス	北陸先端科学技術大学院大学	"	Antoine Fleuret	Japan Advanced Institute of Science and Technology
27	(MnCo) <sub>2</sub> Sbの一次磁気相転移の磁場中圧力効果	小山 佳一	鹿児島大学 大学院理工学研究科	Pressure effect on first order magnetic transition of (MnCo) <sub>2</sub> Sb	Keiichi Koyama	Kagoshima University
28	"	折橋 広樹	鹿児島大学 大学院理工学研究科	"	Hiroti Orihashi	Kagoshima University
29	Dy <sub>2</sub> Ti <sub>2</sub> O <sub>7</sub> のカゴメアイス状態における磁気モノボール	高津 浩	首都大学東京 大学院理工学研究科	Magnetic monopole in the kagome ice state of Dy <sub>2</sub> Ti <sub>2</sub> O <sub>7</sub>	Hiroti Takatsu	Tokyo Metropolitan University

No.	課題名	氏名	所属	Title	Name	Organization
30	Fe <sub>3</sub> Mo <sub>3</sub> Nの高圧下電気抵抗率測定	和氣 剛	京都大学 大学院工学研究科	Resistivity measurement of Fe <sub>3</sub> Mo <sub>3</sub> N under high pressure	Takeshi Waki	Kyoto University
31	Ni-Mn-Ga系強磁性形状記憶合金の磁化の圧力依存性	安達 義也	山形大学 大学院理工学研究科	Pressure Dependence of Magnetization for the Ferrromagnetic Shape-Memory Alloys of Ni-Mn-Ga system	Yoshiya Adachi	Yamagata University
32	"	三浦 友也	山形大学 大学院理工学研究科	"	Tomoya Miura	Yamagata University
33	Pd基ホイスラー合金の高圧下輸送特性	岡田 宏成	東北学院大学 工学部	Transport properties under high pressure in Pd-based Heusler alloys	Hironari Okada	Tohoku Gakuin University
34	PrRu <sub>2</sub> P <sub>2</sub> の高圧力下磁化測定	藤原 哲也	山口大学 大学院理工学研究科	Magnetization measurements under high pressures in PrRu <sub>2</sub> P <sub>2</sub>	Tetsuya Fujiiwara	Yamaguchi University
35	"	巖田 裕也	山口大学 大学院理工学研究科	"	Yuya Kurata	Yamaguchi University
36	TmB <sub>4</sub> の磁気準周期秩序相における圧力効果	伊賀 文後	茨城大学 理学部	Pressure effect on the magnetic quasi-period ordered phase in TmB <sub>4</sub>	Fumitoshi Iga	Ibaraki University
37	"	道村 真司	日本原子力研究開発機構 量子ビーム応用研究部門	"	Shinji Michimura	Japan Atomic Energy Agency
38	TTF-TCNQ類縁物質の高圧物性	村田 恵三	大阪市立大学 大学院理学研究科	High Pressure Properties of TTF-TCNQ Analogue	Keizo Murata	Osaka City University
39	"	福本 雄平	大阪市立大学 理学部	"	Yuhei Fukumoto	Osaka City University
40	セリウム系磁性超伝導体における微小磁気モーメントの圧力下磁化測定	阿曾 尚文	琉球大学 理学部	Magnetization studies under pressure in Ce-based magnetic superconductors with small magnetic moments	Naofumi Aso	University of the Ryukyus
41	"	田中 秀和	琉球大学 大学院理工学研究科	"	Hidekazu Tanaka	University of the Ryukyus
42	圧力下強磁場電子スピinn共鳴測定のためのハイブリッド圧力セルの開発	櫻井 敬博	神戸大学 研究基盤センター	Development of hybrid pressure cell for high field electron spin resonance measurement under pressure	Takahiro Sakurai	Kobe University
43	圧力誘起超伝導体の圧力下輸送特性	中野 智仁	新潟大学 工学部	Transport property of pressure-induced superconductor	Tomohito Nakano	Niigata University
44	"	穴田 泰士	新潟大学 理学部	"	Taishi Anada	Niigata University
45	缶数据動物質の高圧力中輸送特性の研究	仲間 隆男	琉球大学 理学部	Transport properties of valence fluctuation compounds	Takao Nakama	University of the Ryukyus
46	"	山村 愛	琉球大学 大学院理工学研究科	"	Ai Nakamura	University of the Ryukyus

No.	課題名	氏名	所属	Title	Name	Organization
47	磁気運動物質の高圧力中輸送特性の研究	平伸 裕一	琉球大学 大学院理工学 研究科	Transport properties of valence fluctuation compounds	Yuichi Hirakaka	University of the Ryukyus
48	希土類トリテルラジド $\text{RTe}_3$ ( $\text{R} = \text{Ce}, \text{Tb}$ )と $\text{SmS}$ の高圧下物性実験	佐藤 憲昭	名古屋大学 大学院理学研究科	High pressure experiments of $\text{RTe}_3$ ( $\text{R}=\text{Ce}, \text{Tb}$ ) and $\text{SmS}$	Noriaki Sato	Nagoya University
49	"	出口 和彦	名古屋大学 大学院理学研究科	"	Kazuhiro Deguchi	Nagoya University
50	"	今井 祐也	名古屋大学 大学院理学研究科	"	Yuya Imai	Nagoya University
51	希土類強磁性体 $\text{RAL}_2$ の異方的磁気体積効果	大橋 政司	金沢大学 環境デザイン学系 系	Anisotropic magnetovolume effect of rare earth ferrromagnet $\text{RAL}_2$	Masashi Ohashi	Kanazawa University
52	"	澤味 一馬	金沢大学 大学院自然科学研究科	"	Kazuma Sawami	Kanazawa University
53	希土類金属間化合物の高压下における磁性と輸送特性	仲間 隆男	琉球大学 理学部	Magnetism and transport properties of rare-earth intermetallic compounds under high pressure	Takao Nakama	University of the Ryukyus
54	"	内間 清晴	沖縄キリスト教短期大学 沖縄キリスト教短期大学	"	Kiyoharu Uchima	Okinawa Christian Junior College
55	"	竹田 政貴	琉球大学 大学院理工学 研究科	"	Masataka Takeda	University of the Ryukyus
56	"	照屋 淳志	琉球大学 大学院理工学 研究科	"	Atsushi Teruya	University of the Ryukyus
57	強相関型セリカム化合物および合金の量子相転移と磁性	村山 茂幸	室蘭工業大学 大学院工学研究科	Quantum phase transition and magnetism in the strongly correlated Ce compounds and alloys	Shigeyuki Murayama	Muroran Institute of Technology
58	"	雨海 有佑	室蘭工業大学 大学院工学研究科	"	Yusuke Amakai	Muroran Institute of Technology
59	"	森岡 敦	室蘭工業大学 大学院工学研究科	"	Tsutomo Morioka	Muroran Institute of Technology
60	空間反転対称性のない $\text{EuTX}_3$ ( $\text{T}=\text{Fe}, \text{Co}, \text{Ni}; \text{X}=\text{Ge}, \text{Si}$ ) の圧力誘起価移の探索	辺土 正人	琉球大学 理学部	Searching for pressure-induced valence transition of non-inversion symmetry structure $\text{EuTX}_3$ ( $\text{T}=\text{Fe}, \text{Co}, \text{Ni}; \text{X}=\text{Ge}, \text{Si}$ )	Masato Hedo	University of the Ryukyus
61	"	平川 先太郎	琉球大学 大学院理工学 研究科	"	Sendarou Hirakawa	University of the Ryukyus
62	空間反転対称性のない $\text{CeTSi}_3$ ( $\text{T}=\text{Rh}, \text{Ir}$ ) の圧力下電気抵抗	阿曾 尚文	琉球大学 理学部	Electrical resistivity under pressure of non-centrosymmetric magnetic superconductors $\text{CeTSi}_3$ ( $\text{T}=\text{Rh}, \text{Ir}$ )	Naofumi Aso	University of the Ryukyus
63	"	高江洲 義尚	琉球大学 大学院理工学 研究科	"	Yoshimao Takaesu	University of the Ryukyus

No.	課題名	氏名	所属	Title	Name	Organization
64	空間反転対称性のない EuTX <sub>3</sub> (T=Fe,Co,Ni; X=Ge,Si) の圧力誘起価移の探索	田中 秀和	琉球大学 大学院理工学研究科	Searching for pressure-induced valence transition of non-inversion symmetry structure EuTX <sub>3</sub> (T=Fe,Co,Ni; X=Ge,Si)	Hidekazu Tanaka	University of the Ryukyus
65	充填型物質の作成と圧力下物性	中野 智仁	新潟大学 工学部	Magnetic properties under pressure of filled-type compound	Nakano Tomohito	Niigata University
66	"	青山 悠司	新潟大学 大学院自然科学研究科	"	Yoji Aoyama	Niigata University
67	重い電子系新物質Ce <sub>2</sub> Pt <sub>3</sub> Ge <sub>3</sub> の高圧力下磁化測定	藤原 哲也	山口大学 大学院理工学研究科	Magnetization measurements under high pressures in new heavy fermion system Ce <sub>2</sub> Pt <sub>3</sub> Ge <sub>3</sub>	Tetsuya Fujiwara	Yamaguchi University
68	"	長谷川 貴大	山口大学 大学院理工学研究科	"	Takahiro Hasegawa	Yamaguchi University
69	多形性化合物Rh <sub>2</sub> Si <sub>2</sub> の磁気転移	繁岡 透	山口大学 大学院理工学研究科	Magnetic transition of polymorphic compounds Rh <sub>2</sub> Si <sub>2</sub>	Toru Shigeoka	Yamaguchi University
70	"	大河原 遊	山口大学 大学院理工学研究科	"	Yu Okawara	Yamaguchi University
71	大きな管状構造を持つCeRuGe <sub>3</sub> の高压輸送特性	辺土 正人	琉球大学 理学部	Transport properties under high pressure on large cage structure CeRuGe <sub>3</sub>	Masato Hedo	University of the Ryukyus
72	"	渡部 晋太郎	琉球大学 大学院理工学研究科	"	Shintarou Watanabe	University of the Ryukyus
73	逐次転移を示すMn <sub>3</sub> ZnNの圧力効果	飯久保 智	九州工業大学 大学院生命体工学研究科	Pressure Effect on Magnetic Ordering in Mn <sub>3</sub> ZnN	Satoshi Iikubo	Kyushu Institute of Technology
74	中性-イオン性転移物質の超高压下電気伝導度測定	鹿野田 一司	東京大学 大学院工学系研究科	Resistivity measurement of neutral-ionic phase transition materials under extreme high pressure	Kazushi Kanoda	The University of Tokyo
75	"	富川 和也	東京大学 大学院工学系研究科	"	Kazuya Miyagawa	The University of Tokyo
76	"	竹原 陵介	東京大学 大学院工学系研究科	"	Ryosuke Takehara	The University of Tokyo
77	鉄系超伝導体関連物質の圧力効果	余 珊	物質・材料研究機構	Pressure effects of Fe-based superconductor related materials	Yu Shan	National Institute for Materials Science
78	導電性ラングミニア・プロジェクト膜の高压下の電気的性質に関する研究	三浦 康弘	桐蔭横浜大学 大学院工学研究科	Studies on Electrical Properties of Conductive Langmuir-Blodgett Films under High Pressure	Yasuhiro Miura	Toin University of Yokohama
79	高N濃度(In)GaAsN系潤晶薄膜の構造解析(3)	翟谷 茂幸	東京大学 大学院新領域創成科学研究科	Structural analysis of higher-N-content (In)GaAsN films (3)	Shigeyuki Kuboya	The University of Tokyo
80	窒素変調ビームエピタキシ法により作製した窒化物半導体超格子構造の高分解能X線回折測定	小柴 俊	香川大学 工学部	High Resolution XRD Studies of Nitride Semiconductor Superlattices by Modulated Nitrogen Beam Epitaxy	Shyun Koshiha	Kagawa University

No.	課題名	氏名	所属	Title	Name	Organization
81	窒素変調ビームエピタキシ一法により作製した窒化物半導体超格子構造の高分解能X線回折測定	矢内 勝輔	香川大学 大学院工学研究科	High Resolution XRD Studies of Nitride Semiconductor Superlattices by Modulated Nitrogen Beam Epitaxy	Syunsuke Yanai	Kagawa University
82	立方晶窒化物半導体の結晶成長と評価	角田 雅弘	東京大学 大学院新領域創成科学研究科	Crystal growth and characterization of cubic nitride semiconductor	Masahiro Kakuda	The University of Tokyo
83	RF-MBE法を用いた窒化物半導体超格子構造の電気特性評価	小柴 勝	香川大学 工学部	Electric characteristic of nitride semiconductor superlattice grown by radio frequency molecular beam epitaxy using modulated N radical beam method	Shyun Koshiba	Kagawa University
84	"	稻田 雅俊	香川大学 大学院工学研究科	"	Masatoshi Inada	Kagawa University
85	希薄磁性半導体GaGdAsの光学特性・光スピン・ダイナミクスに及ぼす成長条件・Gd濃度の影響	宮川 勇人	香川大学 工学部	Growth Condition Effect on Optical Properties and Opto-spin Dynamics of Diluted Magnetic Semiconductor GaGdAs	Hayato Miyagawa	Kagawa University
86	"	松本 翔太郎	香川大学 大学院工学研究科	"	Shotaro Matsumoto	Kagawa University
87	窒素アルタードープGaAs中の等電子トランプカウチの単一光子発生に関する研究	矢口 裕之	埼玉大学 大学院理工学研究科	Single photon generation from isoelectronic traps in nitrogen delta-doped GaAs	Hiroyuki Yaguchi	Saitama University
88	"	高宮 健吾	埼玉大学 大学院理工学研究科	"	Kengo Takamiya	Saitama University
89	"	吉田 直史	埼玉大学 大学院理工学研究科	"	Naofumi Yoshida	Saitama University
90	Mg <sub>2</sub> Siの高压合成	草場 啓治	名古屋大学 大学院工学研究科	High-pressure synthesis of Mg <sub>2</sub> Si	Keiji Kusaba	Nagoya University
91	"	能丸 大器	名古屋大学 大学院工学研究科	"	Taiki Noumaru	Nagoya University
92	カニ状構造を持つ新奇希土類ニアクチダの探索	闇根 ちひろ	室蘭工業大学 大学院工学研究科	Search for new rare-earth pnictides with cage-like structure	Chihiro Sekine	Muroran Institute of Technology
93	"	川田 友和	室蘭工業大学 大学院工学研究科	"	Tomokazu Kawata	Muroran Institute of Technology
94	新規アルカリ土類金属間化合物の超高圧合成	長谷川 正	名古屋大学 大学院工学研究科	High pressure synthesis of novel alkaline earth metal intermetallic compounds	Masashi Hasegawa	Nagoya University
95	"	江口 邦	名古屋大学 大学院工学研究科	"	Ryo Eguchi	Nagoya University
96	正20面体希土類クラスターの磁気物性	賀戸 孝信	東京理科大学 大学院基礎工学科	Magnetic properties of intermetallic compounds made of icosahedral rare-earth clusters	Takanobu Hiroto	Tokyo University of Science
97	大型プレスを用いた新規遷移金属炭化物の高压合成	舟羽 健	名古屋大学 大学院工学研究科	High pressure synthesis of novel transition metal carbides using large volume press	Ken Niwa	Nagoya University

No.	課題名	氏名	所属	Title	Name	Organization
98	大型プレスを用いた新規遷移金属炭化物の高压合成	野引 浩介	名古屋大学 大学院工学研究科	High pressure synthesis of novel transition metal carbides using large volume press	Kosuke Nobiki	Nagoya University
99	低温合成による層状酸化物の構造物性	小林 洋治	京都大学 大学院工学研究科	Structural properties of layered oxide-pnictide via low temperature synthesis	Yoji Kobayashi	Kyoto University
100	"	矢島 健	京都大学 大学院工学研究科	"	Takeshi Yajima	Kyoto University
101	"	ギヨーム ブイエ	京都大学 大学院工学研究科	"	Guillaume Bouilly	Kyoto University
102	"	中野 晃佑	京都大学 大学院工学研究科	"	Kousuke Nakano	Kyoto University
103	六方晶Eu化合物の低温粉末X線回折	光田 眞弘	九州大学 大学院理学研究院	Powder X-ray diffraction at low temperatures of hexagonal Eu compounds	Akihiro Mitsuda	Kyushu University
104	"	眞鍋 栄樹	九州大学 大学院理学府	"	Shigeki Manabe	Kyushu University
105	エンタングルメント繰り込みを用いた量子三角格子モデルの変分法	原田 健自	京都大学 大学院情報学研究科	Variational method based on an entanglement renormalization for quantum triangular lattice models	Kenji Harada	Kyoto University
106	細胞の自己推進機構の理論的解析	多羅間 充輔	京都大学 大学院理学研究科	Theoretical analysis of the mechanism of cellular spontaneous propulsion	Mitsusuke Tarama	Kyoto University
107	ヒ素の化学結合制の形成・切断を利用した電子物性開拓	野原 実	岡山大学 大学院自然科学研究科	Exploration of novel electronic states out of the arsenic bond making and breaking in solid	Minoru Nohara	Okayama University
108	(Ho,Gd)Rh <sub>6</sub> Si <sub>12</sub> 単結晶の磁気転移Ⅱ	繁岡 透	山口大学 大学院理工学研究科	Magnetic transitions of (Ho,Gd)Rh <sub>6</sub> Si <sub>12</sub> single crystal Ⅱ	Toru Shigeoka	Yamaguchi University
109	"	大河原 遼	山口大学 大学院理工学研究科	"	Yu Okawara	Yamaguchi University
110	LaRu <sub>2</sub> P <sub>2</sub> の上部臨界磁場の圧力効果	藤原 哲也	山口大学 大学院理工学研究科	Pressure effect on the upper critical field of LaRu <sub>2</sub> P <sub>2</sub>	Tetsuya Fujiiwara	Yamaguchi University
111	"	巖田 裕也	山口大学 大学院理工学研究科	"	Yuya Kurata	Yamaguchi University
112	Tb <sub>2</sub> Ti <sub>2</sub> O <sub>7</sub> における量子スピニン液体状態の研究	門脇 広明	首都大学東京 大学院理工学研究科	Quantum spin liquid in Tb <sub>2</sub> Ti <sub>2</sub> O <sub>7</sub>	Hiroaki Kadokawa	Tokyo Metropolitan University
113	"	谷口 智洋	首都大学東京 大学院理工学研究科	"	Tomohiro Taniguchi	Tokyo Metropolitan University
114	近藤半導体YbB <sub>12</sub> のワントーンコイルによる100Tペルス磁場下での強磁場磁化過程	伊賀 文俊	茨城大学 理学部	High field magnetization of Kondo insulator YbB <sub>12</sub> by using one-turn coil in a 100T pulse magnet	Fumitoshi Igai	Ibaraki University

No.	課題名	氏名	所属	Title	Name	Organization
115	DyPd <sub>2</sub> Ge <sub>2</sub> 単結晶の強磁场磁化	繁岡 透	山口大学 大学院理工学 研究科	High field magnetization of DyPd <sub>2</sub> Ge <sub>2</sub> single crystal	Toru Shigeoka	Yamaguchi University
116	"	長谷川 貴大	山口大学 大学院理工学 研究科	"	Takahiro Hasegawa	Yamaguchi University
117	LaCoO <sub>3</sub> 系の強磁场誘起スピinn転移の研究	佐藤 桂輔	茨城工業高等 専門学校	High-Field Induced Spin State Transition in Co perovskite	Keisuke Sato	Ibaraki National College of Technology
118	SrCo <sub>2</sub> P <sub>2</sub> とその周辺化合物における遍歷電子強磁 性量子臨界点近傍の物性	道岡 千城	京都大学 大学院理学研 究科	Physical properties in the vicinity of itinerant ferromagnetic quantum critical point in SrCo <sub>2</sub> P <sub>2</sub> and its family compounds	Chishiro Michioka	Kyoto University
119	"	小林 �慎太郎	京都大学 大学院理学研 究科	"	Shintaro Kobayashi	Kyoto University
120	"	今井 正樹	京都大学 大学院理学研 究科	"	Masaki Imai	Kyoto University
121	$\eta$ -カーバイド型化合物の強磁场磁化測定	和氣 剛	京都大学 大学院工学研 究科	High field magnetization measurement of $\eta$ -carbide-type compounds	Takeshi Waki	Kyoto University
122	"	古澤 大介	京都大学 大学院工学研 究科	"	Daisuke Furusawa	Kyoto University
123	クロミック化合物モリブデン酸コバルトの磁気相転 移と強磁场磁化過程	浅野 貴行	九州大学 大学院理学研 究院	Magnetic Ordering and Magnetization Process in the Chromic Compound CoMoO <sub>4</sub>	Takayuki Asano	Kyushu University
124	"	福井 博章	九州大学 大学院理学府	"	Hiroaki Fukui	Kyushu University
125	スピングラスを持つホイスラー化合物の磁場中比 熱	伊藤 昌和	鹿児島大学 大学院理工学 研究科	Specific heat of Heusler compounds with spin glass under magnetic field	Masakazu Ito	Kagoshima University
126	フラストレートした格子をもつ遷移金属フッ化物の 磁性	植田 浩明	京都大学 大学院理学研 究科	Magnetism of transition-metal fluorides with frustrated lattices	Hiroaki Ueda	Kyoto university
127	"	後藤 真人	京都大学 大学院理学研 究科	"	Masato Goto	Kyoto University
128	希土類カゴ状化合物Ce <sub>3</sub> Pd <sub>20</sub> (Si <sub>1-x</sub> Ge <sub>x</sub> ) <sub>6</sub> の近藤状 態に関する研究	北澤 英明	物質・材料研究 機構	Study of Kondo state in rare-earth clathrate compounds Ce <sub>3</sub> Pd <sub>20</sub> (Si <sub>1-x</sub> Ge <sub>x</sub> ) <sub>6</sub>	Hideaki Kitazawa	National Institute for Materials Science
129	希土類金属間化合物の強磁场物性研究	海老原 孝雄	静岡大学 理学部	Physical phenomena at high magnetic fields in rare earth intermetallic compounds	Takao Ebihara	Shizuoka University
130	"	中井 裕人	静岡大学 大学院理学研 究科	"	Hiroyuki Nakai	Shizuoka University
131	幾何学的フラストレート磁性体の磁化研究	菊池 彦光	福井大学 大学院工学研 究科	Magnetization of the geometrically frustrated magnets	Hikomitsu Kikuchi	University of Fukui

No.	課題名	氏名	所属	Title	Name	Organization
132	幾何学的フランストレート磁性体の磁化研究	藤井 裕	福井大学 遠赤外領域開発研究センター	Magnetization of the geometrically frustrated magnets	Yutaka Fujii	University of Fukui
133	"	中田 勲人	福井大学 大学院工学研究科	"	Hayato Nakata	University of Fukui
134	近藤半導体YtOB <sub>12</sub> の100T級ロングバルス磁場下での強磁場物性	伊賀 文俊	茨城大学 理学部	High field physical property of Kondo insulator YtB <sub>12</sub> up to 100T class in a long pulse magnet	Fumitoshi Iga	Ibaraki University
135	金属ナノクラスターの磁化測定	稻田 貢	関西大学 大学院理工学研究科	Systems of metal nano-clusters under high magnetic field	Mitsuru Inada	Kansai University
136	"	吉原 義浩	関西大学 大学院理工学研究科	"	Yoshihiro Yoshihara	Kansai University
137	金属ナノクラスター集合体の磁気抵抗測定	稻田 貢	関西大学 大学院理工学研究科	Electronic transport properties of metal clusters under high-magnetic field	Mitsuru Inada	Kansai University
138	"	高橋 康輔	関西大学 大学院理工学研究科	"	Kousuke Takahashi	Kansai University
139	単結晶EuNiIn <sub>4</sub> における高磁場磁化	池田 修悟	兵庫県立大学 大学院物質理学研究科	High-field magnetization in EuNiIn <sub>4</sub> single crystals	Shugo Ikeda	University of Hyogo
140	"	田中 佑季	兵庫県立大学 大学院物質理学研究科	"	Yuki Tanaka	University of Hyogo
141	強磁場下での遷移金属酸化物の熱電特性評価	奥田 哲治	鹿児島大学 大学院理工学研究科	Measurements of thermoelectric properties of transition metal oxides in a high magnetic field	Tetsuji Okuda	Kagoshima University
142	スピネル酸化物の強磁場下での振る舞い	香取 浩子	東京農工大学 大学院工学研究院	Magnetic properties of spinel oxides in high magnetic fields	Hiroko Katori	Tokyo University of Agriculture and Technology
143	"	太田 寛人	東京農工大学 工学部	"	Hiroti Ohta	Tokyo University of Agriculture and Technology
144	"	安藤 悠一	東京農工大学 大学院工学府	"	Yuichi Ando	Tokyo University of Agriculture and Technology
145	ペイロクロア型イリジウム酸化物の強磁場下の物性研究	松平 和之	九州工業大学 大学院工学研究科	Transport and Magnetic Properties of Pyrochlore Iridates under High Field Magnetic Field	Kazuyuki Matsunaga	Kyushu Institute of Technology
146	ペルス強磁場中のCu <sub>3</sub> Mo <sub>2</sub> O <sub>9</sub> の磁化・分極測定	黒江 晴彦	上智大学 理工学部	Magnetization and electric polarization measurements in Cu <sub>3</sub> Mo <sub>2</sub> O <sub>9</sub> under strong pulsed magnetic field	Haruhiko Kuroe	Sophia University
147	メタホウ酸銅における電気磁気効果の磁場方位依存性	有馬 孝尚	東京大学 大学院新領域創成科学研究科	Dependence of electric polarization in copper metaborate on magnetic field direction	Taka-hisa Arima	The University of Tokyo
148	"	阿部 伸行	東京大学 大学院新領域創成科学研究科	"	Nobuyuki Abe	The University of Tokyo

No.	課題名	氏名	所属	Title	Name	Organization
149	超強磁場を利用したNiMn基およびFeMn基合金の低温異常現象の観察および起源解明	伊東 航 伊藤 基	仙台高等専門学校	Observation and clarification of the origin of anomalous behaviors at low temperature under strong magnetic field in NiMn based and FeMn based alloys	Wataru Ito	Sendai National College of Technology
150	"	許 震(キヨ キヨウ)	東北大 学工学研 究科	"	Xiao XU	Tohoku University
151	非破壊ペルス強磁场を用いたグラファイトの磁場誘起密度波相の研究	矢口 宏	東京理科大 学	Study of the Magnetic-Field Induced Density-Wave Phase in Graphite Using Non-Destructive Pulsed Magnetic Fields	Hiroshi Yaguchi	Tokyo University of Science
152	銅酸化物高温超伝導体LSCO擬ギャップ相における磁気励起スペクトラムの研究	松浦 直人	東北大 学	Study of spin fluctuations in the pseudogap phase of high-Tc cuprate LSCO	Masato Matsuura	Tohoku University
153	マルチフェロイック薄膜の焦電流換出による電気磁気結合評価	木村 秀夫	物質・材料研究 機構	Evaluation of magneto-electric coupling on multiferroic thin films by pyroelectric current	Hideo Kimura	National Institute for Materials Science
154	Al系準結晶及び近似結晶中の構造欠陥の陽電子子ビーム法による分析	金沢 育三	東京学芸大学	Analysis of structural defects in Al based icosahedral quasicrystals and approximate crystals by slow positron beam	Ikuzo Kanazawa	Tokyo Gakugei University
155	"	齋藤 誠	東京学芸大学	Preparing of carrier-doped Boron clusters and analysis by slow positron beam	Makoto Saito	Tokyo Gakugei University
156	キャリアドープボロンクラスター物質の作製と陽電子子ビーム法による分析	金沢 育三	東京学芸大学	"	Ikuzo Kanazawa	Tokyo Gakugei University
157	"	山田 浩平	東京学芸大学	"	Kouhei Yamada	Tokyo Gakugei University
158	SiC (000-1)上のエピキシャル酸化シリコン超薄膜の高分解能STM/STS測定	柄原 浩	九州大学	High-resolution STM and STS measurements of silicon-oxide ultrathin films formed epitaxially on the SiC(000-1) surface	Hiroshi Tochihara	Kyushu University
159	微傾斜SiC表面に成長したグラフェンの電子物性	中辻 寛	東京工業大 学	Electronic structure of graphene grown on a vicinal SiC substrate	Kan Nakatsui	Tokyo Institute of Technology
160	多重安定性を示す光誘起分子磁性体のサイズ効果の研究	糸井 充恵	日本大学 医学部	Size effect on photo-switchable molecular magnet $K_{0.3}Co[Fe(CN)_{6.07}] \cdot 3.4H_2O$	Miho Itoi	Nihon University
161	重い電子系物質における $^3He$ 温度領域での磁化測定	河江 達也	九州大学	Magnetization measurements in $^3He$ temperature region for heavy fermion systems	Tatsuya Kawai	Kyushu University
162	"	佐藤 由昌	九州大学	"	Yoshiaki Sato	Kyushu University
163	重い電子系Yb化合物の量子臨界と価数振動	富田 崇弘	日本大学 文理学部	valence fluctuation and Quantum Criticality in Heavy Fermion System Yb compound	Takahiro Tomita	Nihon University
164	重い電子系Yb化合物の量子臨界と価数振動	山口 博則	大阪府立大 学	Low-temperature magnetic state of new material with verdazyl radicals	Hironori Yamaguchi	Osaka Prefecture University
165	"	岩瀬 賢治	大阪府立大 学	"	Kenji Iwase	Osaka Prefecture University

No.	課題名	氏名	所属	Title	Name	Organization
166	フェルダジルラジカルを用いた新規磁性体の低温磁気状態	天谷 直樹	大阪府立大学 大学院理学系研究科	Low-temperature magnetic state of new material with verdazyl radicals	Naoki Amaya	Osaka Prefecture University
167	ずれ振動に対する固体ヘリウム4の応答	岩佐 泉	神奈川大学 理学部	Acoustic shear response of solid Helium 4	Izumi Iwasa	Kanagawa University
168	鉄系超伝導体のパルス磁場下量子振動計測	寺嶋 太一	物質・材料研究機構	Pulsed-field quantum oscillation measurements on iron-pnictide superconductors	Taichi Terashima	National Institute for Materials Science
169	FeTiO <sub>3</sub> の誘電性と磁性	山田 重樹	横浜市立大学 国際総合科学部	Dielectric and Magnetic Properties of FeTiO <sub>3</sub>	Shigeki Yamada	Yokohama City University
170	"	清川 貴和	横浜市立大学 大学院生命ナノシステム科学研究所	"	Takayasu Kiyokawa	Yokohama City University
171	Pr-Ca-Co-O系の強磁場下における金属・絶縁体ースピン状態転移	内藤 智之	岩手大学 工学部	Metal-insulator and spin-state transition in Pr-Ca-Co-O system under high magnetic fields	Tomoyuki Naito	Iwate University
172	マルチフェロイック(Sr <sub>0.5</sub> Ba <sub>0.5</sub> )MnO <sub>3</sub> の強磁場下における磁性-強誘電性結合	鈴木 健士	理化学研究所 交差相關物質研究チーム	Coupling between magnetism and ferroelectricity at high magnetic field for multiferroic (Sr <sub>0.5</sub> Ba <sub>0.5</sub> )MnO <sub>3</sub>	Takehito Suzuki	RIKEN
173	表面プラズモンを支持する金属単結晶表面の作成と解析	渡辺 量朗	東京理科大学 大学院総合化学生物研究科	Fabrication and analysis of single crystal metal surfaces supporting surface plasmons	Kazuo Watanabe	Tokyo University of Science
174	"	友部 弥	東京理科大学 大学院総合化学生物研究科	"	Wataru Tomobe	Tokyo University of Science
175	電荷注入された低次元量子スピinn系の結晶育成とその評価	横尾 哲也	高エネルギー加速器研究機構	Single crystal growth and physical properties of charge induced low dimensional quantum spin systems	Tetsuya Yokoo	High Energy Accelerator Research Institute
176	一次元ペイエルス絶縁体の時間分解テラヘルツ分光	武田 淳	横浜国立大学 大学院工学研究科	Time-resolved THz spectroscopy for one-dimensional Peierls insulators	Jun Takeda	Yokohama National University
177	"	片山 郁文	横浜国立大学 大学院工学研究科	"	Ikuhumi Katayama	Yokohama National University
178	"	南 康夫	横浜国立大学 大学院工学研究科	"	Yasuo Minami	Yokohama National University
179	"	大島 扱也	横浜国立大学 大学院工学研究科	"	Takuya Ohshima	Yokohama National University
180	パルス強磁場下における比熱測定技術の開発	稻垣 祐次	九州大学 大学院工学研究科	Specific heat measurements under pulsed high magnetic field	Yūji Imagaki	Kyushu University
181	"	内田 翔也	九州大学 大学院工学研究科	"	Shoya Uchida	Kyushu University
182	LEED I-V法によるCu(001)上のアラニン吸着表面の構造解析	岩井 秀和	宇都宮大学 大学院工学研究科	LEED-IV structure analysis of alanine on Cu(001) surface	Hidetaku Iwai	Utsunomiya University

No.	課題名	氏名	所属	Title	Name	Organization
183 性研究	ペイロクロア型イリジウム酸化物の強磁場下の物	水鳥 雄斗	九州工業大学 大学院工学府	Transport and Magnetic Properties of Pyrochlore Iridates under High Field Magnetic Field	Yuto Mizutori	Kyushu Institute of Technology
184	磁性金属シリサイドの光電子分光	大野 真也	横浜国立大学 大学院工学研究科	Photoemission study of silicide of magnetic metals	Shinya Ohno	Yokohama National University
185 光	シリコン表面上の有機薄膜成長過程の光電子分	大野 真也	横浜国立大学 大学院工学研究科	Photoemission study of organic thin film growth process on silicon surfaces	Shinya Ohno	Yokohama National University
186	"	平賀 健太	横浜国立大学 大学院工学府	"	Kenta Hiraga	Yokohama National University
187	高品質単結晶中性子モノクロメータの開発	平賀 晴弘	東北大学 金属材料研究所	Development of high-quality, single-crystal neutron monochromator	Haruhiro Hiraka	Tohoku University
188	強相関伝導系のハルス磁場中の超音波測定	吉澤 正人	岩手大学 大学院工学研究科	Ultrasonic measurements of strongly correlated systems in pulsed magnetic field	Masahito Yoshizawa	Iwate University
189	"	シャラムジヤンスマイ	岩手大学 大学院工学研究科	"	Shalamujang Simayi	Iwate University
190	"	坂野 幸平	岩手大学 大学院工学研究科	"	Kouhei Sakano	Iwate University
191	空間反転対称性を欠いた系 CeNi <sub>2</sub> Oの圧力下での磁気秩序と超伝導	片野 進	埼玉大学 大学院理工学研究科	Magnetic ordering and superconductivity of the non-centrosymmetric system CeNi <sub>2</sub> O under high pressure	Susumu Katano	Saitama University
192	"	吉田 透	埼玉大学 大学院理工学研究科	"	Toru Yoshida	Saitama University
193 研究	角度分析板厚と空間解像度に関する理論・実験	安藤 正海	東京理科大学 総合研究機構	Theoretical and Experimental Study on Relation between Laue Angle Analyzer and Spatial Resolution	Masami Ando	Tokyo University of Science
194	有機ビラジカルによる低次元量子磁性体の強磁场磁化測定	細越 裕子	大阪府立大学 大学院理学系研究科	Magnetization measurements of organic biradical crystals in high magnetic fields	Yuko Hosokoshi	Osaka Prefecture University
195	"	岩下 健	大阪府立大学 大学院理学系研究科	"	Ken Iwashita	Osaka Prefecture University
196	GaAsNの電子輸送特性およびバンド構造の解明	稻垣 充	豊田工業大学 大学院工学研究科	Clarification of electron transport property and band structure of GaAsN	Makoto Inagaki	Toyota Technological Institute
197	CeRu <sub>2</sub> Al <sub>10</sub> における超高压下反強磁性消失点近傍のパラレク測定	北川 健太郎	高知大学 教育研究部	Bulk experiments around the antiferromagnetism vanishing point of CeRu <sub>2</sub> Al <sub>10</sub> under ultrahigh pressures	Kentaro Kitagawa	Kochi University
198	"	栗原 弘光	高知大学 大学院総合人間自然科学研究科	"	Hironatsu Kurihara	Kochi University
199	量子ホール効果試料の作成	澤田 安樹	京都大学 低温物質科学研究所	Sample Preparation for Quantum Hall Effect	Anju Sawada	Kyoto University

No.	課題名	氏名	所属	Title	Name	Organization
200	圧力下強磁場電子スピン共鳴測定のためのハイブリッド圧力セルの開発	藤本 晃大	神戸大学 大学院理学研究科	Development of hybrid pressure cell for high field electron spin resonance measurement under pressure	Kohdai Fujimoto	Kobe University
201	希土類トリルライド $\text{RTe}_3$ ( $\text{R} = \text{Ce}, \text{Tb}$ )とSmSの高圧下物性実験	松川 周矢	名古屋大学 大学院理学研究科	High pressure experiments of $\text{RTe}_3$ ( $\text{R}=\text{Ce}, \text{Tb}$ ) and SmS	Shuya Matsukawa	Nagoya University
202	偏光顕微鏡による $\text{URu}_2\text{Si}_2$ の隠れた秩序相におけるドメイン構造の観察	網塚 浩	北海道大学 大学院理学研究室	Polarization-Microscope Study on Domain Structure of Hidden Order in $\text{URu}_2\text{Si}_2$	Hiroshi Amitaka	Hokkaido University
203	"	田端 千絵	北海道大学 大学院理学院	"	Chihiro Tabata	Hokkaido University

物質合成・評価設備(備Pクラス)(Materials Synthesis and Characterization P Class Researcher)

No.	課題名	氏名	所属	Title	Name	Organization
1	Ruddlesden-Popper型ペロブスカイトにおける構造相転移	陰山 洋	京都大学 大学院工学研究科	Structural Transition in Ruddlesden-Popper Type Perovskite	Hiroshi Kageyama	Kyoto University
2	"	セドリック タッセル	京都大学 大学院工学研究科	"	Cedric Tassel	Kyoto University
3	"	山本 隆文	京都大学 大学院工学研究科	"	Takafumi Yamamoto	Kyoto University
4	"	吉井 龍太	京都大学 大学院工学研究科	"	Ryuta Yoshii	Kyoto University
5	新規フラストレート磁性体の物性評価	植田 浩明	京都大学 大学院理学研究科	Characterization of novel frustrated magnets	Hiroaki Ueda	Kyoto University
6	"	小林 慎太郎	京都大学 大学院理学研究科	"	Shintaro Kobayashi	Kyoto University
7	"	原口 祐哉	京都大学 大学院理学研究科	"	Yuya Haraguchi	Kyoto University
8	低結晶性クリノニアサイトの非晶質特性の実態と原因の解明	永島 真理子	山口大学 大学院理工学研究科	Properties of low crystallinity clinozoisite	Mariko Nagashima	Yamaguchi University
9	時間分解分光法を用いた超臨界流体中ペルスレーザープラズマによるダイヤモンドイド合成における反応メカニズムの探索	ショウタウスス ヴィエン	東京大学 大学院新領域創成科学研究科	Investigation of the reaction mechanisms of diamondoid synthesis by pulsed laser plasmas generated in supercritical fluids by time-resolved spectroscopy	Sven Strauss	The University of Tokyo
10	"	加藤 暉	東京大学 大学院新領域創成科学研究科	"	Toru Kato	The University of Tokyo
11	強相関系遷移金属酸化物の透過電子顕微鏡法による研究	中山 則昭	山口大学 大学院理工学研究科	TEM study of strongly correlated transition metal oxide systems	Noriaki Nakayama	Yamaguchi University

No.	課題名	氏名	所属	Title	Name	Organization
12	強相関系遷移金属酸化物の透過電子顕微鏡法による研究	寺浦 佳宏	山口大学 大学院理工学研究科	TEM study of strongly correlated transition metal oxide systems	Yoshihiro Teraura	Yamaguchi University
13	ペイクロア型希土類酸化物の単結晶育成と磁気プロストレージョンの研究	松平 和之	九州工業大学 大学院工学研究院	Single crystal growth and study of frustrated magnetism in pyrochlore rare-earth oxides	Kazuyuki Matsuhira	Kyushu Institute of Technology

物質合成・評価設備/備Gクラス(Materials Synthesis and Characterization G Class Researcher)

No.	課題名	氏名	所属	Title	Name	Organization
1	高温高压水中における固体塩基触媒反応の速度論的解析	大友 順一郎	東京大学 大学院新領域創成科学研究科	Kinetic analysis of solid base catalyzed reactions in sub- and supercritical water	Junichiro Otomo	The University of Tokyo
2	"	佐野 恵二	東京大学 大学院新領域創成科学研究科	"	Keiji Sano	The University of Tokyo
3	高温高压水中における固体酸塩基触媒反応の速度論的解析	大友 順一郎	東京大学 大学院新領域創成科学研究科	Kinetic analysis of solid acid and base catalyzed reactions in sub- and supercritical water	Junichiro Otomo	The University of Tokyo
4	"	秋月 信	東京大学 大学院新領域創成科学研究科	"	Makoto Aizuki	The University of Tokyo
5	超臨界水を用いた有機・無機複合廃棄物からのマテリアルリサイクル	大友 順一郎	東京大学 大学院新領域創成科学研究科	Material recycling from organic-inorganic composite waste using supercritical water	Junichiro Otomo	The University of Tokyo
6	"	松本 祐太	東京大学 大学院新領域創成科学研究科	"	Yuta Matsumoto	The University of Tokyo
7	低温下における単結晶YbPdの構造解析	光田 晴弘	九州大学 大学院理学研究院	Structural analysis of single crystal of YbPd at low temperatures	Akihiro Mitsuda	Kyushu University
8	カーボンナイトライドマテリアルの開発とキャラクタリゼーション	佐々木 岳彦	東京大学 大学院新領域創成科学研究科	Development and characterization of carbon-nitride materials	Takehiko Sasaki	The University of Tokyo
9	高温高压水を利用した有機修飾微粒子の連続合成技術の開発	大友 順一郎	東京大学 大学院新領域創成科学研究科	The development of continuous synthesis of organic-modified particles in high temperature and pressure water	Junichiro Otomo	The University of Tokyo
10	"	生駒 健太郎	東京大学 大学院新領域創成科学研究科	"	Kentaro Ikoma	The University of Tokyo
11	幾何学的フラストレーションと強相関に基づく物性開拓	阿部 伸行	東京大学 大学院新領域創成科学研究科	Research of strongly correlated electron systems with geometrical frustration	Nobuyuki Abe	The University of Tokyo
12	"	佐賀山 基	東京大学 大学院新領域創成科学研究科	"	Hajime Sagayama	The University of Tokyo
13	"	植松 大介	東京大学 大学院新領域創成科学研究科	"	Daisuke Uematsu	The University of Tokyo

No.	課題名	氏名	所属	Title	Name	Organization	
14 幾何学的フラストレーションを有する強相関電子系の設計	有馬 孝尚	東京大学	大学院新領域創成科学研究科	Design of strongly correlated electron systems with geometrical frustration	Taka-hisa Arima	The University of Tokyo	
15 幾何学的電子状態の評価	佐賀山 基	東京大学	大学院新領域創成科学研究科	Investigation of strongly correlated electron systems with geometrical frustration	Hajime Sagayama	The University of Tokyo	
16 IT-SOFCならびに金属空気電池のためのセリア系高酸化物イオン伝導性電解質の作製と特性評価	大友 順一郎	東京大学	大学院新領域創成科学研究科	Synthesis and characterization of high ion-conductive electrolytes of Ceria ceramics for intermediate-temperature solid oxide fuel cell and metal-air battery	Junichiro Otomo	The University of Tokyo	
17	"	山本 高史	東京大学	大学院新領域創成科学研究科	"	Takashi Yamamoto	
18 プロトン伝導性中温作動燃料電池電解質および空気極の研究	大友 順一郎	東京大学	大学院新領域創成科学研究科	Synthesis of Electrolyte and Cathode Materials for Intermediate-Temperature Fuel Cells with Proton-Conducting Electrolyte	Junichiro Otomo	The University of Tokyo	
19	"	川村 亮人	東京大学	大学院新領域創成科学研究科	"	Ryoto Kawamura	
20 プロトン伝導性電解質を用いた中温作動燃料電池の開発	大友 順一郎	東京大学	大学院新領域創成科学研究科	Development of an intermediate temperature fuel cell using a proton conducting electrolyte	Junichiro Otomo	The University of Tokyo	
21	"	嶋田 五百里	東京大学	大学院新領域創成科学研究科	"	Iori Shimada	
22 リソ酸チウムガラスセラミックスの合成とリチウムイオン伝導特性評価	大友 順一郎	東京大学	大学院新領域創成科学研究科	Synthesis of lithium phosphate glass ceramics and evaluation of lithium ion conductivity	Junichiro Otomo	The University of Tokyo	
23	"	高坂 文彦	東京大学	大学院新領域創成科学研究科	"	Fumihiro Kosaka	
24 超臨界水を用いたシリコンスマッシュからのシリコンの回収	大友 順一郎	東京大学	大学院新領域創成科学研究科	Recycle of silicon from silicon sludge using supercritical water	Junichiro Otomo	The University of Tokyo	
25	"	横 哲	東京大学	大学院新領域創成科学研究科	"	Akira Yoko	
26 微量成分に着目したSOFCの発電性能及び製造プロセスの評価	大友 順一郎	東京大学	大学院新領域創成科学研究科	Evaluation of SOFC cathode performance based on trace element behavior	Junichiro Otomo	The University of Tokyo	
27	"	大石 淳矢	東京大学	大学院新領域創成科学研究科	"	Junya Oishi	
28 TiNマイクロ・ナノスプリングの成長ペーパンの観察及び微細構造の解析	陳 秀琴	東京理科大学	理工学部	Observation of the growth pattern of the TiN micro/nano springs	Shaoming Yang	Tokyo University of Science	
29	シリサイド系半導体単結晶の光学特性評価	鶴殿 治彦	茨城大学	理工学部	Observation for the morphologies of micro/nano and the solution for their microstructures	Xiuqin Chen	Tokyo University of Science
30	シリサイド系半導体単結晶の光学特性評価	"	工学部	Characterizations of optical properties single crystalline semiconducting silicides	Haruhiko Udono	Ibaraki University	

No.	課題名	氏名	所属	Title	Name	Organization
31	Fe基磁性材料のTEM観察	田村 隆治	東京理科大学 基礎工学部	TEM study of Fe based magnetic materials	Ryujii Tamura	Tokyo University of Science
32	"	今成 慶	東京理科大学 大学院基礎工学科	"	Kei Imanari	Tokyo University of Science
33	MnSiO <sub>3</sub> 成分のMgSiO <sub>3</sub> 組成とCaSiO <sub>3</sub> への分配 塩ベロブスカイトへの分配	李 林	北海道大学 大学院理学院	Partitioning of MnSiO <sub>3</sub> content between MgSiO <sub>3</sub> and CaSiO <sub>3</sub> perovskites	Li Lin	Hokkaido University
34	ナノ構造制御による二次電池等の機能性材料開発	細野 英司	産業技術総合研究所 エネルギー技術研究部門	Development of the functional materials such as secondary battery by the nanostructure control	Eiji Hosono	National Institute of Industrial Science and Technology
35	マイクロミキサを用いた機能性ナノ粒子の連續水熱合成	陶 研	産業技術総合研究所 ナノシステム研究部門	Continuous hydrothermal synthesis of functional nanoparticles using a micronixer	Kiwamu Sue	National Institute of Industrial Science and Technology
36	幾何学的フラストレーションを有するバクロクロア型酸化物の金属絶縁体転移に伴う結晶構造変化の解析	山本 文子	理化学研究所	Analysis of a change in crystal structure of pyrochlore-type oxides showing metal-insulator transition caused by geometrical frustration	Ayako Yamamoto	RIKEN
37	新規磁石材料の微細構造解析	齋藤 哲治	千葉工業大学 工学部	Microstructural studies of newly developed permanent magnet materials	Tetsuji Saito	Chiba Institute of Technology
38	マイクロキャビリリー超臨界流体プラズマによるカーボンナノマテリアルの合成	ショウタクスス エイエヌ	東京大学 大学院新領域創成科学研究科	Synthesis of carbon nanomaterials using supercritical fluid plasma generated in micro capillaries	Sven Strauss	The University of Tokyo
39	"	大島 郁人	東京大学 大学院新領域創成科学研究科	"	Fumito Oshima	The University of Tokyo
40	超臨界キセンン及び二酸化炭素中バルスレーザーによるダイヤモンドイドの合成	ショウタクスス エイエヌ	東京大学 大学院新領域創成科学研究科	Synthesis of diamondoids by pulsed laser plasmas in high-pressure and supercritical CO <sub>2</sub> and Xe	Sven Strauss	The University of Tokyo
41	超臨界二酸化炭素プラズマによるカーボンナノマテリアルの合成、分離及び評価	ショウタクスス エイエヌ	東京大学 大学院新領域創成科学研究科	Synthesis, separation and characterization of carbon nanomaterials using plasmas generated in supercritical CO <sub>2</sub>	Sven Strauss	The University of Tokyo
42	"	石井 千佳子	東京大学 大学院新領域創成科学研究科	"	Chikako Ishii	The University of Tokyo
43	超臨界二酸化炭素中レーザー誘起プラズマによるナノ微粒子合成	ショウタクスス エイエヌ	東京大学 大学院新領域創成科学研究科	Synthesis of nanomaterials by laser induced plasmas in supercritical CO <sub>2</sub>	Sven Strauss	The University of Tokyo
44	"	加藤 智嗣	東京大学 大学院新領域創成科学研究科	"	Satoshi Kato	The University of Tokyo
45	超臨界流体中プラズマによるダイヤモンドイド合成における反応機構の探索	ハイ デイビッド	東京大学 大学院新領域創成科学研究科	Investigation of the reaction mechanisms in the synthesis of diamondoids by plasmas in high-pressure and supercritical fluids	David Pai	The University of Tokyo
46	正20面体準結晶および近似結晶の構造相転移	西本 一恵	東京大学 生産技術研究所	Structural phase transitions in icosahedral quasicrystals and crystalline approximants	Kazue Nishimoto	The University of Tokyo
47	Cu-Ni-Co 系合金中のCo微粒子の析出過程と磁気特性の関係	李 東海	横浜国大 大学院工学府	Precipitation behavior and magnetic properties of fine Co particles in Cu-Ni-Co alloys	Lee dong hae	Yokohama National University

No.	課題名	氏名	所属	Title	Name	Organization
48 キラル銅(II)錯体—機能性金属化合物複合系の磁性	秋津 貴城	東京理科大学 理学部	Magnetism of hybrid assemblies of chiral Cu(II) complexes and functional metal compounds	Takahiro Akitsu	Tokyo University of Science	
49 ハーフメタル型ホイスラー合金の磁性と輸送特性に関する研究	重田 出	鹿児島大学 大学院理工学研究科	Study on the magnetic and transport properties of half-metallic Heusler alloys	Iduru Shigeta	Kagoshima University	
50	"	西迫 裕也	鹿児島大学 大学院理工学研究科	"	Yuya Nishisako	Kagoshima University
51 高温高压合成した銅化合物の磁気特性	草場 啓治	名古屋大学 大学院工学研究科	Magnetic properties of copper compounds synthesized under high pressure and high temperature	Keiji Kusaba	Nagoya University	
52	"	光森 成生	名古屋大学 大学院工学研究科	"	Seiki Mitsunori	Nagoya University
53 高分子前駆体高压合成法で得られた新物質の磁気特性	長谷川 正	名古屋大学 大学院工学研究科	Magnetic properties of noble materials synthesized using high pressure polymer-derived reactions	Masashi Hasegawa	Nagoya University	
54	"	堀部 太嗣	名古屋大学 大学院工学研究科	"	Taishi Horibe	Nagoya University
55 ホイスラー型化合物の磁性と伝導の研究	廣井 政彦	鹿児島大学 大学院理工学研究科	Study on the magnetic and electrical properties of Heusler compounds	Masahiko Hiroi	Kagoshima University	
56	"	諏訪 秀和	鹿児島大学 大学院理工学研究科	"	Suwa Hidekazu	Kagoshima University
57 Mnシリサイド薄膜試料のSQUID測定	服部 賢	奈良先端科学技術大学院大学 物質創成科学研究科	SQUID measurements of Mn-silicide thin films	Ken Hattori	Nara Institute of Science and Technology	
58 金属炭化物微粒子の超伝導磁気特性	吉田 喜孝	いわき明星大学 科学技術学部	Magnetic property in superconducting fine particles of metal carbide	Yositaka Yoshida	Iwaki-Meisei University	
59 Cu-Ni-Fe系合金中における析出ナノ粒子の磁化配向と磁気特性の関係	竹田 真帆人	横浜国立大学 大学院工学研究科	The relationship between microstructure and magnetic properties of nano-scale Fe particles in Cu-Ni-Fe alloys	Mahoto Takeda	Yokohama National University	
60 $Tb_2Ti_2O_7$ における量子スピinn液体状態の研究	門脇 広明	首都大学東京 大学院理工学研究科	Quantum spin liquid in $Tb_2Ti_2O_7$	Hiroaki Kadokawa	Tokyo Metropolitan University	
61	"	谷口 智洋	首都大学東京 大学院理工学研究科	"	Tomohiro Taniguchi	Tokyo Metropolitan University
62 13族クラスター固体の電子物性に関する研究	木村 薫	東京大学 大学院新領域創成科学研究科	Electronic Properties of Group 13 elements-based Cluster Solids	Kaoru Kimura	The University of Tokyo	
63	"	高際 良樹	東京大学 大学院新領域創成科学研究科	"	Yoshiki Takagiwa	The University of Tokyo
64	"	住吉 篤郎	東京大学 大学院新領域創成科学研究科	"	Atsuro Sumiyoshi	The University of Tokyo

No.	課題名	氏名	所属	Title	Name	Organization
65	13族クラスター固体の電子物性に関する研究	北原 功一	東京大学 大学院新領域創成科学科	Electronic Properties of Group 13 elements-based Cluster Solids	Kouichi Kitahara	The University of Tokyo
66	"	松浦 裕介	東京大学 大学院新領域創成科学科	"	Yusuke Matsuura	The University of Tokyo
67	Mnシリサイド薄膜試料のSQUID測定	木村 明日香	奈良先端科学技術大学院大学 大学院新領域創成科学科	SQUID measurements of Mn-silicide thin films	Asuka Kimura	Nara Institute of Science and Technology
68	幾何学的フラストレーションと強相間に基づく物性開拓	新居 陽一	東京大学 大学院新領域創成科学科	Research of strongly correlated electron systems with geometrical frustration	Yoichi Nii	The University of Tokyo

物質合成・評価設備/備Uクラス(Materials Synthesis and Characterization U Class Researcher)

No.	課題名	氏名	所属	Title	Name	Organization
1	結晶膜残留法を用いて濃縮水に含まれるリンと窒素の回収・固定化プロセスの検討	白土 敬介	東京大学 大学院工学系研究科	Recovery and solidification of nutrients from brine in membrane distillation crystallizer	Keisuke Shirado	The University of Tokyo
2	セメント硬化体・セラミック系建材の分光反射率測定と日射熱制御に関する研究	北垣 亮馬	東京大学 大学院工学系研究科	Controlling solar radiation heat by designing surface reflectivity of cementitious/ceramic material for building use	Ryoma Kitagaki	The University of Tokyo
3	AgをドープしたFeSe <sub>0.5</sub> Te <sub>0.5</sub> 超伝導体の構造解析	右田 稔	横浜国立大学 大学院工学府	Structural analysis of Ag doped FeSe <sub>0.5</sub> Te <sub>0.5</sub> superconductor	Minoru Migita	Yokohama National University
4	バルク高温超伝導体および開運磁性酸化物の磁性と構造組織観察	和泉 充	東京海洋大学 大学技術研究所	Magnetism and structural organization of bulk high-temperature superconductor and the related magnetic oxides	Mitsuru Izumi	Tokyo University of Marine Science and Technology
5	"	都築 啓太	東京海洋大学 大学技術研究所	"	Keita Suzuki	Tokyo University of Marine Science and Technology
6	"	周 迪帆	東京海洋大学 大学技術研究所	"	Zhou Difan	Tokyo University of Marine Science and Technology
7	"	李 備戦	東京海洋大学 大学技術研究所	"	Beizhan Li	Tokyo University of Marine Science and Technology
8	"	原 章悟	東京海洋大学 大学技術研究所	"	Shogo Hara	Tokyo University of Marine Science and Technology
9	SPS法によるAl基準結晶の作製と電気抵抗への熱処理の効果	田村 隆治	東京理科大学 基礎工学部	Effect of heat treatment on the electrical resistivity of icosahedral Al-based quasicrystal prepared by the SPS method	Ryuji Tamura	Tokyo University of Science
10	"	中村 敬人	東京理科大学 大学院基礎工学研究科	"	Takahito Nakamura	Tokyo University of Science
11	Vドープβ-ボロンのSEMによる組成分析	金沢 育三	東京学芸大学 自然科学系	Composition analysis of Vanadium doped beta-Boron by Scanning electron microscope	Ikuzo Kanazawa	Tokyo Gakugei University

No.	課題名	氏名	所属	Title	Name	Organization
12	Vドープ $\beta$ -ボロンのSEMによる組成分析	山田 浩平	東京学芸大学 大学院教育学研究科	Composition analysis of Vanadium doped beta-Boron by scanning electron microscope	Kouhei Yamada	Tokyo Gakugei University
13	Al系準結晶の熱電特性及びSEMIによる組成分析	金沢 育三	東京学芸大学 自然科学系	Thermoelectric properties and composition analysis of Al-based icosahedral quasicrystals and approximate crystals, by scanning electron microscope	Ikuzo Kanazawa	Tokyo Gakugei University
14	"	齋藤 誠	東京学芸大学 大学院教育学研究科	"	Makoto Saito	Tokyo Gakugei University

長期留学研究員 (Long Term Young Researcher)

No.	課題名	氏名	所属	Title	Name	Organization
1	極紫外レーザー時間分解光電子分光によるトポロジカル絶縁体の研究	山本 貴士	東京理科大学 大学院理学研究科	Study of Topological insulator using EUV Laser time-resolved photoemission spectroscopy	Takashi Yamamoto	Tokyo University of Science
2	四極子転移を示すPrTr <sub>2</sub> Al <sub>20</sub> の圧力効果と電子状態	田中 斗志貴	日本大学 大学院総合基礎科学研究所	High Pressure effect and Electronic Structure of Quadrupolar Order PrTr <sub>2</sub> Al <sub>20</sub>	Toshiki Tanaka	Nihon University
3	低次元電子系の高周波伝導率の測定	設楽 航	東京理科大学 大学院基礎工学科研究科	Measurement of the high-frequency conductivities of low-dimensional electron systems	Wataru Shitara	Tokyo University of Science

中性子(Neutron Scattering Researcher)

No.	課題名	氏名	所属	Title	Name	Organization
1	GPTAS(汎用3軸中性子分光器)IRT課題	佐藤 卓	東京大学 物性研究所	IRT: GPTAS(Triple Axis Spectrometer)	Taku J Sato	The University of Tokyo
2	La <sub>1-x</sub> U <sub>x</sub> Ru <sub>2</sub> Si <sub>2</sub> ( $x > 0.9$ )における磁気秩序構造と磁気励起	網塙 浩	北海道大学 大学院理学研究院	Magnetic Ordering Structure and excitations in La <sub>1-x</sub> U <sub>x</sub> Ru <sub>2</sub> Si <sub>2</sub> ( $x > 0.9$ )	Hiroshi Amitsuma	Hokkaido University
3	重い電子系URu <sub>2</sub> Si <sub>2</sub> の磁気励起	網塙 浩	北海道大学 大学院理学研究院	Magnetic Excitation of Heavy-Electron Compound URu <sub>2</sub> Si <sub>2</sub>	Hiroshi Amitsuma	Hokkaido University
4	量子臨界点近傍にあるYbCo <sub>2</sub> Zn <sub>20</sub> の磁気励起	阿曾 尚文	琉球大学 理学部	Magnetic excitations in YbCo <sub>2</sub> Zn <sub>20</sub> in vicinity of a quantum critical point	Naofumi Aso	University of the Ryukyus
5	EuCo <sub>2</sub> P <sub>2</sub> の磁気構造解析	藤原 哲也	山口大学 大学院理工学研究科	Magnetic structure analysis of EuCo <sub>2</sub> P <sub>2</sub>	Tetsuya Fujiiwara	Yamaguchi University
6	スピネルイーストにおけるトポジカル相転移	門脇 広明	首都大学東京 大学院理工学研究科	Topological phase transitions in spin ice	Hiroaki Kadokawa	Tokyo Metropolitan University
7	重い電子系物質YbCo <sub>2</sub> Zn <sub>20</sub> における圧力誘起反強磁性秩序の研究	松林 和幸	東京大学 物性研究所	Pressure induced antiferromagnetic order in heavy fermion YbCo <sub>2</sub> Zn <sub>20</sub>	Kazuyuki Matsubayashi	The University of Tokyo

No.	課題名	氏名	所属	Title	Name	Organization
8	時間分割中性子散乱測定による磁気構造変化過程の実時間追跡	元屋 清一郎	東京理科大学 理工学部	Real-time observation of magnetic structural change by means of time-resolved neutron scattering experiments	Kyoichiro Motoya	Tokyo University of Science
9	鉄系超伝導体LiFe(As,P)の磁気揺らぎ	南部 雄亮	東京大学 物性研究所	Magnetic fluctuations in stoichiometric iron-based superconductors LiFe(As,P)	Yusuke Nambu	The University of Tokyo
10	マルチフェロイック物質YMn <sub>2</sub> O <sub>5</sub> の磁気励起と磁気相互作用	野田 幸男	東北大学 多元物質科学研究所	Magnetic interaction and ferroelectricity in multiferroic YMn <sub>2</sub> O <sub>5</sub>	Yukio Noda	Tohoku University
11	強磁性超伝導体UCoGeにおけるスピinn摺らぎの研究	佐藤 憲昭	名古屋大学 大学院理学研究科	Study on spin fluctuations of the superconducting ferromagnet UCoGe	Noriaki Sato	Nagoya University
12	CeTe <sub>3</sub> およびTbTe <sub>3</sub> における量子臨界現象および磁性と超伝導の相関の研究	佐藤 憲昭	名古屋大学 大学院理学研究科	Study on the quantum criticality and correlation of magnetism and superconductivity in CeTe <sub>3</sub> and TbTe <sub>3</sub>	Noriaki Sato	Nagoya University
13	重い電子系超伝導体CeRh <sub>x</sub> Ir(1-x)In <sub>5</sub> における磁性ヒート伝導の相関の研究	佐藤 憲昭	名古屋大学 大学院理学研究科	Study on the correlation of magnetism and superconductivity in CeRh <sub>x</sub> Ir(1-x)In <sub>5</sub>	Noriaki Sato	Nagoya University
14	Dy <sub>3</sub> Al <sub>5</sub> O <sub>12</sub> ガーネットにおけるクーロン相の探索	佐藤 車	東京大学 物性研究所	Search for the Coulomb phase in the Dy <sub>3</sub> Al <sub>5</sub> O <sub>12</sub> garnet	Taku J Sato	The University of Tokyo
15	S=1/2 篦目格子反強磁性体volborthiteの磁気励起	佐藤 車	東京大学 物性研究所	Magnetic excitations in the s=1/2 kagome antiferromagnet volborthite	Taku J Sato	The University of Tokyo
16	強誘電体の相転移機構(変位型及び秩序無秩序型)に関する統一的理解の確立	重松 宏武	山口大学 教育学部	Establishment of the unified explanation about the phase transition mechanism (displacive and order-disorder type) in Ferroelectrics	Hirotake Shigematsu	Shimane University
17	新しいタイプの偏壓電子フラストレート磁性体A <sub>3</sub> B <sub>3</sub> Xの動的スピinn相関	田畠 吉計	京都大学 大学院工学研究科	Dynamic spin correlations in novel itinerant-electron frustrated magnets A <sub>3</sub> B <sub>3</sub> X	Yoshikazu Tabata	Kyoto University
18	導電性三角格子磁性体PdCrO <sub>2</sub> の反強磁性秩序と異常伝導	高津 浩	首都大学東京 大学院理工学研究科	Antiferromagnetism and its relation to the anomalous conductivity in the metallic triangular-lattice magnet PdCrO <sub>2</sub>	Hirosi Takatsu	Tokyo Metropolitan University
19	10GPa級中性子散乱実験用圧力発生装置の開発	上床 美也	東京大学 物性研究所	Development of high pressure apparatus for elastic neutron scattering experiments	Yoshiya Uwatoko	The University of Tokyo
20	新しい籠状物質PrTM <sub>2</sub> Al <sub>20</sub> (TM=V,Cr)の四極子秩序と結晶場効起	山 照夫	東京大学 物性研究所	Quadrupolar order and crystal field excitations in the new cage compound PrTM <sub>2</sub> Al <sub>20</sub> (TM=V,Cr).	Teruo Yamazaki	The University of Tokyo
21	重い電子系ウラン化合物の隠れた秩序に対する横山一軸応力効果	横山 淳	茨城大学 理学部	Effect of uniaxial stress on hidden order in U-based heavy-fermion compound	Makoto Yokoyama	Ibaraki University
22	鉄系超伝導体のスピinn揺動	李 哲虎	産業技術総合研究所 エネルギー技術研究部	Spin fluctuations of iron-based superconductors	Chul-Ho Lee	National Institute of Advanced Industrial Science and Technology
23	UPd <sub>2</sub> Si <sub>2</sub> におけるフラストレートした反強磁性相関の1軸応力および静水圧効果	網塚 浩	北海道大学 大学院理学研究科	Effects of Uniaxial Stress and Hydrostatic Pressure on Frustrated Antiferromagnetic Correlations in UPd <sub>2</sub> Si <sub>2</sub>	Hiroshi Amitaka	Hokkaido University
24	空間反転対称性を持たない超伝導体CeIrSi <sub>3</sub> の非整合磁気構造	阿曾 尚文	琉球大学 理学部	Incommensurate Magnetic Structure in a Non-Centrosymmetric Superconductor CeIrSi <sub>3</sub>	Naofumi Aso	University of the Ryukyus

No.	課題名	氏名	所属	Title	Name	Organization
25	重い電子系新物質Ce <sub>2</sub> Pt <sub>3</sub> Ge <sub>5</sub> の磁気構造解析	藤原 哲也	山口大学 大学院理工学 研究科	Magnetic structure analysis of new heavy fermion material Ce <sub>2</sub> Pt <sub>3</sub> Ge <sub>5</sub>	Tetsuya Fujiiwara	Yamaguchi University
26	EuRu <sub>2</sub> P <sub>2</sub> の磁気構造解析	藤原 哲也	山口大学 大学院理工学 研究科	Magnetic structure analysis of EuRu <sub>2</sub> P <sub>2</sub>	Tetsuya Fujiiwara	Yamaguchi University
27	磁気構造の長時間変化と磁性原子希釈効果 中性子回折法による六方晶フェライト 超交換相互作用の研究	元屋 清一郎	東京理科大学 理工学部	Dilution effect of magnetic atoms on the long-time variation of magnetic structure Study on superexchange interactions of hexagonal ferrites (Ba <sub>1-x</sub> Sr <sub>x</sub> ) <sub>2</sub> Zn <sub>2</sub> Fe <sub>12</sub> O <sub>22</sub> and Ba(Fe <sub>1-x</sub> Sc <sub>x</sub> ) <sub>12</sub> O <sub>19</sub> by neutron diffraction	Kyoichiro Motoya	Tokyo University of Science
28	(Ba <sub>1-x</sub> Sr <sub>x</sub> ) <sub>2</sub> Zn <sub>2</sub> Fe <sub>12</sub> O <sub>22</sub> およびBa(Fe <sub>1-x</sub> Sc <sub>x</sub> ) <sub>12</sub> O <sub>19</sub> の 超交換相互作用の研究	内海 重宜	東京大学 物性研究所	IRT: PONTA(Polarized Neutron Triple Axis Spectrometer)	Shigenori Usumi	Tokyo University of Science, Suwa
29	PONTA(高性能偏極中性子散乱装置)IRT課題 PONTA(高性能偏極中性子散乱装置)IRT課題	益田 隆嗣	東京大学 金属材料研究所	IRT: PONTA(Polarized Neutron Triple Axis Spectrometer)	Takatsugu Masuda	The University of Tokyo
30	偏極中性子線を用いた磁気散乱中性子線ホログラフィー	林 好一	東北大 学 金属材料研究所	Koichi Hayashi	Tohoku University	
31	高エネルギー磁気励起測定によるBi <sub>2201</sub> の磁気励起分散の研究	榎木 勝徳	九州工業大学 大学院工学研究科	Study of magnetic excitation dispersion in Bi <sub>2201</sub> by measurement of high-energy excitation	Masanori Enoki	Kyushu Institute of Technology
32	一次元フラストレート鎖量子磁性体CaCu <sub>2</sub> VO <sub>4</sub> (OD) の磁気励起	萩原 雅人	東京大学 物性研究所	Magnetic excitation of one dimensional quantum frustrated chain magnetism CaCu <sub>2</sub> VO <sub>4</sub> (OD)	Masato HagaHala	The University of Tokyo
33	四面体構造を持つ量子スピン磁性体CaCu <sub>2</sub> VO <sub>4</sub> (OD) の磁気励起	萩原 雅人	東京大学 物性研究所	Magnetic excitation in tetrahedral quantum spin compound Cu <sub>2</sub> (OH) <sub>3</sub> Cl(Clinoatacamite)	Masato HagaHala	The University of Tokyo
34	強磁性ダイマーCs <sub>3</sub> V <sub>2</sub> Cl <sub>9</sub> の中性子散乱	益田 隆嗣	東京大学 物性研究所	Neutron scattering study in ferromagnetic dimer Cs <sub>3</sub> V <sub>2</sub> Cl <sub>9</sub>	Takatsugu Masuda	The University of Tokyo
35	アルカリ超酸化物KO <sub>2</sub> の磁気励起	益田 隆嗣	東京大学 物性研究所	Magnetic excitation in Alkali superoxide KO <sub>2</sub>	Takatsugu Masuda	The University of Tokyo
36	リラクサーPMN-xPTにおける低エネルギー効果 ノードの研究II	松浦 直人	東北大 学 金属材料研究所	Study of extremely low energy phonon mode in PMN-xPT II	Masato Matsuura	Tohoku University
37	時間分割中性子散乱測定による磁気構造変化過程 の実時間追跡	元屋 清一郎	東京理科大学 理工学部	Real-time observation of magnetic structural change by means of time-resolved neutron scattering experiments	Kyoichiro Motoya	Tokyo University of Science
38	磁気構造の長時間変化と磁性原子希釈効果 時間変化へのdisorderの効果	元屋 清一郎	東京理科大学 理工学部	Dilution effect of magnetic atoms on the long-time variation of magnetic structure	Kyoichiro Motoya	Tokyo University of Science
39	多段メタ磁性体Ce <sub>0.8</sub> Co <sub>2</sub> O <sub>6</sub> における磁気構造の 時間変化へのdisorderの効果	茂吉 武人	東京理科大学 理工学部	Effect of Disorder on the Long-Time Variation of Magnetic Structure in a Multistep Metamagnet Ce <sub>0.8</sub> Co <sub>2</sub> O <sub>6</sub>	Taketo Moyoshi	Tokyo University of Science
40	マルチフェロイックCuFeO <sub>2</sub> における2軸圧力による 磁気・誘電・メイン配向制御	中島 多朗	東京理科大学 理学部	Biaxial-pressure control of multiferroic domain structure in spin-driven ME multiferroic CuFeO <sub>2</sub>	Taro Nakajima	Tokyo University of Science
41	NiGa <sub>2</sub> S <sub>4</sub> におけるスピネルマテリック相関の検出	南部 雄亮	東京大学 物性研究所	Detection of spin nematic correlation in the 2D magnet NiGa <sub>2</sub> S <sub>4</sub>	Yusuke Nambu	The University of Tokyo

No.	課題名	氏名	所属	Title	Name	Organization
42	磁性イオンをもつリラクサー誘電体におけるナノ磁気ドメインの電場制御	左右田 稔	東京大学 物性研究所	E+FG14 electric control of nano magnetic domain in relaxor ferroelectrics having magnetic ions	Minoru Soda	The University of Tokyo
43	希釈イシング反強磁性体 $\text{Ho}_x\text{Y}_{1-x}\text{Ru}_2\text{Si}_2$ の磁気秩序相における異常スピンドライナミクス	田畠 吉計	京都大学 大学院工学研究科	Anomalous spin dynamics in the magnetic ordered state of the diluted Ising antiferromagnet $\text{Ho}_x\text{Y}_{1-x}\text{Ru}_2\text{Si}_2$	Yoshikazu Tabata	Kyoto University
44	導電性三角格子磁性体 $\text{PdCrO}_2$ の反強磁性秩序と異常伝導	高津 浩	首都大学東京 大学院理工学研究科	Antiferromagnetism and its relation to the anomalous conductivity in the metallic triangular-lattice magnet $\text{PdCrO}_2$	Hiroshi Takatsu	Tokyo Metropolitan University
45	秩序型ペロブスカイト $\text{CaCu}_3\text{Ti}_4\text{O}_{12}$ のフォノン	留野 泉	秋田大学 教育文化学部	Phonons in ordered perovskite $\text{CaCu}_3\text{Ti}_4\text{O}_{12}$	Izumi Tomono	Akita University
46	立方晶 $\text{BaTiO}_3$ のフォノンの温度依存性	留野 泉	秋田大学 教育文化学部	Temperature dependence of phonons in cubic $\text{BaTiO}_3$	Izumi Tomono	Akita University
47	$\text{FeTe}_{1-x}\text{Se}_x$ 系のフォノン	留野 泉	秋田大学 教育文化学部	Phonons in $\text{FeTe}_{1-x}\text{Se}_x$	Izumi Tomono	Akita University
48	$\text{LaCo}_{1-x}\text{Rh}_x\text{O}_3$ 非磁性状態をend phaseに持つ dopingによって現れる強磁性	安井 幸夫	名古屋大学 大学院理学研究科	$\text{LaCo}_{1-x}\text{Rh}_x\text{O}_3$ ;Ferromagnetism induced by doping between two nonmagnetic end phase	Yukio Yasui	Nagoya University
49	スピノン3/2の反強磁性交換鎖を持つ $\text{RCrGeO}_5$ ( $\text{R}=\text{Sm}, \text{Y}$ or $\text{Nd}$ )のスピニ・ギャップ励起の研究	長谷 正司	物質・材料研究機構	量子ビームエニット中性子散乱グレーブ	Masashi Hase	National Institute for Materials Science
50	偏極中性子を用いた $\text{Cu}_3\text{Mo}_2\text{O}_9$ 単結晶の磁気構造の決定	長谷 正司	物質・材料研究機構	量子ビームエニット中性子散乱グレーブ	Masashi Hase	National Institute for Materials Science
51	$(\text{CuZn})_3\text{Mo}_2\text{O}_9$ 単結晶の磁気反射の測定	長谷 正司	物質・材料研究機構	量子ビームエニット中性子散乱グレーブ	Masashi Hase	National Institute for Materials Science
52	鉄系超伝導体単結晶のフォノン	佐藤 正俊	総合科学研究所	サイエンスユーディネーター	Masatoshi Sato	Comprehensive Research Organization for Science and Society
53	MnRhの低温相及び高温相の磁気構造相転移	松岡 由貴	奈良女子大学 理学部	Magnetic phase transformations in $\text{B}_2^-$ -phase and $\text{L1}_0$ -phase	Yuki Matsuoaka	Nara Women's University
54	三角格子系 $\text{Na}_x\text{NiO}_2$ の磁気構造	茂吉 武人	東京理科大学 理工学部	$\text{Na}_x\text{NiO}_2$	Taketo Moyoshi	Tokyo University of Science
55	3元合金 $\text{CuFePt}_6$ の磁気構造	高橋 美和子	筑波大学 大学院数理物理学研究所	Magnetic structure of a triangular system $\text{Na}_x\text{NiO}_2$	Miwako Takahashi	University of Tsukuba
56	混晶系 $\text{Ba}_{1-x}\text{Ca}_x\text{TiO}_3$ のフォノン	留野 泉	秋田大学 教育文化学部	$\text{CuFePt}_6$ ternary alloy	Izumi Tomono	Akita University
57	TOPAN(東北大理:3軸型偏極中性子分光器)IRI課題	岩佐 和晃	東北大学 大学院理学研究科	Phonons in $(\text{Ba},\text{Ca})\text{TiO}_3$	Kazuaki Iwasa	Tohoku University
58	高精度測定によるFe-LSCOの異方的磁気秩序ピークの起源の研究	藤田 金基	東北大学 金属材料研究所	Origin of anisotropic magnetic peak in Fe-LSCO studied with high resolution measurement	Masaki Fujita	Tohoku University

No.	課題名	氏名	所属	Title	Name	Organization
59	新規T'構造銅酸化物Pr <sub>2-x</sub> Ca <sub>x</sub> CuO <sub>4</sub> における磁気相関のホールドーピング効果	藤田 金基	東北大	金属材料研究所	Masaki Fujita	Tohoku University
60	反強磁性金属Mn <sub>3</sub> Siにおける高温スピノン励起	平賀 晴弘	東北大	金属材料研究所	Haruhiro Hiraka	Tohoku University
61	近藤合金Yb <sub>1-x</sub> Tm <sub>x</sub> B <sub>6</sub> の結晶場遷移	伊賀 文俊	茨城大学	理学部	Fumitoshi Iga	Ibaraki University
62	高い反強磁性転移温度をもつ鉄系化合物TlFe <sub>2</sub> Se <sub>2</sub> の磁性	飯久保 智	九州工業大学	大学院生命体工学科	Kyushu Institute of Technology	
63	PrIr <sub>2</sub> Zn <sub>30</sub> における非Kramers二重項による四極子秩序の検証	岩佐 和晃	東北大	大学院理学研究科	Satoshi Iikubo	
64	近藤半導体CeOs <sub>4</sub> Sb <sub>12</sub> における磁場によってエンハンスされる秩序変数	岩佐 和晃	東北大	大学院理学研究科	Kazuaki Iwasa	Tohoku University
65	電子ドープした重い電子系Pr(Fe <sub>1-x</sub> Co <sub>x</sub> ) <sub>4</sub> P <sub>12</sub> の磁気励起	岩佐 和晃	東北大	大学院理学研究科	Kazuaki Iwasa	Tohoku University
66	CeTeにおける圧力誘起反強四極子秩序	松村 武	広島大学	大学院先端物質科学研究科	Takeshi Matsumura	Hirosima University
67	Ce <sub>0.5</sub> La <sub>0.5</sub> B <sub>6</sub> における磁気八極子秩序の検証	松村 武	広島大学	大学院先端物質科学研究科	Takeshi Matsumura	Hirosima University
68	高温超伝導体LSCOの磁気励起における磁性不純物N置換効果の研究II	松浦 直人	東北大	金属材料研究所	Masato Matsuda	Tohoku University
69	高温超伝導体LSCO擬ギャップ相における磁気励起の温度依存性	松浦 直人	東北大	金属材料研究所	Masato Matsuda	Tohoku University
70	極低温単結晶中性子回折によるYbPdの磁気構造および金属的電荷秩序の検証	光田 眥弘	九州大学	大学院理学研究科	Akihiro Mitsuishi	Kyushu University
71	希薄不純物置換LaCoO <sub>3</sub> 系における巨大磁気モーメントを伴うスピinn分子ポーラロンの研究	富安 啓輔	東北大	大学院理学研究科	Keisuke Tomiyasu	Tohoku University
72	金属絶縁体転移を示す導電性フラストレート系R <sub>2</sub> Ir <sub>2</sub> O <sub>7</sub> における磁気構造と内部磁場の研究	富安 啓輔	東北大	大学院理学研究科	Keisuke Tomiyasu	Tohoku University
73	鉄系超伝導体のスピノン運動	李 哲虎	産業技術総合研究所	エネルギー技術研究部	Chul-Ho Lee	National Institute of Advanced Industrial Science and Technology
74	Ce <sub>0.7</sub> La <sub>0.3</sub> B <sub>6</sub> の一軸圧下中性子回折	桑原 慶太郎	茨城大学	大学院理工学研究科	Keitaro Kuwahara	Ibaraki University
75	HER(高エネルギー分解能3軸型中性子分光器)IRT課題	横山 淳	茨城大学	理学部理学科	Jun Yokoyama	Ibaraki University

No.	課題名	氏名	所属	Title	Name	Organization
76	$\text{La}_{1-x}\text{Ru}_x\text{Si}_2$ ( $x > 0.9$ )における磁気秩序構造と磁気励起	網塚 浩	北海道大学 大学院理学研究科	Magnetic Ordering Structure and excitations in $\text{La}_{1-x}\text{Ru}_x\text{Si}_2$ ( $x > 0.9$ )	Hiroshi Amitsuka	Hokkaido University
77	量子臨界点近傍にある $\text{YbCo}_2\text{Zn}_{20}$ の磁気励起	阿曾 尚文	琉球大学 理学部	Magnetic excitations in $\text{YbCo}_2\text{Zn}_{20}$ in vicinity of a quantum critical point	Naofumi Aso	University of the Ryukyus
78	空間反転対称性をもたない超伝導体 $\text{CeTSi}_3$ ( $T=\text{Rh}, \text{Ir}$ )の磁気励起	阿曾 尚文	琉球大学 理学部	Magnetic Fluctuations in a Non-Centrosymmetric Superconductor $\text{CeTSi}_3$	Naofumi Aso	University of the Ryukyus
79	高エネルギー磁気励起測定による $\text{Bi}2201$ の磁気励起 分散の研究	榎木 勝徳	九州工業大学 大学院工学研究科	Study of magnetic excitation dispersion in $\text{Bi}2201$ by measurement of high-energy excitation	Masanori Enoki	Kyushu Institute of Technology
80	高精度測定による Fe-LSCO の異方的磁気秩序 ピークの起源の研究	藤田 全基	東北大学 金属材料研究所	Origin of anisotropic magnetic peak in Fe-LSCO studied with high resolution measurement	Masaki Fujita	Tohoku University
81	新規 T'構造銅酸化物 $\text{Pr}_{2-x}\text{Ca}_x\text{CuO}_4$ における磁気相関のホールドアブ効果	藤田 全基	東北大学 金属材料研究所	Hole-doping effect on spin correlations in a new cuprate oxide of T'-structured $\text{Pr}_{2-x}\text{Ca}_x\text{CuO}_4$	Masaki Fujita	Tohoku University
82	( $\text{Pr}_{1-x}\text{Ce}_x$ ) $\text{Ru}_x\text{P}_{12}$ のリエンクトント型金属 非金属転移における全対称型高次多極子秩序の研究	岩佐 和晃	東北大学 大学院理学研究科	Studies on totally symmetric higher-rank multipolar ordering on the reentrant metal-nonmetal transition of $(\text{Pr}_{1-x}\text{Ce}_x)\text{Ru}_x\text{P}_{12}$	Kazuaki Iwasa	Tohoku University
83	電子ドープした重い電子系 $\text{Pr}(\text{Fe}_{1-x}\text{Co}_x)_4\text{P}_{12}$ の磁気励起	岩佐 和晃	東北大学 大学院理学研究科	Magnetic excitation in the electron-doped heavy-electron system $\text{Pr}(\text{Fe}_{1-x}\text{Co}_x)_4\text{P}_{12}$	Kazuaki Iwasa	Tohoku University
84	酸素吸着 Cuジカルボン酸の低エネルギー励起	益田 隆嗣	東京大学 物性研究所	Low energy excitation in $\text{O}_2$ adsorbed Cu-dicarboxylic acid	Takatsugu Masuda	The University of Tokyo
85	フラストレート強磁性鎖におけるスピノ・ネマティック相間の検出	益田 隆嗣	東京大学 物性研究所	Detection of spin nematic correlation in frustrated ferromagnetic chain	Takatsugu Masuda	The University of Tokyo
86	強磁性ダイマー— $\text{Cs}_3\text{V}_2\text{Cl}_9$ の中性子散乱	益田 隆嗣	東京大学 物性研究所	Neutron scattering study in ferromagnetic dimer $\text{Cs}_3\text{V}_2\text{Cl}_9$	Takatsugu Masuda	The University of Tokyo
87	スピノ格子結合系 $\text{CuFeO}_2$ のスピノン波分散関係の一軸応力変化	満田 節生	東京理科大学 理学部	Spin wave dispersion relation in a spin-lattice coupled system $\text{CuFeO}_2$ under uni-axial stress	Setsuo Mitsuda	Tokyo University of Science
88	鉄系スピノラダ— $\text{BaFe}_2\text{Se}_3$ の磁気振動	南部 雄亮	東京大学 物性研究所	Spin dynamics of the iron-based spin ladder $\text{BaFe}_2\text{Se}_3$	Yusuke Nambu	The University of Tokyo
89	鉄系超伝導体 $\text{LiFe}(\text{As}, \text{P})$ の磁気振動	南部 雄亮	東京大学 物性研究所	Magnetic fluctuations in stoichiometric iron-based superconductors $\text{LiFe}(\text{As}, \text{P})$	Yusuke Nambu	The University of Tokyo
90	マルチフェロイック物質 $\text{YMn}_2\text{O}_5$ の磁気励起と磁気相互作用	野田 幸男	東北大学 多元物質科学研究所	Magnetic interaction and ferroelectricity in multiferroic $\text{YMn}_2\text{O}_5$	Yukio Noda	Tohoku University
91	強磁性超伝導体 $\text{UCoGe}$ におけるスピノン揺らぎの研究	佐藤 憲昭	名古屋大学 大学院理学研究科	Study on spin fluctuations of the superconducting ferromagnet $\text{UCoGe}$	Noriaki Sato	Nagoya University
92	$\text{CeTe}_3$ より $\text{NbTe}_3$ における量子臨界現象および磁性と超伝導の相関の研究	佐藤 憲昭	名古屋大学 大学院理学研究科	Study on the quantum criticality and correlation of magnetism and superconductivity in $\text{CeTe}_3$ and $\text{NbTe}_3$	Noriaki Sato	Nagoya University

No.	課題名	氏名	所属	Title	Name	Organization
93	重い電子系超伝導体CeRh <sub>x</sub> Ir <sub>1-x</sub> In <sub>5</sub> における磁性と超伝導の相関の研究	佐藤 嘉昭	名古屋大学 大学院理学研究科	Study on the correlation of magnetism and superconductivity in CeRh <sub>x</sub> Ir <sub>1-x</sub> In <sub>5</sub>	Noriaki Sato	Nagoya University
94	Dy <sub>3</sub> Al <sub>5</sub> O <sub>12</sub> ガーネットにおけるクーロン相の探索	佐藤 車	東京大学 物性研究所	Search for the Coulomb phase in the Dy <sub>3</sub> Al <sub>5</sub> O <sub>12</sub> garnet	Taku J Sato	The University of Tokyo
95	量子スピン反強磁性三量体系2b 3CuCl <sub>2</sub> 2H <sub>2</sub> Oの磁気励起	佐藤 車	東京大学 物性研究所	Magnetic Excitations in Quantum Spin Antiferromagnetic Trimer System 2b 3CuCl <sub>2</sub> 2H <sub>2</sub> O	Taku J Sato	The University of Tokyo
96	[Cu <sub>2</sub> (bza) <sub>4</sub> (pyz)]nにおける吸着酸素分子の磁気相關	左右田 稔	東京大学 物性研究所	Magnetic Interaction between Absorbed O <sub>2</sub> Molecules in [Cu <sub>2</sub> (bza) <sub>4</sub> (pyz)]n	Minoru Soda	The University of Tokyo
97	新しいタイプの遍歴電子フラストレート磁性体A <sub>3</sub> B <sub>3</sub> Xの動的スピン相関	田畠 吉計	京都大学 大学院工学研究科	Dynamic spin correlations in novel itinerant-electron frustrated magnets A <sub>3</sub> B <sub>3</sub> X	Yoshikazu Tabata	Kyoto University
98	擬2次元三角格子反強磁性体Ba <sub>3</sub> MSb <sub>2</sub> O <sub>9</sub> (M=Co, Ni)の磁気励起と負の量子再規格化	田中 秀数	東京工業大学 大学院理工学研究科	Negative quantum renormalization of magnetic excitations in quasi-2D triangular-lattice antiferromagnets Ba <sub>3</sub> MSb <sub>2</sub> O <sub>9</sub> (M=Co, Ni)	Hidekazu Tanaka	Tokyo Institute of Technology
99	金属磁性体MnPにおけるDzyaloshinsky-Moriya相互作用の逆効果の検証	山 照夫	東京大学 物性研究所	Verification of the inverse effect of the Dzyaloshinsky-Moriya interaction in metallic magnet MnP	Teruo Yamazaki	The University of Tokyo
100	新しい管状物質PrTM <sub>2</sub> Al <sub>20</sub> (TM=V, Cr)の四極子秩序と結晶場励起	山 照夫	東京大学 物性研究所	Quadrupolar order and crystal field excitations in the new cage compound PrTM <sub>2</sub> Al <sub>20</sub> (TM=V, Cr).	Teruo Yamazaki	The University of Tokyo
101	逐次相転移を示した三角格子物質Co <sub>2</sub> (OD) <sub>3</sub> Brのプラストレーショング・スピンドラッグ	算 旭光	佐賀大学 大学院工学系研究科	Study of the frustrated magnetism and spin fluctuations in triangular-lattice Co <sub>2</sub> (OD) <sub>3</sub> Br	Xu-Guang Zheng	Saga University
102	鉄系超伝導体のスピントラベル	李 哲虎	産業技術総合研究所 エネルギー技術研究部門	Spin fluctuations of iron-based superconductors	Chul-Ho Lee	National Institute of Advanced Industrial Science and Technology
103	高い反磁性転移温度をもつ鉄系化合物TFe <sub>2</sub> Se <sub>2</sub> の磁性	飯久保 智	九州工業大学 大学院生命体工学研究科	Neutron scattering study of high temperature anti-ferromagnet TFe <sub>2</sub> Se <sub>2</sub>	Satoshi Iikubo	Kyushu Institute of Technology
104	量子スピノサイクスの研究	門脇 広明	首都大学東京 大学院理工学研究科	Quantum spin ice	Hiroaki Kadokami	Tokyo Metropolitan University
105	S=1/2擬一次元スピノン・ギャップ物質Pb <sub>2</sub> V <sub>3</sub> O <sub>9</sub> の磁気励起	益田 隆嗣	東京大学 物性研究所	Magnetic excitation in S=1/2 quasi 1D spin-gap compound Pb <sub>2</sub> V <sub>3</sub> O <sub>9</sub>	Takatsugu Masuda	The University of Tokyo
106	PrRh <sub>2</sub> Ge <sub>2</sub> の逐次磁気転移	繁岡 透	山口大学 大学院理工学研究科	Successive magnetic transitions of PrRh <sub>2</sub> Ge <sub>2</sub>	Toru Shigeoka	Yamaguchi University
107	成分分離逐次磁気転移の研究	繁岡 透	山口大学 大学院理工学研究科	Study of component s-separated magnetic transition	Toru Shigeoka	Yamaguchi University
108	TbCu <sub>2</sub> Si <sub>2</sub> の複雑な磁気相図	繁岡 透	山口大学 大学院理工学研究科	Complex magnetic phase diagrams of TbCu <sub>2</sub> Si <sub>2</sub>	Toru Shigeoka	Yamaguchi University
109	希薄不純物置換LaCoO <sub>3</sub> 系における巨大磁気モーメントを伴うスピノン分子ポーラロンの研究	富安 啓輔	東北大学 大学院理学研究科	Molecular spin polaron with colossal magnetic moment in lightly impurity doped LaCoO <sub>3</sub> system	Keisuke Tomiyasu	Tohoku University

No.	課題名	氏名	所属	Title	Name	Organization
110	金属純縁体転移を示す導電性プラスチート系 $R_2Ir_2O_7$ における磁気構造と内部磁場の研究	富安 啓輔	東北大 大学院理学研 究科	Magnetic structure and internal magnetic field in conductive frustrated system $R_2Ir_2O_7$ with metal-insulator transition	Keisuke Tomiyasu	Tohoku University
111	atacamite型四面体構造 $Mn_2(OD)_3Cl$ , $Mn_2(OD)_3Br$ のスピinn揺らぎ	佐賀 大 旭光	佐賀大 大学院工学系 研究科	Investigation of spin fluctuations in atacamite-type pyrochlore compounds $Mn_2(OD)_3Cl$ and $Mn_2(OD)_3Br$	Xu-Guang Zheng	Saga University
112	SANS-U(二次元位置測定小角散乱装置)IRT課 題	柴山 充弘	東京大 物性研究所	IRT: SANS-U(Small Angle Neutron Scattering Instrument, University of Tokyo)	Mitsuhiko Shibayama	The University of Tokyo
113	phosphonate型イオン液体を溶解剤とするセル ロースの溶存状態	藤井 健太	東京大 物性研究所	Solution structure of phosphonate-based ionic liquid containing cellulose	Kenta Fujii	The University of Tokyo
114	新規Fe系超伝導 $BaFe_2(ASiP)_2$ の磁束格子実験	古川 はづき	お茶の水女子 大学	SANS experiment on flux line lattice in $K_{0.8}Fe_2Se_2$	Hazuki Furukawa	Ochanomizu University
115	新規Fe系超伝導 $BaFe_2(ASiP)_2$ の磁束研究	古川 はづき	お茶の水女子 大学	Vortex study on Fe-based superconductor	Hazuki Furukawa	Ochanomizu University
116	中性子小角散乱実験による $Sr_2RuO_4$ の異常金属 状態の研究	古川 はづき	お茶の水女子 大学	Anomalous vortex state in $Sr_2RuO_4$ studied by SANS experiments	Hazuki Furukawa	Ochanomizu University
117	希釈冷凍機温度領域におけるCeIrIn <sub>5</sub> の磁束の磁 気形状因子の異常	古川 はづき	お茶の水女子 大学	Anomalous magnetic form factor in the vortex state on CeIrIn <sub>5</sub>	Hazuki Furukawa	Ochanomizu University
118	高分子流動結晶化における高分子量成分と低分 子量成分の役割	金谷 利治	京都大 化学研究所	Role of high and low molecular weight components in flow induced polymer crystallization	Toshiji Kanaya	Kyoto University
119	抗ガン作用のあるハイブリッドリボソームの構造と 揺らぎの観測	片岡 幹雄	奈良先端科学 技術大学院大 学	The structure and dynamics of hybrid liposome with anticancer function	Mikio Kataoka	Nara Institute of Science and Technology
120	温度応答性界面不活性／界面活性性転移高分子 のビセル形成とナノ構造転移	松岡 秀樹	京都大 学	Micelle Formation and Nanostructure Transition of Temperature Responsive Non-Surface Active/Surface Active Transition Polymers	Hideki Matsuoka	Kyoto University
121	界面不活性イオン性両親性高分子ミセルのナ ノ構造転移—誘電率の効果	松岡 秀樹	京都大 学	Nanostructure Transition of Non-Surface Active Ionic Amphiphilic Diblock Copolymers --- Effect of Dielectric Constant	Hideki Matsuoka	Kyoto University
122	リラクサー誘電体における自己相似プロファイル の研究	松浦 直人	東北大 金属材料研究 所	Investigation of power law profile in relaxor ferroelectrics	Masato Matsura	Tohoku University
123	メソ細孔を発達させたフランタルポーラスシリカの 構造評価	真山 博幸	北海道大 学	Structural investigation of fractal porous silica created by novel template and nano-composite methods	Hiroyuki Mayama	Hokkaido University
124	POPCナノディスクの構造とダイナミクス	中野 実	京都大 学	Structure and Dynamics of POPC Nanodiscs	Minoru Nakano	Kyoto University
125	膜貫通ペプチドのフリップフロップ誘起能の評価	中野 実	京都大 学	Induction of Flip-Flop by Transmembrane Peptides	Minoru Nakano	Kyoto University
126	膜脂質のダイナミクスに及ぼす膜の曲率の評価	中野 実	京都大 学	Effects of Curvature on Dynamics of Membrane Lipids	Minoru Nakano	Kyoto University

No.	課題名	氏名	所属	Title	Name	Organization
127	N-isopropylacrylamide水溶液における相分離挙動と疎水性水和への電解質効果の分子論的解明	西脇 哲士	九州大学 大学院理学研究院	Molecular understanding of the effect of electrolytes on phase separation and hydrophobic hydration in the aqueous solutions of NIPA	Satoshi Okabe	Kyushu University
128	水/有機溶媒/塩混合溶液系の秩序構造に対する圧力の効果	貞包 浩一朗	高エネルギー加速器研究機構 物質構造科学研究所	Pressure-induced phase transition in a mixture of water/organic solvent/salt	Koichiro Sadakane	High Energy Research Organization
129	高压条件下における2成分混合溶液の新奇な臨界挙動	貞包 浩一朗	高エネルギー加速器研究機構 物質構造科学研究所	Novel critical behavior in a mixture of water / organic solvent under high-pressure condition	Koichiro Sadakane	High Energy Research Organization
130	界面不活性の働きをする界面活性剤	貞包 浩一朗	高エネルギー加速器研究機構 物質構造科学研究所	Amphiphilic molecules acting as a surface inactive substance	Koichiro Sadakane	High Energy Research Organization
131	温度応答性部位を有するTetraグエルの構造解析	酒井 崇匡	東京大学 大学院工学系研究科	Structural analysis of thermo-responsive Tetra gel	Takamasa Sakai	The University of Tokyo
132	自発曲率による脂質分子のソーティング	佐久間 由香	お茶の水女子大学 理学部	Lipids Sorting Induced by Membrane Curvature and Geometrical Shape of Lipids	Yuka Sakuma	Ochanomizu University
133	後期エンドソームにおける特異的脂質BMPの分布の非対称性	佐久間 由香	お茶の水女子大学 理学部	Asymmetric Distribution of BMP on Late Endosome	Yuka Sakuma	Ochanomizu University
134	ナノメートルサイズベシクル上でドメインダイナミクス	佐久間 由香	お茶の水女子大学 理学部	Dynamics of Domains on a Nanometer-Sized Vesicle	Yuka Sakuma	Ochanomizu University
135	毛髪の内部構造解析	柴山 充弘	東京大学 物性研究所	Structural analysis of hair	Mitsuhiko Shibayama	The University of Tokyo
136	燃料電池電極用触媒インクの構造解析	柴山 充弘	東京大学 物性研究所	Structural studies on catalyst ink for fuel cell electrodes	Mitsuhiko Shibayama	The University of Tokyo
137	Tetra-PEGオングルの均一網目構造に対するイオン液体の特殊反応場効果	柴山 充弘	東京大学 物性研究所	Effect of ionic liquid type on the structure of Tetra-PEG ion-gel Solvent effect of network structure of Tetra-PEG iongel studied by SANS	Mitsuhiko Shibayama	The University of Tokyo
138	結合不均一性を有するTetra-PEGゲルの延伸下における構造解析	柴山 充弘	東京大学 物性研究所	Structural Analysis of Connective Defects Induced Tetra-PEG gel Under Uniaxial Deformation	Mitsuhiko Shibayama	The University of Tokyo
139	Rheo-FocusingSANSを用いたすり粘稠効果に伴う紡状ミセル伸長機構の解明	柴山 充弘	東京大学 物性研究所	Rheo-Focusing SANS study on shear induced transition of wormlike micelle	Mitsuhiko Shibayama	The University of Tokyo
140	群分割SANS法によるイオン液体中のゲル化反応メカニズム解明	柴山 充弘	東京大学 物性研究所	Gelation process of Tetra-PEG ion gel studied by time-resolved small angle neutron scattering	Mitsuhiko Shibayama	The University of Tokyo
141	中性子小角散乱によるGM1含有Bicelleの構造解析	杉山 正明	京都大学 原子炉実験所	Structural Investigation of GM1-containing Bicelle by Small-Angle Neutron Scattering	Masaaki Sugiyama	Kyoto University
142	マルチドメインタンパク質の動的性質の解明	杉山 正明	京都大学 原子炉実験所	Investigation of Dynamics on Multi-domain Proteins	Masaaki Sugiyama	Kyoto University
143	イオン液体と低分子液体混合系の動的秩序構造の検討	高橋 良輔	九州大学 先導物質化学研究所	Examination of dynamically ordered structure in mixtures of ionic liquid and low molecular weight liquids	Yoshiaki Takahashi	Kyusyu University

No.	課題名	氏名	所属	Title	Name	Organization
144	溶媒極性による硝酸イミダゾリウムの会合挙動の相違	高椋 利幸	佐賀大学 大学院工学系研究科	Aggregation of Imidazolium Nitrate Depending on Solvent Polarities	Toshiyuki Takamuku	Saga University
145	アルカリ電解質が誘起するアセトニトリル水混合溶液の相分離	高椋 利幸	佐賀大学 大学院工学系研究科	Alkali Electrolytes-Induced Phase Separation of Acetonitrile-Water Mixtures	Toshiyuki Takamuku	Saga University
146	イオン液体と界面活性剤の混合物の相分離現象	吉田 享次	福岡大学 理学部	Phase separation of ionic liquids and surfactant mixtures	Koji Yoshida	Fukuoka University
147	環境負荷低減を目指した新規ジエミニ型非イオン性界面活性剤のミセル特性	吉村 優一	奈良女子大学 大学院人間文化研究科	Micelle Properties of Novel Nonionic Gemini Surfactants to Preserve Environment	Tomokazu Yoshimura	Nara Women's University
148	中性子スピinnエコー法を用いたStaphylococcal nucleleaseの水溶液中のメソスコピックダイナミクス研究	遠藤 仁	日本原子力研究開発機構 量子ビーム応用研究部門	Mesoscopic Dynamics of Staphylococcal Nuclease in Aqueous Solution Investigated by Neutron Spin Echo Technique	Hitoshi Endo	Japan Atomic Energy Agency
149	DNA担持ナノ粒子におけるDNA密生相の構造解析	藤田 雅弘	独立行政法人 理化学研究所 前田バイオ工学研究室	Structural study on DNA coronal layer in DNA-functionalized nanoparticle	Masahiro Fujita	RIKEN
150	F-アクチンの構造多形性と運動特性の相関Ⅱ	藤原 恒	日本原子力研究開発機構 量子ビーム応用研究部門	Relationship between the structural polymorphism and the dynamics of F-actin II	Satoru Fujiwara	Japan Atomic Energy Agency
151	アミロイド線維形成初期過程 中間体のダイナミクスⅡ	藤原 恒	日本原子力研究開発機構 量子ビーム応用研究部門	Dynamics of the intermediate structures of the early stages of the amyloid fibril formation II	Satoru Fujiwara	Japan Atomic Energy Agency
152	高世代デンドロンを有する両親媒性デンドリマー会合体の構造解析	岩瀬 裕希	総合科学研究所 機構	Structure analysis of newly synthesized amphiphilic dendrimers with high-generation dendrons in aqueous solution	Hiroki Iwase	Comprehensive Research Organization for Science and Society
153	高分子密集条件下におけるタンパク質の構造とDNAミックス	平井 光博	群馬大学 大学院工学研究科	Structure and dynamics of proteins under crowded polymer conditions	Mitsuhiko Hirai	Gunma University
154	小角中性子散乱によるインスリンアミロイド線維形成機構に関する研究	井上 優太郎	京都大学 化学研究所	Mechanism of insulin amyloid fibril formation as studied by small angle neutron scattering	Rintaro Inoue	Institute for Chemical Research
155	エポキシ樹脂の重合誘起相分離と架橋構造	金谷 利治	京都大学 化学研究所	Polymerization Induced Phase Separation of Epoxy Resin and Network Structure	Toshiji Kanaya	Kyoto University
156	フェノール樹脂ゲル化過程の不均一性解析	柴山 充弘	東京大学 物性研究所	Inhomogeneity of Phenolic Resins during Gelation Process	Mitsuhiko Shibayama	The University of Tokyo
157	水性アクリル樹脂分散体における粒子構造解析	柴山 充弘	東京大学 物性研究所	Particle Structure for Aqueous Acrylic Polymer Dispersion	Mitsuhiko Shibayama	The University of Tokyo
158	ひも状ミセルのシアーベンディング領域における構造の不安定性	高橋 良彰	九州大学 先導物質化学研究所	Structure instability of thread-like micelle in shear banding region	Yoshiaki Takahashi	Kyusyu University
159	セルロースの1-ブチル-3-メチルイミダゾリウムクロリド溶液中の分子量と回転半径	高橋 良彰	九州大学 先導物質化学研究所	Molecular weight and radius of gyration of cellulose in 1-butyl-3-methylimidazolium chloride solution	Yoshiaki Takahashi	Kyusyu University
160	脂質二重膜の曲げ弾性係数に対する面内ネットワーク構造の影響	山田 恒史	高エネルギー加速器研究機構 物質構造科学研究所	Effect of network structure in lipid bilayers on bending modulus	Norifumi Yamada	KENS

No.	課題名	氏名	所属	Title	Name	Organization
161	ULS(極小角散乱装置)IRT課題	大竹 淑恵	理化学研究所	IRT: ULS(Ultra Small Angle Scattering Instrument)	Yoshie Otake	RIKEN
162	C1-3 小型集束型小角散乱装置 IRT課題	古坂 道弘	北海道大学 大学院工学研究科	IRT: mf-SANS(mini-focusing Small Angle Neutron Scattering Instrument)	Michihiro Furusaka	Hokkaido University
163	INSE(中性子スピニコール分光器)IRT課題	柴山 充弘	東京大学 物性研究所	IRT: INSE(New isspp Neutron Spin Echo Spectrometer)	Mitsuhiko Shibayama	The University of Tokyo
164	高分子密閉条件下におけるタンパク質の構造とDNAミックス	平井 光博	群馬大学 大学院工学研究科	Structure and dynamics of proteins under crowded polymer conditions	Mitsuhiko Hirai	Gunma University
165	抗ガン作用のあるハイブリッドリポソームの構造と振らぎの観測	片岡 幹雄	奈良先端科学技術大学院大学 物質創成科学研究所	The structure and dynamics of hybrid liposome with anticancer function	Mikio Kataoka	Nara Institute of Science and Technology
166	POPCナノディスクの構造とダイナミクス	中野 実	京都大学 大学院薬学研究科	Structure and Dynamics of POPC Nanodiscs	Minoru Nakano	Kyoto University
167	N-isopropylacrylamide水溶液における相分離挙動と疎水性水和への電解質効果の分子論的解明	岡部 哲士	九州大学 大学院理学研究科	Molecular understanding of the effect of electrolytes on phase separation and hydrophobic hydration in the aqueous solutions of NIPA	Satoshi Okabe	Kyushu University
168	水/有機溶媒/塩混合溶液系の秩序構造に対する圧力の効果	貞包 浩一朗	高エネルギー加速器研究機構 物質構造科学研究所	Pressure-induced phase transition in a mixture of water/organic solvent/salt	Koichiro Sadakane	High Energy Research Organization
169	マルチドメインタンパク質の動的性質の解明	杉山 正明	京都大学 原子炉実験所	Investigation of Dynamics on Multi-domain Proteins	Masaaki Sugiyama	Kyoto University
170	溶液極性による硝酸ミニマリウムの会合挙動の相違	高椋 利幸	佐賀大学 大学院工学系研究科	Aggregation of Imidazolium Nitrate Depending on Solvent Polarities	Toshiyuki Takamuku	Saga University
171	アルカリ電解質が誘起するアセトニトリル水混合溶液の相分離	高椋 利幸	佐賀大学 大学院工学系研究科	Alkali Electrolytes-Induced Phase Separation of Acetonitrile-Water Mixtures	Toshiyuki Takamuku	Saga University
172	脂質二重膜の曲げ弾性係数に対する面内ネットワーカー構造の影響	山田 悟史	高エネルギー加速器研究機構 物質構造科学研究所	Effect of network structure in lipid bilayers on bending modulus	Norifumi Yamada	KENS
173	イオン液体と界面活性剤の混合物の相分離現象	吉田 亨次	福岡大学 理学部	Phase separation of ionic liquids and surfactant mixtures	Koji Yoshida	Fukuoka University
174	中性子スピニコール法を用いたStaphylococcal nucleleaseの水溶液中のメソスコピックダイナミクス研究	遠藤 仁	日本原子力研究開発機構 量子ビーム応用研究部門	Mesoscopic Dynamics of Staphylococcal Nuclease in Aqueous Solution Investigated by Neutron Spin Echo Technique	Hitoshi Endo	Japan Atomic Energy Agency
175	F-アクチンの構造多形性と運動特性の相関Ⅱ	藤原 恒	日本原子力研究開発機構 量子ビーム応用研究部門	Relationship between the structural polymorphism and the dynamics of F-actin II	Satoru Fujiiwara	Japan Atomic Energy Agency
176	アミロイド線維形成初期過程 中間体のダイナミクスⅡ	藤原 恒	日本原子力研究開発機構 量子ビーム応用研究部門	Dynamics of the intermediate structures of the early stages of the amyloid fibril formation II	Satoru Fujiiwara	Japan Atomic Energy Agency
177	重金属イオンを選択性に認識する配位子がつくる逆ミセルの構造	鈴木 伸一	日本原子力研究開発機構 量子ビーム応用研究部門	Structure of Reverse Micelles Self-Assembled by Organic Ligands with Selective Recognition for Heavy Metal Ion.	Shinichi Suzuki	Japan Atomic Energy Agency

No.	課題名	氏名	所属	Title	Name	Organization
178	ナフイオン-膜イオンチャネル中の水分子のダイナミクス	能田 洋平	日本原子力研究開発機構 量子ビーム応用研究部門	Dynamics of water in ion-channel of Nafion	Yohei Noda	Japan Atomic Energy Agency
179	AGNES(高分解能ノバレス冷中性子分光器)IRT課題	山室 修	東京大学 物性研究所	IRT: AGNES(Angle Focusing Cold Neutron Spectrometer)	Osamu Yamamoto	The University of Tokyo
180	マルチフェロイック物質CuFe <sub>1-x</sub> MnO <sub>2</sub> (M=Al,Mn) の中性子準弾性散乱	木村 慶	東北大学 大学院工学研究科	Quasielastic neutron scattering of multiferroic CuFe <sub>1-x</sub> MnO <sub>2</sub> (M=Al,Mn)	Kei Hayashi	Tohoku University
181	非晶性高分子の分子運動に関する超臨界二酸化炭素の影響	金子 文俊	大阪大学 大学院理学研究科	Influence of supercritical carbon dioxide on dynamical properties of synthetic rubbers	Fumitoshi Kaneko	Osaka University
182	M(OH)(bdc)R(M = Fe, Al, bdc = terephthalate, R = NH <sub>2</sub> , OH, (COOH) <sub>2</sub> )配位高分子の酸発生基によるプロトン伝導性の制御	北川 宏	京都大学 大学院理学研究科	Control of Proton Conductivity in Porous Coordination Polymers, M(OH)(bdc)R(M = Fe, Al, bdc = terephthalate, R = NH <sub>2</sub> , OH, (COOH) <sub>2</sub> )	Hiroshi Kitagawa	Kyoto University
183	中性子準弾性散乱によるアルキルイミダゾリウム系イオン液体におけるアルキル鎖運動の系統的研究	古府 麻衣子	東京大学 物性研究所	Systematic QENS study on dynamics of alkyl-chain in alkylimidazolium ionic liquids	Maiko Kofu	The University of Tokyo
184	メタノール水溶液における疎水性水とによる分子の拡散遅延効果	丸山 健二	新潟大学 理学部	The retardation effect of hydrophobic hydration on diffusion dynamics of water molecules in methanol aqueous solution	Kenji Martiyama	Niigata University
185	有機無機ハイブリッドソーラースリカラ中に閉じ込めた水とメタノールのダイナミクス	山口 敏男	福岡大学 理学部	Dynamics of water and methanol confined in organic-inorganic hybrid mesoporous silica	Toshio Yamaguchi	Fukuoka University
186	規則構造型メソポーラスカーボン中に閉じ込めた分子液体のダイナミクス	山口 敏男	福岡大学 理学部	Dynamics of molecular liquids confined in ordered mesoporous carbon	Toshio Yamaguchi	Fukuoka University
187	両性イオングリシンの水利構造とダイナミクス	山室 憲子	東京電機大学 理工学部	Dynamics and hydration structures of aqueous solutions of zwitterionic glycine	Noriko Yamamoto	Tokyo Denki University
188	逆浸透膜表面における水のダイナミクス	山室 修	東京大学 物性研究所	Dynamics of water on surface of reverse osmosis membranes	Osamu Yamamoto	The University of Tokyo
189	MINEI(京大炉:多層膜中性子干渉計・反射率) IRT課題	日野 正裕	京都大学 原子炉実験所	IRT: MINE(Multilayer Interferometer and Refractometer for Neutron) 1	Masahiro Hino	Kyoto University
190	2次元中性子集光デバイスの開発	日野 正裕	京都大学 原子炉実験所	Development of 2D focusing supermirror device	Masahiro Hino	Kyoto University
191	MIEZE分光法を用いた量子井戸滞在時間の実時間測定	日野 正裕	京都大学 原子炉実験所	Direct measurement of dwell time in quasi-bound state by mean of MIEZE spectroscopy	Masahiro Hino	Kyoto University
192	中性子スピinn位相イメージングを用いた電流分布の可視化 III	田崎 誠司	京都大学 大学院工学研究科	Visualization of electric current distribution using neutron spin phase imaging III	Seiji Tasaki	Kyoto University
193	冷中性子による全断面積測定	田崎 誠司	京都大学 大学院工学研究科	Measurement of total cross section for cold neutron	Seiji Tasaki	Kyoto University
194	中性子スピinn位相コントラスト法による磁気ヒステリシス分布可視化技術の開発	林田 洋寿	日本原子力研究開発機構 J-PARCセンター	Development of imaging technique of magnetic hysteresis distribution with neutron spin phase contrast method	Hirotoshi Hayashida	Japan Atomic Energy Agency

No.	課題名	氏名	所属	Title	Name	Organization
195	MINE2(京大炉)・多層膜中性子干渉計・反射率 計) IRT課題	日野 正裕	京都大学	原子炉実験所	Masahiro Hino	Kyoto University
196	水と接触した多層積層高分子電解質膜の凝集状 態	藤井 義久	九州大学	大学院工学研 究院	Yoshihisa Fujii	Kyushu University
197	経路を完全分離するJamin型冷中性子干渉計の 開発と応用	舟橋 春彦	京都大学	高等教育研究 開発推進機構	Haruhiko Funahashi	Kyoto University
198	2次元中性子集光デバイスの開発	日野 正裕	京都大学	原子炉実験所	Masahiro Hino	Kyoto University
199	MIEZE分光法を用いた量子井戸滯在時間の実時 間測定	日野 正裕	京都大学	原子炉実験所	Masahiro Hino	Kyoto University
200	中性子反射率法による潤滑下摩擦低減のための 金属基板上シリマーブラシ層の膜厚・密度測定	平山 朋子	同志社大学	理工学部	Tomoko Hirayama	Doshisha University
201	中性子反射率法による強水性表面上におけるア ルカン分子の密度測定	平山 朋子	同志社大学	理工学部	Tomoko Hirayama	Doshisha University
202	中性子反射率法による各種DLC被膜／潤滑油界 面の構造解析	平山 朋子	同志社大学	理工学部	Tomoko Hirayama	Doshisha University
203	中性子反射率によるポリメチルメタクリレート薄膜 におけるガラス転移温度の分布	井上 倫太郎	京都大学	化学研究所	Rintaro Inoue	Kyoto University
204	ディップコート薄膜の熱的物性	井上 倫太郎	京都大学	化学研究所	Rintaro Inoue	Kyoto University
205	超冷中性子光学系のためのデバイス開発	北口 雅曉	京都大学	原子炉実験所	Masaaki Kitaguchi	Kyoto University
206	高分子／水界面領域におけるタンパク質吸着状態 に関する研究	松野 寿生	九州大学	大学院工学研 究院	Hisao Matsuno	Kyushu University
207	イオン液体／固体界面におけるイオン多層構造 の中性子反射率測定による研究	西 直哉	京都大学	大学院工学研 究科	Naoya Nishi	Kyoto University
208	偏極超冷中性子輸送ガイドの開発	川崎 真介	京都大学	高エネルギー加 速器研究機構	Kawasaki Shinsuke	KEK
209	混合液体と接触した高分子界面の凝集状態	田中 敬二	九州大学	素粒子原子核 研究所	Keiji Tanaka	Kyushu University
210	中性子スピinn位相イメージングを用いた電流分布 の可視化 III	田崎 誠司	京都大学	大学院工学研 究科	Seiji Tasaki	Kyoto University
211	多層膜冷中性子干渉計による重力起因位相の精 密測定	閑 義穂	理化学研究所	Precision measurement of gravitationally induced phase with multilayer cold neutron interferometer	Yoshihiko Seki	RIKEN

No.	課題名	氏名	所属	Title	Name	Organization
212	HQR(高分解能中性子散乱装置)IRT課題	吉沢 英樹	東京大学 物性研究所	IRT: HQR(High Q Resolution Triple Axis Spectrometer)	Hideki Yoshizawa	The University of Tokyo
213	新規T'構造銅酸化物 $\text{Pr}_{2-x}\text{Ca}_x\text{CuO}_4$ における磁気相関のホールード一効果	藤田 全基	東北大學 金属材料研究所	Hole-doping effect on spin correlations in a new cuprate oxide of T'-structured $\text{Pr}_{2-x}\text{Ca}_x\text{CuO}_4$	Masaki Fujita	Tohoku University
214	$\text{EuCo}_2\text{P}_2$ の磁気構造解析	藤原 哲也	山口大学 大学院理工学研究科	Magnetic structure analysis of $\text{EuCo}_2\text{P}_2$	Tetsuya Fujiwara	Yamaguchi University
215	重い電子系新物質 $\text{Ce}_2\text{Pt}_3\text{Ge}_5$ の磁気構造解析	藤原 哲也	山口大学 大学院理工学研究科	Magnetic structure analysis of new heavy fermion material $\text{Ce}_2\text{Pt}_3\text{Ge}_5$	Tetsuya Fujiwara	Yamaguchi University
216	$\text{EuRu}_2\text{P}_2$ の磁気構造解析	藤原 哲也	山口大学 大学院理工学研究科	Magnetic structure analysis of $\text{EuRu}_2\text{P}_2$	Tetsuya Fujiwara	Yamaguchi University
217	フラストレート強磁性鎖におけるスピinn・ネマティック相関の検出	益田 隆嗣	東京大学 物性研究所	Detection of spin nematic correlation in frustrated ferromagnetic chain	Takatsugu Masuda	The University of Tokyo
218	磁性イオン置換によりフラストレーションを制御したスピinn誘導型強誘電体 $\text{CuFeO}_2$	満田 節生	東京理科大学 理学部	Cross-correlation in spin-driven ME multiferroic $\text{CuFeO}_2$ with Mn-magnetic doping	Setsuo Mitsuuda	Tokyo University of Science
219	スピnn格子結合系 $\text{CuFeO}_2$ のスピnn波分散関係の一軸応力変化	満田 節生	東京理科大学 理学部	Spin wave dispersion relation in a spin-lattice coupled system $\text{CuFeO}_2$ under uni-axial stress	Setsuo Mitsuuda	Tokyo University of Science
220	スピnn誘導型強誘電体 $\text{CuFeO}_2$ における磁気ビエゾ効果	満田 節生	東京理科大学 理学部	spin-mediated piezoelectric effect in spin-driven magneto-electric multiferroic $\text{CuFeO}_2$	Setsuo Mitsuuda	Tokyo University of Science
221	時間分割中性子散乱測定による磁気構造変化過程の美時間追跡	元屋 清一郎	東京理科大学 工学部	Real-time observation of magnetic structural change by means of time-resolved neutron scattering experiments	Kiyoichiro Motoya	Tokyo University of Science
222	磁気構造の長時間変化と磁性原子希釈効果	元屋 清一郎	東京理科大学 工学部	Dilution effect of magnetic atoms on the long-time variation of magnetic structure	Kiyoichiro Motoya	Tokyo University of Science
223	多段メタ磁性体 $\text{Ca}_3\text{C}_{20}\text{O}_6$ における磁気構造の長時間変化へのdisorderの効果	茂吉 武人	東京理科大学 工学部	Effect of Disorder on the Long-Time Variation of Magnetic Structure in a Multistep Metamagnet $\text{Ca}_3\text{C}_{20}\text{O}_6$	Taketo Moyoshi	Tokyo University of Science
224	マルチフェロイック $\text{CuFeO}_2$ における2軸圧力による磁気・強誘電ドメイン配向制御	中島 多朗	東京理科大学 理学部	Biaxial-pressure control of multiferroic domain structure in spin-driven ME multiferroic $\text{CuFeO}_2$	Taro Nakajima	Tokyo University of Science
225	三角格子反強磁性体 $\text{CuCrO}_2$ 磁性と誘電性に対する一軸圧力効果	中島 多朗	東京理科大学 理学部	Uniaxial pressure effect on magnetic and dielectric properties of a triangular lattice antiferromagnet $\text{CuCrO}_2$	Taro Nakajima	Tokyo University of Science
226	$\text{CeTe}_3$ および $\text{TbTe}_3$ における量子臨界現象および磁性と超伝導の相関の研究	佐藤 慧昭	名古屋大学 大学院理学研究科	Study on the quantum criticality and correlation of magnetism and superconductivity in $\text{CeTe}_3$ and $\text{TbTe}_3$	Noriaki Sato	Nagoya University
227	$\text{Rb}_2\text{MoO}_4$ における多形転移とソフトフォノン	重松 宏武	山口大学 教育学部	Polymorph Transition and Soft Phonon in $\text{Rb}_2\text{MoO}_4$	Hirotake Shigematsu	Shimane University
228	強誘電体の相転移機構(変位型及び秩序無秩序型)に関する統一的理理解立	重松 宏武	山口大学 教育学部	Establishment of the unified explanation about the phase transition mechanism (displacive and order-disorder type) in Ferroelectrics	Hirotake Shigematsu	Shimane University

No.	課題名	氏名	所属	Title	Name	Organization
229	PrRh <sub>2</sub> Ge <sub>2</sub> の逐次磁気転移	繁岡 透	山口大学 大学院理工学 研究科	Successive magnetic transitions of PrRh <sub>2</sub> Ge <sub>2</sub>	Toru Shigeoka	Yamaguchi University
230	成分分離逐次磁気転移の研究	繁岡 透	山口大学 大学院理工学 研究科	Study of component s-separated magnetic transition	Toru Shigeoka	Yamaguchi University
231	秩序型ペロブスカイトCaCu <sub>3</sub> Ti <sub>4</sub> O <sub>12</sub> のフォノン	留野 泉	秋田大学 教育文化学部	Phonons in ordered perovskite CaCu <sub>3</sub> Ti <sub>4</sub> O <sub>12</sub>	Izumi Tomono	Akita University
232	立方晶BaTiO <sub>3</sub> のフォノンの温度依存性	留野 泉	秋田大学 教育文化学部	Temperature dependence of phonons in cubic BaTiO <sub>3</sub>	Izumi Tomono	Akita University
233	混晶系Ba <sub>1-x</sub> Ca <sub>x</sub> TiO <sub>3</sub> のフォノン	留野 泉	秋田大学 教育文化学部	Phonons in (Ba,Ca)TiO <sub>3</sub>	Izumi Tomono	Akita University
234	FeTe <sub>1-x</sub> Se <sub>x</sub> 系のフォノン	留野 泉	秋田大学 教育文化学部	Phonons in FeTe <sub>1-x</sub> Se <sub>x</sub>	Izumi Tomono	Akita University
235	マレチフェロイック物質YBaCuFeO <sub>5</sub> の非自明な磁気構造	安井 幸夫	名古屋大学 大学院理学研 究科	Non-trivial Magnetic Structure of Multiferroic System YBaCuFeO <sub>5</sub>	Yukio Yasui	Nagoya University
236	ダブルペロブスカイト酸化物Sr <sub>2</sub> YRuO <sub>6</sub> およびSr <sub>2</sub> CrNbO <sub>6</sub> の磁気構造	安井 幸夫	名古屋大学 大学院理学研 究科	Magnetic Structure of double perovskite oxides Sr <sub>2</sub> YRuO <sub>6</sub> and Sr <sub>2</sub> CrNbO <sub>6</sub>	Yukio Yasui	Nagoya University
237	逐次相転移を示した三角格子物質Co <sub>2</sub> (OD) <sub>3</sub> Brのプラストレーシヨン磁性とスピinningsらぎ	算 旭光	佐賀大学 大学院工学系 研究科	Study of the frustrated magnetism and spin fluctuations in triangular-lattice Co <sub>2</sub> (OD) <sub>3</sub> Br	Xu-Guang Zheng	Saga University
238	atacamite型四面体構造Mn <sub>2</sub> (OD) <sub>3</sub> Cl, Mn <sub>2</sub> (OD) <sub>3</sub> Br のスピinningsらぎ	鄭 旭光	佐賀大学 大学院工学系 研究科	Investigation of spin fluctuations in atacamite-type pyrochlore compounds Mn <sub>2</sub> (OD) <sub>3</sub> Cl and Mn <sub>2</sub> (OD) <sub>3</sub> Br	Xu-Guang Zheng	Saga University
239	空間反転対称性を欠く系CeNiC <sub>2</sub> の複雑な磁気構造	片野 遼	埼玉大学 大学院理工学 研究科	Complex magnetic structures of the non-centrosymmetric system CeNiC <sub>2</sub>	Susumu Katano	Saitama University
240	三角格子系Na <sub>x</sub> NiO <sub>2</sub> の磁気構造	茂吉 武人	東京理科大学 理工学部	Magnetic structure of a triangular system Na <sub>x</sub> NiO <sub>2</sub>	Taketo Moyoshi	Tokyo University of Science
241	TbCu <sub>2</sub> Si <sub>2</sub> の複雑な磁気相図	繁岡 透	山口大学 大学院理工学 研究科	Complex magnetic phase diagrams of TbCu <sub>2</sub> Si <sub>2</sub>	Toru Shigeoka	Yamaguchi University
242	NdCoO <sub>3</sub> の格子ダイナミックス	留野 泉	秋田大学 教育文化学部	Lattice dynamics of NdCoO <sub>3</sub>	Izumi Tomono	Akita University
243	(Sr,Ca)V <sub>2</sub> O <sub>3</sub> のフォノン	留野 泉	秋田大学 教育文化学部	Phonons in (Sr,Ca)V <sub>2</sub> O <sub>3</sub>	Izumi Tomono	Akita University
244	中性子回折を用いたNd <sub>5</sub> Ge <sub>3</sub> における磁場誘起非可逆反強磁性強磁性転移後の研究Ⅱ	萬岡 孝則	広島大学 大学院教育学 研究科	Neutron diffraction studies for Magnetic field induced irreversible antiferromagnetic to ferrimagnetic transition in Nd <sub>5</sub> Ge <sub>3</sub> II	Takanori Tsuruoka	Hiroshima University
245	10GPa級中性子散乱実験用圧力発生装置の開発	上床 美也	東京大学 物性研究所	Development of high pressure apparatus for elastic neutron scattering experiments	Yoshiya Uwاتoko	The University of Tokyo

No.	課題名	氏名	所属	Title	Name	Organization
246	AKANE(東北大企研:三触型中性子分光器)IRT 課題	大山 研司	東北大 金属材料研究所	IRT: AKANE(Advanced Kinken Neutron Spectrometer)	Kenji Ohoyama	Tohoku University
247	高エネルギー磁気励起測定によるBi2201の磁気 励起分散の研究	榎木 勝徳	九州工業大学 大学院工学研究 院	Study of magnetic excitation dispersion in Bi2201 by measurement of high-energy excitation	Masanori Enoki	Kyushu Institute of Technology
248	高精度測定によるFe-LSCOの異方的磁気秩序 ピーカーの起原の研究	藤田 全基	東北大 金属材料研究所	Origin of anisotropic magnetic peak in Fe-LSCO studied with high resolution measurement	Masaki Fujita	Tohoku University
249	反強磁性金属Mn <sub>3</sub> Siにおける高温スピント励起	平賀 晴弘	東北大 金属材料研究所	High-temperature spin excitations in antiferromagnetic metal Mn <sub>3</sub> Si	Haruhiro Hiraka	Tohoku University
250	高い反強磁性転移温度をもつ鉄系化合物 T <sub>1</sub> Fe <sub>2</sub> Se <sub>2</sub> の磁性	飯久保 智	九州工業大学 大学院生命体 工学生理科	Neutron scattering study of high temperature anti-ferromagnet T <sub>1</sub> Fe <sub>2</sub> Se <sub>2</sub>	Satoshi Ikubo	Kyushu Institute of Technology
251	マルチフェロイック物質(Bi,Eu)Mn <sub>2</sub> O <sub>5</sub> )の圧力誘起 磁気秩序と強誘電性	木村 宏之	東北大 多元物質科学 研究所	Pressure induced magnetic order and ferroelectricity in multiferroic (Bi,Eu)Mn <sub>2</sub> O <sub>5</sub>	Hiroyuki Kimura	Tohoku University
252	マルチフェロイックBiMn <sub>2</sub> O <sub>4</sub> の非磁性不純物置換 による強誘電性と磁性の制御	木村 宏之	東北大 多元物質科学 研究所	Control of ferroelectricity and magnetism by non-magnetic impurity substitution in Multiferroic BiMn <sub>2</sub> O <sub>5</sub>	Hiroyuki Kimura	Tohoku University
253	MPO <sub>4</sub> (M:遷移金属) のカイラル磁気構造の検証	高阪 勇輔	青山学院大学 理工学部	Chiral Magnetism in MPO <sub>4</sub> (M: Transition Metal)	Yusuke Kousaka	Aoyama-Gakuin University
254	CrX (Cr=Si, Ge) のカイラル磁気構造の検証	高阪 勇輔	青山学院大学 理工学部	Chiral Magnetic Structure in CrX (X=Si, Ge)	Yusuke Kousaka	Aoyama-Gakuin University
255	幾何学的フラストレート系(Mn,Mg)Cr <sub>2</sub> O <sub>4</sub> における らせん磁気構造のクロスオーバー	高阪 勇輔	青山学院大学 理工学部	Crossover between conical and screw magnetic phase in (Mn,Mg)Cr <sub>2</sub> O <sub>4</sub>	Yusuke Kousaka	Aoyama-Gakuin University
256	Mn <sub>2</sub> Sbのスピinn揺らぎの研究	小山 佳一	鹿児島大学 大学院理工学 研究科	Experimental study of spin fluctuation on Mn <sub>2</sub> Sb	Keiichi Koyama	Kagoshima University
257	Ce <sub>0.5</sub> La <sub>0.5</sub> B <sub>6</sub> における磁気ハバード子秩序の検証	松村 武	広島大学 大学院先端物 質科学研究所	Magnetic Octupole Order in Ce <sub>0.5</sub> La <sub>0.5</sub> B <sub>6</sub>	Takeshi Matsumura	Hirosshima University
258	高温超伝導体LSCOの磁気励起における磁性不 純物Ni置換効果の研究II	松浦 直人	東北大 金属材料研究所	Investigation of Ni-impurity doping effect on magnetic excitations in high-T <sub>c</sub> superconductor LSCO II	Masato Matsutara	Tohoku University
259	極低温単結晶中性子回折によるYbPdの磁気構 造および金属的電荷秩序の検証	光田 瞳弘	九州大学 大学院理学研究 院	Study on metallic charge order of YbPd by single-crystal neutron diffraction at lowest temperature	Akihiro Mitsuda	Kyushu University
260	磁場中中性子回折によるYbPdの金属的電荷秩 序構造の研究	光田 瞳弘	九州大学 大学院理学研究 院	Study on metallic charge order in YbPd by neutron diffraction in a magnetic field	Akihiro Mitsuda	Kyushu University
261	HERMES(東北大企研:中性子粉末回折装置) IRT課題	大山 研司	東北大 金属材料研究所	IRT: HERMES(Kinken Powder Diffractometer for High Efficiency and High Resolution MEasurementS)	Kenji Ohoyama	Tohoku University
262	希土類遷移金属複合化物の磁気構造	土井 貴弘	北海道大学 大学院理学研究 院	Magnetic structure of lanthanide transition metal oxides	Yoshihiro Doi	Hokkaido University

No.	課題名	氏名	所属	Title	Name	Organization
263	二オブ極リチウム型構造をもつ遷移金属酸化物の磁気構造	藤田 晃司	京都大学 大学院工学研究科	Magnetic structure of transition metal oxides with lithium niobate-type structure	Koji Fujita	Kyoto University
264	擬一次元鎖フラストレート磁性体SrCo <sub>2</sub> V <sub>2</sub> O <sub>8</sub> の中性子回折	萩原 雅人	東京大学 物性研究所	Neutron diffraction of quasi-1D frustrated magnetism SrCo <sub>2</sub> V <sub>2</sub> O <sub>8</sub>	Masato Hagihara	The University of Tokyo
265	(Bi,Na)(Ti,Nb,Ta)O <sub>3</sub> 系無鉛圧電セラミックスの結晶構造に与える分極処理の影響	ヰ手本 康	東京理科大学 理工学部	Effect of poling process on crystal structure of (Bi,Na)(Ti,Nb,Ta)O <sub>3</sub> -based lead-free piezoelectric ceramics	Yasushi Idemoto	Tokyo University of Science
266	近藤合金Yb <sub>1-x</sub> Tm <sub>x</sub> B <sub>6</sub> の低温磁気秩序構造	伊賀 文俊	茨城大学 理学部	Magnetic structure of Kondo alloy Yb <sub>1-x</sub> Tm <sub>x</sub> B <sub>6</sub> at low temperatures	Fumitoshi Iga	Ibaraki University
267	高い保磁力を有する水素化FeCoナノ粒子の結晶構造	飯久保 智	九州工業大学 大学院生命体工学科研究科	Crystal structure of a hydrogenated FeCo nano-particle with high coercive force	Satoshi Iikubo	Kyushu Institute of Technology
268	ペロブスカイト型チタン酸水素化物の構造	陰山 洋	京都大学 大学院工学研究科	The structure of perovskite type titanium oxyhydride	Hiroshi Kageyama	Kyoto University
269	層間酸素を含んだ鉄平面4配位酸化物	陰山 洋	京都大学 大学院工学研究科	Square Planar Iron Oxide with Apical Oxygen	Hiroshi Kageyama	Kyoto University
270	異常高原子価鉄を持つ(Ba,Sr)FeO <sub>3</sub> の磁気構造と相対界の解明	陰山 洋	京都大学 大学院工学研究科	Investigation for Magnetic Structure and Phase Boundary of (Ba,Sr)FeO <sub>3</sub> with an Unusually High Valence State of Iron	Hiroshi Kageyama	Kyoto University
271	混晶系マルチフェロイクス(1-x)BiFeO <sub>3-x</sub> PbTiO <sub>3</sub> のMPB相近傍の結晶構造と磁気構造	木村 宏之	東北大学 多元物質科学研究所	Crystal and magnetic structure in MPB phase of multiferroic composite (1-x)BiFeO <sub>3-x</sub> PbTiO <sub>3</sub>	Hiroyuki Kimura	Tohoku University
272	(CuCl)LaNb <sub>2</sub> O <sub>7-x</sub> F <sub>x</sub> の構造決定	小林 洋治	京都大学 大学院工学研究科	Structural determination of (CuCl)LaNb <sub>2</sub> O <sub>7-x</sub> F <sub>x</sub>	Yoji Kobayashi	Kyoto University
273	チタン酸化物のマグネシウム還元	小林 洋治	京都大学 大学院工学研究科	Reduction of titanates with Mg	Yoji Kobayashi	Kyoto University
274	新規カイラル磁性体MPO <sub>4</sub> (M: 遷移金属)の磁気構造解析	高阪 勇輔	青山学院大学 理工学部	Magnetic Structure Analysis in New Chiral Magnetic Compounds MPO <sub>4</sub> (M: Transition Metal)	Yusuke Kousaka	Aoyama-Gakuin University
275	新規カイラル磁性体Cr <sub>2</sub> Geの磁気構造解析	高阪 勇輔	青山学院大学 理工学部	Magnetic Structure Analysis in New Chiral Magnetic Compounds Cr <sub>2</sub> Ge	Yusuke Kousaka	Aoyama-Gakuin University
276	電子ドープ型マンガン酸化物の磁化の反転と磁気構造	松川 倫明	岩手大学 工学部	Magnetization reversal and magnetic structure in electron doped manganites	Michiaki Matsukawa	Iwate University
277	高温超伝導体LSCOの格子における磁性不純物N置換効果の研究	松浦 直人	東北大学 金属材料研究所	Investigation of Ni-impurity doping effect on crystal structure in high-T <sub>c</sub> superconductor LSCO	Masato Matsubara	Tohoku University
278	極低温粉末中性子回折によるYbPdの磁気構造および金属的電荷秩序の検証	光田 晃弘	九州大学 大学院理学研究院	Study on metallic charge order of YbPd by powder neutron diffraction at lowest temperature	Akihiro Mitsuda	Kyushu University
279	二層三角格子反強磁性体Fe <sub>2</sub> Ga <sub>5</sub> S <sub>5</sub> の結晶構造と磁気構造	南部 雄亮	東京大学 物性研究所	Crystal and magnetic structures of the bilayer triangular antiferromagnet Fe <sub>2</sub> Ga <sub>5</sub> S <sub>5</sub>	Yusuke Nambu	The University of Tokyo

No.	課題名	氏名	所属	Title	Name	Organization
280	錯 $\text{Li}_2\text{S} = 3/2$ 三角格子反強磁性体の結晶構造と磁気構造	南部 雄亮	東京大学 物性研究所	Crystal and magnetic structures of a new $S = 3/2$ triangular antiferromagnet	Yusuke Nambu	The University of Tokyo
281	反強磁性三量体2b $3\text{CuCl}_2 \cdot 2\text{H}_2\text{O}$ の磁気構造	佐藤 車	東京大学 物性研究所	Magnetic Structure of Antiferromagnetic Trimer 2b $3\text{CuCl}_2 \cdot 2\text{H}_2\text{O}$	Taku J Sato	The University of Tokyo
282	リチウムイオンを含む新規複合酸化物の合成と結晶構造解析	單 躍進	宇都宮大学 大学院工学研究科	Synthesis and crystal structure analysis of a novel multiple oxide with lithium and tellurium	Yue Jin Shan	Utsunomiya University
283	次世代固体照明用セリウムシリコンナイトライド系螢光体におけるサイト選択性の解明	末廣 隆之	東北大学 多元物質科学研究所	Analyses of site preference in cerium silicon nitride phosphors for solid-state lighting	Takayuki Suehiro	Tohoku University
284	新しいタイプの偏壓電子フラストレート磁性体 $\text{Fe}_3\text{W}_6\text{C}$ における非磁気的秩序相	田畠 吉計	京都大学 大学院工学研究科	Non-magnetic ordered states in novel itinerant-electron frustrated magnets $\text{Fe}_3\text{W}_6\text{C}$	Yoshikazu Tabata	Kyoto University
285	層状金属硫化物 $\text{Co}_x\text{NbS}_2\sigma$ の結晶構造と磁気構造	高橋 美和子	筑波大学 大学院数理物質科学研究生科	Crystal and magnetic structures of $\text{Co}_x\text{NbS}_2\sigma$	Miwako Takahashi	University of Tsukuba
286	酸素空孔をもつ $\text{CaWO}_4$ 系酸化物イオン伝導体の欠陥構造	高井 茂臣	鳥取大学 大学院工学研究科	Defect Structure of $\text{CaWO}_4$ -based O <sub>x</sub> ice Ion Conductor with Oxygen Vacancies	Shigeomi Takai	Tottori University
287	スピ-2電極目格子反強磁性体 $\text{Cs}_2\text{LiMn}_3\text{F}_{12}$ の基底状態	田中 秀数	東京工業大学 大学院理工学研究科	Ground state of spin-2 kagome-lattice antiferromagnet $\text{Cs}_2\text{LiMn}_3\text{F}_{12}$	Hidekazu Tanaka	Tokyo Institute of Technology
288	クロム複硫化物の結晶構造と磁気転移	手塚 勝太郎	宇都宮大学 大学院工学研究科	Crystal Structures and Magnetic Transitions of Chromium Complex Sulfides	Keitaro Tezuka	Utsunomiya University
289	金属絶縁体転移を示す導電性プラスチート系 $\text{R}_2\text{Ir}_2\text{O}_7$ における磁気構造と内部磁場の研究	富安 啓輔	東北大学 大学院理学研究科	Magnetic structure and internal magnetic field in conductive frustrated system $\text{R}_2\text{Ir}_2\text{O}_7$ with metal-insulator transition	Keisuke Tomiyasu	Tohoku University
290	層状鉄オキシカルコゲナイトの磁気構造	分島 亮	北海道大学 大学院理学研究科	Magnetic structures of layered iron oxyhalogenides	Makoto Wakeshima	Hokkaido University
291	巨大な負の熱膨張を示すペロブスカイトの結晶・磁気構造解説	山田 紗也	愛媛大学 大学院理工学研究科	Crystal and Magnetic Structure Analysis of Perovskites Showing Giant Negative Thermal Expansion	Ikuuya Yamada	Ehime University
292	イミダゾリウム系イオン液体の短・中距離構造	山室 修	東京大学 物性研究所	Short- and intermediate-range structures of imidazolium-based ionic liquids	Osamu Yamamoto	The University of Tokyo
293	鉛フリー圧電体ニオブ酸鉄系材料の結晶構造と誘電性	八島 正知	東京工業大学 大学院理工学研究科	Crystal structure and dielectric properties of Pb-free piezoelectric silver niobate-based materials	Masatomo Yashima	Tokyo Institute of Technology
294	層状ペロブスカイト型酸化物の結晶構造とイオン拡散経路	八島 正知	東京工業大学 大学院理工学研究科	Crystal structure and ion conduction pathway of layered perovskite-type oxides	Masatomo Yashima	Tokyo Institute of Technology
295	格子間離素を利用したイオン伝導性セラミックスの結晶構造とイオン拡散経路	八島 正知	東京工業大学 大学院理工学研究科	Crystal structure and diffusion pathway of oxide ions in ionic conducting ceramics via interstitial oxide ions	Masatomo Yashima	Tokyo Institute of Technology
296	排ガス浄化触媒の構造物性	八島 正知	東京工業大学 大学院理工学研究科	Crystal structure catalysts correlation of exhaust gas catalysts	Masatomo Yashima	Tokyo Institute of Technology

No.	課題名	氏名	所属	Title	Name	Organization
297	可視光応答型酸塗化物光触媒の構造物性	八島 正知	東京工業大学 大学院理工学 研究科	Structure–property correlation of visible-light responsive metal–oxynitride photocatalysts	Masatomo Yashima	Tokyo Institute of Technology
298	新しい三角格子系物質M(OD)X [M:Cu,Ni,Co etc; X:Cl,Br,I] の幾何学的(フラストレーシヨン)磁性と磁気構造の解明	佐賀 大学	大学院工学系 研究科	Study of geometric frustration in a new triangular lattice series compounds M(OD)X[M:Cu,Ni,Cu etc; X:Cl,Br,I]	Xu-Guang Zheng	Saga University
299	三角格子系水酸化物M <sub>2</sub> (OD) <sub>3</sub> X[M:Cu,Ni,Cu etc; X:Cl,Br,I] の幾何学的(フラストレーシヨン)磁性と磁気構造の解明 II	佐賀 大学	大学院工学系 研究科	Study of geometric frustration in triangular-lattice M <sub>2</sub> (OD) <sub>3</sub> X[M:Cu,Ni,Cu etc; X:Cl,Br,I] II	Xu-Guang Zheng	Saga University
300	リチウムイオン電池材料の粉末中性子回折	木嶋 優人	産業技術総合 研究所	Neutron Powder Diffraction Studies of Lithium-ion Battery materials	Norihito Kijima	National Institute of Advanced Industrial Science and Technology
301	鉄系超伝導体の結晶構造と超伝導の相關	李 哲虎	産業技術総合 研究所	Relationship between crystal structure and superconductivity in Fe-based superconductors	Chul-Ho Lee	National Institute of Advanced Industrial Science and Technology
302	白金含有ペロブスカイト酸化物の中性子回折測定	野村 勝裕	産業技術総合 研究所	Neutron diffraction study of platinum containing perovskite oxides	Katsuhiro Nomura	National Institute of Advanced Industrial Science and Technology
303	電子ドープVO <sub>2</sub> の磁気構造解析	奥山 大輔	理化学研究所	Magnetic structure analysis on electron-doped VO <sub>2</sub>	Daisuke Okuyama	RIKEN
304	FONDER(中性子4軸回折装置)IRT課題	野田 幸男	東北大学 多元物質科学 研究所	IRT: FONDER(Four-circle-Off-center-type Neutron Diffractometer)	Noda Yukio	Tohoku University
305	マルチフェロイック物質(Bi,Eu)Mn <sub>2</sub> O <sub>5</sub> の圧力誘起磁気秩序と強誘電性	木村 宏之	東北大学 多元物質科学 研究所	Pressure induced magnetic order and ferroelectricity in multiferroic (Bi,Eu)Mn <sub>2</sub> O <sub>5</sub>	Hiroyuki Kimura	Tohoku University
306	マルチフェロイックBMn <sub>2</sub> O <sub>5</sub> の非磁性不純物置換による強誘電性と磁性の制御	木村 宏之	東北大学 多元物質科学 研究所	Control of ferroelectricity and magnetism by non-magnetic impurity substitution in Multiferroic BMn <sub>2</sub> O <sub>5</sub>	Hiroyuki Kimura	Tohoku University
307	塑性歪みを加えたPt <sub>3</sub> Feの反強磁性体における強磁性の発現機構	小林 恒	岩手大学 工学部	Mechanism of ferromagnetism in plastically deformed Pt <sub>3</sub> Fe antiferromagnet	Satoru Kobayashi	Iwate University
308	KH <sub>2</sub> AsO <sub>4</sub> の低温構造と相転移	増山 博行	山口大学 大学院理工学 研究科	Low Temperature Structure and the Phase Transition of KH <sub>2</sub> AsO <sub>4</sub>	Hiroyuki Mashiyama	Yamaguchi University
309	アルカリ超酸化物KO <sub>2</sub> の磁気構造	益田 隆嗣	東京大学 物性研究所	Magnetic structure of Alkali superoxide KO <sub>2</sub>	Takatsugu Masuda	The University of Tokyo
310	磁性イオン置換によりスピinnプラストレーションを制御したスピノン誘導型強誘電体CuFeO <sub>2</sub> (4軸)	溝田 節生	東京理科大学 理学部	Magnetic structures in spin frustration system CuFeO <sub>2</sub> with magnetic doping	Setsuo Mitsuda	Tokyo University of Science
311	三角格子反強磁性体CuCrO <sub>2</sub> 磁性と誘電性に対する一軸圧力効果(4軸)	中島 多朗	東京理科大学 理学部	Effect of uniaxial pressure on a triangular lattice antiferromagnet CuCrO <sub>2</sub> (4-circle neutron diffraction)	Taro Nakajima	Tokyo University of Science
312	マルチフェロイック物質Ca <sub>2</sub> Fe <sub>1.5</sub> Al <sub>0.5</sub> O <sub>5</sub> の磁気構造の解明	佐賀山 基	東京大学 大学院新領域 創成科学研究科	Study of magnetic structure in multiferroic material Ca <sub>2</sub> Fe <sub>1.5</sub> Al <sub>0.5</sub> O <sub>5</sub>	Hajime Sagayama	The University of Tokyo
313	二糖類水和物の結晶構造	高橋 美和子	筑波大学 大学院数理物 質科学研究所	Crystal structure of hydrate disaccharide	Miwako Takahashi	University of Tsukuba

No.	課題名	氏名	所属	Title	Name	Organization
314	Pt(1-x)Mn <sub>x</sub> (x=0.11~0.14)の規則構造と磁性	高橋 美和子	筑波大学 大学院数理物質科学研究所	Structure and magnetism in Pt(1-x)Mn <sub>x</sub> (x=0.11~0.14)	Miwako Takahashi	University of Tsukuba
315	I型クラスレートにおける非調和熱振動	金子 耕士	日本原子力研究開発機構 量子ビーム応用研究部門	Anharmonic thermal motion in type I clathrate compounds	Koji Kaneko	Japan Atomic Energy Agency
316	$\beta$ -ペイロクロア化合物における非調和熱振動	金子 耕士	日本原子力研究開発機構 量子ビーム応用研究部門	Anharmonic thermal motion in beta-pyrochlore compounds	Koji Kaneko	Japan Atomic Energy Agency
317	アクセサリー-IRT課題	上床 美也	東京大学 物性研究所		Yoshiya Uwatoko	The University of Tokyo

# 平成24年度 共同利用課題一覧(後期) Joint Research List (2012 Latter Term)

## 嘱託研究員 (Commission Researcher)

No.	課題名	氏名	所属	Title	Name	Organization
1	$^3\text{He}$ - $^4\text{He}$ 希臘冷凍機を用いた走査トンネル顕微鏡の改良と極低温スピノン偏極STMの開発	河江 達也	九州大学 大学院工学研究院	Development of very Low-temperature spin-polarized STM with a $^3\text{He}$ - $^4\text{He}$ dilution refrigerator	Tatsuya Kawai	Kyushu University
2	二次元超伝導の渦糸に関する理論研究	林 伸彦	大阪府立大学	Theoretical study on vortices in two-dimensional superconductors	Nobuhiko Hayashi	Osaka Prefecture University
3	低温スピノン偏極走査トンネル顕微鏡の開発	山田 豊和	千葉大学	Development of spin-polarized scanning tunneling microscope at low temperatures	Toyokazu Yamada	Chiba University
4	表面薄膜超伝導体の探索	坂本 一之	千葉大学	Search for surface/thin film superconductors	Kazuyuki Sakamoto	Chiba University
5	極性結晶のイオン散乱分光	大西 剛	物質・材料研究機構	International Collaborative Research Project on Ion scattering spectroscopy of polar crystals	Tsuyoshi Ohnishi	National Institute for Materials Science
6	AgPdCu合金圧力セルを用いた磁場中比熱測定	河江 達也	九州大学 大学院工学研究院	Development of pressure cell for specific heat measurements under magnetic field	Tatsuya Kawai	Kyushu University
7	有機伝導体の圧力効果	村田 恵三	大阪市立大学 大学院理学研究科	Effect of pressure on the organic conductor	Keizo Murata	Osaka City University
8	多重極限関連装置の調整	高橋 博樹	日本大学 文理学部	Adjustment of Cubic Anvil apparatus	Hiroki Takahashi	Nihon University
9	C化合物の単結晶試料評価とその圧力効果	藤原 哲也	山口大学 大学院理工学研究科	Effect of Pressure on the Ce Compounds	Tetsuya Fujiiwara	Yamaguchi University
10	磁性体の圧力効果	巨海 玄道	久留米工業大学	Effect of pressure on the Magnetic Materials	Gendo Oomi	Kurume Institute of Technology
11	圧力下NMR測定法に関する開発	藤原 直樹	京都大学 大学院人間・環境学研究科	Development of NMR measurement method under high pressure	Naoki Fujiwara	Kyoto University
12	新しい122化合物の単結晶成長の試みと圧力効果	池田 伸一	産業技術総合研究所 ナノエレクトロニクス研究部門	Pressure effect of new materials	Shinichi Ikeda	National Institute of Industrial Science and Technology
13	中性子回折に用いる圧力装置の開発	片野 進	埼玉大学 大学院理工学研究科	Developments of high pressure cell for neutron diffraction	Susumu Katano	Saitama University
14	第一次元有機物質の圧力下物性研究	糸井 充徳	日本大学 医学部	Study on pressure induced superconductivity of quasi organic conductor	Miho Itoi	Nihon University
15	高压下の比熱測定装置の開発	樋原 出	横浜国立大学 工学部	Development of apparatus for specific heat measurements under high pressure	Izuru Umemura	Yokohama National University

No.	課題名	氏名	所属	Title	Name	Organization
16	NiCrAlを用いた圧力装置の開発	松本 武彦	物質・材料研究機構	The development of the pressure equipment using NiCrAl	Tsukehiko Matsumoto	National Institute for Materials Science
17	磁化測定装置の開発	名嘉 節	物質・材料研究機構	Development of the magnetometer	Takashi Naka	National Institute for Materials Science
18	3d遷移金属化合物の圧力下における磁気特性	鹿又 武	東北学院大学	Investigation of magnetic properties for 3d transition intermetallic compounds under pressure	Takeshi Kanomata	Tohoku Gakuin University
19	重い電子系物質における圧力下電気抵抗測定	礒田 誠	香川大学 教育学部	Effect of Pressure on the Electrical Resistivity of Heavy Fermi Compounds	Makoto Isoda	Kagawa University
20	テラヘルツパルス電磁波によるスピinn秩序の制御の研究	中嶋 誠	千葉大学 理学部	Study of spin order control by pulsed terahertz radiation	Makoto Nakajima	Chiba University
21	高温超伝導体の高分解能光電子分光	藤森 淳	東京大学 大学院理学系研究科	Ultra-high resolution photoemission spectroscopy on high Tc superconductor	Atsushi Fujimori	The University of Tokyo
22	60-eVレーザーを用いた時間分解光電子分光の開発	石坂 香子	東京大学 大学院工学系研究科	The development of time-resolved photoemission using 60eV laser	Kyoko Ishizaka	The University of Tokyo
23	鉄系超伝導体のレーザー光電子分光	下志万 貴博	東京大学 大学院工学系研究科	Laser-ARPES on Fe superconductor	Takahiro Shimojima	The University of Tokyo
24	鉄ニクタードの高分解能光電子分光	吉田 鉄平	東京大学 大学院理学系研究科	Ultra-high resolution photoemission spectroscopy on Fe-based superconductor	Teppei Yoshida	The University of Tokyo
25	B系超伝導体の角度分解光電子分光	竹内 恒博	名古屋大学 エコトピア科学研究所	Angle-resolved photoemission study on high Tc cuprate	Tsunehiro Takeuchi	Nagoya University
26	光電子分光法を用いた各種分子性結晶の電子状態の研究及び装置の低温化	木須 孝幸	大阪大学 大学院基礎工学研究科	Research on electron state of molecular crystals using photoemission spectroscopy	Takayuki Kisu	Osaka University
27	高分解能光電子分光による強相關物質の研究	横谷 尚陸	岡山大学 大学院自然科学研究科	ultra-high resolution study on strongly correlated materials	Takayoshi Yokoya	Okayama University
28	酸化バナジウムの高分解能光電子分光	江口 律子	岡山大学 大学院自然科学研究科	Photoemission study on vanadium oxides	Ritsuko Eguchi	Okayama University
29	有機化合物の光電子分光	金井 要	東京理科大学 理工学部	Photoemission study on organic compounds	Kaname Kanai	Tokyo University of Science
30	準結晶の高分解能光電子分光	田村 隆治	東京理科大学 基礎工学部	High-resolution photoemission study on quasi crystals	Ryuji Tamura	Tokyo University of Science
31	重い電子系ラン化合物の高分解能光電子分光	藤森 伸一	日本原子力研究開発機構 量子ビーム応用部門	Ultra high resolution photoemission study on heavy fermion uranium compounds	Shinichi Fujimori	Japan Atomic Energy Agency
32	レーザーPEEMによる磁性体の研究	小野 寛太	高エネルギー加速器研究機構 物質構造科学研究所	Study on magnetism by laser PEEM	Kanta Ono	High Energy Accelerator Research Institute

No.	課題名	氏名	所属	Title	Name	Organization
33	レーザー光電子分光による酸化物薄膜の研究	津田 後輔	物質・材料研究機構 若手国際研究拠点	Laser-Photoemission Study on Oxide Films	Shunsuke Tsuda	National Institute for Materials Science
34	4f電子系物質の高分解能光電子分光	松波 雅治	自然科学研究機構 分子科学研究所	Photoemission study on 4f materials	Masaharu Matsunami	Institute for Molecular Science
35	超高空間分解能光電子顕微鏡による磁区構造観察	中川 剛志	自然科学研究機構 分子科学研究所	Observation of magnetic domain structures by ultra-high resolution photoemission electron microscopy	Takeshi Nakagawa	Institute for Molecular Science
36	Mn化合物の時間分解光電子分光	大川 万里生	東京理科大学 理学部	Time resolved Photoemission on Mn compounds	Mario Okawa	Tokyo University of Science
37	時間分解光電子分光による重い電子系の研究	関山 明	大阪大学 大学院基礎工学科研究科	Study on heavy Fermion materials by time-resolved Photoemission	Akira Sekiyama	Osaka University
38	高分解能光電子分光による酸化バナジウムの研究	藤原 秀紀	大阪大学 大学院基礎工学科研究科	Study on vanadium oxides by high resolution Photoemission	Hidenori Fujjwara	Osaka University
39	鉄シリコンのFe2性光電子分光の研究	中村 元彦	奈良教育大学 理科教育講座	Study of circular dichroism of photoemission on FeSi	Motohiko Nakamura	Nara University of Education
40	角度分解光電子分光法による遷移金属酸化物の表面/界面電子状態の研究	吉松 公平	東京大学 大学院理学系 研究科	Angle-resolved photoemission study of the interfacial states of transition-metal oxides	Kohei Yoshimatsu	The University of Tokyo
41	X線回折法による表面近傍の半導体微小格子ひずみ解析に関する研究	秋本 見一	日本女子大学 理学部	Analysis of strain field near the surface of semiconductors by surface-sensitive x-ray diffraction	Koichi Akitomo	Japan Women's University
42	高輝度放射光軟X線を用いた時間分解光電子分光による表面ダイナミクス研究	近藤 寛	慶應義塾大学 理工学部	Study of surface dynamics by time-resolved photoemission spectroscopy with high-brilliant soft x-ray synchrotron radiation	Hiroshi Kondoh	Keio University
43	軟X線アンジュレータビームラインの分光光学系の開発研究	雨宮 健太	高エネルギー加速器研究機構 物質構造科学研究所	Research and development of soft X-ray undulator beamline	Kenta Amemiya	High Energy Accelerator Research Institute
44	高輝度光源計画における直入射ビームラインおよびその利用計画の検討	伊藤 健二	高エネルギー加速器研究機構 物質構造科学研究所	Design and case study for the high-resolution atoms- and molecules-spectroscopy beamline at the Super SOR facility	Kenji Ito	High Energy Accelerator Research Institute
45	光電子スピニン検出器の開発・研究	奥田 太一	広島大学 放射光科学研究センター	Research and development of a new photoelectron spin detector	Taichi Okuda	Hirosshima University
46	光電子顕微鏡による磁性ナノ構造物質の磁化過程	木下 豊彦	高輝度光科学 研究センター	Magnetization in process of magnetic nano structure by PEEM	Toyohiko Kinoshita	Japan Synchrotron Radiation Institute
47	高輝度極紫外ビームラインの設計・評価	小野 寛太	高エネルギー加速器研究機構 物質構造科学研究所	Design and characterization of brilliance VUV beamline	Kanta Ono	High Energy Accelerator Research Institute
48	"	木村 真一	自然科学研究機構 分子科学研究所	"	Shinichi Kimura	Institute for Molecular Science
49	高輝度光源ビームラインにおける分光光学系の設計・開発	後藤 俊治	高輝度光科学 研究センター	Design of the new undulator beamline at Spring-8	Shunji Goto	Japan Synchrotron Radiation Institute

No.	課題名	氏名	所属	Title	Name	Organization
50	高輝度光源ビームラインにおける分光光学系の設計・開発	大橋 治彦	高輝度光科学 研究センター	Design of the new undulator beamline at Spring-8	Haruhiko Ohashi	Japan Synchrotron Radiation Institute
51	高輝度軟X線を利用した強相関物質の電子状態 研究	組頭 広志	高エネルギー加速器研究機構 研究所	Study of electronic states in strongly correlated materials with high brilliant soft-Xray.	Hiroshi Kumigashira	High Energy Accelerator Research Institute
52	時間分解光電子分光法による光触媒材料のキャラ クタライジング研究	小澤 健一	東京工業大学	Study of carrier dynamics in photocatalysis materials by time-resolved photoemission spectroscopy	Kenichi Ozawa	Tokyo Institute of Technology
53	軟X線時間分解分光実験による磁性研究 計・開発	木村 昭夫	広島大学	Study of magnetic properties by time-resolved soft X-ray spectroscopy	Akio Kimura	Hirosima University
54	高輝度軟X線を利用する光電子顕微鏡装置の設 計	坂本 一之	千葉大学	Research and designing of a PEEM spectrometer for high brilliance soft X ray	Kazuyuki Sakamoto	Chiba University
55	二次元表示型スピinn分解光電子エネルギー分析 器の開発	大門 寛	奈良先端科学 技術大学院大 学	Development of 2D display type spin resolved photoelectron energy analyzer	Hiroshi Daimon	Nara Institute of Science and Technology
56	軟X線吸収／発光分光法によるチカムイオン電 池電極材料の電子物性研究	朝倉 大輔	産業技術総合 研究所	Study on the electronic property of electrode materials for Li-ion batteries by soft X-ray absorption/emission spectroscopy	Daisuke Asakura	National Institute of Industrial Science and Technology
57	超高分解能軟X線発光分光による水素吸蔵合金 中の水素の波動関数の局在性に関する研究	関場 大一郎	筑波大学	Study on the localization of Wave functions of hydrogen atom in hydrogen storage alloys using ultrahigh resolution soft X-ray emission spectroscopy	Daiichiro Sekiba	University of Tsukuba
58	小型集束型小角散乱装置の高性能化及びそれ による応用研究	古坂 道弘	北海道大学	Development of a compact focusing small-angle neutron scattering instrument and application research using the instrument	Michihiro Furusaka	Hokkaido University
59	中性子極小角散乱実験装置のアップグレード	金子 純一	北海道大学	Upgrade of ULS system	Junichi Kaneko	Hokkaido University
60	中性子散乱装置FONDERのアップグレード後の 研究計画の実施と共同利用の推進	野田 幸男	東北大	Upgrading of neutron diffractometer FONDER and contributing to user collaboration program	Yukio Noda	Tohoku University
61	中性子散乱装置の共同利用・開発による強相関 電子系物質の構造物性の研究	岩佐 和晃	東北大	Structural studies of strongly correlated electron systems by neutron scattering method and instrumental development	Kazuaki Iwasa	Tohoku University
62	中性子モノクロメータの改良と中性子4軸回折計 FONDERの制御プログラムの改良	木村 宏之	東北大	Improvement of neutron monochromator and control program for four circle neutron diffractometer FONDER	Hiroyuki Kimura	Tohoku University
63	中性子散乱装置のアップグレードと共同利用研究 の推進	藤田 全基	東北大	Upgrading of the neutron scattering device and promotion of the research and public use	Masaki Fujita	Tohoku University
64	中性子散乱装置のアップグレード後の研究計画 の実施と共同利用の推進	大山 研司	東北大	Propelling the inter university research cooperation	Kenji Ohoyama	Tohoku University
65	中性子散乱装置のアップグレード後の研究計画 の実施と共同利用の推進	平賀 晴弘	東北大	Implementation of the research plan under the cooperation-use program after upgrading neutron scattering instruments	Haruhiko Hiraka	Tohoku University
66	中性子散乱装置のアップグレード後の研究計画 の実施と共同利用の推進	田畑 吉計	京都大学	Progress of the joint research by using the neutron scattering instruments	Yoshihiko Tabata	Kyoto University

No.	課題名	氏名	所属	Title	Name	Organization
67	中性子散乱装置のアップグレード後の研究計画 の実施と共同利用の推進	松村 武	広島大学 大学院先端物質科学研究所	Promotion of joint research after the upgrade of neutron scattering instruments	Takeshi Matsunura	Hiroshima University
68	J-PARC/MLFとJRR-3共存時代に向けた3軸型中性子散乱装置の高度化	松浦 直人	東北大 金属材料研究所	Upgrade of 3-axis neutron spectrometer for the oncoming coexistence of J-PARC/MLF and JRR-3	Masato Matsuura	Tohoku University
69	中性子分光器を用いた強相関電子系物質の微視的研究	桑原 慶太郎	茨城大学 大学院理工学研究科	Neutron scattering study of strongly correlated electron systems by using neutron triple-axis spectrometers	Keitaro Kuwahara	Ibaraki University
70	高度化した3軸分光器を用いた共同利用の推進 と物質科学研究の実施	横山 淳	茨城大学 理学部	Executing user program and study of material science with the advanced triple-axis spectrometers	Makoto Yokoyama	Ibaraki University
71	冷中性子スピノ干渉計の応用とMINEビームライン の整備	田崎 誠司	京都大学 大学院工学研究科	Development of cold neutron spin interferometry and improvements of MINE beam line	Seiji Tasaki	Kyoto University
72	膜貫通ペプチドのフリップフロップ誘起能の評価	中野 実	富山大学 大学院医学薬学研究部(薬学)	Induction of Phospholipid Flip-Flop by Transmembrane Peptides	Minoru Nakano	University of Toyama
73	C1-3 ULS極小角散乱装置IRT	杉山 正明	京都大学 原子炉実験所	Development of micro-focusing small-angle neutron scattering spectrometer	Masaaki Sugiyama	Kyoto University
74	集光テスト用小型SANSの開発及び冷中性子反射 率計・干渉計のアップグレード	日野 正裕	京都大学 原子炉実験所	Improvement of MIEZE spectrometer and cold neutron reflectometer and interferometer	Masahiro Hino	Kyoto University
75	"	北口 雅曉	京都大学 原子炉実験所	"	Masaaki Kitaguchi	Kyoto University
76	中性子散乱用高圧セルの開発および高圧下における中性子散乱実験	藤原 哲也	山口大学 大学院理工学研究科	Neutron Scattering Experiments under High Pressure and Development of High Pressure Cell for Neutron Scattering	Tetsuya Fujiwara	Yamaguchi University
77	流動場でのソフトマターの構造変化に関する研究	高橋 良彰	九州大学 先導物質化学研究所	Studies on structural change of soft matter under flow field	Yoshiaki Takahashi	Kyushu University
78	三軸分光器を用いた極端条件下における物質科学 学研究の実施	阿曾 尚文	琉球大学 理学部	Material science studies under extreme conditions by using triple-axis spectrometers	Naofumi Aso	University of the Ryukyus
79	非イオン界面活性剤水溶液におけるベシクル系 の高分子添加効果	川端 康平	首都大学東京 大学院理工学研究科	Effect of polymer addition to vesicles in a nonionic surfactant solution	Youhei Kawabata	Tokyo Metropolitan University
80	中性子散乱研究計画の実施と共同利用の推進	伊藤 晋一	高エネルギー加速器研究機構 理学研究所	propelling the inter university research cooperation	Shinichi Itoh	High Energy Accelerator Research Institute
81	冷中性子干渉イメージング装置開発研究	大竹 淑恵	仁科加速器センター 理学研究所	Research and Development of interferometric imaging instruments for cold neutron	Yoshie Otake	RIKEN
82	高度化した三軸分光器を用いた共同利用の推進 とスピンドライナックスの研究	佐藤 卓	東北大 多元物質科学研究所	Promoting user program and investigating spin dynamics using triple-axis spectrometers	Taku Sato	Tohoku University
83	高度化した三軸分光器を用いた強相関電子系物 質の研究	南部 雄亮	東北大 多元物質科学研究所	Study of strongly correlated electron systems using advanced triple-axis spectrometers	Yusuke Nambu	Tohoku University

No.	課題名	氏名	所属	Title	Name	Organization
84	強磁場量子ビーム科学のためのナペルスマグネットの開発	鳴海 康雄	東北大	金属材料研究所	Yasuo Narumi	Tohoku University
85	軟X線吸収／発光分光法によるリチウムイオン電池電極材料の電子物性研究	細野 英司	産業技術総合研究所	エネルギー技術研究部	Eiji Hosono	National Institute of Industrial Science and Technology
86	遷移金属化合物の結晶合成と構造特性	山浦 淳一	東京工業大学	元素戦略研究センター	Jun-ichi Yamaura	Tokyo Institute of Technology

一般研究員 (General Researcher)

No.	課題名	氏名	所属	Title	Name	Organization
1	回転超流動～リチウム3のテクスチャーダイナミクスの研究	佐々木 豊	京都大学	低温物質科学研究センター	Yutaka Sasaki	Kyoto University
2	強相関伝導系のナペルスマグ場中の超音波測定	吉澤 正人	岩手大学	大学院工学研究科	Masahito Yoshizawa	Iwate University
3	"	中西 良樹	岩手大学	大学院工学研究科	"	Iwate University
4	"	シャラムジヤンスマイ	岩手大学	大学院工学研究科	"	Iwate University
5	"	坂野 幸平	岩手大学	大学院工学研究科	"	Iwate University
6	強相関電子系化合物の秩序相に対する結晶対称性および軌道縮退の効果	横山 淳	茨城大学	理学部	Effects of crystal symmetry and orbital degeneracy in ordered states of strongly correlated electron systems	Makoto Yokoyama
7	"	石川 沙羅	茨城大学	大学院理工学研究科	"	Ibaraki University
8	固体～リチウム4の非古典的回転慣性の遮断効果	青木 悠樹	東京工業大学	大学院総合理工学研究科	Blocking effect of Non classical rotational momentum inertia for Solid Helium 4	Sara Ishikawa
9	"	岩佐 泉	神奈川大学	理学部	"	Izumi Iwasa
10	磁気フラストレートした一次元量子スピinnをもつCuO <sub>2</sub> リボン鎖系の磁場相図	安井 幸夫	明治大学	理工学部	Magnetic Phase Diagram of CuO <sub>2</sub> Ribbon Chain System with Frustrated One-Dimensional Quantum Spins	Yukio Yasui
11	重い電子系超伝導体の対称性の決定	町田 一成	岡山大学	大学院自然科学研究科	Determination of pairing symmetry in heavy fermion superconductors	Kazushige Machida
12	新しいスピinnフィルターを用いた超流動～リチウム3スビン流制御の研究	山口 明	兵庫県立大学	大学院物質学研究科	New spin filter for spin current control in superfluid helium-3	Akira Yamaguchi

No.	課題名	氏名	所属	Title	Name	Organization
13	新しいスピンドルレーターを用いた超流動ヘリウム3スビン流制御の研究	鎌田 尚史	兵庫県立大学 大学院物質理学研究科	New spin filter for spin current control in superfluid helium-3	Naofumi Kamada	University of Hyogo
14	量子スピンドルレーターTb <sub>2</sub> Ti <sub>2</sub> O <sub>7</sub> の磁化測定	高津 浩	首都大学東京 大学院理工学研究科	Magnetization measurements of the quantum spin liquid of Tb <sub>2</sub> Ti <sub>2</sub> O <sub>7</sub>	Hiroshi Takatsu	Tokyo Metropolitan University
15	"	谷口 智洋	首都大学東京 大学院理工学研究科	"	Tomohiro Taniguchi	Tokyo Metropolitan University
16	一次元フラストレート磁性体におけるSDW相関とネマティック相関の異方性	吉村 一良	京都大学 大学院理学研究科	Anisotropy of a SDW and a nematic correlations in one-dimensional frustrated magnets	Kazuyoshi Yoshimura	Kyoto University
17	"	那波 和宏	京都大学 大学院理学研究科	"	Kazuhiro Nawa	Kyoto University
18	高温高压下における石英の水素流体への溶解メカニズム	篠崎 彩子	東京大学 大学院理学研究科	Dissolution of quartz into hydrogen fluid under high pressure and temperature	Ayako Shinozaki	The University of Tokyo
19	純良化試料を用いた擬二次元磁性体Sr <sub>2</sub> VO <sub>4</sub> の磁気低温相の解明	那波 和宏	京都大学 大学院理学研究科	Investigation of a low-temperature magnetic phase in a quasi-two-dimensional magnet Sr <sub>2</sub> VO <sub>4</sub> using a purified sample	Kazuhiro Nawa	Kyoto University
20	有機薄膜の低温物性測定	鳥塚 潔	法政大学 理工学部	Measurements of Low Temperature Properties of Organic Thin Films	Kiyoshi Torizuka	Hosei University
21	有機薄膜素子の物性研究	松田 真生	熊本大学 大学院自然科学研究科	Studies on organic thin film devices	Masaki Matsuda	Kumamoto University
22	"	清島 啓太	熊本大学 大学院自然科学研究科	"	Keita Kiyoshima	Kumamoto University
23	1/4フィルド・チエッカーボードハバードモデルの基底状態相図	山下 靖文	日本大学 工学部総合教育	Ground-state phase diagram of the checkerboard Hubbard model at 1/4 filling	Yasufumi Yanashita	Nihon University
24	太陽電池応用を目指したエネルギー材料の研究	伊高 健治	弘前大学 北日本新エネルギー研究所	Research of the energy materials for solar cell application	Kenji Itaka	Hirosaki University
25	パレスレーザー堆積法による多成分系ナノ相分離酸化物薄膜の構造と物性	松本 祐司	東京工業大学 応用セラミックス研究所	Structural and material-property characterization of multi-component oxide films with nano-scale phase separation	Yuji Matsumoto	Tokyo Institute of Technology
26	Pb置換Bi2201相超伝導体のCu価数とホール濃度の精密測定	神戸 土郎	山形大学 大学院理工学研究科	Precise measurement of Cu valence and hole density for Pb-substituted Bi2201 superconductor	Shiro Kambe	Yamagata University
27	グラフィン表面の化学修飾	エムディ キール ホサイ	群馬大学 先端科学研究中心	Chemical modification of graphene	Md. Zakir Hossain	Gunma University
28	機械的応力のシリコン表面化学への影響に関する研究	成島 哲也	自然科学研究機構 分子科学研究所	Effect on Silicon Surface Chemistry under External Mechanical Stress	Tetsuya Narushima	Institute for Molecular Science
29	表面プラズモンを支持する金属単結晶表面の作成と解析(2)	渡辺 量朗	東京理科大学 大学院総合化学生物学研究科	Fabrication and analysis of single crystal metal surfaces supporting surface plasmons (2)	Kazuo Watanabe	Tokyo University of Science

No.	課題名	氏名	所属	Title	Name	Organization
30	表面プラズモンを支持する金属単結晶表面の作成と解析(2)	長井 健太	東京理科大学 大学院総合化学生物研究科	Fabrication and analysis of single crystal metal surfaces supporting surface plasmons (2)	Kenta Nagai	Tokyo University of Science
31	Al系準結晶及び近似結晶中の構造欠陥の陽電子ビーム法による分析	金沢 育三	東京学芸大学 自然科学系	Analysis of structural defects in Al based icosahedral quasicrystals and approximate crystals by slow positron beam	Ikuzo Kanazawa	Tokyo Gakugei University
32	"	齋藤 誠	東京学芸大学 大学院教育学研究科	"	Makoto Saito	Tokyo Gakugei University
33	Mo及びSiC上のエピタキシャル酸化シリコン超薄膜の作製とSTM/STS観察	柄原 浩	九州大学 大学院総合理工学研究院	Formation of an epitaxial silicon-oxide ultrathin film on Mo and SiC surfaces and STM/STS measurement	Hiroshi Tochihara	Kyushu University
34	キャリアドープがロンクラスター物質の作製と陽電子ビーム法による分析する。	金沢 育三	東京学芸大学 自然科学系	Preparing of carrier-doped Boron clusters and analysis by slow positron beam	Ikuzo Kanazawa	Tokyo Gakugei University
35	"	山田 浩平	東京学芸大学 大学院教育学研究科	"	Kouhei Yamada	Tokyo Gakugei University
36	金属／半導体表面上ナノ構造の形成とその非線形発光の時間分解測定	河村 紀一	日本放送協会 放送技術研究所	Time resolved spectroscopy of harmonics from nano-structures on Cu surfaces	Norikazu Kawamura	NHK Science and Technology Research Laboratory
37	磁性金属シリサイドの光電子分光	大野 真也	横浜国立大学 大学院工学研究科	Photoemission study of silicide of magnetic metals	Shinya Ohno	Yokohama National University
38	半導体基板上に成長したグラフェンおよびシリシングの電子物性	中辻 寛	東京工業大学 大学院総合理工学研究院	Electronic structure of graphene and silicene grown on semiconductor substrates	Kan Nakatsuji	Tokyo Institute of Technology
39	エピタキシャルシリセンの低温走査トンネル顕微鏡観察	高村 由起子	北陸先端科学技術大学院大学	Low temperature scanning tunneling microscopy investigations of epitaxial silicene	Yukiko Takamura	Japan Advanced Institute of Science and Technology
40	"	ライナー・フリードライン	北陸先端科学技術大学院大学	"	Rainer FRIEDLEIN	Japan Advanced Institute of Science and Technology
41	"	アントワーヌ・フロランス	北陸先端科学技術大学院大学	"	Antoine FLEURENCE	Japan Advanced Institute of Science and Technology
42	(Ho,Gd)Rh <sub>2</sub> Si <sub>2</sub> 単結晶の磁気転移	繁岡 透	山口大学 大学院理工学研究科	Magnetic transitions of (Ho,Gd)Rh <sub>2</sub> Si <sub>2</sub> single crystal	Toru Shigeoka	Yamaguchi University
43	"	大河原 遊	山口大学 大学院理工学研究科	"	Yu Okawara	Yamaguchi University
44	CeTeにおける圧力誘起四極子秩序と近藤効果	松村 武	広島大学 大学院先端物質科学研究科	Pressure induced quadrupole order and Kondo effect in CeTe	Takeshi Matsumura	Hirosima University
45	"	林 佑弥	広島大学 大学院先端物質科学研究科	"	Yuya Hayashi	Hirosima University
46	Dy <sub>2</sub> Ti <sub>2</sub> O <sub>7</sub> のスピンドイナミクスと磁気モノポール	高津 浩	首都大学東京 大学院理工学研究科	Spin dynamics and magnetic monopole in Dy <sub>2</sub> Ti <sub>2</sub> O <sub>7</sub>	Hirosi Takatsu	Tokyo Metropolitan University

No.	課題名	氏名	所属	Title	Name	Organization
47	Dy <sub>2</sub> Ti <sub>2</sub> O <sub>7</sub> のスピンドライナミクスと磁気モノポール	後藤 和基	首都大学東京 大学院理工学 研究科	Spin dynamics and magnetic monopole in Dy <sub>2</sub> Ti <sub>2</sub> O <sub>7</sub>	Kazuki Goto	Tokyo Metropolitan University
48	EuRu <sub>2</sub> P <sub>2</sub> の高圧力下磁化測定	藤原 哲也	山口大学 大学院理工学 研究科	Magnetization measurements under high pressures in EuRu <sub>2</sub> P <sub>2</sub>	Tetsuya Fujiiwara	Yamaguchi University
49	"	廣田 裕也	山口大学 大学院理工学 研究科	"	Yuya Kurata	Yamaguchi University
50	HoRh <sub>2</sub> Si <sub>2</sub> の単結晶育成	藤原 哲也	山口大学 大学院理工学 研究科	Single crystal growth of HoRh <sub>2</sub> Si <sub>2</sub>	Tetsuya Fujiiwara	Yamaguchi University
51	"	長谷川 貴大	山口大学 大学院理工学 研究科	"	Takahiro Hasegawa	Yamaguchi University
52	Mn <sub>2-x</sub> Co <sub>x</sub> Sbの高圧下磁気緩和	小山 佳一	鹿児島大学 大学院理工学 研究科	Magnetic relaxation in Mn <sub>2-x</sub> Co <sub>x</sub> Sb under high pressure	Keiichi Koyama	Kagoshima University
53	"	折橋 広樹	鹿児島大学 大学院理工学 研究科	"	Hiroki Orihashi	Kagoshima University
54	セリウム系磁性超伝導体における微小磁気モーメントの圧力下磁化測定II	阿曾 尚文	琉球大学 理学部	Magnetization studies under pressure in Ce-based magnetic superconductors with small magnetic moments II	Naofumi Aso	University of the Ryukyus
55	"	田中 秀和	琉球大学 大学院理工学 研究科	"	Hidekazu Tanaka	University of the Ryukyus
56	ホイスラー化合物Fe <sub>2</sub> MnSiの圧力下電気抵抗率	伊藤 昌和	鹿児島大学 大学院理工学 研究科	Transport properties of Heusler alloy Fe <sub>2</sub> MnSi under pressure.	Masakazu Ito	Kagoshima University
57	圧力下での磁気および電荷移動が生み出すEu化合物の新しい電子状態の探索	杉山 清寛	大阪大学 大学院理学研 究科	Investigation of exotic electronic properties of Eu compounds driven by magnetic and valence fluctuation under high pressure	Kiyohiro Sugiyama	Osaka University
58	"	大貫 憲陸	琉球大学 理学部	"	Yoshichika Onuki	University of the Ryukyus
59	圧力下での磁気および電荷移動が生み出すEu化合物の新しい電子状態の探索	本多 史憲	東北大学 金属材料研究 所	Investigation of exotic electronic properties of Eu compounds driven by magnetic and valence fluctuation under high pressure	Fuminori Honda	Tohoku University
60	"	廣瀬 雄介	新潟大学 大学院自然科 学研究科	"	Yusuke Hirose	Niigata University
61	"	森 晶宣	大阪大学 大学院理学研 究科	"	Akinobu Mori	Osaka University
62	圧力下磁場中点接合分光実験の試み	本山 岳	兵庫県立大学 大学院物質理 学研究科	Development of a new method of Point-Contact-Spectroscopy under pressure	Gaku Motoyama	University of Hyogo
63	"	大刀掛 勇哉	兵庫県立大学 大学院物質理 学研究科	"	Yuya Tachikake	University of Hyogo

No.	課題名	氏名	所属	Title	Name	Organization
64	偏数転移及び価数秩序を示すEu化合物の高压下物性	光田 晴弘	九州大学 大学院理学研究科	Physical properties under high pressure of Eu compounds performing valence transition and valence ordering	Akihiro Mitsuda	Kyushu University
65	"	眞鍋 栄樹	九州大学 大学院理学府	"	Shigeki Manabe	Kyushu University
66	偏数振動物質の高压力中輸送特性の研究	仲間 隆男	琉球大学 理学部	Transport properties of valence fluctuation compounds	Takao Nakama	University of the Ryukyus
67	"	仲村 愛	琉球大学 大学院理工学研究科	"	Ai Nakamura	University of the Ryukyus
68	"	平仲 裕一	琉球大学 大学院理工学研究科	"	Yuichi Hirahaka	University of the Ryukyus
69	希土類化合物における低温物性の圧力効果	中野 智仁	新潟大学 工学部	Pressure effect of low-temperature properties of the rare-earth compound.	Tomohito Nakano	Niigata University
70	"	武田 大地	新潟大学 大学院自然科学研究科	"	Daichi Takeda	Niigata University
71	希土類金属間化合物の高压下における磁性ヒューリズム特性	仲間 隆男	琉球大学 理学部	Magnetism and transport properties of rare-earth intermetallic compounds under high pressure	Takao Nakama	University of the Ryukyus
72	"	内間 清晴	沖縄キリスト教短期大学 総合教育系	"	Kiyoharu Nakama	Okinawa Christian Junior College
73	"	照屋 淳志	琉球大学 大学院理工学研究科	"	Atsushi Teruya	University of the Ryukyus
74	強磁性Ce化合物の高压下における量子臨界点の探索	杉山 清寛	大阪大学 大学院理学研究科	Investigation of a quantum critical point of ferromagnetic Ce compound under high pressure	Kiyohiro Sugiyama	Osaka University
75	"	大貫 憲陸	琉球大学 理学部	"	Yoshichika Onuki	University of the Ryukyus
76	"	本多 史憲	東北大 金属材料研究所	"	Fuminori Honda	Tohoku University
77	"	廣瀬 雄介	新潟大学 大学院自然科学研究科	"	Yusuke Hirose	Niigata University
78	"	石田 一裕	大阪大学 大学院理学研究科	"	Kazuhiro Ishida	Osaka University
79	強相関型セリウム化合物および合金の量子相転移と磁性	村山 茂幸	室蘭工業大学 大学院工学研究科	Quantum phase transition and magnetism in the strongly correlated Ce compounds and alloys	Shigeyuki Murayama	Muroran Institute of Technology
80	"	雨海 有佑	室蘭工業大学 大学院工学研究科	"	Yusuke Amakai	Muroran Institute of Technology

No.	課題名	氏名	所属	Title	Name	Organization
81	複合バンドギャップ半導体FeSb <sub>2</sub> の高圧下精密磁化測定	小山 基一	鹿児島大学 大学院理工学研究科	Precise magnetization measurement of narrow-gap semiconductor FeSb <sub>2</sub> under high pressure	Keiichi Koyama	Kagoshima University
82	"	出口 拓也	鹿児島大学 大学院理工学研究科	"	Takuya Deguchi	Kagoshima University
83	空間反転対称性のないCeTSi <sub>3</sub> (T=Rh,Ir)の圧力下電気抵抗II	阿曾 尚文	琉球大学 理学部	Electrical resistivity under pressure of non-centrosymmetric magnetic superconductors CeTSi <sub>3</sub> (T=Rh,Ir) II	Naofumi Aso	University of the Ryukyus
84	"	高江洲 義尚	沖縄キリスト教短期大学	"	Yoshinao Takaesu	Okiawa Christian Junior College
85	"	田中 秀和	琉球大学 大学院理工学研究科	"	Hidekazu Tanaka	University of the Ryukyus
86	固体ヘリウムの超流動的挙動に対する回転効果	白濱 圭也	慶應義塾大学 理工学部	Rotation Effect on Supersolid Behavior of Solid <sup>4</sup> He	Keiya Shirahama	Keio University
87	"	高橋 大輔	足利工業大学 共通課程	"	Daisuke Takahashi	Ashikaga Institute of Technology
88	"	立木 智也	慶應義塾大学 大学院理工学研究科	"	Tomoya Tsuiki	Keio University
89	磁化測定用対抗アンビル型高圧力発生装置の開発	藤原 哲也	山口大学 大学院理工学研究科	Development of opposed-anvil type high pressure apparatus for magnetization measurement	Tetsuya Fujiwara	Yamaguchi University
90	"	長谷川 貴大	山口大学 大学院理工学研究科	"	Takahiro Hasegawa	Yamaguchi University
91	充填スッテルダイト化合物LaFe <sub>4</sub> P <sub>12</sub> における超伝導の圧力効果	関根 ちひろ	室蘭工業大学 大学院工学研究科	Pressure Effect of Superconductivity on Filled Skutterudite LaFe <sub>4</sub> P <sub>12</sub>	Chihiro Sekine	Muroran Institute of Technology
92	"	川村 幸裕	室蘭工業大学 大学院工学研究科	"	Yukihiro Kawamura	Muroran Institute of Technology
93	"	川合 拓馬	室蘭工業大学 大学院工学研究科	"	Takuma Kawai	Muroran Institute of Technology
94	重い電子系物質における <sup>3</sup> He温度領域での磁化測定	河江 達也	九州大学 大学院工学研究院	Magnetization measurements in <sup>3</sup> He temperature region for heavy fermion systems	Tatsuya Kawai	Kyushu University
95	"	佐藤 由昌	九州大学 大学院工学府	"	Yoshiaki Sato	Kyushu University
96	新規希土類化合物の作成と圧力下物性	中野 智仁	新潟大学 工学部	Magnetic properties under pressure of the new rare earth compound	Tomohito Nakano	Niigata University
97	"	青山 悠司	新潟大学 自然科学大学院研究科	"	Yuji Aoyama	Niigata University

No.	課題名	氏名	所属	Title	Name	Organization
98	層状有機物質(BPDT-TTF) <sub>2</sub> I <sub>3</sub> の超高圧下新電子相探索	谷口 弘三	埼玉大学 大学院理工学研究科	Search for novel electronic phase in a layered organic material, (BPDT-TTF) <sub>2</sub> I <sub>3</sub> under ultra-high pressure	Hironi Taniguchi	Saitama University
99	"	新川 貴晃	埼玉大学 大学院理工学研究科	"	Takaaki Shinkawa	Saitama University
100	導電性ランギュア・ブロジェット膜の高圧下の電気的性質に関する研究	三浦 康弘	桐蔭横浜大学 大学院工学研究科	Studies on Electrical Properties of Conductive Langmuir-Blodgett Films under High Pressure	Yasuhiro Miura	Toin University of Yokohama
101	超流動ヘリウム3-A相の新奇渦状態の探索	石川 修六	大阪市立大学 大学院理学研究科	Investigation of novel quantum vortex of superfluid <sup>3</sup> He-A	Osamu Ishikawa	Osaka City University
102	"	國松 貴之	大阪市立大学 大学院理学研究科	"	Takayuki Kunitatsu	Osaka City University
103	空間反転対称を持つない炭化物CeNiC <sub>2</sub> の圧力下での磁気秩序の安定性	片野 進	埼玉大学 大学院理工学研究科	Stability of magnetic ordering of the non-centrosymmetric carbide CeNiC <sub>2</sub> under high pressure	Susumu Katano	Saitama University
104	角度分析板厚と空間解像度に関する理論・実験研究	安藤 正海	東京理科大学 総合研究機構	Theoretical and Experimental Study on Relation between Thickness of Laue Angle Analyzer and Spatial Resolution	Masami Ando	Tokyo University of Science
105	高N濃度(In)GaAsN系混晶薄膜の構造解析(4)	窪谷 茂幸	東京大学 大学院新領域創成科学研究所	Structural analysis of higher-N-content (In)GaAsN films (4)	Shigeyuki Kuboya	The University of Tokyo
106	歪み半導体の表面近傍の歪み量の精密測定	武田 さくら	奈良先端科学技術大学院大学 物質創成科学研究所	Precise measurement of Strain beneath the surface of strained semiconductors	Sakura Takeda	Nara Institute of Science and Technology
107	窒素デルタープGaAs中の等電子トライプかきのつ発光の光子相関測定	矢口 裕之	埼玉大学 大学院理工学研究科	Photon correlation measurement of luminescence from isoelectronic traps in nitrogen delta-doped GaAs	Hiroyuki Yaguchi	Saitama University
108	"	高宮 健吾	埼玉大学 大学院理工学研究科	"	Kengo Takamiya	Saitama University
109	"	吉田 直史	埼玉大学 大学院理工学研究科	"	Naofumi Yoshida	Saitama University
110	新規遷移金属炭化物の高圧合成と物性評価	丹羽 健	名古屋大学 大学院理工学研究科	High pressure synthesis and characterization of new transition metal carbides	Ken Niwa	Nagoya University
111	正20面体準結晶およびその近似結晶の磁性	廣戸 孝信	東京理科大学 大学院基礎工学研究科	Magnetic properties of icosahedral quasicrystals and their approximants	Takanobu Hiroto	Tokyo University of Science
112	超高压プレスを用いた新規プロトニクス酸化物のソフト化学的合成法の検討	山口 周	東京大学 大学院工学系研究科	Oxide-Protonics materials synthesis by combined use of soft chemical method and high pressure	Shu Yamaguchi	The University of Tokyo
113	"	三好 正悟	東京大学 大学院工学系研究科	"	Shogo Miyoshi	The University of Tokyo
114	"	田中 和彦	東京大学 大学院工学系研究科	"	Kazuhiko Tanaka	The University of Tokyo

No.	課題名	氏名	所属	Title	Name	Organization
115	超高压プレスを用いた新規プロトニクス酸化物のソフト化学的合成法の検討	ドロクサリブル ラス ティシナル	東京大学 大学院工学系 研究科	Oxide-Protonics materials synthesis by combined use of soft chemical method and high pressure	Doloksaribu Rolas Timbul	The University of Tokyo
116	超伝導を示すAs系充填スクッテルダイト化合物の探索	関根 ちひろ	室蘭工業大学 大学院工学研 究科	Search for As-based filled-skutterudite compounds show superconductivity	Chihiro Sekine	Muroran Institute of Technology
117	超伝導を示すAs系充填スクッテルダイト化合物の探索	川田 友和	室蘭工業大学 大学院工学研 究科	Search for new rare-earth pnictides with cage-like structure	Tomokazu Kawada	Muroran Institute of Technology
118	溶融亜鉛メッキ合金相の応力誘起変態	山口 周	東京大学 大学院工学系 研究科	Stress-induced phase transformation of Fe-Zn alloy formed in hot-dip process	Shu Yamaguchi	The University of Tokyo
119	"	三好 正悟	東京大学 大学院工学系 研究科	"	Shogo Miyoshi	The University of Tokyo
120	"	田中 和彦	東京大学 大学院工学系 研究科	"	Kazuhiko Tanaka	The University of Tokyo
121	イオン交換性層状酸化物を基にしたアモルファス酸化物の合成とキャラクタリゼーション	小林 洋治	京都大学 大学院工学研 究科	Synthesis and Characterization of Amorphous Oxides Based on Ion-exchangeable Layered Oxides	Yoji Kobayashi	Kyoto University
122	"	スボード ガネ サン ポッティ	京都大学 大学院工学研 究科	"	Subodh Ganesan Potti	Kyoto University
123	"	淺井 啓	京都大学 大学院工学研 究科	"	Kei Asai	Kyoto University
124	高品質単結晶中性子モノクロメータの開発	平賀 晴弘	東北大学 金属材料研究 所	Development of high-quality, single-crystal neutron monochromator	Haruhiro Hiraka	Tohoku University
125	三角スピンドループのスピンドライナミクス	真中 浩貴	鹿児島大学 大学院理工学 研究科	Spin dynamics of triangular spin tubes	Hirotaka Manaka	Kagoshima University
126	中性子散乱研究用大型単結晶試料の結晶性評価	阿曾 尚文	琉球大学 理学部	Crystal Quality Evaluation of large single crystals for neutron scattering	Naofumi Aso	University of the Ryukyus
127	電荷注入された低次元量子スピinn系の結晶育成とその評価	横尾 哲也	高エネルギー加速器研究機構 物質構造科学 研究所	Single crystal growth and physical properties of charge induced low dimensional quantum spin systems	Tetsuya Yokoo	High Energy Accelerator Research Institute
128	通歴反強磁性体Ni(SSe) <sub>2</sub> における磁気励起スペクトラムの研究	松浦 直人	東北大学 金属材料研究 所	Study of spin fluctuations in the itinerant antiferromagnet Ni(SSe) <sub>2</sub>	Masato Matsura	Tohoku University
129	Tb <sub>2</sub> (Sn <sub>1-x</sub> Ti <sub>x</sub> ) <sub>2</sub> O <sub>7</sub> におけるスピinn液体状態の研究	門脇 広明	首都大学東京 大学院理工学 研究科	Spin liquid state in Tb <sub>2</sub> (Sn <sub>1-x</sub> Ti <sub>x</sub> ) <sub>2</sub> O <sub>7</sub>	Hiroaki Kadokawa	Tokyo Metropolitan University
130	"	松澤 光司	首都大学東京 大学院理工学 研究科	"	Koji Matsuzawa	Tokyo Metropolitan University
131	Tb <sub>2</sub> Ti <sub>2</sub> O <sub>7</sub> における量子スピinn液体状態の研究	門脇 広明	首都大学東京 大学院理工学 研究科	Quantum spin liquid in Tb <sub>2</sub> Ti <sub>2</sub> O <sub>7</sub>	Hiroaki Kadokawa	Tokyo Metropolitan University

No.	課題名	氏名	所属	Title	Name	Organization
132	Tb <sub>2</sub> Ti <sub>2</sub> O <sub>7</sub> における量子スピinn液体状態の研究	谷口 智洋	首都大学東京 大学院理工学 研究科	Quantum spin liquid in Tb <sub>2</sub> Ti <sub>2</sub> O <sub>7</sub>	Tomohiro Taniguchi	Tokyo Metropolitan University
133	重い電子系新物質Ce <sub>2</sub> Pt <sub>3</sub> Ge <sub>5</sub> の比熱測定	藤原 哲也	山口大学 大学院理工学 研究科	Specific heat measurement in new heavy fermion system Ce <sub>2</sub> Pt <sub>3</sub> Ge <sub>5</sub>	Tetsuya Fujiiwara	Yamaguchi University
134	"	廣田 裕也	山口大学 大学院理工学 研究科	"	Yuya Kurata	Yamaguchi University
135	多形性化合物TbIr <sub>2</sub> Si <sub>2</sub> の磁気転移	繁岡 透	山口大学 大学院理工学 研究科	Magnetic transition of polymorphic compounds TbIr <sub>2</sub> Si <sub>2</sub>	Toru Shigeoka	Yamaguchi University
136	"	大河原 遼	山口大学 大学院理工学 研究科	"	Yu Okawara	Yamaguchi University
137	鉄系超伝導体111系の比熱測定	佐藤 車	東北大学 多元物質科学 研究所	Specific heat measurement of the 111 systems among iron-based superconductors	Taku Sato	Tohoku University
138	鉄系超伝導体Fe <sub>1+y</sub> Te <sub>1-x</sub> S <sub>x</sub> における酸素中アーニルによる物性変化	矢口 宏	東京理科大学 理工学部	Progress of physical property by annealing in Fe-based superconductor in Fe <sub>1+y</sub> Te <sub>1-x</sub> S <sub>x</sub>	Hiroshi Yaguchi	Tokyo University of Science
139	"	山崎 照夫	東京理科大学 理工学部	"	Teruo Yamazaki	Tokyo University of Science
140	"	櫻井 辰弥	東京理科大学 大学院理工学 研究科	"	Tatsuya Sakurai	Tokyo University of Science
141	HoRh <sub>2</sub> Si <sub>2</sub> 単結晶における磁化の角度依存	繁岡 透	山口大学 大学院理工学 研究科	Angular dependence of magnetization on a HoRh <sub>2</sub> Si <sub>2</sub> single crystal	Toru Shigeoka	Yamaguchi University
142	"	長谷川 貴大	山口大学 大学院理工学 研究科	"	Takahiro Hasegawa	Yamaguchi University
143	クロミック化合物の結晶粒径と磁気的性質の相関	浅野 貴行	九州大学 大学院理学研 究院	Correlation between grain size and magnetic property in chromic compound	Takayuki Asano	Kyushu University
144	"	福井 博章	九州大学 大学院理学府	"	Hiroaki Fukui	Kyushu University
145	パルス強磁場下における比熱測定技術の開発	稻垣 祐次	九州大学 大学院工学研 究院	Specific heat measurements under pulsed high magnetic field	Yujii Imagaki	Kyushu University
146	ホイスラー化合物Ru <sub>2-x</sub> Fe <sub>x</sub> CrSiの強磁場磁化	廣井 政彦	鹿児島大学 大学院理工学 研究科	Magnetization of Heusler compounds Ru <sub>2-x</sub> Fe <sub>x</sub> CrSi in high magnetic field	Masahiko Hiroi	Kagoshima University
147	缶数据動Eu化合物の強磁場磁化過程	光田 晃弘	九州大学 大学院理学研 究院	Magnetization in a pulsed magnetic field of valence fluctuating Eu compounds	Akihiro Mitsuda	Kyushu University
148	"	浜野 車	九州大学 大学院理学府	"	Suguru Hamano	Kyushu University

No.	課題名	氏名	所属	Title	Name	Organization
149	希土類金属間化合物の強磁場物性研究	海老原 孝雄	静岡大学 理学部	Physical Phenomena at high magnetic fields in rare earth intermetallic compounds	Takao Ebihara	Shizuoka University
150	"	中井 裕人	静岡大学 大学院理学研究科	"	Hirohito Nakai	Shizuoka University
151	幾何学的フラストレート磁性体の磁化研究	菊池 彦光	福井大学 大学院工学研究科	Magnetization of the geometrically frustrated magnets	Hikomitsu Kikuchi	University of Fukui
152	"	藤井 裕	福井大学 遠赤外領域開発研究センター	"	Yutaka Fujii	University of Fukui
153	"	高田 晋弥	福井大学 大学院工学研究科	"	Shinya Takada	University of Fukui
154	強磁場を用いたトポロジカル絶縁体の輸送特性に関する研究	柏木 隆成	筑波大学 数理物質系	Study of the transport properties of topological insulator under high magnetic fields.	Takanari Kashiwagi	University of Tsukuba
155	"	鈴木 悠介	筑波大学 大学院数理物質科学研究所	"	Yusuke Suzuki	University of Tsukuba
156	金属ナノクラスターネットワークの磁気抵抗測定	稻田 貢	関西大学 システム理工学部	Electronic transport properties of metal cluster networks under high-magnetic field	Mitsuru Inada	Kansai University
157	"	小川 智矢	関西大学 大学院理工学研究科	"	Tomoya Ogawa	Kansai University
158	金属ナノクラスターの磁化測定	稻田 貢	関西大学 システム理工学部	Magnetic properties of metal nano-clusters under high magnetic field	Mitsuru Inada	Kansai University
159	"	吉原 義浩	関西大学 大学院理工学研究科	"	Yoshihiro Yoshihara	Kansai University
160	新規フッ化物ラストレート磁性体の強磁場磁性	植田 浩明	京都大学 大学院理学研究科	Magnetism of novel frustrated magnetic fluorides under very strong magnetic field	Hiroaki Ueda	Kyoto University
161	"	原口 祐哉	京都大学 大学院理学研究科	"	Yuya Haraguchi	Kyoto University
162	複合極限装置のためのワイドボアハルスマグネットの開発	萩原 政幸	大阪大学 極限量子科学研究中心	Development of a wide-bore pulse magnet for experimental apparatus used under multiple extreme conditions	Masayuki Hagiwara	Osaka University
163	"	谷口 一也	大阪大学 極限量子科学研究中心	"	Kazuya Taniguchi	Osaka University
164	通歴電子メタ磁性体SrCo <sub>2</sub> P <sub>2</sub> 周辺物質の強磁场測定	道岡 千城	京都大学 大学院理学研究科	High field magnetization of the itinerant electron metamagnet SrCo <sub>2</sub> P <sub>2</sub> and its family compounds	Chihiro Michioka	Kyoto University
165	"	小林 健太郎	京都大学 大学院理学研究科	"	Shintaro Kobayashi	Kyoto University

No.	課題名	氏名	所属	Title	Name	Organization
166	偏極電子メタ磁性体Sr <sub>2</sub> Co <sub>3</sub> P <sub>2</sub> 周辺物質の強磁场測定	今井 正樹	京都大学 大学院理学研究科	High field magnetization of the itinerant electron metamagnet SrCo <sub>2</sub> P <sub>2</sub> and its family compounds	Masaki Imai	Kyoto University
167	LaCoO <sub>3</sub> 系の強磁场誘起スピン転移の研究	佐藤 桂輔	茨城工業高等専門学校	High-Field Induced Spin State Transition in Co perovskite	Keisuke Sato	Ibaraki National College of Technology
168	GaAsNの電子輸送特性およびバンド構造の解明	稻垣 充	豊田工業大学 大学院工学研究科	Clarification of electron transport property and band structure of GaAsN	Makoto Inagaki	Toyota Technological Institute
169	コバルト酸化物の磁気形状記憶効果	佐藤 桂輔	茨城工業高等専門学校	Magnetic shape memory effect in cobalt oxide	Keisuke Sato	Ibaraki National College of Technology
170	ペイクロア型イリジウム酸化物の強磁场下の物理性研究	松平 和之	九州工業大学 大学院工学研究院	Transport and Magnetic Properties of Pyrochlore Iridates under High Field Magnetic Field	Kazuyuki Matsuhira	Kyushu Institute of Technology
171	"	水鳥 雄斗	九州工業大学 大学院工学府	"	Yuto Mizutori	Kyushu Institute of Technology
172	パレス強磁场を用いたグラファイトの強磁场相の研究	矢口 宏	東京理科大学 理工学部	Study of High Magnetic Field Phase in Graphite Using Pulsed Magnetic Fields	Hiroshi Yaguchi	Tokyo University of Science
173	幾何学的フ拉斯トレート磁性体の強磁场下での振る舞い、	香取 浩子	東京農工大学 大学院工学研究院	Properties of geometrically frustrated magnets in high magnetic fields	Hiroko Katori	Tokyo University of Agriculture and Technology
174	"	安藤 悠一	東京農工大学 大学院工学府	"	Yuichi Ando	Tokyo University of Agriculture and Technology
175	偏極電子系磁性体の強磁场下での振る舞い、	太田 寛人	東京農工大学 大学院工学府	Magnetic behavior of itinerant electronic magnets under high magnetic field	Hiroyuki Ohta	Tokyo University of Agriculture and Technology
176	"	野口 大介	東京農工大学 大学院工学府	"	Daisuke Noguchi	Tokyo University of Agriculture and Technology
177	Mn <sub>3</sub> Siの超強磁场磁化測定	小山 佳一	鹿児島大学 大学院理工学研究科	High field magnetization measurement of Mn <sub>3</sub> Si	Keiichi Koyama	Kagoshima University
178	"	折橋 広樹	鹿児島大学 大学院理工学研究科	"	Hiroki Orihashi	Kagoshima University
179	EuNiSi <sub>3</sub> の圧力誘起価数転移の探索と低温異常の解明	仲間 隆男	琉球大学 理学部	Searching for pressure-induced valence transition and resolution of low temperature anomalies on EuNiSi <sub>3</sub>	Takao Nakama	University of the Ryukyus
180	"	平川 先太郎	琉球大学 大学院理工学研究科	"	Sentaro Hirakawa	University of the Ryukyus
181	立方晶 CeTSn <sub>3</sub> (T=Ni, Rh) の高压輸送特性	仲間 隆男	琉球大学 理学部	High pressure transport properties of cubic structure CeTSn <sub>3</sub> (T=Ni, Rh)	Takao Nakama	University of the Ryukyus
182	"	渡部 晋太郎	琉球大学 大学院理工学研究科	"	Shintaro Watanabe	University of the Ryukyus

No.	課題名	氏名	所属	Title	Name	Organization
183	スピンドロスオーバー伝導体に対する光照射効果の観測	高橋 一志	神戸大学 大学院理学研究科	Photo effect on spin crossover conductors	Kazuyuki Takahashi	Kobe University
184	スピンドロスオーバー錯体の誘電率測定	高橋 一志	神戸大学 大学院理学研究科	Permittivity measurements of spin-crossover complexes	Kazuyuki Takahashi	Kobe University
185	"	川向 希昂	神戸大学 大学院理学研究科	"	Kiko Kawamukai	Kobe University
186	量子ホール効果試料の作成	澤田 安樹	京都大学	Sample Preparation for Quantum Hall Effect	Anju Sawada	Kyoto University
187	Pd-Mn-Sn合金のマルテンサイト変態の圧力効果	岡田 宏成	東北学院大学 工学部	Pressure effect on martensitic transition in Pd-Mn-Sn alloy	Hironari Okada	Tohoku Gakuin University
188	Ni-Mn-Ga系強磁性形状記憶合金の磁化の圧力依存性	安達 義也	山形大学 大学院理工学研究科	Pressure Dependence of Magnetization for the Ferromagnetic Shape-Memory Alloys of Ni-Mn-Ga system	Yoshiya Adachi	Yamagata University
189	"	三浦 友也	山形大学 大学院理工学研究科	"	Tomoya Miura	Yamagata University
190	部分酸化型一次元複核白金錯体の伝導挙動の圧力依存性	満身 稔	兵庫県立大学 大学院物質科学研究科	Pressure Dependence of Electrical Conductivity of Partially Oxidized One-Dimensional Diplatinum Complex	Minoru Mitsuishi	University of Hyogo
191	超強磁場を利用したNiMn基およびCoCr基合金の低温異常現象の観察および起源解明	伊藤 航	仙台高等専門学校 マテリアル環境工学科	Observation and clarification of the origin of anomalous behaviors at low temperature under strong magnetic field in NiMn based and CoCr based alloys	Wataru Ito	Sendai National College of Technology
192	"	許 震(キヨウ)	東北大 大学院工学研究科	"	Xiao XU	Tohoku University
193	低次元有機ラジカル磁性体の極低温磁化測定	山口 博則	大阪府立大学 大学院理学系研究科	Magnetization measurements of organic low-dimensional magnets at low temperature	Hironori Yamaguchi	Osaka Prefecture University
194	"	岩瀬 賢治	大阪府立大学 大学院理学系研究科	"	Kenji Iwase	Osaka Prefecture University
195	"	奥 雄太	大阪府立大学 大学院理学系研究科	"	Yuta Oku	Osaka Prefecture University
196	マルチフェロイック物質の低エネルギー励起状態の研究	佐賀山 基	東京大学 大学院新領域創成科学研究科	Research of low-energy excitations in multiferroics	Hajime Sagayama	The University of Tokyo
197	"	阿部 伸行	東京大学 大学院新領域創成科学研究科	"	Nobuyuki Abe	The University of Tokyo
198	強磁場下における酸化コバルト反強磁性相のハイアンタ再配列現象の観察	寺井 智之	大阪大学 大学院工学研究科	Observation of variant rearrangement of CoO antiferromagnetic phase under high magnetic field	Tomoyuki Terai	Osaka University
199	In <sub>2</sub> Ga <sub>3</sub> CuO <sub>7</sub> の単結晶合成	萩原 政幸	大阪大学 極限量子科学研究センター	Growth of single crystals of In <sub>2</sub> Ga <sub>3</sub> CuO <sub>7</sub>	Masayuki Hagiwara	Osaka University

No.	課題名	氏名	所属	Title	Name	Organization
200	In <sub>2</sub> Ga <sub>2</sub> CuO <sub>7</sub> の単結晶合成	奥谷 躍	大阪大学 大学院理学研究科	Growth of single crystals of In <sub>2</sub> Ga <sub>2</sub> CuO <sub>7</sub>	Akira Okutani	Osaka University
201	強相関型セリウム化合物および合金の量子相転移と磁性	野本 光春	室蘭工業大学 大学院工学研究科	Quantum phase transition and magnetism in the strongly correlated Ce compounds and alloys	Mitsuharu Nomoto	Muroran Institute of Technology
202	フラーイド単結晶の伝導性と磁性	森山 広思	東邦大学 理学部	Magnetic and Transport Properties of Fullereide Single Crystals	Hiroshi Moriyama	Toho University
203	"	山本 翔平	東邦大学 大学院理学研究科	"	Shohei Yamamoto	Toho University
204	配向制御されたニオブ酸カリウム系非鉛圧電材料に關する研究	森田 剛	東京大学 大学院新領域創成科学研究所	Orientation controlled KN family piezoelectric material with hydrothermal synthesis powder	Takeshi Morita	The University of Tokyo
205	"	藤内 由紀子	東京大学 大学院新領域創成科学研究所	"	Yukiko Fujuchi	The University of Tokyo
206	TmB <sub>4</sub> の磁気準周期秩序相における圧力効果	伊賀 文後	茨城大学 理学部	Pressure effect on the magnetic quasi-period ordered phase in TmB <sub>4</sub>	Fumitoshi Iga	Ibaraki University
207	"	道村 真司	埼玉大学 研究機構科学分析支援センター	"	Shinji Michimura	Saitama University
208	水溶性シリコンナノ結晶の作製と機能デバイスへの応用	佐藤 井一	兵庫県立大学 大学院物質理化学研究科	Fabrication of hydrophilic silicon nanocrystals and application to functional devices	Seiichi Sato	University of Hyogo
209	BiCo <sub>1-x</sub> Fe <sub>x</sub> O <sub>3</sub> のバルス強磁場中スピンドル状態転移	岡 研吾	東京工業大学 応用セラミックス研究所	Field Induced Spin-State Transition in BiCo <sub>1-x</sub> Fe <sub>x</sub> O <sub>3</sub>	Kengo Oka	Tokyo Institute of Technology
210	S=2一次元ハイゼンベルグ反強磁性体の極低温磁化測定	萩原 政幸	大阪大学 極限量子科学研究所	Magnetization measurements on an S=2 one-dimensional Heisenberg antiferromagnet at ultra-low temperatures	Masayuki Hagiwara	Osaka University
211	"	池田 真実	大阪大学 大学院理学研究科	"	Masami Ikeda	Osaka University

物質合成・評価設備Pクラス(Materials Synthesis and Characterization P Class Researcher)

No.	課題名	氏名	所属	Title	Name	Organization
1	Ruddlesden-Popper型ペロブスカイト酸化物における構造相転移	陰山 洋	京都大学 大学院工学研究科	Structural Transition in Ruddlesden-Popper Type Perovskite oxides	Hirosi Kageyama	Kyoto University
2	"	セドリック タッセル	京都大学 大学院工学研究科	"	Cedric Tassel	Kyoto University
3	"	山本 隆文	京都大学 大学院工学研究科	"	Takafumi Yamamoto	Kyoto University

No.	課題名	氏名	所属	Title	Name	Organization
4	Ruddlesden-Popper 型ペロブスカイト酸化物における構造相転移	吉井 龍太	京都大学 大学院工学研究科	Structural Transition in Ruddlesden-Popper Type Perovskite oxides	Ryuta Yoshii	Kyoto University
5	スピノン・電荷・軌道の自由度を有する新規フラストレート磁性体の物性評価	植田 浩明	京都大学 大学院理学研究科	characterization of novel frustrated magnets with spin-charge-orbital degrees of freedom	Hiroaki Ueda	Kyoto University
6	"	小林 憲太郎	京都大学 大学院理学研究科	"	Shintaro Kobayashi	Kyoto University
7	"	後藤 真人	京都大学 大学院理学研究科	"	Masato Goto	Kyoto University
8	時間分解分光法を用いた超臨界流体中パルスレーザープラズマによるダイヤモンドイド合成における反応メカニズムの探索	ショウタクスス ジョン	東京大学 大学院新領域創成科学研究科	Investigation of the reaction mechanisms of diamondoid synthesis by pulsed laser plasmas generated in supercritical fluids by time-resolved spectroscopy	Sven Strauss	The University of Tokyo
9	"	加藤 暉	東京大学 大学院新領域創成科学研究科	"	Toru Kato	The University of Tokyo
10	炭素質コンドライト隕石にみられる水質変成組織の微細組織観察	瀬戸 雄介	神戸大学 大学院理学研究科	Microscopic characterization of aqueous alteration texture in carbonaceous chondrites	Yusuke Seto	Kobe University
11	"	松本 恵	神戸大学 大学院理学研究科	"	Megumi Matsumoto	Kobe University
12	"	宇津木 純香	神戸大学 大学院理学研究科	"	Ayaka Utsuki	Kobe University
13	強相関系遷移金属酸化物の透過電子顕微鏡法による研究	中山 則昭	山口大学 大学院理工学研究科	TEM study of strongly correlated transition metal oxide systems	Noriaki Nakayama	Yamaguchi University
14	ハイクロア型希土類酸化物の単結晶育成と磁気プロトトレーションの研究	松平 和之	九州工業大学 大学院工学研究科	Single crystal growth and study of frustrated magnetism in pyrochlore rare-earth oxides	Kazuyuki Matsuhira	Kyushu Institute of Technology
物質合成・評価設備Gクラス(Materials Synthesis and Characterization G Class Researcher)						
No.	課題名	氏名	所属	Title	Name	Organization
1	高温高压水中における固体酸塩基触媒反応の速 度論的解析	大友 順一郎	東京大学 大学院新領域創成科学研究科	Kinetic analysis of solid acid and base catalyzed reactions in sub- and supercritical water	Junichiro Otomo	The University of Tokyo
2	"	秋月 信	東京大学 大学院新領域創成科学研究科	"	Makoto Akizuki	The University of Tokyo
3	高温高压水中における固体酸触媒反応の速度論 的解析	大友 順一郎	東京大学 大学院新領域創成科学研究科	Kinetic analysis of solid acid catalyzed reactions in sub- and supercritical water	Junichiro Otomo	The University of Tokyo
4	"	佐野 恵二	東京大学 大学院新領域創成科学研究科	"	Keiji Sano	The University of Tokyo

No.	課題名	氏名	所属	Title	Name	Organization
5 重 造	電子系反強磁性体Yb(Ni <sub>1-x</sub> Cu <sub>x</sub> ) <sub>3</sub> Al <sub>9</sub> の結晶構 造	大原 駿男	名古屋工業大學	Structure study of heavy-fermion antiferromagnet; Yb(Ni <sub>1-x</sub> Cu <sub>x</sub> ) <sub>3</sub> Al <sub>9</sub>	Shigeo Ohara	Nagoya Institute of Technology
6 マテリアルリサイクル	超臨界水を用いた有機・無機複合廃棄物からの マテリアルリサイクル	大友 順一郎	東京大学	Material recycling from organic-inorganic composite waste using supercritical water	Junichiro Otomo	The University of Tokyo
7	"	松本 祐太	東京大学	"	Yuta Matsumoto	The University of Tokyo
8 ケミカルループ法における酸素キャリア材料 の酸化還元応答特性と担体効果	大友 順一郎	東京大学	大学院新領域 創成科学研究科	Reduction and Oxidation Kinetics of Iron Oxide Carriers and effect of support materials for Chemical Looping Combustion	Junichiro Otomo	The University of Tokyo
9	"	磯貝 俊介	東京大学	大学院新領域 創成科学研究科	"	Shunsuke Isogai
10 固体酸化物形燃料電池の劣化挙動におけるイオン ビーダンススペクトルの解析	大友 順一郎	東京大学	大学院新領域 創成科学研究科	Analysis of electrochemical impedance spectra for the identification of degradation mechanisms in solid oxide fuel cells	Junichiro Otomo	The University of Tokyo
11	"	伊原 冬樹	東京大学	大学院新領域 創成科学研究科	"	Fuyuki Ihara
12 高温高压水を利用した有機修飾微粒子の連続式 合成技術の開発	大友 順一郎	東京大学	大学院新領域 創成科学研究科	The development of continuous synthesis of organic-modified particles in high temperature and pressure water	Junichiro Otomo	The University of Tokyo
13	"	生駒 健太郎	東京大学	大学院新領域 創成科学研究科	"	Kentaro Ikoma
14 酸化セリウムナノマテリアルのキャラクタリゼーション	佐々木 岳彦	東京大学	大学院新領域 創成科学研究科	Characterization for cerium oxide nanomaterials	Takehiko Sasaki	The University of Tokyo
15	"	梶 智大	東京大学	大学院新領域 創成科学研究科	"	Tomohiro Kajii
16 酸化物イオン伝導体とプロトン伝導体を用いた新 規二次電池の開発	大友 順一郎	東京大学	大学院新領域 創成科学研究科	Development of novel rechargeable battery using oxide ion and proton conductors	Junichiro Otomo	The University of Tokyo
17	"	櫻井 健一朗	東京大学	大学院新領域 創成科学研究科	"	Kenichiro Sakurai
18 中温作動プロトン伝導型燃料電池における多様 な燃料の直接利用	大友 順一郎	東京大学	大学院新領域 創成科学研究科	Direct use of diverse fuels in a proton-conducting intermediate temperature fuel cell	Junichiro Otomo	The University of Tokyo
19	"	嶋田 五百里	東京大学	大学院新領域 創成科学研究科	"	Iori Shimada
20 中温作動型燃料電池におけるプロトン伝導型固 体電解質の開発	大友 順一郎	東京大学	大学院新領域 創成科学研究科	Development of proton conducting electrolyte for intermediate temperature fuel cells	Junichiro Otomo	The University of Tokyo
21	"	庄野 淳平	東京大学	大学院新領域 創成科学研究科	"	Yohei Shono

No.	課題名	氏名	所属	Title	Name	Organization
22	複合固体電解質の合成と大容量蓄電池の開発	大友 順一郎	東京大学 大学院新領域 創成科学研究科	Synthesis of glass ceramics composite electrolyte and development of novel rechargeable battery.	Junichiro Otomo	The University of Tokyo
23	"	高坂 文彦	東京大学 大学院新領域 創成科学研究科	"	Fumihiko Kosaka	The University of Tokyo
24	プロトン伝導性中温作動燃料電池における新規りん酸ガラス-セラミックス電解質の開発	大友 順一郎	東京大学 大学院新領域 創成科学研究科	Development of Phosphate Glass-Ceramics Electrolyte for Intermediate-Temperature Fuel Cells with Proton-Conducting Electrolyte	Junichiro Otomo	The University of Tokyo
25	"	川村 亮人	東京大学 大学院新領域 創成科学研究科	"	Ryoto Kawamura	The University of Tokyo
26	幾何学的フラストレーションを有する強相関電子系の設計	有馬 孝尚	東京大学 大学院新領域 創成科学研究科	Design of strongly correlated electron systems with geometrical frustration	Taka-hisa Arima	The University of Tokyo
27	"	阿部 伸行	東京大学 大学院新領域 創成科学研究科	"	Nobuyuki Abe	The University of Tokyo
28	"	佐賀山 基	東京大学 大学院新領域 創成科学研究科	"	Hajime Sagayama	The University of Tokyo
29	"	新居 陽一	東京大学 大学院新領域 創成科学研究科	"	Yoichi Nii	The University of Tokyo
30	"	ヌイエン ドゥイー カー ン	東京大学 大学院新領域 創成科学研究科	"	Nguyen Duy Khanh	The University of Tokyo
31	"	豊田 新悟	東京大学 大学院新領域 創成科学研究科	"	Shingo Toyoda	The University of Tokyo
32	SOFC空気極における製造プロセス由来微量元素 分の電極特性に対する影響評価	大友 順一郎	東京大学 大学院新領域 創成科学研究科	Evaluation of correlation between SOFC cathode performance and trace element behavior in a SOFC production process	Junichiro Otomo	The University of Tokyo
33	"	大石 淳矢	東京大学 大学院新領域 創成科学研究科	"	Junya Oisii	The University of Tokyo
34	超臨界水を反応場としたナノ材料の創成	大友 順一郎	東京大学 大学院新領域 創成科学研究科	Synthesis of nano-materials using supercritical water as a reaction medium	Junichiro Otomo	The University of Tokyo
35	"	横 哲	東京大学 大学院新領域 創成科学研究科	"	Akira Yoko	The University of Tokyo
36	複合型酸化物イオン伝導体の合成と金属-空気 二次電池への応用	大友 順一郎	東京大学 大学院新領域 創成科学研究科	Synthesis and utilization of nanocomposite materials for highly oxide ion conducting electrolytes of metal-air secondary battery	Junichiro Otomo	The University of Tokyo
37	"	山本 高史	東京大学 大学院新領域 創成科学研究科	"	Takashi Yamamoto	The University of Tokyo
38	超臨界二酸化炭素中ハルスレーザープラズマに よるナノ微粒子の合成	シェタウス ス ヴィエン	東京大学 大学院新領域 創成科学研究科	Synthesis of nanomaterials by pulsed-laser plasmas in high-pressure and supercritical CO <sub>2</sub>	Sven Strauss	The University of Tokyo

No.	課題名	氏名	所属	Title	Name	Organization
39	超臨界二酸化炭素中バルスレーザープラズマによるナノ微粒子の合成	加藤 智嗣	東京大学 大学院新領域創成科学研究科	Synthesis of nanomaterials by pulsed-laser plasmas in high-pressure and supercritical CO <sub>2</sub>	Satoshi Kato	The University of Tokyo
40	超臨界二酸化炭素中レーーザープラズマ生成現象の分子光学的基礎研究	古部 繼一郎	東京大学 大学院新領域創成科学研究科	Spectroscopic investigation of laser plasma generation mechanisms in supercritical carbon-dioxide	Keiichiro Urabe	The University of Tokyo
41	超臨界流体中プラズマによるダイヤモンドイド合成における反応機構の探索	ハイ デイビッド	東京大学 大学院新領域創成科学研究科	Investigation of the reaction mechanisms in the synthesis of diamondoids by plasmas in high-pressure and supercritical fluids. Investigation of the reaction mechanisms in the synthesis of diamondoids by plasmas in high-pressure and supercritical fluids	David Pai	The University of Tokyo
42	Al系準結晶の熱電特性及びSEMIによる組成分析	金沢 育三	東京学芸大学 大学院教育学研究科	Thermoelectric properties and composition analysis of Al-based icosahedral quasicrystals and approximate crystals, by scanning electron microscope	Ikuzo Kanazawa	Tokyo Gakugei University
43	"	齋藤 誠	東京学芸大学 大学院教育学研究科	"	Makoto Saito	Tokyo Gakugei University
44	SPS法によるAl基準結晶の作製と電気抵抗への熱処理の効果	田村 隆治	東京理科大学 基礎工学部	Effect of heat treatment on the electrical resistivity of icosahedral Al-based quasicrystal prepared by the SPS method	Ryuji Tamura	Tokyo University of Science
45	SPS法によるAl基準結晶の作製と電気抵抗への熱処理の効果	中村 敬人	東京理科大学 大学院基礎工学研究科	The electrical properties of icosahedral Al-based quasicrystal prepared by the SPS method	Takahito Nakamura	Tokyo University of Science
46	Vドーブβ-ボロンのSEMIによる組成分析	金沢 育三	東京学芸大学 自然科学系	Composition analysis of Vanadium doped beta-Boron by scanning electron microscope	Ikuzo Kanazawa	Tokyo Gakugei University
47	"	山田 浩平	東京学芸大学 大学院教育学研究科	"	Kouhei Yamada	Tokyo Gakugei University
48	ナノ構造制御による二次電池等の機能性材料開発	細野 英司	産業技術総合研究所 エネルギー技術研究部	Development of the functional materials such as secondary battery by the nanostructure control	Eiji Hosono	National Institute of Industrial Science and Technology
49	下水汚泥の超臨界水ガス化プロセスにおける栄養塩回収・固定化の実験的検討	澤井 理	東京大学 環境安全研究センター	Recovery and immobilization of nutrients salts in the supercritical water gasification process of municipal sewage sludge	Osamu Sawai	The University of Tokyo
50	高温高压水とマイクロミキサを用いた機能性ナノ粒子の連続合成	陶 宏	産業技術総合研究所 ナノシステム研究部	Continuous hydrothermal synthesis of functional nanoparticles using a micromixer	Kiwamu Sue	National Institute of Industrial Science and Technology
51	新規磁石材料の微細構造解析	齋藤 哲治	千葉工業大学 工学部	Microstructural studies of newly developed permanent magnet materials	Tetsuji Saito	Chiba Institute of Technology
52	低結晶性クリノゾイサイトの非晶質特性の実態と原因の解明	永嶌 真理子	山口大学 大学院理工学研究科	Properties of low crystallinity clinozoisite	Mariko Nagashima	Yamaguchi University
53	鉄カルコゲナイト超伝導体FeTe <sub>1-x</sub> S <sub>x</sub> における表面の酸化状態と超伝導性	山崎 照夫	東京理科大学 理工学部	Superconductivity and the state of oxidation on the surface in iron calcogenide superconductors	Teruo Yamazaki	Tokyo University of Science
54	"	櫻井 辰弥	東京理科大学 大学院理工学研究科	"	Tatsuya Sakurai	Tokyo University of Science
55	様々な不純物をドープした超伝導体の結晶構造解析	右田 稔	横浜国立大学 大学院工学府	Structure analysis of the superconductor which doped various impurities	Minoru Migit	Yokohama National University

No.	課題名	氏名	所属	Title	Name	Organization
56	MnSiO <sub>3</sub> 成分のMgSiO <sub>3</sub> 組成とCaSiO <sub>3</sub> 組成のケイ酸塩ペロブスカイトへの分配	李 林	北海道大学 大学院理学院	Partitioning of MnSiO <sub>3</sub> content between MgSiO <sub>3</sub> and CaSiO <sub>3</sub> perovskites	Li Lin	Hokkaido University
57	Cu-Ni-Co 系合金中のCo 微粒子の析出過程と磁気特性の関係	李 東海	横浜国立大学 大学院工学府	Precipitation behavior and magnetic properties of fine Co particles in Cu-Ni-Co alloys	Lee Dong Hae	Yokohama National University
58	バルク高温超伝導体および開運磁性酸化物の磁性と構造組織観察	和泉 充	東京海洋大学 大学院海洋科学技術研究所	Magnetism and structural organization of bulk high-temperature superconductor and the related magnetic oxides	Mitsuru Izumi	Tokyo University of Marine Science and Technology
59	"	都築 啓太	東京海洋大学 大学院海洋科学技術研究所	"	Keita Tsuzuki	Tokyo University of Marine Science and Technology
60	"	周 迪帆	東京海洋大学 大学院海洋科学技術研究所	"	Zhou Difan	Tokyo University of Marine Science and Technology
61	"	李 備戦	東京海洋大学 大学院海洋科学技術研究所	"	Li Beizhan	Tokyo University of Marine Science and Technology
62	"	原 章悟	東京海洋大学 大学院海洋科学技術研究所	"	Shogo Hara	Tokyo University of Marine Science and Technology
63	正20面体クラスター固体の構造に関する研究	西本 一恵	東京大学 生産技術研究所	The structural studies of icosahedral cluster solids	Kazue Nishimoto	The University of Tokyo
64	Mnシリサイド薄膜試料のSQUID測定	服部 賢	奈良先端科学技術大学院大学 物質創成科学研究所	SQUID measurements of Mn-silicide thin films	Ken Hattori	Nara Institute of Science and Technology
65	"	木村 明日香	奈良先端科学技術大学院大学 物質創成科学研究所	"	Asuka Kimura	Nara Institute of Science and Technology
66	ハーフメタル型ホイスラー合金の磁性と輸送特性にに関する研究	重田 出	鹿児島大学 大学院理工学研究科	Study on the magnetic and transport properties of half-metallic Heusler alloys	Iduru Shigeta	Kagoshima University
67	"	春森 浩平	鹿児島大学 大学院理工学研究科	"	Kouhei Harumori	Kagoshima University
68	バルスレーザー堆積法により作製したTaO <sub>2</sub> 薄膜の物性評価	村岡 祐治	岡山大学 大学院自然科学研究科	Characterization of physical properties for TaO <sub>2</sub> thin films prepared by pulsed laser deposition method	Yuki Muraoka	Okayama University
69	"	藤本 佑樹	岡山大学 大学院自然科学研究科	"	Yuki Fujimoto	Okayama University
70	ホイスラー型化合物の磁性と伝導の研究	廣井 政彦	鹿児島大学 大学院理工学研究科	Study on the magnetic and electrical properties of Heusler compounds	Masahiko Hiroi	Kagoshima University
71	"	諫訪 秀和	鹿児島大学 大学院理工学研究科	"	Hidekazu Suwa	Kagoshima University
72	金属炭化物微粒子の超伝導磁気特性	吉田 喜孝	いわき明星大学 科学技術学部	Magnetic property in superconducting fine particles of metal carbides	Yositaka Yosida	Iwaki-Meisei University

No.	課題名	氏名	所属	Title	Name	Organization
73	13族クラスター固体に関する研究	木村 薫	東京大学 大学院新領域 創成科学研究 科	Electronic Properties of Group 13 elements-based Cluster Solids	Kaoru Kimura	The University of Tokyo
74	"	住吉 篤郎	東京大学 大学院新領域 創成科学研究 科	"	Atsuro Sumiyoshi	The University of Tokyo
75	"	北原 功一	東京大学 大学院新領域 創成科学研究 科	"	Kouichi Kitahara	The University of Tokyo
76	"	松浦 裕介	東京大学 大学院工学研 究院	"	Yusuke Matsuuwa	The University of Tokyo
77	Cu-Ni-Co系合金中のCo微粒子析出過程と磁 気特性の関係	竹田 真帆人	横浜国立大学 大学院新領域 創成科学研究 科	Precipitation behavior and magnetic properties of fine Co particles in Cu-Ni-Co based alloys	Mahoto Takeda	Yokohama National University
78	ホウ化物セラミックスサンプルの相形成及び酸化 挙動の研究およびアーク風洞の開発	桜沢 愛	東京大学 大学院工学研 究院	Investigation on phase formation and oxidation behavior of boride ceramics, and development of arc-heater	Ai Momozawa	The University of Tokyo
79	多重安定性を示す光誘起分子磁性体のサイス効 果の研究	糸井 充恵	日本大学 医学部	Size effect on photo-switchable molecular magnet $K_{0.3}Co[Fe(CN)_{6.77}\cdot 3.4H_2O$	Miho Itoi	Nihon University
80	セメント硬化体・セラミック系建材の分光反射率測 定と日射熱制御に関する研究	北垣 亮馬	東京大学 大学院工学系 研究科	Controlling solar radiation heat by designing surface reflectivity of cementitious/ceramic material for building use	Ryoma Kitagaki	The University of Tokyo

物質合成・評価設備Uクラス(Materials Synthesis and Characterization U Class Researcher)

No.	課題名	氏名	所属	Title	Name	Organization
1	炭素材料の高分解能透過電子顕微鏡による微細 構造解析	齋藤 幸恵	東京大学 大学院農学生 命科学研究所	Structural analysis of carbon materials using high resolution transmission electron microscopy	Yukie Saito	The University of Tokyo
2	シリカム酸化物系の結晶構造評価	有馬 孝尚	東京大学 大学院新領域 創成科学研究 科	Characterization of the crystal structure in iridate materials	Taka-hisa Arima	The University of Tokyo
No.	課題名	氏名	所属	Title	Name	Organization
3	シリカム酸化物系の結晶構造評価	植松 大介	東京大学 大学院新領域 創成科学研究 科	Characterization of the crystal structure in iridate materials	Daisuke Uematsu	The University of Tokyo
4	シリサイド系半導体単結晶の光学特性評価	鶴殿 治彦	茨城大学 工学部	Characterizations of optical properties single crystalline Semiconducting Silicides	Haruhiko Udone	Ibaraki University

# ISSP publications

## Division of New Materials Science

### Takigawa group

We have been performing nuclear magnetic resonance experiments on various quantum spin systems and strongly correlated electron systems to explore novel quantum phases with exotic ordering and fluctuation phenomena. The major achievements in the year 2011 include: (1) Investigation in high magnetic field of anisotropic spin dynamics of LiCuVO<sub>4</sub>, a quasi 1D frustrated antiferromagnet with a ferromagnetic nearest neighbor interaction, which enabled us to find evidence for the two-magnon bound state in the field range where the spin density wave order takes place at low temperatures, (2) Search for a spin nematic order in LiCuVO<sub>4</sub> in very high magnetic fields immediately below the saturation, (3) Detailed and systematic NMR experiments on the distorted Kagome spin system volborthite, which allowed us to determine the precise phase diagram with unusual spin order and fluctuation effects in high magnetic fields.

1. \*High-Field Phase Diagram and Spin Structure of Volborthite Cu<sub>3</sub>V<sub>2</sub>O<sub>7</sub>(OH)<sub>2</sub>·2H<sub>2</sub>O: M. Yoshida, M. Takigawa, S. Krämer, S. Mukhopadhyay, M. Horvatić, C. Berthier, H. Yoshida, Y. Okamoto and Z. Hiroi, J. Phys. Soc. Jpn. **81** (2012) 024703(1-9).
2. Magnetic Coulomb Fields of Monopoles in Spin Ice and Their Signatures in the Internal Field Distribution: G. Sala, C. Castelnovo, R. Moessner, S. Sondhi, K. Kitagawa, M. Takigawa, R. Higashinaka and Y. Maeno, Phys. Rev. Lett. **108** (2012) 217203(1-5).
3. \*Magnetic Order in the Spin-1/2 Kagome Antiferromagnet Vesignieite: M. Yoshida, Y. Okamoto, M. Takigawa and Z. Hiroi, J. Phys. Soc. Jpn. **82** (2013) 013702(1-5).
4. \*Incomplete Devil's Staircase in the Magnetization Curve of SrCu<sub>2</sub>(BO<sub>3</sub>)<sub>2</sub>: M. Takigawa, M. Horvatic, T. Waki, S. Kramer, C. Berthier, F. L. Bertrand, I. Sheikin, H. Kageyama, Y. Ueda and F. Mila, Phys. Rev. Lett. **110** (2013) 067210(1-5).
5. フラストレートした磁性体ボルボサイトのゆらぎと秩序: 吉田 誠, 瀧川 仁, 日本物理学会誌 **67** (2012) 179-183.
6. 容積効率にこだわった高圧セルによる 10GPa 級 NMR 測定: 北川健太郎, 松林 和幸, 後藤 弘匡, 松本 武彦, 上床 美也, 八木 健彦, 瀧川 仁, 高圧力の科学と技術 **22** (2012) 198-205.

### Sakakibara group

We study magnetism and superconductivity of materials having low characteristic temperatures. These include heavy-electron systems, quantum spin systems and frustrated spin systems. The followings are some selected achievements in the fiscal year 2012. (1) Field and temperature variations of the specific heat  $C(H,T)$  of the heavy fermion superconductor CeCu<sub>2</sub>Si<sub>2</sub> ( $T_c=0.6$  K) were examined at temperatures down to 50 mK. Quite unexpectedly, the low temperature  $C(H,T)$  indicates an exponential decay with a two-gap feature in its temperature variation, along with a linear dependence as a function of  $H$ . The results strongly indicate that the superconducting gap is fully opened, in sharp contrast to the general belief that CeCu<sub>2</sub>Si<sub>2</sub> is a  $d$ -wave superconductor. (2) We examined the low temperature magnetization of the Yb dimer compound Yb<sub>2</sub>Pt<sub>3</sub>Pb. The results confirm the model, proposed in a preceding study by Ochiai et al., in which Yb<sup>3+</sup> has an Ising-type Kramers doublet in the crystalline electric field ground state. Interestingly, the system exhibits a spin-flop like phase at low temperatures and in high fields. This unusual behavior of the magnetization is explained by assuming a pseudo-spin flop of the doublet, which can be stabilized by introducing a high-rank multipole interaction. (3) We measured the magnetization of the S=1/2 one dimensional Heisenberg antiferromagnet CuPzN (interaction parameter  $J \sim 10$  K) at temperatures down to 80 mK in magnetic fields up to 15 T. At the base temperature ( $T/J=0.008$ ), the field variation of the magnetization is found to closely follow the exact solution obtained by the Bethe ansatz.

1. <sup>†</sup>Nonmagnetic ground states and phase transitions in the caged compounds  $\text{PrT}_2\text{Zn}_{20}$ (T = Ru, Rh and Ir): T. Onimaru, K. T. Matsumoto, N. Nagasawa, Y. F. Inoue, K. Umeo, R. Tamura, K. Nishimoto, S. Kittaka, T. Sakakibara and T. Takabatake, *J. Phys.: Condens. Matter* **24** (2012) 294207(1-5).
2. \*Field dependence of the specific heat in a heavy-fermion superconductor  $\text{CeIrIn}_5$ : Y. Aoki, S. Kittaka, T. Sakakibara, A. Sakai, S. Nakatsuji, Y. Tsutsumi, M. Ichioka and K. Machida, *J. Phys. Soc. Jpn.* **81** (2012) SB014(1-4).
3. Low Temperature Magnetization of  $\text{Yb}_2\text{Pt}_2\text{Pb}$  with the Shastry–Sutherland Type Lattice and a High-Rank Multipole Interaction: Y. Shimura, T. Sakakibara, K. Iwakawa, K. Sugiyama and Y. Onuki, *J. Phys. Soc. Jpn.* **81** (2012) 103601(1-4).
4. \*Multiferroicity on the Zigzag-Chain Antiferromagnet  $\text{MnWO}_4$  in High Magnetic Fields: H. Mitamura, T. Sakakibara, H. Nakamura, T. Kimura and K. Kindo, *J. Phys. Soc. Jpn.* **81** (2012) 054705(1-7).
5. Superconducting Gap Structure of the Cage Compound  $\text{Sc}_5\text{Rh}_6\text{Sn}_{18}$ : N. Kase, S. Kittaka, T. Sakakibara and J. Akimitsu, *J. Phys. Soc. Jpn.* **81** (2012) SB016(1-4).
6. <sup>†</sup>Simultaneous superconducting and antiferroquadrupolar transitions in  $\text{PrRh}_2\text{Zn}_{20}$ : T. Onimaru, N. Nagasawa, K. T. Matsumoto, K. Wakiya, K. Umeo, S. Kittaka, T. Sakakibara, Y. Matsushita and T. Takabatake, *Phys. Rev. B* **86** (2012) 184426(1-7).
7. \*Superconducting gap structure of  $\text{CeIrIn}_5$  from field-angle-resolved measurements of its specific heat: S. Kittaka, Y. Aoki, T. Sakakibara, A. Sakai, S. Nakatsuji, Y. Tsutsumi, M. Ichioka and K. Machida, *Phys. Rev. B* **85** (2012) 060505(1-4).
8. 力ゴ状化合物  $\text{Pr}_{1-2-20}$  系における非クラマース二重項と多彩な相転移現象: 鬼丸 孝博, 榊原 俊郎, 固体物理 **47** (2012) 565-576.
9. Destruction of the Kondo effect in the cubic heavy-fermion compound  $\text{Ce}_3\text{Pd}_{20}\text{Si}_6$ : J. Custers, K.-A. Lorenzer, M. Müller, A. Prokofiev, A. Sidorenko, H. Winkler, A. M. Strydom, Y. Shimura, T. Sakakibara, R. Yu, Q. Si and S. Paschen, *Nature Mater.* **11** (2012) 189-194.
10. Field-Induced Ordering in the Heavy Fermion Compound  $\text{YbCo}_2\text{Zn}_{20}$ : Y. Shimura, T. Sakakibara, S. Yoshiuchi, F. Honda, R. Settai and Y. Onuki, *J. Phys.: Conf. Ser.* **391** (2012) 012066(1-4).
11. Field-temperature phase diagram of superconductivity in  $\text{Sr}_2\text{RuO}_4$ -Ru under out-of-plane uniaxial pressure: H. Taniguchi, S. Kittaka, S. Yonezawa, H. Yaguchi and Y. Maeno, *J. Phys.: Conf. Ser.* **391** (2012) 012108(1-5).
12. \* $T/B$  scaling of magnetization in the mixed valent compound  $\beta$ - $\text{YbAlB}_4$ : Y. Matsumoto, S. Nakatsuji, K. Kuga, Y. Karaki, Y. Shimura, T. Sakakibara, A. H. Nevidomskyy and P. Coleman, *J. Phys.: Conf. Ser.* **391** (2012) 012041(1-4).
13. Probing Spin Chirality of the Equilateral Triangular-Lattice Antiferromagnet  $\text{RbFe}(\text{MoO}_4)_2$  through Multiferroicity: H. Mitamura, R. Watanuki, N. Onozaki, Y. Shimura, S. Kittaka, T. Sakakibara and K. Suzuki, *J. Phys.: Conf. Ser.* **391** (2012) 012099(1-4).
14. Searching for the in-plane anisotropy of the specific heat of  $\text{UPt}_3$  in rotating fields: S. Kittaka, K. An, T. Sakakibara, Y. Haga, E. Yamamoto, N. Kimura, Y. Onuki and K. Machida, *J. Phys.: Conf. Ser.* **391** (2012) 012031(1-4).
15. Anomalous Field-Angle Dependence of the Specific Heat of Heavy-Fermion Superconductor  $\text{UPt}_3$ : S. Kittaka, K. An, T. Sakakibara, Y. Haga, E. Yamamoto, N. Kimura, Y. Onuki and K. Machida, *J. Phys. Soc. Jpn.* **82** (2013) 024707(1-5).
16. <sup>†</sup>Coexistence of Ising and XY Spin Systems on a Single Tb Atom in  $\text{TbCoGa}_5$ : N. Sanada, Y. Amou, R. Watanuki, K. Suzuki, I. Yamamoto, H. Mitamura, T. Sakakibara, M. Akatsu, Y. Nemoto and T. Goto, *J. Phys. Soc. Jpn.* **82** (2013) 044713(1-7).
17. \*Evidence of a High-Field Phase in  $\text{PrV}_2\text{Al}_{20}$  in a [100] Magnetic Field: Y. Shimura, Y. Ohta, T. Sakakibara, A. Sakai and S. Nakatsuji, *J. Phys. Soc. Jpn.* **82** (2013) 043705(1-4).
18. <sup>†\*</sup>High-Field Phase Diagram of  $\text{SmRu}_4\text{P}_{12}$  Determined by Ultrasonic Measurements in Pulsed Magnetic Field up to 55 T: M. Yoshizawa, H. Mitamura, F. Shichinomiya, S. Fukuda, Y. Nakanishi, H. Sugawara, T. Sakakibara and K. Kindo, *J. Phys. Soc. Jpn.* **82** (2013) 033602(1-5).
19. <sup>†\*</sup>Long-range order and spin-liquid states of polycrystalline  $\text{Tb}_{2+x}\text{Ti}_{2-x}\text{O}_{7+y}$ : T. Taniguchi, H. Kadowaki, H. Takatsu, B. Fåk, J. Ollivier, T. Yamazaki, T. J. Sato, H. Yoshizawa, Y. Shimura, T. Sakakibara, T. Hong, K. Goto, L. R. Yaraskavitch and J. B. Kycia, *Phys. Rev. B* **87** (2013) 060408R(1-5).

20. Determining the Surface-To-Bulk Progression in the Normal-State Electronic Structure of  $\text{Sr}_2\text{RuO}_4$  by Angle-Resolved Photoemission and Density Functional Theory: C. N. Veenstra, Z. -H. Zhu, B. Ludbrook, M. Capsoni, G. Levy, A. Nicolaou, J. A. Rosen, R. Comin, S. Kittaka, Y. Maeno, I. S. Elfimov and A. Damascelli, Phys. Rev. Lett. **110** (2013) 097004(1-5).
21. <sup>†</sup>Unconventional Magnetic and Thermodynamic Properties of  $S=1/2$  Spin Ladder with Ferromagnetic Legs: H. Yamaguchi, K. Iwase, T. Ono, T. Shimokawa, H. Nakano, Y. Shimura, N. Kase, S. Kittaka, T. Sakakibara, T. Kawakami and Y. Hosokoshi, Phys. Rev. Lett. **110** (2013) 157205(1-5).

## Mori group

We have successfully developed and characterized the functional molecular materials. The major achievements in 2012 are (1) to develop the purely organic single-component organic conductor  $\kappa\text{-H}_3(\text{Cat-EDT-ST})_2$  which shows metallic state under 1GPa, (2) to develop the proton-electron coupled conductor with the proton arrangement driven by the charge ordering, and (3)to develop the pressure-induced superconductor beta-(meso-DMBEDT-TTF)<sub>2</sub> $\text{AsF}_6$  which shows the checkerboard-type charge ordering at ambient pressure.

1. Recent Topics of Organic Superconductors: A. Ardavan, S. Brown, S. Kagoshima, K. Kanoda, K. Kuroki, H. Mori, M. Ogata, S. Uji and J. Wosnitza, J. Phys. Soc. Jpn. **81** (2012) 011004(27 pages).
2. Charge-order driven proton arrangement in a hydrogen-bonded charge-transfer complex based on a pyridyl-substituted TTF derivative: S. C. Lee, A. Ueda, H. Kamo, K. Takahashi, M. Uruichi, K. Yamamoto, K. Yakushi, A. Nakao, R. Kumai, K. Kobayashi, H. Nakao, Y. Murakami and H. Mori, Chem. Commun. **48** (2012) 8673-8675.
3. Reversible iodine absorption by alkali-TCNQ salts with associated changes in physical properties: A. Funabiki, T. Mochida, K. Takahashi, H. Mori, T. Sakurai, H. Ohtad and M. Uruich, J. Mater. Chem. **344** (2012) 8361-8366.
4. Development of chiral molecular crystals: S. J. Krivickas, C. Hashimoto, K. Takahashi, J. D. Wallis and H. Mori, Phys. Status Solidi C **9** (5) (2012) 1146-1148.
5. \*Magnetism in crown-ether-substituted nitronyl nitroxide derivatives and their metal complexes: T. Sugano, S. J. Blundell, W. Hayes, H. Tajima and H. Mori, Phys. Status Solidi C **9**(5) (2012) 1205-1207.
6. Thermoelectric and thermal properties of novel  $\tau$ -type organic conductors as thermoelectric materials: H. Yoshino, H. Nakada, S. J. Krivickas, H. Mori, G. C. Anyfantis, G. C. Papavassiliou and K. Murata, Phys. Status Solidi C **9**(5) (2012) 1193-1195.
7. \*Cooperative spin transition and thermally quenched high-spin state in new polymorph of  $[\text{Fe}(\text{qsal})_2]\text{I}_3$ : K. Takahashi, T. Sato, H. Mori, H. Tajima, Y. Einaga and O. Sato, Hyp. Int. **1-5** (2012) 206(1-3).
8. Manipulation of the heme electronic structure by external stimuli and ligand field: Y. Ohgo, M. Takahashi, K. Takahashi, Y. Namatame, H. Konaka, H. Mori, S. Neya, S. Hayami, D. Hashizume and M. Nakamura, Hyp. Int. **23-33** (2012) 206(1-3).
9. Spectroscopic characterization of charge order fluctuations in BEDT-TTF metals and superconductors: A. Girlando, M. Masino, S. Kaiser, Y. Sun N. Drichko, M. Dressel and H. Mori, Phys. Status Solidi B **24** (2012) 953-956.
10. Synthesis and properties of catechol-fused tetrathiafulvalene derivatives and their hydrogen-bonded conductive charge-transfer salts: H. Kamo, A. Ueda, T. Isono, K. Takahashi and H. Mori, Tetrahedron Letters **53** (2012) 4385-4388.
11. Magnetism and Pressure-Induced Superconductivity of Checkerboard-Type Charge-Ordered Molecular Conductor  $\beta$ -(meso-DMBEDT-TTF)<sub>2</sub>X (X =  $\text{PF}_6^-$  and  $\text{AsF}_6^-$ ): T. Shikama, T. Shimokawa, S. Lee, T. Isono, A. Ueda, K. Takahashi, A. Nakao, R. Kumai, H. Nakao, K. Kobayashi, Y. Murakami, M. Kimata, H. Tajima, K. Matsubayashi, Y. Uwatoko, Y. Nishio, K. Kajita and H. Mori, Crystals **2** (2012) 1502-1513.
12. Pyridone derivatives carrying radical moieties: Hydrogen-bonded structures, magnetic properties, and metal coordination: M. Ueda, T. Mochida and H. Mori, Polyhedron **52** (2013) 755-760.
13. Fabrication of a field effect transistor structure using charge-ordered organic materials  $\alpha$ -(BEDT-TTF)<sub>2</sub> $\text{I}_3$  and  $\alpha'$ -(BEDT-TTF)<sub>2</sub> $\text{IBr}_2$ : M. Kimata, T. Ishihara, A. Ueda, H. Mori and H. Tajima, Synthetic Metals **173** (2013) 43-45.
14. Hydrogen bond-promoted metallic state in a purely organic single-component conductor under pressure: T. Isono, H. Kamo, A. Ueda, K. Takahashi, A. Nakao, R. Kumai, H. Nakao, K. Kobayashi, Y. Murakami and H. Mori, Nature Commun. **4** (2013) 1344-1349.

## Tajima group

Our main subject is the electrical properties on molecular assemblies especially on organic thin films and conducting molecular crystals. The major achievements in 2012 include (1) spin injection experiments into a organic conductive polymer PEDOT:PSS, (2) a detailed report on a new technique for determining a trap density function based on the photo-CELIV measurements, and (3) magnetic torque studies on conducting phthalocyanine salts.

1. Electrostatic Charge Carrier Injection into the Charge-Ordered Organic Material  $\alpha$ -(BEDT-TTF)<sub>2</sub>I<sub>3</sub>: M. Kimata, T. Ishihara and H. Tajima, J. Phys. Soc. Jpn. **81** (2012) 073704(1-4).
2. \*Magnetism in crown-ether-substituted nitronyl nitroxide derivatives and their metal complexes: T. Sugano, S. J. Blundell, W. Hayes, H. Tajima and H. Mori, Phys. Status Solidi C **9(5)** (2012) 1205-1207.
3. \*Cooperative spin transition and thermally quenched high-spin state in new polymorph of [Fe(qsal)<sub>2</sub>]I<sub>3</sub>: K. Takahashi, T. Sato, H. Mori, H. Tajima, Y. Einaga and O. Sato, Hyp. Int. **1-5** (2012) 206(1-3).
4. Direct determination of trap density function based on the photoinduced charge carrier extraction technique: H. Tajima, T. Suzuki and M. Kimata, Organic Electronics **13** (2012) 2272-2280.
5. \*Observation of Phonon-Assisted Magnon Absorption in Spin–Orbit Coupling Induced Mott Insulator Sr<sub>2</sub>IrO<sub>4</sub>: Y. Hirata, H. Tajima and K. Ohgushi, J. Phys. Soc. Jpn. **82** (2013) 035002(1-2).
6. \*Mechanism of Enhanced Optical Second-Harmonic Generation in the Conducting Pyrochlore-Type Pb<sub>2</sub>Ir<sub>2</sub>O<sub>7-x</sub> Oxide Compound: Y. Hirata, M. Nakajima, Y. Nomura, H. Tajima, Y. Matsushita, K. Asoh, Y. Kiuchi, A. G. Eguiluz, R. Arita, T. Suemoto and K. Ohgushi, Phys. Rev. Lett. **110** (2013) 187402(1-5).
7. Characteristics of organic light-emitting devices consisting of dye-doped spin crossover complex films: M. Matsuda, K. Kiyoshima, R. Uchida, N. Kinoshita and H. Tajima, Thin Solid Films **531** (2013) 451-453.
8. Electrochemically Fabricated Phthalocyanine-Based Molecular Conductor Films and Their Potential Use in Organic Electronic Devices: M. Matsuda, N. Kinoshita, M. Fujishima, S. Tanaka, H. Tajima and H. Hasegawa, Appl. Phys. Express **6** (2013) 021602 1-3.
9. 新著紹介「太陽電池の物理」: 田島 裕之, 日本物理学会誌 **68** (2013) 186-187.
10. 固体の分光測定: 田島 裕之, 「大学院講義物理化学 (第2版) 3 固体の化学と物性」, 7, 近藤 保, (東京化学同人, 2012), 190-198.

## Nakatsuji group

Our group explores novel quantum phases and phase transitions in rare-earth and transition metal based compounds. The followings are some relevant results obtained in 2012. (1) We have found that Pr<sub>2</sub>Zr<sub>2</sub>O<sub>7</sub>, the sister insulating compound of Pr<sub>2</sub>Ir<sub>2</sub>O<sub>7</sub>, has strong quantum monopolar fluctuations in the spin ice state. This suggests the monopole in this exchange-based spin ice may propagate coherently in the lattice, in contrast with the diffusive motion of the classical counterpart. (2) We discovered heavy fermion superconductivity in the ferroquadrupolar state in the quadrupolar Kondo lattice system PrTi<sub>2</sub>Al<sub>20</sub>. (3) The strong temperature and field dependence of the Hall resistivity of  $\beta$ -YbAlB<sub>4</sub> indicates that the low coherence temperature of 40 K in comparison with the valence fluctuation scale of 300 K. The results further suggest the band dependence of the localized and itinerant characters of *f*-electrons.

1. \*Field dependence of the specific heat in a heavy-fermion superconductor CeIrIn<sub>5</sub>: Y. Aoki, S. Kittaka, T. Sakakibara, A. Sakai, S. Nakatsuji, Y. Tsutsumi, M. Ichioka and K. Machida, J. Phys. Soc. Jpn. **81** (2012) SB014(4 pages).
2. Low Temperature Properties of the Cubic Kondo Lattice Systems SmTr<sub>2</sub>Al<sub>20</sub> (Tr = Ti, V, Cr): A. Sakai and S. Nakatsuji, J. Phys. Soc. Jpn. **81** (2012) SB049 (5 pages).
3. Microscopic Evidence for Long-Range Magnetic Ordering in the  $\Gamma$ 8 Ground Quartet Systems SmTr<sub>2</sub>Al<sub>20</sub> (Tr: Ti, V, Cr): T. U. Ito, W. Higemoto, K. Ninomiya, A. Sakai and S. Nakatsuji, J. Phys. Soc. Jpn. **81** (2012) SB050 (4 pages).
4. Superconductivity in the Ferroquadrupolar State in the Quadrupolar Kondo Lattice PrTi<sub>2</sub>Al<sub>20</sub>: A. Sakai, K. Kuga and S. Nakatsuji, J. Phys. Soc. Jpn. **81** (2012) 083702 (4 pages).
5. Continuous transition between antiferromagnetic insulator and paramagnetic metal in the pyrochlore iridate Eu<sub>2</sub>Ir<sub>2</sub>O<sub>7</sub>: J. Ishikawa, E. C. T. O'Farrell and S. Nakatsuji, Phys. Rev. B **85** (2012) 245109(1-6).

6. Evidence for an exotic magnetic transition in the triangular spin system  $\text{FeGa}_2\text{S}_4$ : P. Dalmas de Réotier, A. Yaouanc, D. E. MacLaughlin, S. Zhao, T. Higo, S. Nakatsuji, Y. Nambu, C. Marin, G. Lapertot, A. Amato and C. Baines, Phys. Rev. B **85** (2012) 140407(1-5).
7. Ferroquadrupolar ordering in  $\text{PrTi}_2\text{Al}_{20}$ : T. Sato, S. Ibuka, Y. Nambu, T. Yamazaki, T. Hong, A. Sakai and S. Nakatsuji, Phys. Rev. B **86** (2012) 184419(1-8).
8. Magnetic order induced by Fe substitution of Al site in the heavy-fermion systems  $\alpha$ -YbAlB<sub>4</sub> and  $\beta$ -YbAlB<sub>4</sub>: K. Kuga, G. Morrison, L. Treadwell, J. Y. Chan and S. Nakatsuji, Phys. Rev. B **86** (2012) 224413(1-6).
9. Pressure-tuned insulator to metal transition in  $\text{Eu}_2\text{Ir}_2\text{O}_7$ : F. Tafti, J. Ishikawa, A. McCollam, S. Nakatsuji and S. Julian, Phys. Rev. B **85** (2012) 205104(1-6).
10. Spin dynamics and spin freezing in the triangular lattice antiferromagnets  $\text{FeGa}_2\text{S}_4$  and  $\text{NiGa}_2\text{S}_4$ : S. Zhao, P. Dalmas de Réotier, A. Yaouanc, D. MacLaughlin, J. Mackie, O. Bernal, Y. Nambu, T. Higo and S. Nakatsuji, Phys. Rev. B **86** (2012) 064435(1-11).
11. \*Superconducting gap structure of  $\text{CeIrIn}_5$  from field-angle-resolved measurements of its specific heat: S. Kittaka, Y. Aoki, T. Sakakibara, A. Sakai, S. Nakatsuji, Y. Tsutsumi, M. Ichioka and K. Machida, Phys. Rev. B **85** (2012) 060505(1-4).
12. Evolution of c-f Hybridization and Two-Component Hall Effect in  $\beta$ -YbAlB<sub>4</sub>: E. O'Farrell, Y. Matsumoto and S. Nakatsuji, Phys. Rev. Lett. **109** (2012) 176405(1-5).
13. \*Pressure-Induced Heavy Fermion Superconductivity in the Nonmagnetic Quadrupolar System  $\text{PrTi}_2\text{Al}_{20}$ : K. Matsubayashi, T. Tanaka, A. Sakai, S. Nakatsuji, Y. Kubo and Y. Uwatoko, Phys. Rev. Lett. **109** (2012) 187004(1-5).
14. Thermoelectric Response Near a Quantum Critical Point of  $\beta$ -YbAlB<sub>4</sub> and  $\text{YbRh}_2\text{Si}_2$ : A Comparative Study: Y. Machida, K. Tomokuni, C. Ogura, K. Izawa, K. Kuga, S. Nakatsuji, G. Lapertot, G. Knebel, J. -P. Brison and J. Flouquet, Phys. Rev. Lett. **109** (2012) 156405(1-5).
15. Yb 系の重い電子化合物における量子臨界性と超伝導: 中辻 知, 固体物理 **47** (2012) 521-535.
16. Spin-Orbital Short-Range Order on a Honeycomb-Based Lattice: S. Nakatsuji, K. Kuga, K. Kimura, R. Satake, N. Katayama, E. Nishibori, H. Sawa, R. Ishii, M. Hagiwara, F. Bridges, T. U. Ito, W. Higemoto, Y. Karaki, M. Halim, A. Nugroho, J. A. Rodriguez-Rivera, M. A. Green and C. Broholm, Science **336** (2012) 559-563.
17. 磁気秩序なしに起こる新しい巨大ホール効果: 中辻 知, パリティ **27-7** (2012) P.11-17.
18. New magnetic phase diagram of  $(\text{Sr,Ca})_2\text{RuO}_4$ : J. P. Carlo, T. Goko, I. M. Gat-Malureanu, P. L. Russo, A. T. Savici, A. A. Aczel, G. J. MacDougall, J. A. Rodriguez, T. J. Williams, G. M. Luke, C. R. Wiebe, Y. Yoshida, S. Nakatsuji, Y. Maeno, T. Taniguchi and Y. J. Uemura, Nature Mater. **11** (2012) 323-328.
19. \* $T/B$  scaling of magnetization in the mixed valent compound  $\beta$ -YbAlB<sub>4</sub>: Y. Matsumoto, S. Nakatsuji, K. Kuga, Y. Karaki, Y. Shimura, T. Sakakibara, A. H. Nevidomskyy and P. Coleman, J. Phys.: Conf. Ser. **391** (2012) 012041(1-4).
20. Shubnikov-de Haas oscillations in the heavy fermion  $\alpha$ -YbAlB<sub>4</sub>: E. C. T. O'Farrell, D. A. Tompsett, N. Horie, S. Nakatsuji and M. L. Sutherland, J. Phys.: Conf. Ser. **391** (2012) 012053(1-4).
21. Thermal properties of the nonmagnetic cubic  $\Gamma_3$  Kondo lattice systems  $\text{Pr}Tr_2\text{Al}_{20}$  ( $Tr = \text{Ti}, \text{V}$ ): A. Sakai and S. Nakatsuji, J. Phys.: Conf. Ser. **391** (2012) 012058(1-4).
22. Structure and physical properties of single crystal  $\text{PrCr}_2\text{Al}_{20}$  and  $\text{CeM}_2\text{Al}_{20}$  ( $M = \text{V}, \text{Cr}$ ): comparison of compounds adopting the  $\text{CeCr}_2\text{Al}_{20}$  structure type: M. J. Kangas, D. Schmitt, A. Sakai, S. Nakatsuji and J. Y. Chan, Journal of Solid State Chemistry **196** (2012) 274-281.
23. Discovery of the Novel Quantum Liquid Robust Against Disorder in Pseudo-Honeycomb Lattice Antiferromagnet  $\text{Ba}_3\text{CuSb}_2\text{O}_9$ : N. Katayama, R. Satake, E. Nishibori, H. Sawa and S. Nakatsuji, SPring-8 Information **17**, No.4 (2012) 297-303.
24. \*Evidence of a High-Field Phase in  $\text{PrV}_2\text{Al}_{20}$  in a [100] Magnetic Field: Y. Shimura, Y. Ohta, T. Sakakibara, A. Sakai and S. Nakatsuji, J. Phys. Soc. Jpn. **82** (2013) 043705(1-4).
25. Determination of long-range all-in-all-out ordering of Ir<sup>4+</sup> moments in a pyrochlore iridate  $\text{Eu}_2\text{Ir}_2\text{O}_7$  by resonant x-ray diffraction: H. Sagayama, D. Uematsu, T. Arima, K. Sugimoto, J. J. Ishikawa, E. O'Farrell and S. Nakatsuji, Phys. Rev. B **87** (2013) 100403(4 pages).

26. Dynamical spin-orbital correlation in the frustrated magnet  $\text{Ba}_3\text{CuSb}_2\text{O}_9$ : Y. Ishiguro, K. Kimura, S. Nakatsuji, S. Tsutsui, A. Q. R. Baron, T. Kimura and Y. Wakabayashi, *Nature Commun.* **4** (2013) 1-11, in print.
27. Chemical effects of high-resolution  $\text{YbL}\gamma_4$  emission spectra: a possible probe for chemical analysis: H. Hayashi, N. Kanai, N. Kawamura, Y. H. Matsuda, K. Kuga, S. Nakatsuji, T. Yamashita and S. Ohara, *X-Ray Spectrometry* (2013) 1-18, in print.
28. Quantum fluctuations in spin-ice-like  $\text{Pr}_2\text{Zr}_2\text{O}_7$ : K. Kimura, S. Nakatsuji, J. J. Wen, C. Broholm, M. B. Stone and E. Nishibori & H. Sawa, *Nature Commun.* **4** (2013) 1-6, in print.
29. 銅酸化物における乱れに強い量子液体状態: 中辻 知, 澤 博, 「超伝導現象と高温超伝導体」, 新日本編集企画, (NTS 出版社, 2013), 475-481.

## Ohgushi group

Our group is focused on an exploratory synthesis and characterization of oxides, chalcogenides, and intermetallics. The major achievements in the fiscal year 2012 are (1) investigation of electronic properties of Fe-based ladder compounds, and (2) elucidation of magnetic and orbital structures of 5d transition metal oxides by means of resonant x-ray diffraction.

1. <sup>†\*</sup>Abrupt change in the energy gap of superconducting  $\text{Ba}_{1-x}\text{K}_x\text{Fe}_2\text{As}_2$  single crystals with hole doping: W. Malaeb, T. Shimojima, Y. Ishida, K. Okazaki, Y. Ota, K. Ohgushi, K. Kihou, T. Saito, C. H. Lee, S. Ishida, M. Nakajima, S. Uchida, H. Fukazawa, Y. Kohori, A. Iyo, H. Eisaki, C. -T. Chen, S. Watanabe, H. Ikeda and S. Shin, *Phys. Rev. B* **86** (2012) 165117 (1-7).
2. \*Block magnetism coupled with local distortion in the iron-based spin-ladder compound  $\text{BaFe}_2\text{Se}_3$ : Y. Nambu, K. Ohgushi, S. Suzuki, F. Du, M. Avdeev, Y. Uwatoko, K. Munakata, H. Fukazawa, S. Chi, Y. Ueda and T. Sato, *Phys. Rev. B* **85** (2012) 064413(1-5).
3. Doping dependence of Hall coefficient and evolution of coherent electronic state in the normal state of the Fe-based superconductor  $\text{Ba}_{1-x}\text{K}_x\text{Fe}_2\text{As}_2$ : K. Ohgushi and Y. Kiuchi, *Phys. Rev. B* **85** (2012) 064522(1-5).
4. \*Stripelike magnetism in a mixed-valence insulating state of the Fe-based ladder compound  $\text{CsFe}_2\text{Se}_3$ : F. Du, K. Ohgushi, Y. Nambu, T. Kawakami, M. Avdeev, Y. Hirata, Y. Watanabe, T.-J. Sato and Y. Ueda, *Phys. Rev. B* **85** (2012) 214436(1-5).
5. \*Tetrahedral Magnetic Order and the Metal-Insulator Transition in the Pyrochlore Lattice of  $\text{Cd}_2\text{Os}_2\text{O}_7$ : J. Yamaura, K. Ohgushi, H. Ohsumi, T. Hasegawa, I. Yamauchi, K. Sugimoto, S. Takeshita, A. Tokuda, M. Takata, M. Udagawa, M. Takigawa, H. Harima, T. Arima and Z. Hiroi, *Phys. Rev. Lett.* **108** (2012) 247205(1-5).
6. \*Insitu observation of shear stress-induced perovskite to post-perovskite phase transition in  $\text{CaIrO}_3$  and the development of its deformation texture in a diamond-anvil cell up to 30 GPa: K. Niwa, N. Miyajima, Y. Seto, K. Ohgushi, H. Gotou and T. Yagi, *Phys. Earth Planet. Inter.* **194–195** (2012) 10–17.
7. \*Observation of Phonon-Assisted Magnon Absorption in Spin–Orbit Coupling Induced Mott Insulator  $\text{Sr}_2\text{IrO}_4$ : Y. Hirata, H. Tajima and K. Ohgushi, *J. Phys. Soc. Jpn.* **82** (2013) 035002(1-2).
8. Complex orbital state stabilized by strong spin-orbit coupling in a metallic iridium oxide  $\text{IrO}_2$ : Y. Hirata, K. Ohgushi, J.-I. Yamaura, H. Ohsumi, S. Takeshita, M. Takata and T. Arima, *Phys. Rev. B* **87** (2013) 161111(1-5).
9. Magnetoelasticity in  $\text{ACr}_2\text{O}_4$  spinel oxides ( $A = \text{Mn, Fe, Co, Ni, and Cu}$ ): V. Kocsis, S. Bordács, D. Varjas, K. Penc, A. Abouelsayed, C. A. Kuntscher, K. Ohgushi, Y. Tokura and I. Kézsmárki, *Phys. Rev. B* **87** (2013) 064416(1-9).
10. \*Mechanism of Enhanced Optical Second-Harmonic Generation in the Conducting Pyrochlore-Type  $\text{Pb}_2\text{Ir}_2\text{O}_{7-x}$  Oxide Compound: Y. Hirata, M. Nakajima, Y. Nomura, H. Tajima, Y. Matsushita, K. Asoh, Y. Kiuchi, A. G. Eguiluz, R. Arita, T. Suemoto and K. Ohgushi, *Phys. Rev. Lett.* **110** (2013) 187402(1-5).
11. Resonant X-ray Diffraction Study of the Strongly Spin-Orbit-Coupled Mott Insulator  $\text{CaIrO}_3$ : K. Ohgushi, J.-I. Yamaura, H. Ohsumi, K. Sugimoto, S. Takeshita, A. Tokuda, H. Takagi, M. Takata and T.-H. Arima, *Phys. Rev. Lett.* **110** (2013) 217212(1-5).
12. <sup>†</sup>Suppression of Intersite Charge Transfer in Charge-Disproportionated Perovskite  $\text{YC}_{\text{u}3}\text{Fe}_4\text{O}_{12}$ : H. Etani, I. Yamada, K. Ohgushi, N. Hayashi, Y. Kusano, M. Mizumaki, J. Kim, N. Tsuji, R. Takahashi, N. Nishiyama, T. Inoue, T. Irifune and M. Takano, *J. Am. Chem. Soc.* **135** (2013) 6100–6106.

13.  ${}^{\dagger}B$ -Site Deficiencies in A-site-Ordered Perovskite  $\text{LaCu}_3\text{Pt}_{3.75}\text{O}_{12}$ : M. Ochi, I. Yamada, K. Ohgushi, Y. Kusano, M. Mizumaki, R. Takahashi, S. Yagi, N. Nishiyama, T. Inoue and T. Irifune, Inorg. Chem. **52** (2013) 3985-3989.
14.  ${}^{\dagger}\text{Pd}^{2+}$ -Incorporated Perovskite  $\text{CaPd}_3\text{B}_4\text{O}_{12}$  ( $B = \text{Ti}, \text{V}$ ): K. Shiro, I. Yamada, N. Ikeda, K. Ohgushi, M. Mizumaki, R. Takahashi, N. Nishiyama, T. Inoue and T. Irifune, Inorg. Chem. **52** (2013) 1604-1609.

## Division of Condensed Matter Theory

### K. Ueda group

Following the previous year, the problem of the Kondo effect of a magnetic ion vibrating in a metal was investigated. In 2011, we investigated the nature of Kondo effect in the weak electron correlation regime from a different point of view. It has turned out that the essential physics in this regime can be understood by the concept of electric dipolar Kondo effect. As another topic, our group focused on shot noise observed in the Kondo tunneling through the dot with orbital degeneracy. The Fano factor determined by the Wilson ratio was calculated by employing the NRG calculation. This approach was also applied to the FQH edge states. Analyzing shot noise at finite temperatures, we proposed a way to observe the fractional statistics for Laughlin quasi-particles.

1. Dimensional Reduction and Odd-Frequency Pairing of the Checkerboard-Lattice Hubbard Model at 1/4-Filling: Y. Yanagi, Y. Yamashita and K. Ueda, J. Phys. Soc. Jpn. **81** (2012) 123701(1-4).
2. Electric Dipolar Kondo Effect Emerging from a Vibrating Magnetic Ion: T. Hotta and K. Ueda, Phys. Rev. Lett. **108** (2012) 247214(1-5).
3. 固体物理特集号「重い電子系の物理の最近の発展」はじめに: 上田 和夫, 固体物理 **67** (2012) 509-510.
4. 高温超伝導-理論-: 上田 和夫, 「物性物理学ハンドブック」, 川畑有郷・鹿児島誠一・北岡良雄・上田正仁, (朝倉書店, 2012), 175-182.

### Takada group

Employing several techniques including the Green's-function approach, the density-matrix renormalization group, quantum Monte Carlo simulations, band-structure calculations, and several types of variational approaches, we are studying various aspects of quantum many-body problems in condensed matter physics, based mainly on the first-principles Hamiltonian. This year we have studied the following issues: (1) With use of both the diffusion Monte Carlo method and the density functional theory, a detailed analysis is made on the system of a proton embedded in an electron gas with a view of clarifying the difference between this first-principles system and the impurity Anderson model devised for investigating the Kondo physics. With the decrease of the electron density of the electron gas, the electronic state around the proton changes in three steps, i.e., from the hydron  $\text{H}^+$  with itinerant metallic screening to the totally localized hydride  $\text{H}^-$  through the Kondo-resonant nonmagnetic neutral hydrogen  $\text{H}$ . The transition of each step is abrupt. (2) With use of analytical methods as well as the powerful self-consistent numerical scheme of GWT, we have discovered an electron-like elementally excitation (pseudoelectron) in the Luttinger liquid. The pseudoelectron is considered as a spinon-(anti)holon composite particle. Although it manifests itself only as the small cusp behavior in the one-electron spectral function near the Fermi level, it constitutes the main structure if the momentum is far away from the Fermi momentum. (3) With a better functional form for  $\Gamma$  always satisfying not only the Ward identity but also the momentum conservation law, we have investigated the low-density electron gas in the GWT scheme to find an anomalous mass reduction as a result of avoiding the collapse of the normal state into a spontaneously excited electron-hole liquid (excitonic liquid).

1. \*Coulomb Frustrated Phase Separation in Quasi-Two-Dimensional Organic Conductors on the Verge of Charge Ordering: K. Yoshimi and H. Maebashi, J. Phys. Soc. Jpn. **81** (2012) 063003(1-4).
2. Superconductivity in a Correlated  $E \otimes e$  Jahn-Teller System: C. Hori, H. Maebashi and Y. Takada, J. Supercond. Nov. Magn. **25** (2012) 1369-1373.
3. 超伝導転移温度の第一原理計算: 高田 康民, 「岩波講座: 計算科学 「計算と物質」」, 第8章, 押山淳, (岩波書店, 2012), 221-267.

## Oshikawa group

We studied a wide range of fundamental problems in condensed matter theory and statistical mechanics. In particular, we discussed doping of holes into the spin liquid phases of the Quantum Dimer Model (QDM). A fundamental issue is the possible existence of a superconducting phase in such systems and its properties. For this purpose, the question of the statistics of the mobile holes (or “holons”) was addressed first. We proved a general “statistical transmutation” symmetry of such doped QDM by using composite operators of dimers and holes. This exact transformation enables to define duality equivalence classes (or families) of doped QDM, and provides the analytic framework to analyze dynamical statistical transmutations. We then discussed possible superconducting phases of the system. In particular, the possibility of an exotic superconducting phase originating from the condensation of (bosonic) charge-e holons was examined. It was shown that flux quantization does not distinguish such an exotic superconducting phase from a standard one due to Cooper pairing. Thus we proposed a new gauge-invariant holon Green’s function, as a mean to detect the exotic phase. A numerical evidence supported its existence in the doped QDM on a triangular lattice.

1. <sup>†</sup>Correlation effects in two-dimensional topological insulators: Y. Tada, R. Peters, M. Oshikawa, A. Koga, N. Kawakami and S. Fujimoto, Phys. Rev. B **85** (2012) 165138(1-18).
2. <sup>†</sup>Field theory analysis of S=1 antiferromagnetic bond-alternating chains in the dimer phase: J. Tamaki and M. Oshikawa, Phys. Rev. B **85** (2012) 134431(1-10).
3. <sup>†</sup>General method for calculating the universal conductance of strongly correlated junctions of multiple quantum wires: A. Rahmani, C.-Y. Hou, A. Feiguin, M. Oshikawa, C. Chamon and I. Affleck, Phys. Rev. B **85** (2012) 045120(1-24).
4. Mass ratio of elementary excitations in frustrated antiferromagnetic chains with dimerization: S. Takayoshi and M. Oshikawa, Phys. Rev. B **86** (2012) 144408 (1-6).
5. <sup>†</sup>Quasiparticle statistics and braiding from ground-state entanglement: Y. Zhang, T. Grover, A. Turner, M. Oshikawa and A. Vishwanath, Phys. Rev. B **85** (2012) 235151(1-15).
6. <sup>†</sup>Symmetry protection of topological phases in one-dimensional quantum spin systems: F. Pollmann, E. Berg, A. M. Turner and M. Oshikawa, Phys. Rev. B **85** (2012) 075125(1-9).
7. <sup>†</sup>Thermodynamic properties of quantum sine-Gordon spin chain system KCuGaF<sub>6</sub>: I. Umegaki, H. Tanaka, T. Ono, M. Oshikawa and K. Sakai, Phys. Rev. B **85** (2012) 144423(1-9).
8. <sup>†</sup>Boundary Resonances in S=1/2 Antiferromagnetic Chains Under a Staggered Field: S. C. Furuya and M. Oshikawa, Phys. Rev. Lett. **109** (2012) 247603(1-5).
9. <sup>†</sup>Electron Spin Resonance Shift in Spin Ladder Compounds: S. C. Furuya, P. Bouillot, C. Kollath, M. Oshikawa and T. Giamarchi, Phys. Rev. Lett. **108** (2012) 037204(1-5).
10. <sup>†</sup>Instability in Magnetic Materials with a Dynamical Axion Field: H. Ooguri and M. Oshikawa, Phys. Rev. Lett. **108** (2012) 161803(1-5).
11. Superconductivity Induced by Longitudinal Ferromagnetic Fluctuations in UCoGe: T. Hattori, Y. Ihara, Y. Nakai, K. Ishida, Y. Tada, S. Fujimoto, N. Kawakami, E. Osaki, K. Deguchi, N. Sato and I. Satoh, Phys. Rev. Lett. **108** (2012) 066403(1-5).
12. <sup>†</sup>Electron spin resonance shifts in S=1 antiferromagnetic chains: S. C. Furuya, Y. Maeda and M. Oshikawa, Phys. Rev. B **87** (2013) 125122 (1-10).
13. <sup>†</sup>Hole statistics and superfluid phases in quantum dimer models: C. A. Lamas, A. Ralko, M. Oshikawa, D. Poilblanc and P. Pujol, Phys. Rev. B **87** (2013) 104512(1-20).

## Tsunetsugu group

We have investigated p-wave superconductivity near a transverse saturation field in easy-axis ferromagnets and demonstrated that soft-magnon excitations lead to enhancement and re-entrance of the superconducting transition temperature. This explains the enhanced superconducting transition temperature in the reentrant superconductivity in URhGe under transverse magnetic fields.

We have also extended our earlier analysis about phonon coupled Kondo systems. We have constructed a boundary conformal field theory (BCFT) with non-magnetic SO(5) degrees of freedom, which successfully explains earlier numerical results. We have further developed a powerful continuous-time quantum Monte Carlo algorithm for general phonon-assisted hybridization Anderson models and checked the validity of the results by the BCFT.

We have also clarified various details of transport criticality in electric conductivity near the Mott transition in a frustrated Hubbard model, using large-scale numerical simulations based on the cluster dynamical mean-field theory.

- \*Rattling Good Superconductor: the  $\beta$ -Pyrochlore Oxide  $\text{AOs}_2\text{O}_6$ : Z. Hiroi, J. Yamaura and K. Hattori, *J. Phys. Soc. Jpn.* **81** (2012) 011012 (24 pages).
- Transport Criticality in Triangular Lattice Hubbard Model: T. Sato, K. Hattori and H. Tsunetsugu, *J. Phys. Soc. Jpn.* **81** (2012) 083703 (4 pages).
- Bipolaron-SO(5) Non-Fermi Liquid in a Two-channel Anderson Model with Phonon-assisted Hybridizations: K. Hattori, *Phys. Rev. B* **85** (2012) 214411 (14 pages).
- Conventional and charge-six superfluids from melting hexagonal Fulde-Ferrell-Larkin-Ovchinnikov phases in two dimensions: D. F. Agterberg, M. Geracie and H. Tsunetsugu, *Phys. Rev. B* **84** (2012) 014513 (7 pages).
- Non-Fermi liquid, unscreened scalar chirality, and parafermions in a frustrated tetrahedron Anderson model: K. Hattori and H. Tsunetsugu, *Phys. Rev. B* **86** (2012) 054421 (6 pages).
- Transport criticality at the Mott transition in a triangular-lattice Hubbard model: T. Sato, K. Hattori and H. Tsunetsugu, *Phys. Rev. B* **86** (2012) 235137 (13 pages).
- Continuous-Time Quantum Monte Carlo Approach for Impurity Anderson Models with Phonon-Assisted Hybridizations: K. Hattori, *J. Phys. Soc. Jpn.* **82** (2013) 064709 (5 pages).
- Exotic disordered phases in the quantum J1-J2 model on the honeycomb lattice: H. Zhang and C. A. Lamas, *Phys. Rev. B* **87** (2013) 024415 (10 pages).
- p-wave superconductivity near a transverse saturation field: K. Hattori and H. Tsunetsugu, *Phys. Rev. B* **87** (2013) 064501 (5 pages).

## Kohmoto group

Twisted bilayer graphen is studied. Especially energy versus magnetic field shows a fractal Hofstadter butterfly. Since supercell is large one can expect nontrivial Hall conductance (TKNN integer) may be observed in a high magnetic field experiment. Also edge states at the interface between monolayer and bilayer are studied and its properties of applied electric field is clarified. Fibonacci optical lattice are studied and it is shown that soliton states and critical states can coexist multifractal analysis.

- Electric-field Induced Penetration of Edge States at the Interface between Monolayer and Bilayer Graphene: Y. Hasegawa and M. Kohmoto, *Phys. Rev. B* **85** (2012) 125430(1-9).
- Multifractals Competing with Solitons on Fibonacci Optical Lattices: M. Takahashi, H. Katsura, M. Kohmoto and T. Koma, *New J. Phys.* **14** (2012) 113012-113027.
- Time-Reversal Symmetry in Non-Hermitian Systems: M. Sato, K. Hasebe, K. Esaki and M. Kohmoto, *Prog. Theor. Phys.* **127** (2012) 937-974.
- Theory of tunneling conductance and surface-state transition in superconducting topological insulators: A. Yamakage, K. Yada, M. Sato and Y. Tanaka, *Phys. Rev. B* **85** (2012) 180509(R)(1-5).
- Topological Field Theory for p-wave Superconductors: T. H. Hansson, A. Karlhede and M. Sato, *New J. Phys.* **14** (2012) 063017(10pages).
- Symmetry and Topology in Superconductors —Odd-Frequency Pairing and Edge States—: Y. Tanaka, M. Sato and N. Nagaosa, *J. Phys. Soc. Jpn.* **81** (2012) 011013(1-34).

## Sugino group

The activity of Sugino group consists of (1) investigation of the property of materials related to energy-conversion, (2) developing density functional methods for computing dynamical process in matters, and (3) developing a many-body scheme to calculate the ground-state and the excited-state energies. Particularly, there was breakthrough in the algorithm of handling the many-body wavefunctions, possibly leading to one of the post density functional theories (post-DFT).

- Possible magnetic behavior in oxygen-deficient  $\beta$ -PtO<sub>2</sub>: Y. Yang, O. Sugino and T. Ohno, *Phys. Rev. B* **85** (2012) 035204(1-13).
- First-Principles Molecular Dynamics at a Constant Electrode Potential: N. Bonnet, T. Morishita, O. Sugino and M. Otani, *Phys. Rev. Lett.* **109** (2012) 266101(1-5).

3. Symmetric Tensor Decomposition Description of Fermionic Many-Body Wave Functions: W. Uemura and O. Sugino, Phys. Rev. Lett. **109** (2012) 253001(1-5).
4. A GW+Bethe-Salpeter calculation on photoabsorption spectra of  $(\text{CdSe})_3$  and  $(\text{CdSe})_6$  clusters: Y. Noguchi, O. Sugino, M. Nagaoka, S. Ishii and K. Ohno, J. Chem. Phys. **137** (2012) 024306 (1-5).
5. Analytical expression for the excited-state force from density-functional perturbation theory: T. Tsukagoshi and O. Sugino, Phys. Rev. A **86** (2012) 064501(1-4).
6. Quantum dissipative dynamics using the Doebner–Goldin equation: T. Tsukagoshi and O. Sugino, Physics Letters A **376** (2012) 3033-3037.
7. Band gap of  $\beta$ -PtO<sub>2</sub> from first-principles: Y. Yang, O. Sugino and T. Ohno, AIP Advances **2** (2012) 022172(1-7).
8. The charged interface between Pt and water: First principles molecular dynamics simulations: T. Ikeshoji, M. Otani, I. Hamada, O. Sugino, Y. Morikawa, Y. Okamoto, Y. Qian and I. Yagi, AIP Advances **2** (2012) 032182(1-10).
9. Nonadiabatic couplings from time-dependent density functional theory: Formulation by the Kohn-Sham derivative matrix within density functional perturbation theory: C. Hu, T. Tsukagoshi, O. Sugino and K. Watanabe, Phys. Rev. B **87** (2013) 035421(1-7).
10. Electronic structures of oxygen-deficient Ta<sub>2</sub>O<sub>5</sub>: Y. Yang, H.-H. Nahm, O. Sugino and T. Ohno, AIP Advances **3** (2013) 042101(1-8).

## Kato group

The main research subject in our laboratory is theory of nonequilibrium properties in nanoscale devices. We have studied nonequilibrium noise of the Kondo regime in quantum dot systems by considering effect of Hund's exchange interaction, and purity of single photons in semiconductor microcavity. Dielectric properties in ferroelectric relaxors made from perovskite oxides have been studied by the Monte Carlo method. We have also studied spin diffusion length in normal metals in the context of anti-localization analysis in collaboration with Otani group.

1. \*Coulomb Frustrated Phase Separation in Quasi-Two-Dimensional Organic Conductors on the Verge of Charge Ordering: K. Yoshimi and H. Maebashi, J. Phys. Soc. Jpn. **81** (2012) 063003(1-4).
2. Full Counting Statistics for Orbital-Degenerate Impurity Anderson Model with Hund's Rule Exchange Coupling: R. Sakano, Y. Nishikawa, A. Oguri, A. C. Hewson and S. Tarucha, Phys. Rev. Lett. **108** (2012) 266401(1-5).
3. Properties of a Single Photon Generated by a Solid-State Emitter: Effects of Pure Dephasing: E. Iyoda, T. Kato, T. Aoki, K. Edamatsu and K. Koshino, J. Phys. Soc. Jpn. **82** (2013) 014301(1-10).
4. Relaxor Behavior and Morphotropic Phase Boundary in a Simple Model: Y. Tomita and T. Kato, J. Phys. Soc. Jpn. **82** (2013) 063002(1-5).
5. 量子ドットの近藤効果による非平衡電流の完全係数統計: 阪野 墓, 小栗 章, 小林 研介, 固体物理 **47** (2013) 475-485.

## Division of Nanoscale Science

### Iye group

Thermoelectric effect in GaAs/AlGaAs 2DEG in the quantum Hall regime is studied by using a Corbino geometry. Thermopower generally contains contributions from two distinct mechanisms: diffusion and phonon drag. In order to selectively extract the diffusion contribution, microwave-heating technique is used to raise the electron temperature with the lattice temperature kept at the bath temperature. The measurement of the diagonal thermopower  $S_{rr}$  provides a unique opportunity to probe the entropy of the system in the QH plateau regions. The measured  $S_{rr}$  takes large values on the order of 1 meV/K in the regions where  $\sigma_{rr} = 0$ , alternating the sign at exact even integer fillings, in accordance with the theoretical prediction.

1. \*Geometric resonances in the magnetoresistance of hexagonal lateral superlattices: Y. Kato, A. Endo, S. Katsumoto and Y. Iye, Phys. Rev. B **86** (2012) 235315(1-10).
2. \*Magnetization dependent rectification in (Ga,Mn)As tri-layer tunnel junctions: Y. Hashimoto, H. Amano, Y. Iye and S. Katsumoto, J. Phys.: Conf. Ser. **400** (2012) 042016(1-4).

3. \*Novel blockade due to spin-filtering with spin-orbit interaction: S. W. Kim, Y. Hashimoto, Y. Iye and S. Katsumoto, J. Phys.: Conf. Ser. **400** (2012) 042032(1-4).
4. \*Suppression of Andreev current due to transverse current flow in an InAs two-dimensional electrons: Y. Takahashi, Y. Hashimoto, Y. Iye and S. Katsumoto, Journal of Crystal Growth **378** (2013) S0022024813000705(1-4).
5. \*Control of magnetic anisotropy in (Ga,Mn)As with etching depth of specimen boundaries: Y. Hashimoto, Y. Iye and S. Katsumoto, J. Cryst. Growth **378** (2013) S0022024812008329(1-4).
6. Commensurability oscillations in the rf conductivity of unidirectional lateral superlattices: measurement of anisotropic conductivity by coplanar waveguide: A. Endo, T. Kajioka and Y. Iye, J. Phys. Soc. Jpn **82** (2013) 054710(1-7).
7. Diffusion Thermopower of Quantum Hall States Measured in Corbino Geometry: S. Kobayakawa, A. Endo and Y. Iye, J. Phys. Soc. Jpn **82** (2013) 053702(1-4).

## Katsumoto group

We have investigated the supercurrent through semiconductor 2-dimensional systems by applying spin current created with the spin Hall effect. We found the superconductivity established through the formation of the Andreev bound states is easily broken by small amount of spin current. This phenomenon seems to be promising in the application to low energy consumption logic devices.

1. Evidence of Spin-Filtering in Quantum Constrictions with Spin-Orbit Interaction: S. W. Kim, Y. Hashimoto, Y. Iye and S. Katsumoto, J. Phys. Soc. Jpn. **81** (2012) 054706 (1-5).
2. Detection of spin polarization utilizing singlet and triplet states in a single-lead quantum dot: T. Otsuka, Y. Sugihara, J. Yoneda, S. Katsumoto and S. Tarucha, Phys. Rev. B **86** (2012) 081308(1-4).
3. \*Geometric resonances in the magnetoresistance of hexagonal lateral superlattices: Y. Kato, A. Endo, S. Katsumoto and Y. Iye, Phys. Rev. B **86** (2012) 235315(1-10).
4. \*Magnetization dependent rectification in (Ga,Mn)As tri-layer tunnel junctions: Y. Hashimoto, H. Amano, Y. Iye and S. Katsumoto, J. Phys.: Conf. Ser. **400** (2012) 042016(1-4).
5. \*Novel blockade due to spin-filtering with spin-orbit interaction: S. W. Kim, Y. Hashimoto, Y. Iye and S. Katsumoto, J. Phys.: Conf. Ser. **400** (2012) 042032(1-4).
6. Robustness of spin filtering against current leakage in a Rashba-Dresselhaus-Aharonov-Bohm interferometer: S. Matityahu, A. Aharonov, O. Entin-Wohlman and S. Katsumoto, Phys. Rev. B **87** (2013) 205438(1-8).
7. \*Suppression of Andreev current due to transverse current flow in an InAs two-dimensional electrons: Y. Takahashi, Y. Hashimoto, Y. Iye and S. Katsumoto, Journal of Crystal Growth **378** (2013) S0022024813000705(1-4).
8. \*Control of magnetic anisotropy in (Ga,Mn)As with etching depth of specimen boundaries: Y. Hashimoto, Y. Iye and S. Katsumoto, J. Cryst. Growth **378** (2013) S0022024812008329(1-4).
9. Energy level spectroscopy of a quantum dot with a side coupled satellite dot: S. W. Kim, Y. Kuwabara, T. Otsuka, Y. Iye and S. Katsumoto, in: *AIP Conference Proceedings*, edited by Jisoon Ihm, Hyeonsik Cheong (American Institute of Physics, 2012), 393-394.

## Otani group

This year we put our focus on the following three topics including the skew scattering mechanism of spin Hall effects, spin relaxation mechanism in lateral spin valve structures, and collective dynamics of coupled magnetic vortices. Concerning the first topic, we have performed collaborative research with German and French groups to find best combination of materials to induce large spin Hall effects originating from the skew scattering mechanisms. Based on these theoretical studies we have succeeded in demonstrating the giant spin Hall effect by doping copper with small amount of bismuth. Apart from the skew scattering studies, we have shown for the first time a possibility to use spin Hall effect as a means to detect higher order spin fluctuation. As to the second topic on the lateral spin valve, we have found the contribution of the surface spin flip scattering was non-negligible at low temperatures and was suppressed significantly by the surface capping layer of MgO. Thereby we were able to clarify that the spin relaxation process was well described in the framework of Elliot-Yafet mechanism. Furthermore we have demonstrated the non-local spin valve effect in the lateral spin valve structure consisting of silicon nano-wire and permalloy. As to the third topic on vortex dynamics, our final goal is to realize magnonic crystals. For this, we have been studying collective spin dynamics mediated by the dynamic dipolar interaction. When the nano-scale ferromagnetic

elements are very closely spaced with a separation of 50 nm, a gradual transition from completely uniform collective regime to a completely non-collective regime was observed as the azimuthal angle varies from 0° to 45°.

1. Anisotropy in collective precessional dynamics in arrays of Ni<sub>80</sub>Fe<sub>20</sub> nanoelements: B. Rana, D. Kumar, S. Barman, S. Pal, R. Mandal, Y. Fukuma, Y. Otani, S. Sugimoto and A. Barman, *J. Appl. Phys.* **111** (2012) 07D503(1-3).
2. Nonlinear motion of magnetic vortex cores during fast magnetic pulses: K. Fukumoto, K. Arai, T. Kimura, Y. Otani and T. Kinoshita, *Phys. Rev. B* **85** (2012) 134414(1-4).
3. Giant Spin Hall Effect Induced by Skew Scattering from Bismuth Impurities inside Thin Film CuBi Alloys: Y. Niimi, Y. Kawanishi, D. H. Wei, C. Deranlot, H. X. Yang, M. Chshiev, T. Valet, A. Fert and Y. Otani, *Phys. Rev. Lett.* **109** (2012) 156602(1-5).
4. Spin relaxation mechanism in silver nanowires covered with MgO protection layer: H. Idzuchi, Y. Fukuma, L. Wang and Y. Otani, *Appl. Phys. Lett.* **101** (2012) 022415(1-4).
5. Temperature Evolution of Spin-Polarized Electron Tunneling in Silicon Nanowire–Permalloy Lateral Spin Valve System: J. Tarun, S. Huang, Y. Fukuma, H. Idzuchi, Y. Otani, N. Fukata, K. Ishibashi and S. Oda, *Appl. Phys. Express* **5** (2012) 045001(1-3).
6. Optically Induced Tunable Magnetization Dynamics in Nanoscale Co Antidot Lattices: R. Mandal, S. Saha, D. Kumar, S. Barman, S. Pal, K. Das, A. K. Raychaudhuri, Y. Fukuma, Y. Otani and A. Barman, *ACS Nano* **6** (2012) 3397-3403.
7. The spin Hall effect as a probe of nonlinear spin fluctuations: D. H. Wei, Y. Niimi, B. Gu, T. Ziman, S. Maekawa and Y. Otani, *Nature Commun.* **3** (2012) 1058(1-5).
8. Towards coherent spin precession in pure-spin current: H. Idzuchi, Y. Fukuma and Y. Otani, *Sci. Rep.* **2** (2012) 628(1-5).
9. Perfect Alloys for Spin Hall Current-Induced Magnetization Switching: M. Gradhand, D. V. Fedorov, P. Zahn, I. Mertig, Y. Otani, Y. Niimi, L. Vila and A. Fert, *SPIN* **02** (2012) 1250010(1-8).

## Komori group

Electronic and atomic structures of the Au-adsorbed Ge(111) surface are studied by ARPES and STM. A triangle structure, which is mobile at room temperature on the surface, selectively dopes the electron-like metallic surface band. A band gap over 0.3 eV was found by ARPES in a regular array of the graphene nanoribbons that were formed selectively on the terrace of vicinal SiC(0001) surfaces by molecular beam epitaxy. The width of each nanoribbon is 10 nm. The gap size increases with decreasing the width of the nanoribbons. Regular arrays of square CrN islands were thermally fabricated on the Cu(001) surface. A short-range attractive interaction among the islands is the origin of the self-assembly.

1. <sup>†</sup>Uniaxial deformation of graphene Dirac cone on a vicinal SiC substrate: K. Nakatsuji, T. Yoshimura, F. Komori, K. Morita and S. Tanaka, *Phys. Rev. B* **85** (2012) 195416(1-6).
2. \*Epitaxial Rh-doped SrTiO<sub>3</sub> thin film photocathode for water splitting under visible light irradiation: S. Kawasaki, K. Nakatsuji, J. Yoshinobu, F. Komori, R. Takahashi, M. Lippmaa, K. Mase and A. Kudo, *Appl. Phys. Lett.* **101** (2012) 033910 (1-4).
3. \*Elucidation of Rh-Induced In-Gap States of Rh:SrTiO<sub>3</sub> Visible-Light-Driven Photocatalyst by Soft X-ray Spectroscopy and First-Principles Calculations: S. Kawasaki, K. Akagi, K. Nakatsuji, S. Yamamoto, I. Matsuda, Y. Harada, J. Yoshinobu, F. Komori, R. Takahashi, M. Lippmaa, C. Sakai, H. Niwa, M. Oshima, K. Iwashina and A. Kudo, *J. Phys. Chem. C* **116** (2012) 24445-24448.
4. Selective doping in a surface band and atomic structures of the Ge(111) ( $\sqrt{3} \times \sqrt{3}$ )R30°–Au surface: K. Nakatsuji, Y. Motomura, R. Niikura and F. Komori, *J. Phys.: Condens. Matter* **25** (2013) 045007 (9).
5. Fabrication and characterization of strain-driven self-assembled CrN nanoislands on Cu(001): P. Krukowski, T. Iimori, K. Nakatsuji, M. Yamada and F. Komori, *J. Appl. Phys.* **113** (2013) 174309 (5).
6. <sup>†</sup>Graphene nanoribbons on vicinal SiC surfaces by molecular beam epitaxy: T. Kajiwara, Y. Nakamori, A. Visikovskiy, T. Iimori, F. Komori, K. Nakatsuji, K. Mase and S. Tanaka, *Phys. Rev. B* **87** (2013) 121407R (4).
7. Growth and structure of CrN nanoislands on Cu(001) studied by scanning tunneling microscopy and X-ray photoemission spectroscopy: P. Krukowski, T. Iimori, K. Nakatsuji, M. Yamada and F. Komori, *Thin Solid Films* **531** (2013) 251-254.

8. <sup>†</sup>エピタキシャルグラフェンの成長と電子物性: 田中 悟, 中辻 寛, 小森 文夫, 日比野 浩樹, 触媒 **54** (2012) 386-391.
9. 表面磁性: 小森 文夫, 「現代表面科学シリーズ 3巻 表面物性」, 第4章, 坂本 一之, (共立出版, 東京都文京区小日向4丁目6番19号, 2012), 132-172.
10. エピタキシャルグラフェンの電子状態: 中辻 寛, 小森 文夫, 「ポストシリコン半導体-ナノ成膜ダイナミクスと基板・界面効果-」, 6章 2.2, 財満 鎮明, (NTS, 東京都文京区湯島 2-16-16, 2013), in print.

### **Yoshinobu group**

We conducted several research projects in the fiscal year 2012. (1) The kinetic and geometric isotope effects and energy-level alignment of cyclohexane on clean and H-preadsorbed Rh(111) surfaces using IRAS, TPD, STM, SPA-LEED and SR-PES. (2) The adsorption states of CO<sub>2</sub> on Cu(997) studied by SR-PES and IRAS. (3) The thin film growth and electronic states of pentacene film on chemically modified Si(100) surfaces using PES and 4-probe surface conductivity measurements. (4) Spectroscopic characterization and transport properties of aromatic monolayers covalently attached to Si(111) surfaces by wet-chemical methods.

1. \*Epitaxial Rh-doped SrTiO<sub>3</sub> thin film photocathode for water splitting under visible light irradiation: S. Kawasaki, K. Nakatsuji, J. Yoshinobu, F. Komori, R. Takahashi, M. Lippmaa, K. Mase and A. Kudo, *Appl. Phys. Lett.* **101** (2012) 033910 (1-4).
2. Kinetic and geometric isotope effects originating from different potential energy surfaces: cyclohexane on Rh(111): T. Koitaya, S. Shimizu, K. Mukai, S. Yoshimoto and J. Yoshinobu, *J. Chem. Phys.* **136** (2012) 214705 (9 pages).
3. \*Elucidation of Rh-Induced In-Gap States of Rh:SrTiO<sub>3</sub> Visible-Light-Driven Photocatalyst by Soft X-ray Spectroscopy and First-Principles Calculations: S. Kawasaki, K. Akagi, K. Nakatsuji, S. Yamamoto, I. Matsuda, Y. Harada, J. Yoshinobu, F. Komori, R. Takahashi, M. Lippmaa, C. Sakai, H. Niwa, M. Oshima, K. Iwashina and A. Kudo, *J. Phys. Chem. C* **116** (2012) 24445-24448.
4. Chemically homogeneous and thermally reversible oxidation of epitaxial graphene: Md. Zakir Hossain, J. E. Johns, K. H. Bevan, H. J. Karmel, Y. T. Liang, S. Yoshimoto, K. Mukai, T. Koitaya, J. Yoshinobu, M. Kawai, A. M. Lear, L. L. Kesmodel, S. L. Tait and M. C. Hersam, *Nature Chem.* **4** (2012) 305-309.
5. Energy level alignment of cyclohexane on Rh(111): the importance of interfacial dipole and final-state screening: T. Koitaya, K. Mukai, S. Yoshimoto and J. Yoshinobu, *J. Chem. Phys.* **138** (2013) 044702 (9 pages).
6. Site-specific chemical states of adsorbed CO on Pt(997): a high resolution XPS study: S. Shimizu, H. Noritake, T. Koitaya, K. Mukai, S. Yoshimoto and J. Yoshinobu, *Surf. Sci.* **608** (2013) 220-225.
7. Spectroscopic Characterization and Transport Properties of Aromatic Monolayers Covalently Attached to Si(111) Surfaces: Y. Harada, T. Koitaya, K. Mukai, S. Yoshimoto and J. Yoshinobu, *J. Phys. Chem. C* **117** (2013) 7497-7505.
8. 「読書のススメ」: 吉信 淳, *化学 Vol.67* (2012) 58.
9. Potential Energy Surface of NO on Pt(997): Adsorbed States and Surface Diffusion: N. Tsukahara and J. Yoshinobu, *Advances in Physical Chemistry* **2012** (2012) Article ID 571657 (9 pages).

### **Hasegawa group**

We have developed spin-polarized scanning tunneling microscopy (SP-STM), and studied magnetic properties of nano-size Co island structures, whose dimension ranges 10-30 nm in lateral size and 1 nm in thickness, formed on Ag(111). From the Moiré intensities observed in STM images, we found two structurally different Co islands on the substrate. Magnetic properties revealed by the SP-STM are also different; one has an out-of-plane magnetization while the other does not. As pristine hcp Co has strong magnetocrystalline anisotropy along the c-axis whereas in fcc Co thin films shape anisotropy prefers in-plane magnetization, we assign the two structures as hcp and fcc Co structures, respectively. We also developed a scanning potentiometry, which enables us to visualize nanoscale spatial distribution of electrical potential under current flow. The potential drops due to finite electrical resistance at grain boundaries were clearly observed in a Au thin film. The method will be applied to two-dimensional surface electron systems that show superconductivity at low temperatures.

1. Thermally assisted penetration and exclusion of single vortex in mesoscopic superconductors: S.-Z. Lin, T. Nishio, L. Bulaevskii, M. Graf and Y. Hasegawa, *Phys. Rev. B* **85** (2012) 134534(1-7).
2. Development of Scanning Tunneling Potentiometry for Semiconducting Samples: M. Hamada and Y. Hasegawa, *Jpn. J. Appl. Phys.* **51** (2012) 125202.

3. 電子定在波とフリーデル振動: 長谷川 幸雄, 小野 雅紀, 鈴木 孝将, 江口 豊明, 日本物理学会誌 **67** (2012) 6-13.
4. Observation of Vortex Clustering in Nano-Size Superconducting Pb Island Structures by Low-Temperature Scanning Tunneling Microscopy/ Spectroscopy: T. Tominaga, T. Sakamoto, T. Nishio, T. An, T. Eguchi, Y. Yoshida and Y. Hasegawa, J. Supercond. Nov. Magn. **25** (2012) 1375-1378.
5. 放射光励起走査トンネル顕微鏡による高分解能元素分析: 江口豊明・奥田太一・木下豊彦・長谷川幸雄, 顕微鏡 **47** (2012) 14-17.
6. Trapping and squeezing of vortices in voids directly observed by scanning tunneling microscopy and spectroscopy: T. Tominaga, T. Sakamoto, H. Kim, T. Nishio, T. Eguchi and Y. Hasegawa, Phys. Rev. B **87** (2013) 195434.
7. 低温走査トンネル顕微鏡によるナノサイズ超伝導体の研究: 坂本 崇樹, 富永 貴亮, 西尾 隆宏, 江口 豊明, 吉田 靖雄, 長谷川 幸雄, 表面科学 **33** (2012) 443-448.

### Lippmaa group

This year saw progress on three main fronts: photocatalytic materials, spin filters, and the pyroelectric analysis of ferroelectrics. In the catalyst project, we analyzed the electronic structure of Rh-doped SrTiO<sub>3</sub> and showed that the valence state of the Rh dopant can be controlled by a suitable selection of crystal growth parameters. The presence of a mid-gap acceptor state in Rh<sup>4+</sup>:SrTiO<sub>3</sub> was confirmed, explaining the reduced solar energy conversion efficiency. The tunnel junction project culminated with a successful construction of spin-filter tunnel junctions based on ferromagnetic insulator barrier layers. Record-making magnetoresistance ratios were observed in the tunnel junctions. A pyroelectric analysis system was used to analyze the presence of ferroelectricity in Magnetite thin films. A new buffer layer technique was developed for growing perfectly oriented magnetite thin films.

1. Sub-bandgap photocurrent effects on dynamic pyroelectric measurement in Pt/PbTiO<sub>3</sub>/Nb:SrTiO<sub>3</sub> heterostructures: R. Takahashi, T. Tybell and M. Lippmaa, J. Appl. Phys. **112** (2012) 014111(1-6).
2. Pyroelectric detection of spontaneous polarization in magnetite thin films: R. Takahashi, H. Misumi and M. Lippmaa, Phys. Rev. B **86** (2012) 144105 (1-7).
3. Development of a new laser heating system for thin film growth by chemical vapor deposition: E. Fujimoto, M. Sumiya, T. Ohnishi, M. Lippmaa, M. Takeguchi, H. Koinuma and Y. Matsumoto, Rev. Sci. Instrum. **83** (2012) 094701(1-6).
4. Spin-Filter Tunnel Junction with Matched Fermi Surfaces: T. Harada, I. Ohkubo, M. Lippmaa, Y. Sakurai, Y. Matsumoto, S. Muto, H. Koinuma and M. Oshima, Phys. Rev. Lett. **109** (2012) 076602(1-5).
5. \*Epitaxial Rh-doped SrTiO<sub>3</sub> thin film photocathode for water splitting under visible light irradiation: S. Kawasaki, K. Nakatsuji, J. Yoshinobu, F. Komori, R. Takahashi, M. Lippmaa, K. Mase and A. Kudo, Appl. Phys. Lett. **101** (2012) 033910 (1-4).
6. \*Elucidation of Rh-Induced In-Gap States of Rh:SrTiO<sub>3</sub> Visible-Light-Driven Photocatalyst by Soft X-ray Spectroscopy and First-Principles Calculations: S. Kawasaki, K. Akagi, K. Nakatsuji, S. Yamamoto, I. Matsuda, Y. Harada, J. Yoshinobu, F. Komori, R. Takahashi, M. Lippmaa, C. Sakai, H. Niwa, M. Oshima, K. Iwashina and A. Kudo, J. Phys. Chem. C **116** (2012) 24445-24448.
7. Self-Template Growth of Orientation-Controlled Fe<sub>3</sub>O<sub>4</sub> Thin Films: R. Takahashi, H. Misumi and M. Lippmaa, Cryst. Growth Des. **12** (2012) 2679-2683.
8. †Photo-Electrochemical Synthesis of Silver-Oxide Clathrate Ag<sub>7</sub>O<sub>8</sub>NO<sub>3</sub> on SrTiO<sub>3</sub>: R. Tanaka, S. Takata, R. Takahashi, J. K. Grepstad, T. Tybell and Y. Matsumoto, Electrochim. Solid-State Lett. **15** (2012) E19-E22.
9. Large Tunnel Magnetoresistance in Epitaxial Oxide Spin-Filter Tunnel Junctions: T. Harada, I. Ohkubo, M. Lippmaa, Y. Sakurai, Y. Matsumoto, S. Muto, H. Koinuma and M. Oshima, Adv. Funct. Mater. **22** (2012) 4471-4475.
10. Nonmagnetic Sc Substitution in a Perovskite Ferromagnetic Insulator Pr<sub>0.8</sub>Ca<sub>0.2</sub>MnO<sub>3</sub>: T. Harada, R. Takahashi and M. Lippmaa, J. Phys. Soc. Jpn. **82** (2013) 014801 (1-5).
11. Combinatorial Nanoscience and Technology for Solid-state Materials: H. Koinuma, R. Takahashi, M. Lippmaa, S.-Y. Jeong, Y. Matsumoto, T. Chikyo and S. Suzuki, in: *Handbook of Advanced Ceramics*, Ch 11.1.11, edited by S. Somiya, (Academic Press, Amsterdam, 2013), 1103-1124.

# Division of Physics in Extreme Conditions

## Uwatoko group

We report the discovery of a pressure-induced heavy fermion superconductivity in a nonmagnetic orbital ordering state in the cubic compound  $\text{PrTi}_2\text{Al}_{20}$ . The strong orbital fluctuations may provide a nonmagnetic glue for Cooper pairing. The results suggest a generic phase diagram hosting unconventional superconductivity on the border of orbital order, paving a new path for further research on novel quantum criticality and superconductivity due to orbital fluctuations. We have performed XAS, NMR, magnetization measurements in relatively large fields and specific heat up to 3 T on heavy fermion  $\text{YbCo}_2\text{Zn}_{20}$  to investigate the possibility that magnetic field gives rise to the delocalization of 4f electrons. Correlations between Yb moments are weak without significant enhancement in the  $\chi(\mathbf{q})$  spectrum at least in a field, which may explain the lack of magnetic order in  $\text{YbCo}_2\text{Zn}_{20}$  in spite of the existence of distinct local moments. We measured the microwave surface impedances and obtained the superfluid density and flux flow resistivity in single crystals of a phosphor-doped iron-based superconductor  $\text{SrFe}_2(\text{As}_{0.7}\text{P}_{0.3})_2$  single crystals ( $T_C = 25$  K). These results indicate the presences of line nodes on at least one band and modulated nodeless gap with deep minimum on the same bands and or other bands. We report a comprehensive high-pressure study on the triple-layer  $\text{T}'\text{-La}_4\text{Ni}_3\text{O}_8$  with a suite of experimental probes, including structure determination, magnetic, and transport properties up to 50 GPa. The presence of isolated Ni sites with apical oxygen in the  $\text{T}'$  structure leads to a variable-range-hopping conductivity in the LS phase. The high pressure structural study reveals that a new  $\text{T}^+$  structure is stabilized under  $P > 21$  GPa. We have performed inelastic neutron scattering measurements in the ferroelectric noncollinear magnetic phase of  $\text{CuFe}_{0.965}\text{Ga}_{0.035}\text{O}_2$  under applied uniaxial pressure. The reduction of the spin-lattice coupling, which reflects the partial release of the magnetic frustration due to the nonmagnetic substitution, can also contribute to the emergence of the noncollinear incommensurate magnetic ground state. We have measured the temperature-dependent resistivity of  $(\text{TMTTF})_2\text{PF}_6$  up to 7 GPa using a turnbuckle-type diamond anvil cell (DAC) and at magnetic fields of up to 5 T. The Ginzburg–Landau coherence lengths for three different axes obtained from this work show that  $(\text{TMTTF})_2\text{PF}_6$  is an anisotropic three-dimensional superconductor. We have developed a high-pressure and high-field ESR system using the combination of a commercially available SQUID magnetometer up to 5 T and a clamp-type piston cylinder pressure cell up to 1.5 GPa.

1. \*Block magnetism coupled with local distortion in the iron-based spin-ladder compound  $\text{BaFe}_2\text{Se}_3$ : Y. Nambu, K. Ohgushi, S. Suzuki, F. Du, M. Avdeev, Y. Uwatoko, K. Munakata, H. Fukazawa, S. Chi, Y. Ueda and T. Sato, Phys. Rev. B **85** (2012) 064413(1-5).
2. Effect of pressure on the neutron spin resonance in the unconventional superconductor  $\text{FeTe}_{0.6}\text{Se}_{0.4}$ : K. Marty, A. D. Christianson, A. M. dos Santos, B. Sipos, K. Matsubayashi, Y. Uwatoko, J. A. Fernandez-Baca, C. A. Tulk, T. A. Maier, B. C. Sales and M. D. Lumsden, Phys. Rev. B **86** (2012) 220509(1-5).
3. <sup>†</sup>Investigation of the superconducting gap structure in  $\text{SrFe}_2(\text{As}_{0.7}\text{P}_{0.3})_2$  by magnetic penetration depth and flux flow resistivity analysis: H. Takahashi, T. Okada, Y. Imai, K. Kitagawa, K. Matsubayashi, Y. Uwatoko and A. Maeda, Phys. Rev. B **86** (2012) 144525(1-5).
4. Magnetic anisotropy of Kondo semiconductor  $\text{CeT}_2\text{Al}_{10}$  ( $T = \text{Ru, Os}$ ) in the ordered state: H. Tanida, Y. Nonaka, D. Tanaka, M. Sera, Y. Kawamura, Y. Uwatoko, T. Nishioka and M. Matsumura, Phys. Rev. B **85** (2012) 205208(1-11).
5. Magnetic interactions in the multiferroic phase of  $\text{CuFe}_{1-x}\text{Ga}_x\text{O}_2$  ( $x=0.035$ ) refined by inelastic neutron scattering with uniaxial-pressure control of domain structure: T. Nakajima, S. Mitsuda, J. T. Haraldsen, R. S. Fishman, T. Hong, N. Terada and Y. Uwatoko, Phys. Rev. B **85** (2012) 144405 (1-7).
6. Microwave surface-impedance measurements of the electronic state and dissipation of magnetic vortices in superconducting LiFeAs single crystals: T. Okada, H. Takahashi, Y. Imai, K. Kitagawa, K. Matsubayashi, Y. Uwatoko and A. Yamada, Phys. Rev. B **2** (2012) 064516 (1-5).
7. Weakly ferromagnetic metallic state in heavily doped  $\text{Ba}_{1-x}\text{K}_x\text{Mn}_2\text{As}_2$ : JK. Bao, H. Jiang, YL. Sun, WH. Jiao, CY. Shen, HJ. Guo, Y. Chen, CM. Feng, HQ. Yuan, ZA. Xu, GH. Cao, R. Sasaki, T. Tanaka, K. Matsubayashi and Y. Uwatoko, Phys. Rev. B **85** (2012) 144523(1-6).
8. \*Pressure-Induced Heavy Fermion Superconductivity in the Nonmagnetic Quadrupolar System  $\text{PrTi}_2\text{Al}_{20}$ : K. Matsubayashi, T. Tanaka, A. Sakai, S. Nakatsuji, Y. Kubo and Y. Uwatoko, Phys. Rev. Lett. **109** (2012) 187004(1-5).
9. <sup>†</sup>Correlation between superconductivity and structural properties under high pressure of iron pnictide superconductor  $\text{Ce}_{0.6}\text{Y}_{0.4}\text{FeAsO}_{0.8}\text{F}_{0.2}$ : M. Kanagaraj, S. Arumugam, RS. Kumar, NRT. Selvan, SE. Muthu, H. Yoshino, K. Murata, K. Matsubayashi, Y. Uwatoko, S. Sinogeikin, A. Cornelius, AK. Ganguli and YS. Zhao, Appl. Phys. Lett. **100** (2012) 052601(1-4).

10. Conductivity and Incommensurate Antiferromagnetism of  $\text{Fe}_{1.02}\text{Se}_{0.10}\text{Te}_{0.90}$  under pressure: N. Katayama, K. Matsubayashi, Y. Nomura, S. J. Leao, M. A. Green, T. J. Sato, Y. Uwatoko, M. Fujita, K. Yamada, R. Arita and S. H. Lee, *Europhys. Lett.* **98** (2012) 37002 (1-6).
11. <sup>†</sup>Uniaxial-stress enhancement of spin-driven ferroelectric polarization in a multiferroic  $\text{CuFe}_{1-x}\text{Ga}_x\text{O}_2$ : S. Mitsuda, K. Yoshitomi, T. Nakajima, C. Kaneko, H. Yamazaki, M. Kosaka, N. Aso, Y. Uwatoko, Y. Noda, M. Matsuura, N. Terada, S. Wakimoto, M. Takeda and K. Kakurai, *J. Phys.: Conf. Series* **340** (2012) 012062(1-8).
12. Uniaxial-Pressure Control of Magnetic Phase Transitions in a Frustrated Magnet  $\text{CuFe}_{1-x}\text{Ga}_x\text{O}_2$  ( $x=0, 0.018$ ): T. Nakajima, S. Mitsuda, K. Takahashi, K. Yoshitomi, K. Masuda, C. Kaneko, Y. Honma, S. Kobayashi, H. Kitazawa, M. Kosaka, N. Aso, Y. Uwatoko, N. Terada, S. Wakimoto, M. Takeda and K. Kakurai, *J. Phys. Soc. Jpn* **81** (2012) 094710(1-8).
13. Heat Capacity Measurement of Heavy Fermion  $\text{YbCo}_2\text{Zn}_{20}$  under Magnetic Field: R. Yamanaka, K. Matsubayashi, Y. Saiga, T. Kawae and Y. Uwatoko, *J. Phys.: Conf. Ser.* **391** (2012) 012078.
14. <sup>†</sup>Anisotropy of Upper Critical Field in a One-Dimensional Organic System,  $(\text{TMTTF})_2\text{PF}_6$  under High Pressure: M. Kano, M. Hatsumi, K. Matsubayashi, M. Itoi, M. Hedo, T. P. Murphy, S. W. Tozer, Y. Uwatoko and T. Nakamura, *J. Phys. Soc. Jpn.* **81** (2012) 024716 (1-7).
15. <sup>†</sup>Magnetic Properties of  $\text{TbPd}_2\text{Si}_2$  Single Crystal: Y. Zhang, T. Fujiwara, Y. Uwatoko and T. Shigeoka, *J. Phys. Soc. Jpn.* **81** (2012) 044702(1-5).
16. Mechanism of Field Induced Fermi Liquid State in Yb-Based Heavy-Fermion Compound: X-ray Absorption Spectroscopy and Nuclear Magnetic Resonance Studies of  $\text{YbCo}_2\text{Zn}_{20}$ : T. Mito, T. Koyama, K. Nakagawara, T. Ishida, K. Ueda, T. Kohara, K. Matsubayashi, Y. Saiga, K. Munakata, Y. Uwatoko, M. Mizumaki, N. Kawamura, B. Idzikowski and M. Reiffers, *J. Phys. Soc. Jpn.* **81** (2012) 033706(1-4).
17. Pressure effects on the superconducting transition of ytterbium doped  $\text{Ce}_{0.6}\text{Yb}_{0.4}\text{FeAsO}_{0.9}\text{F}_{0.1}$ : S. Arumugam, M. Kanagaraj, N. R. T. Selvan, S. E. Muthu, J. Prakash, G. S. Thakur, A. K. Ganguli, H. Yoshino, K. Murata, K. Matsubayashi and Y. Uwatoko, *Phys. Status Solidi: Rapid Res. Lett.* **6** (2012) 220-222.
18. Scanning tunneling microscopy/spectroscopy of vortices in LiFeAs: T. Hanaguri, K. Kitagawa, K. Matsubayashi, Y. Mazaki, Y. Uwatoko and H. Takagi, *Phys. Rev. B* **85** (2012) 214505(1-9).
19. Pressure-induced positive electrical resistivity coefficient in Ni-Nb-Zr-H glassy alloy: M. Fukuhara, C. Gangli, K. Matsubayashi and Y. Uwatoko, *Appl. Phys. Lett.* **100** (2012) 253114(1-3).
20. Pressure Effect on the Structural Transition and Suppression of the High-Spin State in the Triple-Layer  $T'_{-}\text{La}_4\text{Ni}_3\text{O}_8$ : J. G. Cheng, J. S. Zhou, J. B. Goodenough, H. D. Zhou, K. Matsubayashi, Y. Uwatoko, P. P. Kong, C. Q. Jin, W. G. Yang and G. Y. Shen, *Phys. Rev. Lett.* **108** (2012) 236403(1-5).
21. Development of high-pressure and high-field ESR system using SQUID magnetometer: T. Sakurai, K. Fujimoto, R. Goto, S. Okubo, H. Ohta and Y. Uwatoko, *Journal of Magnetic Resonance* **223** (2012) 41-45.
22. <sup>†\*</sup>High-Field Phase Diagram of  $\text{SmRu}_4\text{P}_{12}$  Determined by Ultrasonic Measurements in Pulsed Magnetic Field up to 55 T: M. Yoshizawa, H. Mitamura, F. Shichinomiya, S. Fukuda, Y. Nakanishi, H. Sugawara, T. Sakakibara and K. Kindo, *J. Phys. Soc. Jpn.* **82** (2013) 033602(1-5).
23. <sup>†</sup>Pressure and Substitution Effects on Transport and Magnetic Properties of  $\text{Y}_{1-x}\text{R}_x\text{Co}_2$  Systems with Static Magnetic Disorder: M. Takeda, A. Teruya, S. Watanabe, S. Hirakawa, Y. Hiranaka, A. Nakamura, Y. Takaesu, K. Uchima, M. Hedo, T. Nakama, K. Yagasaki, K. Matsubayashi, Y. Uwatoko and A. T. Burkov, *J. Phys. Soc. Jpn.* **82** (2013) 014708 (1-6).
24. <sup>†</sup>Low energy excitations inside the vortex core of LiFe(As, P) single crystals investigated by microwave-surface impedance: T. Okada, H. Takahashi, Y. Imai, K. Kitagawa, K. Matsubayashi, Y. Uwatoko and A. Maeda, *J. Magn. Magn. Mater.* **331** (2013) 98-101.
25. Dielectric properties of single crystal spinels in the series  $\text{FeV}_2\text{O}_4$ ,  $\text{MnV}_2\text{O}_4$ , and  $\text{CoV}_2\text{O}_4$  in high magnetic fields: A. Kismaraha, J. S. Brooks, H. D. Zhou, E. S. Choi, K. Matsubayashi and Y. Uwatoko, *Phys. Rev. B* **87** (2013) 054432 (1-10).
26. Magnetic properties of spinel  $\text{CuCrZrS}_4$  under pressure: M. Ito, N. Kado, K. Matsubayashi, Y. Uwatoko, N. Terada, S. Ebisu and S. Nagata, *J. Magn. Magn. Mater.* **331** (2013) 98-101.
27. <sup>†</sup>High Field Magnetization of  $\text{TbPd}_2\text{Ge}_2$  Single Crystal: T. Shigeoka, T. Hasegawa, T. Fujiwara, A. Kondo, K. Kindo and Y. Uwatoko, *J. Low. Temp. Phys.* **170** (2013) 248-254.

## Osada group

(1) We have discussed the mechanism of interlayer surface transport due to helical edge state accompanying the quantum Hall ferromagnetic state in multilayer Dirac fermion systems by employing the tunneling picture. Since this surface state is not topologically protected, it must be diffusive due to spin-inversion scattering. This fact justifies the tunneling picture, in which inter-edge tunneling is regarded as a perturbation. We have concluded that the interlayer tunneling due to the helical surface state is allowed only when the magnetic field is parallel to the side surface of the crystal. (2) We have confirmed the above theoretical prediction by performing the experiment on organic Dirac fermion system  $\alpha$ -(BEDT-TTF)<sub>2</sub>I<sub>3</sub>. The saturation odf interlayer resistance occurs when the magnetic field was parallel to the stacking direction. Observed features are well explained by the above picture. This agreement indicates the appearance of the QH ferromagnetic phase with the helical edge state in  $\alpha$ -(BEDT-TTF)<sub>2</sub>I<sub>3</sub>.

1. Observation of Angle-Dependent Stark Cyclotron Resonance in a Layered Organic Conductor: A. Kumagai, T. Konoike, K. Uchida and T. Osada, J. Phys. Soc. Jpn. **81** (2012) 023708(1-4).
2. Specific Heat of the Multilayered Massless Dirac Fermion System: T. Konoike, K. Uchida and T. Osada, J. Phys. Soc. Jpn. **81** (2012) 043601(1-4).
3.  $\alpha$ -(BEDT-TTF)<sub>2</sub>I<sub>3</sub> におけるディラック電子系の比熱とその磁場効果: 鴻池 貴子, 内田 和人, 長田 俊人, 固体物理 **47** (2012) 301-307.
4. Specific heat study of massless Dirac fermion system  $\alpha$ -(BEDT-TTF)<sub>2</sub>I<sub>3</sub> under pressure: T. Konoike, K. Uchida and T. Osada, Phys. Status Solidi C **9** (2012) 1177-1179.
5. Magnetotransport in organic Dirac fermion system at the quantum limit: Interlayer Hall effect and surface transport via helical edge states: T. Osada, Phys. Status Solidi B **249** (2012) 962-966.
6. Angle-Dependent Magnetoresistance Oscillations and Charge Density Wave in the Organic Conductor  $\alpha$ -(BEDT-TTF)<sub>2</sub>KHg(SCN)<sub>4</sub>: K. Uchida, R. Yamaguchi, T. Konoike, T. Osada and W. Kang, J. Phys. Soc. Jpn. **82** (2013) 043714(1-4).
7. 強磁場下電気伝導に現れるサイクロトロン共鳴: 長田 俊人, 熊谷 篤, 内田 和人, 鴻池 貴子, 固体物理 **48** (2013) 65-73.
8. 角度依存シユタルクサイクロトロン共鳴とその応用: 鴻池 貴子, パリティ **28(4)** (2013) 42-45.
9. 角度依存シユタルクサイクロトロン共鳴法の開発: 長田 俊人, パリティ **28(1)** (2013) 20-23.
10. グラフェンの量子ホール伝導: 長田 俊人, 「グラフェンの機能と応用展望 II」, 16, 斎木 幸一郎, (シーエムシー出版, 東京, 2012), 169-184.

## Materials Design and Characterization Laboratory

### Y. Ueda group

The materials mainly studied in 2012 are (1) hollandites, (2) A-site ordered manganites, (3) iron-based spin ladder compounds, and (4) low dimensional or frustrated magnetic materials. The main findings in each material group are (1) novel structural distortion accompanied by metal-insulator transition in K<sub>2</sub>Cr<sub>8</sub>O<sub>16</sub> and charge order driven by K-vacancy order in K<sub>x</sub>Mn<sub>8</sub>O<sub>16</sub>, (2) Korringa-like relaxation in YBaMn<sub>2</sub>O<sub>6</sub>, (3) block and stripelike magnetism in BaFe<sub>2</sub>Se<sub>3</sub> and CsFe<sub>2</sub>Se<sub>3</sub>, respectively, and (4) magnetic phases up to 600 T in ZnCr<sub>2</sub>O<sub>4</sub> and incomplete devil's staircase magnetization curve in SrCu<sub>2</sub>(BO<sub>3</sub>)<sub>2</sub>.

1. \*Magnetic Phases of ZnCr<sub>2</sub>O<sub>4</sub> Revealed by Magneto-Optical Studies under Ultra-High Magnetic Fields up to 600 T: A. Miyata, H. Ueda, Y. Ueda, Y. Motome, N. Shannon, K. Penc and S. Takeyama, J. Phys. Soc. Jpn. **81** (2012) 114701(1-8).
2. Observation of Structural Change in the Novel Ferromagnetic Metal-Insulator Transition of K<sub>2</sub>Cr<sub>8</sub>O<sub>16</sub>: A. Nakao, Y. Yamaki, H. Nakao, Y. Murakami, K. Hasegawa, M. Isobe and Y. Ueda, J. Phys. Soc. Jpn. **81** (2012) 054710(1-6).
3. \*Synthesis, Structure and Electromagnetic Properties of Manganese Hollandite, K<sub>x</sub>Mn<sub>8</sub>O<sub>16</sub>: T. Kuwabara, M. Isobe, H. Gotou, T. Yagi, D. Nishio-Hamane and Y. Ueda, J. Phys. Soc. Jpn. **81** (2012) 104701(1-5).
4. Antiferromagnetism in the spin-gap system NaV<sub>2</sub>O<sub>5</sub>: Muon spin rataion measurements: V. G. Storchak, O. E. Parfenov, D. G. Eshchenko, R. L. Lichti, P. W. Mengyan, M. Isobe and Y. Ueda, Phys. Rev. B **85** (2012) 094406(1-6).

5. \*Block magnetism coupled with local distortion in the iron-based spin-ladder compound  $\text{BaFe}_2\text{Se}_3$ : Y. Nambu, K. Ohgushi, S. Suzuki, F. Du, M. Avdeev, Y. Uwatoko, K. Munakata, H. Fukazawa, S. Chi, Y. Ueda and T. Sato, Phys. Rev. B **85** (2012) 064413(1-5).
6.  $\mu\text{SR}$  investigation of magnetically ordered states in the A-site ordered perovskite manganites  $R\text{BaMn}_2\text{O}_6$  ( $R = \text{Y}$  and  $\text{La}$ ): Y. Kawasaki, T. Minami, Y. Kishimoto, T. Ohno, K. H. Satoh, A. Koda, R. Kadono, J. L. Gavilano, H. Luetkens, T. Nakajimna and Y. Ueda, Phys. Rev. B **86** (2012) 125141(1-8).
7.  $\mu^+\text{SR}$  study on ferromagnetic hollandites,  $\text{K}_2\text{Cr}_8\text{O}_{16}$  and  $\text{Rb}_2\text{Cr}_8\text{O}_{16}$ : J. Sugiyama, H. Nozaki M. Mänsson, K. Prša, D. Andreica, A. Amato, M. Isobe and Y. Ueda, Phys. Rev. B **85** (2012) 214407(1-8).
8. Infrared phonons and specific heat in the gapped quantum magnet  $\text{Ba}_3\text{Cr}_2\text{O}_8$ : Z. Wang, M. Schmidt, A. Günther, F. Mayr, Y. Wan, S. -H. Lee, H. Ueda, Y. Ueda, A. Loidl and J. Deisenhofer, Phys. Rev. B **85** (2012) 224304(1-5).
9. Korringa-like relaxation in the high-temperature phase of A-site ordered  $\text{YBaMn}_2\text{O}_6$ : S. Schaile, H. -A. Krug von Nidda, J. Deisenhofer, A. Loidl, T. Nakajima and Y. Ueda, Phys. Rev. B **85** (2012) 205121(1-5).
10. \*Stripelike magnetism in a mixed-valence insulating state of the Fe-based ladder compound  $\text{CsFe}_2\text{Se}_3$ : F. Du, K. Ohgushi, Y. Nambu, T. Kawakami, M. Avdeev, Y. Hirata, Y. Watanabe, T.-J. Sato and Y. Ueda, Phys. Rev. B **85** (2012) 214436(1-5).
11.  $^{51}\text{V-NMR}$  study of antiferromagnetic state and spin dynamics in quasi-one-dimensional  $\text{BaCo}_2\text{V}_2\text{O}_8$ : Y. Ideta, Y. Kawasaki, Y. Kishimoto, T. Ohno, Y. Michihiro, Z. He, Y. Ueda and M. Itoh, Phys. Rev. B **86** (2012) 094433(1-5).
12. Two-dimensional charge fluctuation in  $\beta\text{-Na}_{0.33}\text{V}_2\text{O}_5$ : K. Ohwada, T. Yamauchi, Y. Fujii and Y. Ueda, Phys. Rev. B **85** (2012) 134102(1-4).
13.  ${}^{\dagger*}$ Quadruple-layered perovskite  $(\text{CuCl})\text{Ca}_2\text{NaNb}_4\text{O}_{13}$ : A. Kitada, Y. Tsujimoto, T. Yamamoto, Y. Kobayashi, Y. Narumi, K. Kindo, A. A. Aczel, G. M. Luke, Y. J. Uemura, Y. Kiuchi, Y. Ueda, K. Yoshimura, Y. Ajiro and H. Kageyama, J. Solid State Chem. **185** (2012) 10-17.
14. Orbital order in layered manganites probed with  $^{57}\text{Fe}$  Mössbauer spectroscopy: Y. Ueda, K. Nomura and A. I. Rykov, Hyp. Int. **208** (2012) 19-23.
15. Ferromagnetic hollandite  $\text{K}_2\text{Cr}_8\text{O}_{16}$ : J. Sugiyama, H. Nozaki, M. Mansson, K. Prsa, A. Amato, M. Isobe and Y. Ueda, Physics Procedia **30** (2012) 186-189.
16.  $\mu\text{SR}$  Investigation of the Hollandite Vanadate  $\text{K}_2\text{V}_8\text{O}_{16}$ : K. H. Chow, M. Mansson, Y. Ikeda, J. Sugiyama, O. Ofer, E. J. Ansaldo, J. H. Brewer, M. Isobe, H. Gotou, T. Yagi, Y. Ueda and C. Baines, Physics Procedia **30** (2012) 117-120.
17. Revisiting the layered  $\text{LiNi}_{0.4}\text{Mn}_{0.4}\text{Co}_{0.2}\text{O}_2$ : a magnetic approach: X. Bie, L. Liu, H. Ehrenberg, Y. Wei, K. Nikolowski, C. Wang, Y. Ueda, H. Chen, G. Chen and F. Du, RSC Advances **2** (2012) 9986-9992.
18. \*Incomplete Devil's Staircase in the Magnetization Curve of  $\text{SrCu}_2(\text{BO}_3)_2$ : M. Takigawa, M. Horvatic, T. Waki, S. Kramer, C. Berthier, F. L. Bertrand, I. Sheikin, H. Kageyama, Y. Ueda and F. Mila, Phys. Rev. Lett. **110** (2013) 067210(1-5).

## Hiroi group

Various novel compounds are presented. For example, a unique type of frustrated lattice is found in two A-site ordered spinel oxides,  $\text{LiGaCr}_4\text{O}_8$  and  $\text{LiInCr}_4\text{O}_8$ . Because of the large size mismatch between  $\text{Li}^+$  and  $\text{Ga}^{3+}/\text{In}^{3+}$  ions at the A site, the pyrochlore lattice made up of  $\text{Cr}^{3+}$  ions carrying spin 3/2 becomes an alternating array of small and large tetrahedra, i.e., a “breathing” pyrochlore lattice.  $\text{YCr}_6\text{Ge}_6$ , comprising a kagome lattice made up of Cr atoms, is a plausible candidate compound for a kagome metal that is expected to exhibit anomalous phenomena such as flat-band ferromagnetism. A unique structural transition in single crystals of the spin-1/2 quasi-kagomé antiferromagnet volborthite,  $\text{Cu}_3\text{V}_2\text{O}_7(\text{OH})_2 \cdot 2\text{H}_2\text{O}$ , is found, whereby the unpaired electron “switches” from one  $d$  orbital to another upon cooling, so that it is called the orbital switching transition. Tetrahedral magnetic order and the metal-insulator transition in the pyrochlore lattice of  $\text{Cd}_2\text{Os}_2\text{O}_7$  are studied in detail. Rattling and superconducting properties of the cage compound  $\text{Ga}_x\text{V}_2\text{Al}_{20}$  are reported.

1. The spin dynamics in distorted kagome lattices: a comparative Raman study: D. Wulferding, P. Lemmens, H. Yoshida, Y. Okamoto and Z. Hiroi, J. Phys.: Condens. Matter **24** (2012) 185602(1-4).
2. Distorted Kagome Lattice Generated by a Unique Orbital Arrangement in the Copper Mineral  $\text{KCu}_3\text{As}_2\text{O}_7(\text{OH})_3$ : Y. Okamoto, H. Ishikawa, J. G. Nilsen and Z. Hiroi, J. Phys. Soc. Jpn. **81** (2012) 033707(1-4).

3. \*High-Field Phase Diagram and Spin Structure of Volborthite  $\text{Cu}_3\text{V}_2\text{O}_7(\text{OH})_2 \cdot 2\text{H}_2\text{O}$ : M. Yoshida, M. Takigawa, S. Krämer, S. Mukhopadhyay, M. Horvatić, C. Berthier, H. Yoshida, Y. Okamoto and Z. Hiroi, *J. Phys. Soc. Jpn.* **81** (2012) 024703 (1-9).
4. Large Diamagnetism of  $\text{AV}_2\text{Al}_{20}$  (A=Y and La): A. Onosaka, Y. Okamoto, J.-I. Yamaura, T. Hirose and Z. Hiroi, *J. Phys. Soc. Jpn.* **81** (2012) 123702(1-4).
5. \*Pressure Dependence of Upper Critical Field in  $\beta$ -Pyrochlore Oxides: D. Iguchi, T. Isono, Y. Machida, K. Izawa, B. Salce, J. Flouquet, H. Ogusu, J. Yamaura and Z. Hiroi, *J. Phys. Soc. Jpn.* **80** (2012) SA040.
6. Rattling and Superconducting Properties of the Cage Compound  $\text{Ga}_x\text{V}_2\text{Al}_{20}$ : Z. Hiroi, A. Onosaka, Y. Okamoto, J.-I. Yamaura and H. Harima, *J. Phys. Soc. Jpn.* **81** (2012) 124707(1-11).
7. \*Rattling Good Superconductor: the  $\beta$ -Pyrochlore Oxide  $\text{AOs}_2\text{O}_6$ : Z. Hiroi, J. Yamaura and K. Hattori, *J. Phys. Soc. Jpn.* **81** (2012) 011012 (24 pages).
8. \*Superconductivity in the Einstein Solid  $\text{A}_x\text{V}_2\text{Al}_{20}$  (A = Al and Ga): A. Onosaka, Y. Okamoto, J. Yamaura and Z. Hiroi, *J. Phys. Soc. Jpn.* **81** (2012) 023703(1-4).
9. \*Synthesis, Structure and Electromagnetic Properties of Manganese Hollandite,  $\text{K}_x\text{Mn}_8\text{O}_{16}$ : T. Kuwabara, M. Isobe, H. Gotou, T. Yagi, D. Nishio-Hamane and Y. Ueda, *J. Phys. Soc. Jpn.* **81** (2012) 104701(1-5).
10. Large and homogeneous mass enhancement in the rattling-induced superconductor  $\text{KOs}_2\text{O}_6$ : T. Terashima, N. Kurita, A. Kiswandhi, E.-S. Choi, J. S. Brooks, K. Sato, J.-I. Yamaura, Z. Hiroi, H. Harima and S. Uji, *Phys. Rev. B* **85** (2012) 180503(1-5).
11. Giant Phonon Softening and Enhancement of Superconductivity by Phosphorus Doping of  $\text{BaNi}_2\text{As}_2$ : K. Kudo, M. Takasuga, Y. Okamoto, Z. Hiroi and M. Nohara, *Phys. Rev. Lett.* **109** (2012) 097002(1-5).
12. \*Tetrahedral Magnetic Order and the Metal-Insulator Transition in the Pyrochlore Lattice of  $\text{Cd}_2\text{Os}_2\text{O}_7$ : J. Yamaura, K. Ohgushi, H. Ohsumi, T. Hasegawa, I. Yamauchi, K. Sugimoto, S. Takeshita, A. Tokuda, M. Takata, M. Udagawa, M. Takigawa, H. Harima, T. Arima and Z. Hiroi, *Phys. Rev. Lett.* **108** (2012) 247205(1-5).
13. Crystal chemistry and magnetic properties of manganese zinc alloy “ $\text{YMn}_2\text{Zn}_{20}$ ” comprising a Mn pyrochlore lattice: Y. Okamoto, T. Shimizu, J.-I. Yamaura and Z. Hiroi, *J. Solid State Chem.* **191** (2012) 246-256.
14. Spin Reorientation in the Square-Lattice Antiferromagnets  $\text{RMnAsO}$  (R = Ce, Nd): Density Functional Analysis of the Spin-Exchange Interactions between the Rare-Earth and Transition-Metal Ions: C. Lee, E. Kan, H. Xiang, R. K. Kremer, S.-H. Lee, Z. Hiroi and M.-H. Whangbo, *Inorg. Chem.* **51** (2012) 6890-6897.
15. A novel crystal polymorph of volborthite,  $\text{Cu}_3\text{V}_2\text{O}_7(\text{OH})_2 \cdot 2\text{H}_2\text{O}$ : H. Ishikawa, J.-I. Yamaura, Y. Okamoto, H. Yoshida, G. J. Nilsen and Z. Hiroi, *Acta Cryst.* **68** (2012) i41-i44.
16. †\*Electrospinning Synthesis of Wire-Structured  $\text{LiCoO}_2$  for Electrode Materials of High-Power Li-Ion Batteries: Y. Mizuno, E. Hosono, T. Saito, M. Okubo, D. Nishio-Hamane, K. Ohishi, T. Kudo and H. Zhou, *J. Phys. Chem. C* **116** (2012) 10774-10780.
17. †\*Miyahisaite,  $(\text{Sr,Ca})_2\text{Ba}_3(\text{PO}_4)_3\text{F}$ , a new mineral of the hedyphane group in the apatite supergroup from the Shimoharai mine, Oita Prefecture, Japan: D. Nishio-Hamane, Y. Ogoshi and T. Minakawa, *Journal of Mineralogical and Petrological Sciences* **107** (2012) 121-126.
18. †\*An Energy Storage Principle using Bipolar Porous Polymeric Frameworks: K. Sakaushi, G. Nickerl, F. M. Wisser, D. Nishio-Hamane, E. Hosono, H. Zhou, S. Kaskel and J. Eckert, *Angew. Chem. Int. Ed.* **51** (2012) 7850-7854.
19. Orbital switching in a frustrated magnet: H. Yoshida, J.-I. Yamaura, M. Isobe, Y. Okamoto, G. J. Nilsen and Z. Hiroi, *Nature Commun.* **3** (2012) 860(1-5).
20. Study on the Microstructures and the Magnetic Properties of Precipitates in a  $\text{Cu}_{75}\text{-Fe}_5\text{-Ni}_{20}$  Alloy: S. Kang, M. Takeda, M. Takeuchi, Z. Hiroi, G.-W. Kim, D.-S. Bae, C.-G. Lee and B.-H. Koo, *J. Nanosci. Nanotech.* **12** (2012) 1337-1340.
21. †\*Hulsite from Sengendera skarn deposit, Miyazaki, Japan: Y. Ogoshi, T. Minakawa and D. Hamane, *Japanese Magazine of Mineralogical and Petrological Sciences* **41** (2012) 61-66.
22. †\*Gold nanoparticles stabilized on nanocrystalline magnesium oxide as an active catalyst for reduction of nitroarenes in aqueous medium at room temperature: K. Layek, M. Lakshmi Kantam, M. Shirai, D. Nishio-Hamane, T. Sasaki and H. Maheswaran, *Green Chem.* **14** (2012) 3164-3174.

23. \*Magnetic Order in the Spin-1/2 Kagome Antiferromagnet Vesignieite: M. Yoshida, Y. Okamoto, M. Takigawa and Z. Hiroi, J. Phys. Soc. Jpn. **82** (2013) 013702(1-5).
24. YCr<sub>6</sub>Ge<sub>6</sub> as a Candidate Compound for a Kagome Metal: Y. Ishii, H. Harima, Y. Okamoto, J.-I. Yamaura and Z. Hiroi, J. Phys. Soc. Jpn. **82** (2013) 023705(1-4).
25. Breathing Pyrochlore Lattice Realized in A-Site Ordered Spinel Oxides LiGaCr<sub>4</sub>O<sub>8</sub> and LiInCr<sub>4</sub>O<sub>8</sub>: Y. Okamoto, G. J. Nilsen, J. Paul Attfield and Z. Hiroi, Phys. Rev. Lett. **110** (2013) 097203(1-5).
26. †\*Iseite, Mn<sub>2</sub>Mo<sub>3</sub>O<sub>8</sub>, a new mineral from Ise, Mie Prefecture, Japan: D. Nishio-Hamane, N. Tomita, T. Minakawa and S. Inaba, Journal of Mineralogical and Petrological Sciences **108** (2013) 37-41.
27. †\*Synthesis of LiNi<sub>0.5</sub>Mn<sub>1.5</sub>O<sub>4</sub> and 0.5Li<sub>2</sub>MnO<sub>3</sub>-0.5LiNi<sub>1/3</sub>Co<sub>1/3</sub>Mn<sub>1/3</sub>O<sub>2</sub> hollow nanowires by electrospinning: E. Hosono, T. Saito, J. Hoshino, Y. Mizuno, M. Okubo, D. Asakura, K. Kagesawa, D. Nishio-Hamane, T. Kudo and H. Zhou, CrystEngComm **15** (2013) 2592-2597.

### Kawashima group

We investigated quantum spin/boson systems and frustrated systems by means of large-scale numerical simulation. We also developed several new numerical techniques. This year we discovered the following facts in particular: (1) super-solid state exists at the commensurate filling in the soft-core Bose-Hubbard model in two and three dimensions, (2) the phase diagram was obtained for hard-core Bose-Hubbard model with dipolar interaction, and (3) the solution of the finite-temperature Gross-Pitaevski equation agree with the Quantum Monte Carlo results even quantitatively.

1. Ground-state phase diagram of the two-dimensional extended Bose-Hubbard model: T. Ohgroe, T. Suzuki and N. Kawashima, Phys. Rev. B **86** (2012) 054520(1-9).
2. Quantum phases of hardcore bosons with long-range interactions on a square lattice: D. Yamamoto, A. Masaki and I. Danshita, Phys. Rev. B **86** (2012) 054516(1-17).
3. Commensurate supersolid of three-dimensional lattice bosons: T. Ohgroe, T. Suzuki and N. Kawashima, Phys. Rev. Lett. **108** (2012) 185302 (4 pages).
4. Finite-Temperature Transition of the Antiferromagnetic Heisenberg Model on a Distorted kagome Lattice: H. Masuda, T. Okubo and H. Kawamura, Phys. Rev. Lett. **109** (2012) 057201(1-5).
5. Bimodal Momentum Distribution of the High-Density Supersolid State: T. Ohgroe, T. Suzuki and N. Kawashima, J. Low Temp. Phys. **171** (2012) 309.
6. Phase diagram and universality of the Lennard-Jones gas-liquid system: H. Watanabe, N. Ito and C.-K. Hu, J. Chem. Phys. **136** (2012) 204102 (7 pages).
7. Quantum phases of hard-core bosons on two-dimensional lattices with anisotropic dipole-dipole interaction: T. Ohgroe, T. Suzuki and N. Kawashima, Phys. Rev. A **86** (2012) 063635(1-6).
8. Usefulness of an equal-probability assumption for out-of-equilibrium states: a master equation approach: T. Nogawa, N. Ito and H. Watanabe, Phys. Rev. E **86** (2012) 41133(1-8).
9. Validity of projected Gross-Pitaevskii simulation: Comparison with quantum Monte Carlo: T. Sato, Y. Kato, T. Suzuki and N. Kawashima, Phys. Rev. E **85** (2012) 050105 (1-4).
10. Localization of Bose-Fermi Mixtures in One-Dimensional Incommensurate Lattices: A. Masaki and H. Mori, J. Phys.: Conf. Series **400** (2012) 012043.
11. Double peaks in the momentum distribution of cold polar molecules in the supersolid state: T. Ohgroe, T. Suzuki and N. Kawashima, J. Phys.: Conf. Ser. **400** (2012) 012058.
12. Second-Order Phase Transition in Heisenberg Model on Triangular Lattice with Competing Interactions: R. Tamura, S. Tanaka and N. Kawashima, Phys. Rev. B (2013), accepted for publication.
13. Visibility Pattern of Bose-Fermi Mixtures in One-Dimensional Incommensurate Lattices: A. Masaki and H. Mori, Philosophical Magazine (2013), accepted for publication.

## Noguchi group

We have studied the structure formation of binary mixtures of two surfactants. We found that various micelles such as bicelles and octopus-like shapes are formed depending on the critical micelle concentration and the ratio of hydrophobic and hydrophilic segments of the molecules. We also studied the dynamics of red blood cells in capillary flow and dynamic-mode correlation in a glass system.

1. Relationship between bond-breakage correlations and four-point correlations in heterogeneous glassy dynamics: Configuration changes and vibration modes: H. Shiba, T. Kawasaki and A. Onuki, *Phys. Rev. E* **86** (2012) 041504(1-14).
2. Ordering and arrangement of deformed red blood cells in flow through microcapillaries: J. L. McWhirter, H. Noguchi and G. Gompper, *New J. Phys.* **14** (2012) 085026(1-23).
3. Line tension of branching junctions of bilayer membranes: H. Noguchi, *Soft Matter* **8** (2012) 3146-3153.
4. Structure formation in binary mixtures of surfactants: vesicle opening-up to bicelles and octopus-like micelles: H. Noguchi, *Soft Matter* **8** (2012) 8926-8935.
5. 生体膜の粗視化シミュレーション: 野口 博司, アンサンブル **57** (2012) 1-4.
6. Structure formation in binary mixtures of lipids and detergents: Self-assembly and vesicle division: H. Noguchi, *J. Chem. Phys.* **138** (2013) 024907(1-9).
7. Effects of anchored flexible polymers on mechanical properties of model biomembranes: H. Wu and H. Noguchi, *AIP Conf. Proc.* **1518** (2013) 649-653.
8. Hierarchical heterogeneous glassy dynamics of configuration changes and vibration modes: T. Kawasaki, H. Shiba and A. Onuk, *AIP Conf. Proc.* **1518** (2013) 784-791.
9. Structure formation of lipid membranes: Membrane self-assembly and vesicle opening-up to octopus-like micelles: H. Noguchi, *AIP Conf. Proc.* **1518** (2013) 566-570.
10. 脂質膜の構造形成の粗視化シミュレーション: 野口 博司, *生物物理* **53** (2013) 11-14.
11. Multiscale modeling of blood flow: from single cells to blood rheology: D. A. Fedosov, H. Noguchi and G. Gompper, *Biomech. Model. Mechanobiol.* (2013), in print.
12. Structure formation of surfactant membranes under shear flow: H. Shiba, H. Noguchi and G. Gompper, *J. Chem. Phys.* (2013), accepted for publication.
13. Entropy-driven aggregation in multilamellar membranes: H. Noguchi, *EPL* (2013), accepted for publication.

## Materials Synthesis and Characterization group

1. \*Pressure Dependence of Upper Critical Field in  $\beta$ -Pyrochlore Oxides: D. Iguchi, T. Isono, Y. Machida, K. Izawa, B. Salce, J. Flouquet, H. Oguisu, J. Yamaura and Z. Hiroi, *J. Phys. Soc. Jpn.* **80** (2012) SA040.
2. \*Superconductivity in the Einstein Solid  $A_xV_2Al_{20}$  ( $A = Al$  and  $Ga$ ): A. Onosaka, Y. Okamoto, J. Yamaura and Z. Hiroi, *J. Phys. Soc. Jpn.* **81** (2012) 023703(1-4).
3. \*Synthesis, Structure and Electromagnetic Properties of Manganese Hollandite,  $K_xMn_8O_{16}$ : T. Kuwabara, M. Isobe, H. Gotou, T. Yagi, D. Nishio-Hamane and Y. Ueda, *J. Phys. Soc. Jpn.* **81** (2012) 104701(1-5).
4. †\*Electrospinning Synthesis of Wire-Structured  $LiCoO_2$  for Electrode Materials of High-Power Li-Ion Batteries: Y. Mizuno, E. Hosono, T. Saito, M. Okubo, D. Nishio-Hamane, K. Ohishi, T. Kudo and H. Zhou, *J. Phys. Chem. C* **116** (2012) 10774-10780.
5. †\*Miyahisaite,  $(Sr,Ca)_2Ba_3(PO_4)_3F$ , a new mineral of the hedyphane group in the apatite supergroup from the Shimoharai mine, Oita Prefecture, Japan: D. Nishio-Hamane, Y. Ogoshi and T. Minakawa, *Journal of Mineralogical and Petrological Sciences* **107** (2012) 121-126.
6. †\*An Energy Storage Principle using Bipolar Porous Polymeric Frameworks: K. Sakaushi, G. Nickerl, F. M. Wisser, D. Nishio-Hamane, E. Hosono, H. Zhou, S. Kaskel and J. Eckert, *Angew. Chem. Int. Ed.* **51** (2012) 7850-7854.

7. <sup>†\*</sup>Gold nanoparticles stabilized on nanocrystalline magnesium oxide as an active catalyst for reduction of nitroarenes in aqueous medium at room temperature: K. Layek, M. Lakshmi Kantam, M. Shirai, D. Nishio-Hamane, T. Sasaki and H. Maheswaran, *Green Chem.* **14** (2012) 3164-3174.
8. <sup>†\*</sup>Iseite,  $Mn_2Mo_3O_8$ , a new mineral from Ise, Mie Prefecture, Japan: D. Nishio-Hamane, N. Tomita, T. Minakawa and S. Inaba, *Journal of Mineralogical and Petrological Sciences* **108** (2013) 37-41.
9. <sup>†\*</sup>Synthesis of  $LiNi_{0.5}Mn_{1.5}O_4$  and  $0.5Li_2MnO_3-0.5LiNi_{1/3}Co_{1/3}Mn_{1/3}O_2$  hollow nanowires by electrospinning: E. Hosono, T. Saito, J. Hoshino, Y. Mizuno, M. Okubo, D. Asakura, K. Kagesawa, D. Nishio-Hamane, T. Kudo and H. Zhou, *CrystEngComm* **15** (2013) 2592-2597.

## Neutron Science Laboratory

### Shibayama group

Shibayama group has been exploring the structure and dynamics of soft matter, especially polymer gels, micelles, and phenolic resin, utilizing a combination of small-angle neutron scattering (SANS), neutron spin echo (NSE), and dynamic light scattering (DLS). The objectives are to elucidate the mysterious relationship between the structure and variety of novel properties/functions of polymer gels/resins. The highlights of 2012 include that (1) upgrade of the small-angle neutron scattering instrument, SANS-U by introducing a focusing collimation and high-resolution area detector, (2) examination of the theories of rubber elasticity using an ideal polymer network, i.e., Tetra-PEG gels, (3) Rheo-SANS of threadlike micelles, (4) structural characterization of phenolic resin, and so on.

1. Stress relaxation and hysteresis of nanocomposite gel investigated by SAXS and SANS measurement: T. Nishida, A. Obayashi, K. Haraguchi and M. Shibayama, *Polymer* **53** (2012) 4533-4538.
2. Experimental evidences for molecular origin of low-Q peak in neutron/x-ray scattering of 1-alkyl-3-methylimidazolium bis: K. Fujii, R. Takamuku and T. Kameda, *J. Chem. Phys.* **135** (2012) 244502(1-11).
3. Relationship between mesoscale dynamics and shear relaxation of ionic liquids with long alkyl chain: T. Yamaguchi, K.-I. Mikawa, S. Koda, K. Fujii, H. Endo, M. Shibayama, H. Hamano and Y. Umebayashi, *J. Chem. Phys.* **137** (2012) 104511(1-7).
4. Rubber elasticity for incomplete polymer networks: K. Nishi, M. Chijiishi, Y. Katsumoto, T. Nakao, K. Fujii, U.-I. Chung, H. Noguchi, T. Sakai and M. Shibayama, *J. Chem. Phys.* **137** (2012) 224903(1-7).
5. Star-Shaped Trimeric Quaternary Ammonium Bromide Surfactants: Adsorption and Aggregation Properties: T. Yoshimura, T. Kusano, H. Iwase, M. Shibayama, T. Ogawa and H. Kurata, *Langmuir* **28** (2012) 9322-9331.
6. Structural and Rheological Studies on Growth of Salt-Free Wormlike Micelles Formed by Star-Type Trimeric Surfactants: T. Kusano, H. Iwase, T. Yoshimura and M. Shibayama, *Langmuir* **28** (2012) 16798-16806.
7. Kinetic Study for AB-Type Coupling Reaction of Tetra-Arm Polymers: K. Nishi, K. Fujii, M. Chijiishi, Y. Katsumoto, U.-I. Chung, T. Sakai and M. Shibayama, *Macromolecules* **45** (2012) 1031-1036.
8. Pressure Effects on Cononsolvency Behavior of Poly(*N*-isopropylacrylamide) in Water/DMSO Mixed Solvents: N. Osaka and M. Shibayama, *Macromolecules* **45** (2012) 2171-2174.
9. Structural Analysis of High Performance Ion-Gel Comprising Tetra-PEG Network: H. Asai, K. Fujii, T. Ueki, T. Sakai, U.-I. Chung, M. Watanabe, Y.-S. Han, T.-H. Kim and M. Shibayama, *Macromolecules* **45** (2012) 3902-3909.
10. Anomalous volume phase transition in a polymer gel with alternative hydrophilic-amphiphilic sequence: H. Kamata, U. Chung, M. Shibayama and T. Sakai, *Soft Matter* **8** (2012) 6876-6879.
11. Atomistic molecular dynamics study of cross-linked phenolic resins: A. Izumi, T. Nakao and M. Shibayama, *Soft Matter* **8** (2012) 5283-5292.
12. Effect of swelling and deswelling on the elasticity of polymer networks in the dilute to semi-dilute region: T. Sakai, M. Kurakazu, Y. Akagi, M. Shibayama and U.-I. Chung, *Soft Matter* **8** (2012) 2730-2736.
13. High-performance ion gel with tetra-PEG network: K. Fujii, H. Asai, T. Ueki, T. Sakai, S. Imaizumi, U.-I. Chung, M. Watanabe and M. Shibayama, *Soft Matter* **8** (2012) 1756-1759.

14. \*Microscopic insights into Ion Gel dynamics using neutron spectroscopy: M. Kofu, T. Someya, S. Tatsumi, K. Ueno, T. Ueki, M. Watanabe, T. Matsunaga, M. Shibayama, V. G. Sakai, M. Tyagi and O. Yamamuro, *Soft Matter* **8** (2012) 7888-7897.
15. Structural analysis of cured phenolic resins using complementary small-angle neutron and X-ray scattering and scanning electron microscopy: A. Izumi, T. Nakao, H. Iwase and M. Shibayama, *Soft Matter* **8** (2012) 8438-8445.
16. Structure-mechanical property relationship of tough hydrogels: M. Shibayama, *Soft Matter* **8** (2012) 8030-8038.
17. Optimization of the thickness of a ZnS/(LiF)-Li-6 scintillator for a high-resolution detector installed on a focusing small-angle neutron scattering spectrometer (SANS-U): H. Iwase, M. Katagiri and M. Shibayama, *J Appl Crystallogr* **45** (2012) 507-512.
18. Mechanical properties of a polymer network of Tetra-PEG gel: A. Sugimura, M. Asai, T. Matsunaga, Y. Akagi, T. Sakai, H. Noguchi and M. Shibayama, *Polym J* **45** (2012) 300-306.
19. 中性子による材料評価・構造解析: 柴山 充弘, *表面科学* **33** (2012) 258-263.
20. 中性子による材料評価・構造解析: 柴山 充弘, *表面科学* **33** (2013) 258-263.
21. 溶液中での重水素化ノボラックのコンフォメーション: 和泉 篤士, 中尾 俊夫, 柴山 充弘, ネットワークポリマー **33** (2013) 204-208.
22. Fabrication, Structure, Mechanical Properties, and Application of Tetra-PEG Hydrogels Oren Scherman and Xian Jun Loh, Eds.: M. Shibayama and T. Sakai, in: *Polymeric and Self Assembled Hydrogels: Fundamentals to Applications, Chapt. 2*, edited by RSC Publishing, (RSC Publishing, 2013), 2-38.

### **Yoshizawa group**

A systematic study on spin dynamics in two-dimensional transition-metal oxides have been carried out with use of the high resolution chopper spectrometer installed at BL12 in the Material and Life Science Facility, J-PARC. In the highly hole-doped region in the layered nickelate, conventional spin wave excitations change its character to metal-like behavior. Spin dynamics in non-centrosymmetric superconductors CeRhSi<sub>3</sub> and CeIrSi<sub>3</sub> were also studied.

1. <sup>†</sup>\*Long-range order and spin-liquid states of polycrystalline Tb<sub>2+x</sub>Ti<sub>2-x</sub>O<sub>7+y</sub>: T. Taniguchi, H. Kadowaki, H. Takatsu, B. Fåk, J. Ollivier, T. Yamazaki, T. J. Sato, H. Yoshizawa, Y. Shimura, T. Sakakibara, T. Hong, K. Goto, L. R. Yaraskavitch and J. B. Kycia, *Phys. Rev. B* **87** (2013) 060408R(1-5).
2. Structural and magnetic properties in the quantum S=1/2 dimer system Ba<sub>3</sub>(Cr<sub>1-x</sub>V<sub>x</sub>)<sub>2</sub>O<sub>8</sub> with site disorder: T. Hong, L. Y. Zhu, X. Ke, V. O. Garlea, Y. Qiu, Y. Nambu, H. Yoshizawa, M. Zhu, G. E. Granroth, A. T. Savici, Z. Gai and H. D. Zhou, *Phys. Rev. B* **87** (2013) 144427(1-9).

### **Yamamuro group**

Our laboratory is studying chemical physics of complex condensed matters by using neutron scattering, X-ray diffraction, calorimetric, dielectric, and viscoelastic techniques. Our target materials are glasses, liquids, and various disordered systems. The first topic of this year is that we developed a calorimetric system for metal hydrides and measured the heat of hydrogen adsorption to palladium and the heat capacities of palladium hydrides. We have clarified that “50 K anomaly”, which has been a long mystery in this material, is due to a glass transition, i.e., freezing of the motion of the hydrogen atoms disordered among the octahedral sites of the palladium fcc lattice. The second topic is that we succeeded to observe magnetic relaxations in a single molecule magnet (SMM) as a clear quasielastic neutron scattering (QENS) for the first time. The third topic is that we found the diffusion of hydrogen molecules in clathrate hydrates stabilized by tetrahydrofuran by means of a QENS technique. Other than these three, we have made some progresses in the studies on porous coordination polymers and ionic liquids.

1. Structures and Low-energy Excitations of Amorphous Gas Hydrates: T. Kikuchi, Y. Inamura, N. Onoda-Yamamuro and O. Yamamuro, *J. Phys. Soc. Jpn.* **81** (2012) 094604 (5 pages).
2. Hydration properties and compressive strength development of Low Heat Cement: K. Mori, T. Fukunaga, M. Sugiyama, K. Iwase, K. Oishi and O. Yamamuro, *J. Phys. Chem. Solids* **73** (2012) 1274-1277.
3. Thermodynamic Study of Simple Molecular Glasses: Universal Features in Their Heat Capacity and the Size of the Cooperatively Rearranging Regions: S. Tatsumi, S. Aso and O. Yamamuro, *Phys. Rev. Lett.* **109** (2012) 045701 (5 pages).

4. Heat Capacities and Glass Transitions of Ion Gels: O. Yamamuro, T. Someya, M. Kofu, T. Ueki, K. Ueno and M. Watanabe, *J. Phys. Chem. B* **116** (2012) 10935-10940.
5. Relationship between the Local Dynamics and Gas Permeability of Para-Substituted Poly(1-chloro-2-phenylacetylenes): R. Inoue, T. Kanaya, T. Masuda, K. Nishida and O. Yamamuro, *Macromolecules* **45** (2012) 6008-6014.
6. Direct Observation of Supercooled Water in Mortar Materials by Quasi-elastic Neutron Scattering: K. Mori, K. Iwase, M. Sugiyama, T. Fukunaga and O. Yamamuro, *Trans. Mater. Res. Soc. Jpn.* **37** (2012) 139-142.
7. Neutron scattering studies of Ti-Cr-V bcc alloy with the residual hydrogen and deuterium: K. Mori, K. Iwase, M. Sugiyama, M. Kofu, O. Yamamuro, Y. Onodera, T. Otomo and T. Fukunaga, *J. Phys.: Conf. Series* **340** (2012) 012103 (5 pages).
8. \*Microscopic insights into Ion Gel dynamics using neutron spectroscopy: M. Kofu, T. Someya, S. Tatsumi, K. Ueno, T. Ueki, M. Watanabe, T. Matsunaga, M. Shibayama, V. G. Sakai, M. Tyagi and O. Yamamuro, *Soft Matter* **8** (2012) 7888-7897.
9. 単純分子ガラスの熱力学的研究: 山室 修, 辰巳 創一, レオロジー学会誌 **40** (2012) 137-142.
10. Heterogeneous Slow Dynamics of Imidazolium Based Ionic Liquids Studied by Neutron Spin Echo: M. Kofu, M. Nagao, T. Ueki, Y. Kitazawa, Y. Nakamura, S. Sawamura, M. Watanabe and O. Yamamuro, *J. Phys. Chem. B* **117** (2013) 2773-2781.
11. Linear trinuclear Zn(II)-Ce(III)-Zn(II) complex which behaves as a single-molecule magnet: S. Hino, M. Maeda, K. Yamashita, Y. Kataoka, M. Nakano, T. Yamamura, H. Nojiri, M. Kofu, O. Yamamuro and T. Kajiwara, *Dalton Trans.* **42** (2013) 2683-2686.
12. Thermal behaviour, structure and dynamics of low-temperature water confined in mesoporous organosilica by differential scanning calorimetry, X-ray diffraction and quasi-elastic neutron scattering: M. Aso, K. Ito, H. Sugino, K. Yoshida, T. Yamada, O. Yamamuro, S. Inagaki and T. Yamaguchi, *Pure and Appl. Chem.* **85** (2013) 289-305.
13. Phase Transition and Dynamics of Water Confined in Hydroxyethyl Copper Rubenate Hydrate: T. Yamada, T. Yamada, M. Tyagi, M. Nagao, H. Kitagawa and O. Yamamuro, *J. Phys. Soc. Jpn.* (2013), accepted for publication.
14. Mode distribution analysis of quasi-elastic neutron scattering and application to liquid water: T. Kikuchi, K. Nakajima, S. Ohira-Kawamura, Y. Inamura, O. Yamamuro, M. Kofu, Y. Kawakita, K. Suzuya, M. Nakamura and M. Arai, *Phys. Rev. E* (2013), accepted for publication.
15. 中性子散乱と回折: 山室 修, 「大学院講義物理化学(第2版) III. 固体の化学と物性」, 7.3, 小谷正博, 幸田清一郎, 染田清彦, 阿波賀邦夫, (東京化学同人, 2012), 181-190.
16. ガラス状態: 山室 修, 「イオン液体の科学 新世代液体への挑戦」, 1.4.3, 西川恵子, 大内幸雄, 伊藤俊幸, 大野弘幸, 渡邊正義, (丸善, 2012), 82-89.

## Masuda group

The correlation of the higher order of the spin operator has attracted theoretical interest in terms of hidden order in spin disordered state. The challenge is that the experimental probe to identify the correlation is absent. Meanwhile in multiferroic compound that exhibits spontaneous order both in magnetism and dielectricity, the electric polarization is expressed by second order tenors of the spin operators, and the spin nematic operator comes to visible. In this fiscal year our group demonstrated the existence of the spin nematic interaction in an easy-plane type antiferromagnet Ba<sub>2</sub>CoGe<sub>2</sub>O<sub>7</sub> by exploring the magnetic anisotropy and spin dynamics. Combination of neutron scattering and magnetization measurements reveals that the dominant origin of the observed in-plane anisotropy is the antiferro-type interaction of spin nematic operator instead of conventional single-ion anisotropy. The structure of the spontaneous polarization is consistent with the antiferro-nematic order. The introduction of the spin nematic interaction is useful to understand the physics of spin and electric dipole in multiferroic compounds.

1. <sup>63,65</sup>Cu Nuclear Resonance Study of the Coupled Spin Dimers and Chains Compound Cu<sub>2</sub>Fe<sub>2</sub>Ge<sub>4</sub>O<sub>13</sub>: J. Kikuchi, S. Nagura, K. Murakami, T. Masuda and G. J. Redhammer, *J. Phys. Soc. Jpn.* **82** (2013) 034710(1-10).
2. 1次元フラストレート強磁性鎖のスピン密度波と Bond Nematic 相関: 萩原 雅人, 益田 隆嗣, 波紋 **23** (2013) 14-18.

# International MegaGauss Science Laboratory

## Takeyama group

We have developed a magnetization measurement technique for special use in a vertically aligned single-turn coil, capable of generating ultra-high magnetic fields over 100 T. Compensation ratios of an order as high as  $10^{-4}$  were achieved by self-compensation in parallel twin-pickup coils without using compensation circuit mixing of the signal from an auxiliary coil. High performance cryogenics was employed with a liquid Helium container that was also manufactured to fit the system. The high magnetic field magnetization measurements were applied to a manganite  $\text{Bi}_{0.5}\text{Ca}_{0.5}\text{MnO}_3$  at room temperature, and also to a geometrically frustrated spinel oxide,  $\text{CdCr}_2\text{O}_4$  at very low temperatures. Not only the transition field, but also the absolute value of the magnetization was shown to be evaluated within a 3% degree of accuracy in magnetic fields over 100 T by means of a 14-mm inner-diameter single-turn coil.

1. \*Magnetic Phases of  $\text{ZnCr}_2\text{O}_4$  Revealed by Magneto-Optical Studies under Ultra-High Magnetic Fields up to 600 T: A. Miyata, H. Ueda, Y. Ueda, Y. Motome, N. Shannon, K. Penc and S. Takeyama, J. Phys. Soc. Jpn. **81** (2012) 114701(1-8).
2. \*Precise Magnetization Measurements by Parallel Self-Compensated Induction Coils in a Vertical Single-Turn Coil up to 103 T: S. Takeyama, R. Sakakura, Y. H. Matsuda, A. Miyata and M. Tokunaga, J. Phys. Soc. Jpn. **81** (2012) 014702(1-7).
3. クロムスピネル幾何学的フラストレート磁性体の超強磁場磁気相 -600 Tまでの磁気光学精密測定から: 宮田 敦彦, 嶽山 正二郎, 固体物理 **47**(8) (2012) 17-25.
4. 「電磁濃縮法による室内世界最高磁場発生と物性物理への応用」: 嶽山 正二郎, 日本物理学会誌 **67**(3) (2012) 170-178.
5. Magneto-photoluminescence of charged excitons from  $\text{Mg}_x\text{Zn}_{1-x}\text{O}/\text{ZnO}$  heterojunctions: T. Makino, Y. Segawa, A. Tsukazaki, H. Saito, S. Takeyama, S. Akasaka, K. Nakahara and M. Kawasaki, Phys. Rev. B **87** (2013) 085312(1-7).
6. Precise measurement of a magnetic field generated by the electromagnetic flux compression technique: D. Nakamura, H. Sawabe, Y. H. Matsuda and S. Takeyama, Rev. Sci. Instrum. **84** (2013) 044702(1-10).
7. Magnetization Studies of Field-Induced Transitions by Using a Single-Turn Coil Technique: N. Abe, Y. H. Matsuda, S. Takeyama, K. Sato, H. Kageyama and Y. Nishiwaki, J. Low Temp. Phys. **170** (2013) 452–456.
8. Precision of an Ultra-high Magnetic Field Generated by the Electro-magnetic Flux Compression: D. Nakamura, Y. H. Matsuda and S. Takeyama, J. Low Temp. Phys. **170** (2013) 457–462.
9. \*Magneto-Absorption in the  $\alpha$  Phase of Solid Oxygen at Megagauss Magnetic Fields: T. Nomura, Y. H. Matsuda, J. L. Her, S. Takeyama, A. Matsuo, K. Kindo and T. C. Kobayashi, J Low Temp Phys **170** (2013) 372-376.

## Kindo group

New mono-coil was developed to generate 85.8 T non-destructively. The maximum field beyond 85 T is the world highest field as generated by a non-destructive mono-coil. The coil has an inner bore of 18 mm and the pulse duration is about 4 msec.

1. †\*High-Magnetic-Field X-ray Absorption and Magnetic Circular Dichroism Spectroscopy in the Mixed-Valent Compound  $\text{YbAgCu}_4$ : T. Nakamura, Y. H. Matsuda, J.-L. Her, K. Kindo, S. Michimura, T. Inami, M. Mizumaki, N. Kawamura, M. Suzuki, B. Chen, H. Ohta, K. Yoshimura and A. Kotani, J. Phys. Soc. Jpn. **81** (2012) 114702(1-11).
2. \*Multiferroicity on the Zigzag-Chain Antiferromagnet  $\text{MnWO}_4$  in High Magnetic Fields: H. Mitamura, T. Sakakibara, H. Nakamura, T. Kimura and K. Kindo, J. Phys. Soc. Jpn. **81** (2012) 054705(1-7).
3. †Soft-X-ray Magnetic Circular Dichroism under Pulsed High Magnetic Fields at Eu  $M_{4,5}$  Edges of Mixed Valence Compound  $\text{EuNi}_2(\text{Si}_{0.18}\text{Ge}_{0.82})_2$ : T. Nakamura, T. Hirono, T. Kinoshita, Y. Narumi, M. Hayashi, H. Nojiri, A. Mitsuda, H. Wada, K. Kodama, K. Kindo and A. Kotani, J. Phys. Soc. Jpn. **81** (2012) 103705(1-4).
4. †\*Valence Fluctuation in  $\text{YbAgCu}_4$  at High Magnetic Fields: Y. H. Matsuda, T. Nakamura, J.-L. Her, K. Kindo, S. Michimura, T. Inami, M. Mizumaki, N. Kawamura, M. Suzuki, B. Chen, H. Ohta and K. Yoshimura, J. Phys. Soc. Jpn. **81** (2012) 015002(1-2).

5. High magnetic field study of the Gd-Co exchange interactions in  $\text{GdCo}_{12}\text{B}_6$ : O. Isnard, Y. Skourski, L. V. B. Diop, Z. Arnold, A. V. Andreev, J. Wosnitza, A. Iwasa, A. Kondo, A. Matsuo and K. Kindo, *J. Appl. Phys.* **111** (2012) 093916(1-5).
6. <sup>†</sup>Ferromagnetism induced in the anisotropic stacked kagome lattice antiferromagnet  $\text{Cs}_2\text{Cu}_3\text{CeF}_{12}$ : T. Amemiya, I. Umegaki, H. Tanaka, T. Ono, A. Matsuo and K. Kindo, *Phys. Rev. B* **85** (2012) 144409(1-9).
7. <sup>†</sup>Short-range correlations and persistent spin fluctuations in the undistorted kagome lattice Ising antiferromagnet  $\text{Co}_3\text{Mg}(\text{OH})_6\text{Cl}_2$ : M. Fujihala, X. G. Zheng, Y. Oohara, H. Morodomi, T. Kawae, A. Matsuo and K. Kindo, *Phys. Rev. B* **85** (2012) 012402(1-5).
8. <sup>†\*</sup>Suppression of f-electron itinerancy in  $\text{CeRu}_2\text{Si}_2$  by a strong magnetic field: Y. H. Matsuda, T. Nakamura, J. L. Her, S. Michimura, T. Inami, K. Kindo and T. Ebihara, *Phys. Rev. B* **86** (2012) 041109(R)(1-4).
9. <sup>†</sup>Experimental Realization of a Spin-1/2 Triangular-Lattice Heisenberg Antiferromagnet: Y. Shirata, H. Tanaka, A. Matsuo and K. Kindo, *Phys. Rev. Lett.* **108** (2012) 057205(1-5).
10. <sup>†\*</sup>Quadruple-layered perovskite  $(\text{CuCl})\text{Ca}_2\text{NaNb}_4\text{O}_{13}$ : A. Kitada, Y. Tsujimoto, T. Yamamoto, Y. Kobayashi, Y. Narumi, K. Kindo, A. A. Aczel, G. M. Luke, Y. J. Uemura, Y. Kiuchi, Y. Ueda, K. Yoshimura, Y. Ajiro and H. Kageyama, *J. Solid State Chem.* **185** (2012) 10-17.
11. <sup>†</sup>Field-induced valence transition in  $\text{EuPtP}_{1-x}\text{As}_x$ : A. Mitsuda, T. Okuma, M. Sugishima, H. Wada, K. Sato and K. Kindo, *Eur. Phys. J. B* **85** (2012) 71-75.
12. Collapse of Magnetic Order of the Quasi One-Dimensional Ising-Like Antiferromagnet  $\text{BaCo}_2\text{V}_2\text{O}_8$  in Transverse Fields: S. Kimura, K. Okunishi, M. Hagiwara, K. Kindo, Z. He, T. Taniyama, M. Itoh, K. Koyama and K. Watanabe, *J. Phys. Soc. Jpn.* **82** (2013) 033706(1-4).
13. <sup>†\*</sup>High-Field Phase Diagram of  $\text{SmRu}_4\text{P}_{12}$  Determined by Ultrasonic Measurements in Pulsed Magnetic Field up to 55 T: M. Yoshizawa, H. Mitamura, F. Shichinomiya, S. Fukuda, Y. Nakanishi, H. Sugawara, T. Sakakibara and K. Kindo, *J. Phys. Soc. Jpn.* **82** (2013) 033602(1-5).
14. <sup>†</sup>Marked Change in the Ground State of  $\text{CeRu}_2\text{Al}_{10}$  Induced by Small Amount of Rh Substitution: A. Kondo, K. Kindo, K. Kunimori, H. Nohara, H. Tanida, M. Sera, R. Kobayashi, T. Nishioka and M. Matsumura, *J. Phys. Soc. Jpn.* **82** (2013) 054709(1-5).
15. <sup>†</sup>Crystal structure and magnetic properties of honeycomb-like lattice antiferromagnet p-BIP-V<sub>2</sub>: H. Yamaguchi, S. Nagata, M. Tada, K. Iwase, T. Ono, S. Nishihara, Y. Hosokoshi, T. Shimokawa, H. Nakano, H. Nojiri, A. Matsuo, K. Kindo and T. Kawakami, *Phys. Rev. B* **87** (2013) 125120(1-8).
16. <sup>\*</sup>Magneto-Absorption in the  $\alpha$  Phase of Solid Oxygen at Megagauss Magnetic Fields: T. Nomura, Y. H. Matsuda, J. L. Her, S. Takeyama, A. Matsuo, K. Kindo and T. C. Kobayashi, *J Low Temp Phys* **170** (2013) 372-376.
17. <sup>\*</sup>Observation of Field-induced Anomaly in High-field Magnetization on a Complex Spin-Driven Multiferroic Compound,  $\text{LiCu}_{2-z}\text{Zn}_z\text{O}_2$ : J. L. Her, H. C. Hsu, Y. H. Matsuda, K. Kindo and F. C. Chou, *J Low Temp Phys* **170** (2013) 285-290.
18. <sup>†</sup>Present Status and Future Plan at High Magnetic Field Laboratory in Osaka University: M. Hagiwara, T. Kida, K. Taniguchi and K. Kindo, *J Low Temp Phys* **170** (2013) 531-540.
19. <sup>†</sup>Itinerant electron magnetism of  $\eta$ -carbides  $\text{Co}_6\text{M}_6\text{C}$  and  $\text{Ni}_6\text{M}_6\text{C}$  (M=Mo and W): T. Waki, D. Furusawa, Y. Tabata, C. Michioka, K. Yoshimura, A. Kondo, K. Kindo and H. Nakamura, *Journal of Alloys and Compounds* **554** (2013) 21-24.

## Tokunaga group

Through the measurements of magnetoresistance up to 65 T, we found field-induced melting of the antiferromagnetic spin order in single crystals of  $\text{Fe}_{1+y}\text{Te}_{1-x}\text{S}_x$ . Concomitant melting of the orbital order was visually demonstrated through the high-speed polarizing microscopy in pulsed fields.

1. Field-Induced Magnetostructural Transitions in Antiferromagnetic  $\text{Fe}_{1+y}\text{Te}_{1-x}\text{S}_x$ : M. Tokunaga, T. Kihara, Y. Mizuguchi and Y. Takano, *J. Phys. Soc. Jpn.* **81** (2012) 063703(1-4).

2. \*Precise Magnetization Measurements by Parallel Self-Compensated Induction Coils in a Vertical Single-Turn Coil up to 103 T: S. Takeyama, R. Sakakura, Y. H. Matsuda, A. Miyata and M. Tokunaga, *J. Phys. Soc. Jpn.* **81** (2012) 014702(1-7).
3. Multiferroic properties of an åkermanite  $\text{Sr}_2\text{CoSi}_2\text{O}_7$  single crystal in high magnetic fields: M. Akaki, H. Iwamoto, T. Kihara, M. Tokunaga and H. Kuwahara, *Phys. Rev. B* **86** (2012) 060413(1-4).
4. Giant Magnetoresistance Effect in the Metal–Insulator Transition of Pyrochlore Oxide  $\text{Nd}_2\text{Ir}_2\text{O}_7$ : K. Matsuhira, M. Tokunaga, M. Wakshima, Y. Hinatsu and S. Takagi, *J. Phys. Soc. Jpn.* **82** (2013) 023706(1-4).
5. Thermal Transport and Magnetotransport Properties of  $\text{CuCr}_{1-x}\text{Mg}_x\text{O}_2$  with a Spin-3/2 Antiferromagnetic Triangular Lattice: T. Okuda, S. Oozono, T. Kihara and M. Tokunaga, *J. Phys. Soc. Jpn.* **82** (2013) 014706(1-7).
6. Magnetic control of electric polarization in the noncentrosymmetric compound  $(\text{Cu},\text{Ni})\text{B}_2\text{O}_4$ : N. D. Khanh, N. Abe, K. Kubo, M. Akaki, M. Tokunaga, T. Sasaki and T. Arima, *Phys. Rev. B* **87** (2013) 184416(1-5).
7. Shubnikov–de Haas oscillations in the bulk Rashba semiconductor  $\text{BiTeI}$ : C. Bell, M. S. Bahramy, H. Murakawa, J. G. Checkelsky, R. Arita, Y. Kaneko, Y. Onose, M. Tokunaga, Y. Kohama, N. Nagaosa, Y. Tokura and H. Y. Hwang, *Phys. Rev. B* **87** (2013) 081109(R)(1-5).
8. Field-Induced Magnetostructural Transitions in Antiferromagnetic  $\text{Fe}_{1+y}\text{Te}_{1-x}\text{S}_x$ : M. Tokunaga, T. Kihara, Y. Mizuguchi and Y. Takano, *J. Low Temp. Phys.* **170** (2013) 340-345.
9. High Magnetic Field Dependence of Magnetodielectric Properties in  $\text{Sr}_2\text{CoSi}_2\text{O}_7$  Crystal: M. Akaki, T. Tadokoro, T. Kihara, M. Tokunaga and H. Kuwahara, *J. Low Temp. Phys.* **170** (2013) 291-295.
10. Studies on multiferroic materials in high magnetic fields: M. Tokunaga, *Front. Phys.* **7** (2012) 386-398.

## **Y. Matsuda group**

Valence states of rare-earth ions in heavy fermion compounds at high magnetic fields have been investigated. A distinct magnetic field-induced valence transition was observed in  $\text{YbAgCu}_4$  by the x-ray absorption spectroscopy. The metamagnetism was also found at the valence transition. This findings support the theoretical proposal that  $\text{YbAgCu}_4$  is located at near the quantum critical point of the valence transition. Moreover, a small magnetic field-induced valence change was detected in a typical Kondo lattice  $\text{CeRu}_2\text{Si}_2$ . The observed valence reduction of Ce ion towards 3+ indicates the reduction of the itinerancy of the f-electrons. Apart from the valence states, the microscopic magnetic field-induced spin-crossover phenomenon was observed in a complex molecule Mn III(taa) using the high magnetic field x-ray spectroscopy. The techniques of the x-ray spectroscopy in a pulsed high magnetic field were reported, especially focusing on the portable type capacitor bank and miniature magnets. We have succeeded in making the ultrahigh magnetic field magnetization measurement up to 103 T, and demonstrated the magnetization curves in several magnetic materials.

1. †\*High-Magnetic-Field X-ray Absorption and Magnetic Circular Dichroism Spectroscopy in the Mixed-Valent Compound  $\text{YbAgCu}_4$ : T. Nakamura, Y. H. Matsuda, J.-L. Her, K. Kindo, S. Michimura, T. Inami, M. Mizumaki, N. Kawamura, M. Suzuki, B. Chen, H. Ohta, K. Yoshimura and A. Kotani, *J. Phys. Soc. Jpn.* **81** (2012) 114702(1-11).
2. \*Precise Magnetization Measurements by Parallel Self-Compensated Induction Coils in a Vertical Single-Turn Coil up to 103 T: S. Takeyama, R. Sakakura, Y. H. Matsuda, A. Miyata and M. Tokunaga, *J. Phys. Soc. Jpn.* **81** (2012) 014702(1-7).
3. †\*Valence Fluctuation in  $\text{YbAgCu}_4$  at High Magnetic Fields: Y. H. Matsuda, T. Nakamura, J.-L. Her, K. Kindo, S. Michimura, T. Inami, M. Mizumaki, N. Kawamura, M. Suzuki, B. Chen, H. Ohta and K. Yoshimura, *J. Phys. Soc. Jpn.* **81** (2012) 015002(1-2).
4. †Magnetic field-induced spin-crossover transition in [MnIII(taa)] studied by x-ray absorption spectroscopy: J. L. Her, Y. H. Matsuda, M. Nakano, Y. Niwa and Y. Inada, *J. Appl. Phys.* **111** (2012) 053921(1-4).
5. †\*Suppression of f-electron itinerancy in  $\text{CeRu}_2\text{Si}_2$  by a strong magnetic field: Y. H. Matsuda, T. Nakamura, J. L. Her, S. Michimura, T. Inami, K. Kindo and T. Ebihara, *Phys. Rev. B* **86** (2012) 041109(R)(1-4).
6. X-ray Spectroscopies in Pulsed High Magnetic Fields: New Frontier with Flying Magnets and Rolling Capacitor Banks: Y. Narumi, T. Nakamura, T. Kinoshita, Y. H. Matsuda and H. Nojiri, *Synchrotron Radiation News* **25** (2012) 12-17.
7. X-ray Diffraction and Absorption Spectroscopy in Pulsed High Magnetic Fields: Y. H. Matsuda and T. Inami, *J. Phys. Soc. Jpn.* **82** (2013) 021009 (17 pages).

8. \*Precise measurement of a magnetic field generated by the electromagnetic flux compression technique: D. Nakamura, H. Sawabe, Y. H. Matsuda and S. Takeyama, Rev. Sci. Instrum. **84** (2013) 044702 (10 pages).
9. Effect of surface roughness on electrical characteristics in amorphous InGaZnO thin-film transistors with high- $\kappa$  Sm<sub>2</sub>O<sub>3</sub> dielectrics: F.-H. Chen, M.-N. Hung, J.-F. Yang, S.-Y. Kuo, J.-L. Her, Y. H. Matsuda and T.-M. Pan, Journal of Physics and Chemistry of Solids **74** (2013) 570-574.
10. \*Magnetization Studies of Field-Induced Transitions by Using a Single-Turn Coil Technique: N. Abe, Y. H. Matsuda, S. Takeyama, K. Sato, H. Kageyama and Y. Nishiwaki, J Low Temp Phys **170** (2013) 452-456.
11. \*Magneto-Absorption in the  $\alpha$  Phase of Solid Oxygen at Megagauss Magnetic Fields: T. Nomura, Y. H. Matsuda, J. L. Her, S. Takeyama, A. Matsuo, K. Kindo and T. C. Kobayashi, J Low Temp Phys **170** (2013) 372-376.
12. \*Observation of Field-induced Anomaly in High-field Magnetization on a Complex Spin-Driven Multiferroic Compound, LiCu<sub>2-z</sub>Zn<sub>z</sub>O<sub>2</sub>: J. L. Her, H. C. Hsu, Y. H. Matsuda, K. Kindo and F. C. Chou, J Low Temp Phys **170** (2013) 285-290.
13. \*Precision of an Ultra-high Magnetic Field Generated by the Electro-magnetic Flux Compression: D. Nakamura, Y. H. Matsuda and S. Takeyama, J Low Temp Phys **170** (2013) 457-462.

## Center of Computational Materials Science

### Todo group

The main subject of the research in Todo group in FY2012 is as follows: (1) Optimization of transition kernel of Markov chain Monte Carlo. (2) Quantum Monte Carlo level spectroscopy and spin liquid phase in two dimensions. (3) Finite-size scaling with dynamical recovery of isotropy for anisotropic spin systems. (4) Quantum Monte Carlo method for measuring the local Z<sub>2</sub> Berry phase. (5) Deconfined critical phenomena in SU(N) quantum antiferromagnets. We have also developed the ALPS framework for large-scale parallel simulations using quantum Monte Carlo, numerical diagonalization, etc, in order to advance our own research on quantum phase transitions and quantum critical phenomena by eliciting high performance of the modern supercomputers, such as the K computer.

1. Ordering and excitation in orbital compass model on a checkerboard lattice: J. Nasu, S. Todo and S. Ishihara, Phys. Rev. B **85** (2012) 205141(1-12).
2. Path-integral Monte Carlo method for the local Z<sub>2</sub> Berry phase: Y. Motoyama and S. Todo, Phys. Rev. E **87** (2013) 021301(1-5).
3. Loop Algorithm: S. Todo, in: *Strongly Correlated Systems: Numerical Methods (Springer Series in Solid-State Sciences)*, Ch 6, edited by A. Avella and F. Mancini, (Springer-Verlag, Berlin, 2013), 153-184.

## Laser and Synchrotron Research Center

### Suemoto group

The spin reorientation transition in a weak ferromagnet ErFeO<sub>3</sub> has been detected by observing the free induction decay signal due to the spin precession motion of the aligned spins, using the terahertz time domain spectroscopy. This demonstrates ultrafast detection of spin orientation with femtojoule pulses which gives practically no thermal disturbance on the sample. The ultrafast hole dynamics, which was hard to access, has been deduced from a comparison of time-resolved luminescence and photoemission data. We propose this type of combined measurements as a new methodology for investigating the hole dynamics in luminescent materials.

1. <sup>†</sup>Anomalous behavior of high-frequency zero-field ferromagnetic resonance in aluminum-substituted  $\varepsilon$ -Fe<sub>2</sub>O<sub>3</sub>: M. Yoshiakiyo, A. Namai, M. Nakajima, T. Suemoto and S. Ohkoshi, J. Appl. Phys. **111** (2012) 07A726(1-3).
2. <sup>†</sup>Ultrafast dynamics of reversible photoinduced phase transitions in rubidium manganese hexacyanoferrate investigated by CN vibration spectroscopy: A. Asahara, M. Nakajima, R. Fukaya, H. Tokoro, S. Ohkoshi and T. Suemoto, Phys. Rev. B **86** (2012) 195138(1-9).
3. <sup>†</sup>Picosecond Soft-X-ray Laser Interferometer for Probing Nanometer Surface Structure: Y. Ochi, K. Terakawa, N. Hasegawa, M. Yamamoto, T. Tomita, T. Kawachi, Y. Minami, M. Nishikino, T. Imazono, M. Ishino and T. Suemoto, Jpn. J. Appl. Phys. **51** (2012) 016601(1-3).

4. <sup>†</sup>Experimental verification of femtosecond laser ablation schemes by time-resolved soft x-ray reflective imaging: T. Tomita, M. Yamamoto, N. Hasegawa, K. Terakawa, Y. Minami, M. Nishikino, M. Ishino, T. Kaihori, Y. Ochi, T. Kawachi, M. Yamagawa and T. Suemoto, *Optics Express* **20** (2012) 29329-29337.
5. <sup>†</sup>Dependence of the cutoff in lithium plasma harmonics on the delay between the prepulse and the main pulse: M. Suzuki, M. Baba, R. A. Ganeev, L. E. Bom, H. Kuroda and T. Ozaki, *J. Phys. B: At. Mol. Opt. Phys.* **45** (2012) 065601(5 pages).
6. <sup>†</sup>Growth Dynamics of Photoinduced Phase Domainin Cyano-Complex Studied by Boundary Sensitive Raman Spectroscopy: A. Asahara, M. Nakajima, R. Fukaya, H. Tokoro, S. Ohkoshi and T. Suemoto, *Acta Physica Polonica A* **121** (2012) 375-378.
7. Ultrafast Coherent Control of Spin Precession Motion by Terahertz Magnetic Pulses: M. Nakajima, K. Yamaguchi and T. Suemoto, *Acta Physica Polonica A* **121** (2012) 343-346.
8. <sup>†</sup>Hard magnetic ferrite with a gigantic coercivity and high frequency millimetre wave rotation: A. Namai, M. Yoshiyuki, K. Yamada, S. Sakurai, T. Goto, T. Yoshida, T. Miyazaki, M. Nakajima, T. Suemoto, H. Tokoro and S. Ohkoshi, *Nature Commun.* **3** (2012) 1035(1-6).
9. \*Mechanism of Enhanced Optical Second-Harmonic Generation in the Conducting Pyrochlore-Type  $Pb_2Ir_2O_{7-x}$  Oxide Compound: Y. Hirata, M. Nakajima, Y. Nomura, H. Tajima, Y. Matsushita, K. Asoh, Y. Kiuchi, A. G. Eguiluz, R. Arita, T. Suemoto and K. Ohgushi, *Phys. Rev. Lett.* **110** (2013) 187402(1-5).
10. <sup>†</sup>Terahertz Time-Domain Observation of Spin Reorientation in Orthoferrite  $ErFeO_3$  through Magnetic Free Induction Decay: K. Yamaguchi, T. Kurihara, Y. Minami, M. Nakajima and T. Suemoto, *Phys. Rev. Lett.* **110** (2013) 137204(1-5).
11. <sup>†</sup>High-power THz wave generation in plasma induced by polarization adjusted two-color laser pulses: Y. Minami, T. Kurihara, K. Yamaguchi, M. Nakajima and T. Suemoto, *Appl. Phys. Lett.* **102** (2013) 041105(1-4).
12. <sup>†</sup>Longitudinal THz wave generation from an air plasma filament induced by a femtosecond lase: Y. Minami, T. Kurihara, K. Yamaguchi, M. Nakajima and T. Suemoto, *Appl. Phys. Lett.* **102** (2013) 151106(1-3).
13. <sup>†</sup>Pulsed laser ablation plasmas generated in  $CO_2$  under high-pressure conditions up to supercritical fluid: T. Kato, S. Stauss, S. Kato, K. Urabe, M. Baba, T. Suemoto and K. Terashima, *Appl. Phys. Lett.* **101** (2013) 224013(1-4).
14. テラヘルツパルス磁場によるインパルシブなスピントリクス起とコヒーレント制御: 中嶋 誠, 山口 啓太, 末元 徹, 応用物理 **81-4** (2012) 317-320.

## Shin group

We studied high Tc Fe-pnictide superconductors using 7-eV laser. High resolution photoemission study with polarization dependence is very powerful for the study of the superconducting mechanism. Orbital fluctuation mechanism is also important in addition to the spin fluctuation mechanism.

1. Corrigendum: Determination of the absolute chirality of tellurium using resonant diffraction with circularly polarized x-rays: Y. Tanaka, S. P. Collins, S. W. Lovesey, M. Matsunami, T. Moriwaki and S. Shin, *J. Phys.: Condens. Matter* **24** (2012) 159501(1 page).
2. Photoemission Evidence for Valence Fluctuations and Kondo Resonance in  $YbAl_2$ : M. Matsunami, A. Chainani, M. Taguchi, R. Eguchi, Y. Takata, M. Oura, M. Yabashi, K. Tamasaku, Y. Nishino, T. Ishikawa, M. Kosaka and S. Shin, *J. Phys. Soc. Jpn.* **81** (2012) 073702(1-4).
3. <sup>†\*</sup>Abrupt change in the energy gap of superconducting  $Ba_{1-x}K_xFe_2As_2$  single crystals with hole doping: W. Malaeb, T. Shimojima, Y. Ishida, K. Okazaki, Y. Ota, K. Ohgushi, K. Kihou, T. Saito, C. H. Lee, S. Ishida, M. Nakajima, S. Uchida, H. Fukazawa, Y. Kohori, A. Iyo, H. Eisaki, C. -T. Chen, S. Watanabe, H. Ikeda and S. Shin, *Phys. Rev. B* **86** (2012) 165117 (1-7).
4. Correlation effects, circular dichroism, and Fermi surfaces of bulk nickel from soft x-ray angle-resolved photoemission: J. Braun, J. Minar, H. Ebert, A. Chainani, J. Miyawaki, Y. Takata, M. Taguchi, M. Oura and S. Shin, *Phys. Rev. B* **85** (2012) 165105(1-5).
5. Evolution of magnetic phases in single crystals of  $SrFe_{1-x}Co_xO_3$  solid solution: Y. W. Long, Y. Kaneko, S. Ishiwata, Y. Tokunaga, T. Matsuda, H. Wadati, Y. Tanaka, S. Shin, Y. Tokura and Y. Taguchi, *Phys. Rev. B* **86** (2012) 064436(1-8).

6. Observation of two fine structures related to the hidden order in the spectral functions of URu<sub>2</sub>Si<sub>2</sub>: R. Yoshida, M. Fukui, Y. Haga, E. Yamamoto, Y. Onuki, M. Okawa, W. Malaeb, S. Shin, Y. Muraoka and T. Yokoya, Phys. Rev. B **85** (2012) 241102(1-4).
7. <sup>†\*</sup>Ultrahigh resolution soft x-ray emission spectrometer at BL07LSU in SPring-8: Y. Harada, M. Kobayashi, H. Niwa, Y. Senba, H. Ohashi, T. Tokushima, Y. Horikawa and S. Shin, Rev. Sci. Instrum. **83** (2012) 013116(1-6).
8. Incommensurate Orbital Modulation behind Ferroelectricity in CuFeO<sub>2</sub>: Y. Tanaka, N. Terada, T. Nakajima, M. Taguchi, T. Kojima, Y. Takata, S. Mitsuda, M. Oura, Y. Senba, H. Ohashi and S. Shin, Phys. Rev. Lett. **109** (2012) 127205(1-5).
9. Octet-line node structure of superconducting order parameter in KFe<sub>2</sub>As<sub>2</sub>: K. Okazaki, Y. Ota, Y. Kotani, W. Malaeb, Y. Ishida, T. Shimojima, T. Kiss, S. Watanabe, C. -T. Chen, K. Kihou, C. H. Lee, A. Iyo, H. Eisaki, T. Saito, H. Fukazawa, Y. Kohori, K. Hashimoto, T. Shibauchi, Y. Matsuda, H. Ikeda, H. Miyahara, R. Arita, A. Chainani and S. Shin, Science **337** (2012) 1314-1317.
10. Special fingerprint in x-ray absorption for hydrogen-bonded dimer formation of acetic acids in solution: Y. Horikawa, H. Arai, T. Tokushima and S. Shin, Chem. Phys. Lett. **522** (2012) 33-37.
11. The Effect of Tetraphenylphosphonium Chloride on Phase Behavior and Nanoscale Structures in a Mixture of D<sub>2</sub>O and 3-Methylpyridine: K. Sadakane, Y. Horikawa, M. Nagao and H. Seto, Chem. Lett. **41** (2012) 1075-1077.
12. Quasiparticles and Fermi liquid behavior in an organic metal: T. Kiss, A. Chainai, H. M. Yamamoto, T. Miyazaki, T. Akimoto, T. Shimojima, K. Ishizaka, S. Watanabe, C. T. Chen, A. Fukaya, R. Kato and S. Shin, Nature Commun. **3** (2012) 1089(1-6).
13. \* 液体水分子の内殻電子励起ダイナミクスと局所構造: 原田 慶久, 徳島 高, 堀川 裕加, 丹羽 秀治, 木内 久雄, 小林 正起, 尾嶋 正治, 辛 塤, しょうとつ **10** (2013) 14-20.

### Takahashi group

We have been studying the structure and phase transition of surfaces and interfaces with diffraction techniques. Bismuth attracts much attention from a viewpoint of topological insulators. It was shown that a single bilayer of Bi(001) on Bi<sub>2</sub>Te<sub>3</sub>(111) is strongly distorted compared to the bulk Bi, resulting in a large change in the band structure. We have also successfully applied a novel method, analyzing the surface structure as an electron density distribution model-independently, to the structure of a few layers of pentacene on Bi(001).

1. Surface relaxation of topological insulators: Influence on the electronic structure: N. Fukui, T. Hirahara, T. Shirasawa, T. Takahashi, K. Kobayashi and S. Hasegawa, Phys. Rev. B **85** (2012) 115426(1-4).
2. Atomic and Electronic Structure of Ultrathin Bi(111) Films Grown on Bi<sub>2</sub>Te<sub>3</sub>(111) Substrates: Evidence for a Strain-Induced Topological Phase Transition: T. Hirahara, N. Fukui, T. Shirasawa, M. Yamada, M. Aitani, H. Miyazaki, M. Matsunami, S. Kimura, T. Takahashi, S. Hasegawa and K. Kobayashi, Phys. Rev. Lett. **109** (2012) 227401(1-5).
3. 多波長同時分散型光学系を用いた結晶トランケーションロッド散乱プロファイルの迅速測定法の開発: 白澤 徹郎, 荒川 悅雄, W. Voegeli, 高橋 敏男, 松下 正, 放射光 **25 No.4** (2012) 229-237.
4. Structure of a Bi/Bi<sub>2</sub>Te<sub>3</sub> heteroepitaxial film studied by x-ray crystal truncation rod scattering: T. Shirasawa, J. Tsunoda, T. Hirahara and T. Takahashi, Phys. Rev. B **87** (2013) 075449(1-5).
5. A method for measuring the specular X-ray reflectivity with millisecond time resolution: W. Voegeli, T. Matsushita, E. Arakawa, T. Shirasawa, T. Takahashi and Y. F. Yano, J. Phys.: Conf. Ser. **425** (2013) 092003(1-4).
6. X-ray intensity and beam trajectory for the Laue-case off-Bragg conditions: T. Takahashi, T. Shirasawa, W. Voegeli, E. Arakawa and T. Matsushita, in: *Silicon Single Crystal:Insatiable Pursuit towards Ideal Quality as Crop in Semiconductor Industry and X-ray Optical Element in Synchrotron Science* (High Energy Accelerator Research Organization(KEK), 2012), 105-105.
7. X 線 CTR 散乱ホログラフィによる表面・界面原子イメージング: 白澤 徹郎, 高橋 敏男, X 線結像光学ニューズレター **No.36** (2012) 5-7.
8. X 線物理学の基礎: 雨宮 慶幸, 高橋 敏男, 百生 敦, 篠原 佑也, 白澤 徹郎, 矢代 航, ((株) 講談社, 東京都文京区音羽 2-12-21, 2012).

## Akiyama group

In 2012, we intensively studied physics of short-pulse generation via gain switching of various semiconductor lasers, such as InGaAsP distributed-feedback (DFB) lasers, InGaAs Fabry-Perot (FP) lasers, and InGaN vertical-cavity surface-emitting lasers (VCSELs). We developed quantitative optical spectroscopy and analysis using detailed-balance relations to study non-equilibrium nature of photo-excited carriers in non-doped semiconductor quantum wells, fluorescent radiation thermometry, quantum-wire lasers, and tandem solar cells. We achieved quantitative measurements of color change in spectra of firefly bioluminescence due to modification of enzyme protein structures in site-directed-mutant luciferase and to temperature change. We also accomplished in-situ absorption and fluorescence spectroscopy of firefly oxyluciferin in the wild-type and red-mutant luciferase. Collaborations of theoretical calculations with TD-DFT of electronic states for luciferin and oxyluciferin in water were made to interpret these experiments.

1. Fano-Resonance Gain by Dephasing Electron–Hole Cooper Pairs in Semiconductors: K. Kamide, M. Yoshita, H. Akiyama, M. Yamaguchi and T. Ogawa, *J. Phys. Soc. Jpn.* **81** (2012) 093706(1-4).
2. Observation of high Rydberg states of one-dimensional excitons in GaAs quantum wires by magneto-photoluminescence excitation spectroscopy: M. Okano, Y. Kanemitsu, S. Chen, T. Mochizuki, M. Yoshita, H. Akiyama, L. N. Pfeiffer and K. W. West, *Phys. Rev. B* **86** (2012) 085312(1-5).
3. Analysis of gain-switching characteristics including strong gain saturation effects in low-dimensional semiconductor lasers: S. Chen, M. Yoshita, T. Ito, T. Mochizuki, H. Akiyama, H. Yokoyama, K. Kamide and T. Ogawa, *Jpn. J. Appl. Phys.* **51** (2012) 098001(1-2).
4. Waveguide-two-points-differential-excitation method for quantitative absorption measurements of nano-structures: T. Mochizuki, M. Yoshita, S. Maruyama, C. Kim, K. Fukuda, H. Akiyama, L. N. Pfeiffer and K. W. West, *Jpn. J. Appl. Phys.* **51** (2012) 106601(1-5).
5. Applicability of continuum absorption in semiconductor quantum wells to absolute absorption-strength standards: M. Yoshita, K. Kamide, H. Suzuura and H. Akiyama, *Appl. Phys. Lett.* **101** (2012) 032108(1-4).
6. Blue 6-ps short-pulse generation in gain-switched InGaN vertical-cavity surface-emitting lasers via impulsive optical pumping: S. Chen, M. Okano, B. Zhang, M. Yoshita, H. Akiyama and Y. Kanemitsu, *Appl. Phys. Lett.* **101** (2012) 191108(1-3).
7. Metal-to-insulator transition in anatase TiO<sub>2</sub> thin films induced by growth rate modulation: T. Tachikawa, M. Minohara, Y. Nakanishi, Y. Hikita, M. Yoshita, H. Akiyama, C. Bell and H. Y. Hwang, *Appl. Phys. Lett.* **101** (2012) 022104(1-4).
8. Quantitative absorption spectra of quantum wires measured by analysis of attenuated internal emissions: M. Yoshita, T. Okada, H. Akiyama, M. Okano, T. Ihara, L. N. Pfeiffer and K. W. West, *Appl. Phys. Lett.* **100** (2012) 112101(1-4).
9. <sup>†</sup>Electrical and Optical Properties of GaNAs/GaAs MQW p-i-n Junctions: K. Arimoto, M. Shiraga, H. Shirai, S. Takeda, M. Ohmori, H. Akiyama, T. Mochizuki, K. Yamaguchi, H. Miyagawa, N. Tsurumachi, S. Nakanishi and S. Koshiba, *Transactions of the Materials Research Society of Japan* **37** (2012) 193-196.
10. <sup>†</sup>Biexciton Luminescence from Individual Isoelectronic Traps in Nitrogen δ-Doped GaAs: K. Takamiya, T. Fukushima, S. Yagi, Y. Hijikata, T. Mochizuki, M. Yoshita, H. Akiyama, S. Kuboya, K. Onabe, R. Katayama and H. Yaguchi, *Appl. Phys. Express* **5** (2012) 111201(1-3).
11. Sub-5-ps optical pulse generation from a 155-μm distributed-feedback laser diode with nanosecond electric pulse excitation and spectral filtering: S. Chen, A. Sato, T. Ito, M. Yoshita, H. Akiyama and H. Yokoyama, *Opt. Express* **20** (2012) 24843-24849.
12. Theoretical Study of Absorption and Fluorescence Spectra of Firefly Luciferin in Aqueous Solutions: M. Hiyama, H. Akiyama, K. Yamada and N. Koga, *Photochemistry and Photobiology* **88** (2012) 889-898.
13. Fluorescent Radiation Thermometry at Cryogenic Temperatures Based on Detailed Balance Relation: T. Mochizuki, T. Ihara, M. Yoshita, S. Maruyama, H. Akiyama, L. N. Pfeiffer and K. W. West, *Appl. Phys. Express* **6** (2013) 056602(1-3).
14. Dynamics of short-pulse generation via spectral filtering from intensely excited gain-switched 155-μm distributed-feedback laser diodes: S. Chen, M. Yoshita, A. Sato, T. Ito, H. Akiyama and H. Yokoyama, *Opt. Express* **21** (2013) 10597-10605.
15. Gain-switched pulses from InGaAs ridge-quantum-well lasers limited by intrinsic dynamical gain suppression: S. Chen, M. Yoshita, T. Ito, T. Mochizuki, H. Akiyama and H. Yokoyama, *Opt. Express* **21** (2013) 7570-7576.

16. Theoretical Study of Firefly Luciferin p*K<sub>a</sub>* Values-Relative Absorption Intensity in Aqueous Solutions: M. Hiyama, H. Akiyama, K. Yamada and N. Koga, *Photochem Photobiol* **89** (2013) 571-578.
17. <sup>†</sup>Electroluminescence of GaNAs/GaAs MQWs p-i-n junctions grown by RF-MBE using modulated nitrogen radical beam source: N. Ohta, K. Arimoto, M. Shiraga, K. Ishii, M. Inada, S. Yanai, Y. Nakai, H. Akiyama, T. Mochizuki, T. Takahashi, N. Takahashi, H. Miyagawa, N. Tsurumachi, S. Nakanishi and S. Koshiba, *Journal of Crystal Growth* (2013) S002202481300081X, in print.
18. Double-core-slab-waveguide semiconductor lasers for end optical pumping: T. Nakamura, T. Mochizuki, C. Kim, S. Chen, M. Yoshita and H. Akiyama, *Applied Physics Express* (2013), in print.
19. Intrinsic radiative lifetime derived via absorption cross section of one-dimensional excitons: S. Chen, M. Yoshita, A. Ishikawa, T. Mochizuki, S. Maruyama, H. Akiyama, Y. Hayamizu, L. N. Pfeiffer and K. W. West, *Scientific Reports* (2013), in print.
20. Theoretical Study of Oxyuciferin p*K<sub>a</sub>* Values; Relative Absorption Intensity in Aqueous Solutions: M. Hiyama, H. Akiyama, Y. Wang and N. Koga, *Chem. Phys. Lett* (2013), in print.
21. Spectroscopic study on oxyluciferinluciferase complex in firefly bioluminescent reaction solution and clues to understand the color tuning mechanism: Y. Wang, Y. Hayamizu and H. Akiyama, in: *7th International Symposium on Bioluminescence and Chemiluminescence* (ISBC2012, 2012), 172.

## I. Matsuda group

We have carried out developments and experiments of the advanced spectroscopies using vacuum ultraviolet and soft X-rays.  
 1) Time-resolved soft X-ray photoemission researches have been performed at high brilliant soft X-ray beamline SPring-8 BL07LSU with the ultrashort pulse laser. By the pump-probe method, relaxation of photoexcited carriers after the surface photovoltage effect at various semiconductor surfaces are traced in real time in the picoseconds to nanoseconds-time scale.

2) The M-edge resonant magneto-optical Kerr effect (RMOKE) of a transition metal film was examined by measurement of the rotating analyzer ellipsometry method and by theoretical simulation based on the resonant scattering theory. The giant Kerr rotation angle over 10 degree at room temperature was observed with vacuum ultraviolet synchrotron radiation at KEK-PB BL-18A. Significant roles of lifetime of the intermediate state during the scattering process and the Fano-resonance were identified. The time-resolved measurement of RMOKE was demonstrated with the SCSS free-electron laser to trace relaxation after the photo-induced demagnetization.

3) The SPring-8 BL07LSU is equipped with a crossed-type long undulator that is designed to generate high-brilliant soft X-rays with various light polarizations. Degrees of linear (horizontal/vertical) and circular (left/right) polarizations were evaluated with soft X-ray polarimeter using the rotating analyzer ellipsometry method.

1. Electronic structure study of ultra thin Ag(111) films modified by Si(111) substrate and by the  $\sqrt{3} \times \sqrt{3}$ -Ag<sub>2</sub>Bi surface: M. Ogawa, P. M. Sheverdyeva, P. Moras, D. Topwal, A. Harasawa, K. Kobayashi, C. Carbone and I. Matsuda, *J. Phys.: Condens. Matter* **24** (2012) 115501(1-6).
2. Atomic configuration and phase transition of Pt-induced nanowire on Ge(001) surface studied by scanning tunneling microscopy, reflection high-energy positron diffraction and angle resolved photo-emission spectroscopy: I. Mochizuki, Y. Fukaya, A. Kawasuso, K. Wada, T. Hyodo, K. Yaji, A. Harasawa and I. Matsuda, *Phys. Rev. B* **85** (2012) 245438(1-6).
3. \*Development of soft X-ray time-resolved photoemission spectroscopy systemwith a two-dimensional angle-resolved time-of-flight analyzer at SPring-8 BL07LSU: M. Ogawa, S. Yamamoto, Y. Kousa, F. Nakamura, R. Yukawa, A. Fukushima, A. Harasawa, H. Kondo, Y. Tanaka, A. Kakizaki and I. Matsuda, *Rev. Sci. Instrum.* **83** (2012) 023109(1-7).
4. Controlling the topology of Fermi surfaces in metal nanofilms: M. Ogawa, A. Gray, P. M. Sheverdyeva, P. Moras, H. Hong, L. -C. Huang, S. -J. Tang, K. Kobayashi, C. Carbone, T. -C. Chiang and I. Matsuda, *Phys. Rev. Lett.* **109** (2012) 026802(1-4).
5. Hydrogen-induced surface metallization of SrTiO<sub>3</sub>(001): M. D'Angelo, R. Yukawa, K. Ozawa, S. Yamamoto, T. Hirahara, S. Hasegawa, M. G. Silly, F. Sirotti and I. Matsuda, *Phys. Rev. Lett.* **108** (2012) 116802(1-5).
6. \*Elucidation of Rh-Induced In-Gap States of Rh:SrTiO<sub>3</sub> Visible-Light-Driven Photocatalyst by Soft X-ray Spectroscopy and First-Principles Calculations: S. Kawasaki, K. Akagi, K. Nakatsuji, S. Yamamoto, I. Matsuda, Y. Harada, J. Yoshinobu, F. Komori, R. Takahashi, M. Lippmaa, C. Sakai, H. Niwa, M. Oshima, K. Iwashina and A. Kudo, *J. Phys. Chem. C* **116** (2012) 24445-24448.

7. Atomic and electronic structures of Si(111)- $\sqrt{21} \times \sqrt{21}$  superstructure: Y. Fukaya, K. Kubo, T. Hirahara, S. Yamazaki, W. H. Choi, H. W. Yeom, S. Hasegawa, A. Kawasuso and I. Matsuda, *e-J. Surf. Sci. Nanotechnology* **10** (2012) 310-314.
8. Structural analysis of Si(111)- $\sqrt{21} \times \sqrt{21}$ -(Ag, Cs) surface by reflection high-energy positron diffraction: Y. Fukaya, I. Matsuda, R. Yukawa and A. Kawasuso, *Surface Science* **606** (2012) 1918-1921.
9. Time-resolved photoelectron spectroscopies using synchrotron radiation: Past, present, and future: S. Yamamoto and I. Matsuda, *J. Phys. Soc. Jpn.* **82** (2013) 021003(1-18).
10. Electronic structure of the hydrogen-adsorbed SrTiO<sub>3</sub>(001) surface studied by polarization-dependent photoemission spectroscopy: R. Yukawa, S. Yamamoto, K. Ozawa, M. D'Angelo, M. Ogawa, M. G. Silly, F. Sirotti and I. Matsuda, *Phys. Rev. B* **87** (2013) 115314(1-6).
11. 金属超薄膜内に閉じ込められた電子系のフェルミ面トポロジー制御-量子効果で銀細工: 永村 直佳, 小河 愛実, 松田 巍, *固体物理* **48** (2013) 13-19.

## Kobayashi group

We have developed a Dual-comb spectroscopy setup, Multi-GHz repetition-rate mode-locked laser, and precision spectroscopy in VUV.

1. Chirped-pulse direct frequency-comb spectroscopy of two-photon transitions: A. Ozawa and Y. Kobayashi, *Phys. Rev. A* **86** (2012) 022514(1-6).
2. \*Generation of soft x-ray and water window harmonics using a few-cycle, phase-locked, optical parametric chirped-pulse amplifier: N. Ishii, S. Adachi, Y. Nomura, A. Kosuge, Y. Kobayashi, T. Kanai, J. Itatani and S. Watanabe, *Opt. Lett.* **37** (2012) 97-99.
3. †Vacuum ultraviolet frequency combs generated by a femtosecond enhancement cavity in the visible: B. Bernhardt, A. Ozawa, A. Vernaleken, I. Pupeza, J. Kaster, Y. Kobayashi, R. Holzwarth, E. Fill, F. Krausz, T. W. Hänsch and T. Udem, *Opt. Lett.* **37** (2012) 503-505.
4. Injection locking of Yb-fiber based optical frequency comb: N. Kuse, A. Ozawa, Y. Nomura, I. Ito and Y. Kobayashi, *Optics Express* **20** (2012) 10509-10518.
5. Kerr-lens mode-locked Yb:KYW laser at 4.6-GHz repetition rate: M. Endo, A. Ozawa and Y. Kobayashi, *Optics Express* **20** (2012) 12191-12197.
6. Comb-Resolved Dual-Comb Spectroscopy Stabilized by Free-Running Continuous-Wave Lasers: N. Kuse, A. Ozawa and Y. Kobayashi, *Appl. Phys. Express* **5** (2012) 112402(1-3).
7. vuv frequency-comb spectroscopy of atomic xenon: A. Ozawa and Y. Kobayashi, *Phys. Rev. A* **87** (2013) 022507(1-4).

## Itatani group

We have developed a novel BIBO-based intense optical parametric amplifier system that produces 0.55-mJ, 9-fs pulses at 1.6  $\mu\text{m}$  at a repetition rate of 1 kHz with stable carrier-envelope phases. High harmonics are successfully produced with this light source, and we observed CEP-dependent coherent soft x rays that extend to  $\sim 330$  eV in photon energies. This is the first observation of CEP-dependent soft-x-ray high harmonics that extend to the water window. The observed high harmonic spectra agree quantitatively well with quantum simulation that suggests the generation of isolated attosecond pulses in soft x rays. This result is an important milestone to extend the attosecond optical science from extremely ultraviolet (EUV) to soft x rays. We have also started to work on high harmonics beamlines for time-and-angle-resolved photoemission spectroscopy (TARPES) and ultrafast magneto-optical Kerr effect (MOKE) spectroscopy for collaborative research on material sciences.

1. \*Generation of soft x-ray and water window harmonics using a few-cycle, phase-locked, optical parametric chirped-pulse amplifier: N. Ishii, S. Adachi, Y. Nomura, A. Kosuge, Y. Kobayashi, T. Kanai, J. Itatani and S. Watanabe, *Opt. Lett.* **37** (2012) 97-99.
2. Sub-two-cycle, carrier-envelope phase-stable, intense optical pulses at 16  $\mu\text{m}$  from a BiB<sub>3</sub>O<sub>6</sub> optical parametric chirped-pulse amplifier: N. Ishii, K. Kaneshima, K. Kitano, T. Kanai, S. Watanabe and J. Itatani, *Opt. Lett.* **37** (2012) 4182-4184.
3. 高強度レーザーによる再衝突物理: 板谷 治郎, パリティ **27** (2012) 11-19.

## **Harada group**

1) We have upgraded our ultrahigh resolution soft X-ray emission spectrometer to increase the detection efficiency by implementing a pre-focusing mirror in front of the grating. The upgrade was successful and has improved the performance of the spectrometer by a factor of three without losing energy resolving power.

2) We have studied hydrogen bond property of water using O 1s resonant X-ray emission spectroscopy (XES). Spectroscopic evidence of inhomogeneity in liquid water, i.e. tetrahedrally coordinated and highly distorted hydrogen bond picture of water, depends on the character of the pre-edge peak in the O 1s X-ray absorption spectrum (XAS). In the recombination emission spectrum at resonant excitation to the pre-edge, we have observed vibrational excitations characteristic of a highly broken hydrogen bond, which strengthen the inhomogeneous picture of liquid water.

3) Determination of oxygen reduction active site in carbon based fuel cell cathode catalyst is a critical issue to systematically improve the catalytic activity. This year we have studied the problem by the following two *in situ* and one *in operando* experiments; i) *In situ* C 1s, N 1s and O 1s XAS, XPS and XES experiments to elucidate O<sub>2</sub> adsorption property of nitrogen doped HOPG as a model of the carbon based catalyst. ii) *In situ* N 1s and O 1s XAS and XES to elucidate O<sub>2</sub> adsorption property of highly active carbon based catalyst mixed with Nafion211. iii) *In operando* XAS and XES to elucidate O<sub>2</sub> adsorption property of carbon based catalyst embedded in a membrane electrolyte assembly (MEA). We have fabricated an original cell for the MEA experiments. The electronic structure of metals in metallo-phthalocyanine derived fuel cell cathode catalysts under operation (gas condition/ bias application) was obtained for the first time. Combining these three experiments we concluded that nitrogen should contribute to the high oxygen reduction activity at high pyrolysis temperatures above 800 °C while at low (< 600 °C) temperatures the residual iron regains oxygen adsorption property through mixture with Nafion and possibly contribute to the oxygen reduction activity.

1. <sup>†\*</sup>Ultrahigh resolution soft x-ray emission spectrometer at BL07LSU in SPring-8: Y. Harada, M. Kobayashi, H. Niwa, Y. Senba, H. Ohashi, T. Tokushima, Y. Horikawa and S. Shin, Rev. Sci. Instrum. **83** (2012) 013116(1-6).
2. \*Elucidation of Rh-Induced In-Gap States of Rh:SrTiO<sub>3</sub> Visible-Light-Driven Photocatalyst by Soft X-ray Spectroscopy and First-Principles Calculations: S. Kawasaki, K. Akagi, K. Nakatsuji, S. Yamamoto, I. Matsuda, Y. Harada, J. Yoshinobu, F. Komori, R. Takahashi, M. Lippmaa, C. Sakai, H. Niwa, M. Oshima, K. Iwashina and A. Kudo, J. Phys. Chem. C **116** (2012) 24445-24448.
3. \* 液体水分子の内殻電子励起ダイナミクスと局所構造: 原田 慶久, 徳島 高, 堀川 裕加, 丹羽 秀治, 木内 久雄, 小林 正起, 尾嶋 正治, 辛 塤, じょうとつ **10** (2013) 14-20.

## **Joint Use Projects**

### **Jointuse group**

1. <sup>†\*</sup>Electrospinning Synthesis of Wire-Structured LiCoO<sub>2</sub> for Electrode Materials of High-Power Li-Ion Batteries: Y. Mizuno, E. Hosono, T. Saito, M. Okubo, D. Nishio-Hamane, K. Ohishi, T. Kudo and H. Zhou, J. Phys. Chem. C **116** (2012) 10774-10780.
2. <sup>†\*</sup>Hulsite from Sengendera skarn deposit, Miyazaki, Japan: Y. Ogoshi, T. Minakwa and D. Hamane, Japanese Magazine of Mineralogical and Petrological Sciences **41** (2012) 61-66.

<sup>†</sup> Joint research with outside partners.

\* Joint research between groups within ISSP.